

Medical University of South Carolina

MEDICA

MUSC Theses and Dissertations

1996

Studies on ARA-C-Induced DNA Damage and Apoptosis in Acute Myeloid Leukemia Cells which Overexpress p26Bcl-2

Gloria Joan Bullock

Medical University of South Carolina

Follow this and additional works at: <https://medica-musc.researchcommons.org/theses>

Recommended Citation

Bullock, Gloria Joan, "Studies on ARA-C-Induced DNA Damage and Apoptosis in Acute Myeloid Leukemia Cells which Overexpress p26Bcl-2" (1996). *MUSC Theses and Dissertations*. 187.

<https://medica-musc.researchcommons.org/theses/187>

This Dissertation is brought to you for free and open access by MEDICA. It has been accepted for inclusion in MUSC Theses and Dissertations by an authorized administrator of MEDICA. For more information, please contact medica@muscd.edu.

**STUDIES ON ARA-C-INDUCED DNA DAMAGE AND APOPTOSIS
IN ACUTE MYELOID LEUKEMIA CELLS
WHICH OVEREXPRESS p26Bcl-2**

by

Gloria Joan Bullock

A dissertation submitted to the faculty of
the Medical University of South Carolina
in partial fulfillment of the requirement for
the degree of Doctor of Philosophy
in the College of Graduate Studies.

Molecular and Cellular Biology and Pathobiology Program

June 1996

Approved by:

Kapil Bhalla, M.D.

Chairman, Advisory Committee

Ronald J. Fernandez

James
Chen, M.D.

Robert K. Deans

Mark Cuddy

<u>TABLE OF CONTENTS</u>	<u>Page</u>
General abstract	v
Acknowledgements	vii
List of Figures	ix
List of Tables	xi
Glossary of terms and abbreviations used	xii
<u>Chapter I. General Introduction</u>	1
A. Apoptosis.	2
1. Distinction from necrosis	2
2. Definition of programmed cell death, apoptosis, and its characteristics	3
3. Occurrence and mediators of apoptosis	4
4. Genes which regulate apoptosis	7
B. Bcl-2.	10
1. <i>bcl-2</i> gene structure	10
2. Regulation of <i>bcl-2</i> gene expression: Indications for transcriptional, or post-transcriptional/translation modification	14
3. The <i>bcl-2</i> gene product blocks a final common pathway of apoptosis	15
4. Speculations of the mechanisms of action of Bcl-2	17
4a. Motifs in <i>bcl-2</i> sequence	17
4b. Bcl-2 as an antioxidant	18
4c. Bcl-2 and regulation of Ca ²⁺ flux	19
4d. Bcl-2 and interaction with Ras	21
4e. Bcl-2 and transport of nuclear proteins	22
5. <i>bcl-2</i> -related family of genes	23
6. Expression of <i>bcl-2</i> and related genes in malignancies	36
C. Acute myeloid leukemia.	38
1. Definition, history, and classification	38
2. Presentation at diagnosis	40
3. Treatment of AML	40
D. Ara-C.	42
1. Intracellular metabolism of Ara-C	42
2. Mechanism of action of Ara-C	43
3. Other targets of Ara-C	45
E. Objectives of this dissertation	50
Hypotheses	51
<u>Chapter II. Development of <i>in vitro</i> AML cell model</u>	52
A. Choice of a model cell line.	53
1. Expression of Bcl-2 and related proteins in AML cell lines	53
2. HL-60 cell line	54
B. The LacSwitch Inducible Mammalian Expression System	60
Introduction	60
Materials and Methods	64

Results	68
Discussion	69
Figure Legends	71
Figures	72
C. Retroviral-mediated transfer of <i>bcl-2</i> cDNA to AML cells	73
Introduction	73
Materials and Methods	73
Results	76
Discussion	77
Figure Legends	79
Figures	80
<u>Chapter III. Bcl-2 blocks Ara-C-induced DNA fragmentation associated with apoptosis but not early events of intracellular Ara-C metabolism</u>	82
Abstract	83
Introduction	84
Materials and Methods	85
Results	91
Discussion	94
Figure Legends	97
Figures	98
<u>Chapter IV.</u>	105
<u>Part A. The level of Bcl-2 overexpression determines the response to Ara-C-induced apoptosis over time in human AML HL-60 cells.</u>	
<u>Part B. <i>bcl-2</i> expression is induced in human AML cells which survive treatment with high-dose Ara-C.</u>	
Abstract	106
Introduction	107
Materials and Methods	109
Results	113
Discussion	120
Figure Legends	133
Figures	136
<u>Chapter V. Overexpression of p26Bcl-2 in acute myeloid leukemia cells blocks Ara-C-induced apoptosis, but does not increase repair of Ara-C-induced DNA damage.</u>	154
Abstract	155
Introduction	156
Materials and Methods	160
Results	164
Discussion	170
Figure Legends	175
Figures	177

<u>Chapter VI. Mechanism(s) of action of Bcl-2: General Discussion and Future Studies.</u>	190
A. Introduction	191
B. Disparate levels of gene expressions induced in HIDAC-treated HL-60/Bcl-2 cells as compared with HIDAC-treated HL-60/neo cells	192
1. <i>c-jun</i> mRNA hyperinduction in HIDAC-treated HL-60/Bcl-2 cells	192
2. Increased <i>c-myc</i> mRNA expression in HL-60/Bcl-2 cells	194
C. Proposal for Bcl-2-mediated blockade of p34^{cdc2} kinase trafficking or premature activation, and review of other documented mechanisms.	195
D. Proposal for Bcl-2-mediated blockade of protease cascade(s) preceding the onset of apoptosis.	196
E. Further speculations.	203
Figure Legends	205
Figures	207
<u>List of references</u>	213
<u>Biographical Sketch</u>	248

GLORIA JOAN BULLOCK.**Bcl-2 BLOCKS ARA-C-INDUCED APOPTOSIS BUT NOT ARA-C-INDUCED DNA DAMAGE IN HUMAN ACUTE MYELOID LEUKEMIA CELLS.**

Under the direction of Kapil N. Bhalla, M.D. Division of Hematology/Oncology, Medical University of South Carolina, Charleston, SC and Winship Cancer Center, Emory University, Atlanta, GA.

High expression of p26Bcl-2 in patient-derived AML cells has been associated with poor response to chemotherapy including Ara-C. It has been well established that Bcl-2 overexpression blocks apoptosis or programmed cell death induced by a wide variety of stimuli including chemotherapeutic drugs. However, the exact mechanism of action of Bcl-2 in promoting this blockade is still largely unknown. To determine the types of Ara-C-induced DNA damage with which Bcl-2 specifically interferes, HL-60/neo and HL-60/Bcl-2 cells were created via retroviral-mediated transfection of the *bcl-2* gene. These transfectants served as *in vitro* AML cell models that expressed different levels of p26Bcl-2. The clone with the highest Bcl-2 levels contained 5- to 10-fold greater Bcl-2 by Western blot and immunofluorescence as compared to HL-60/neo cells. HL-60/Bcl-2 cells are resistant to Ara-C-induced apoptosis, which was evident in HL-60/neo cells as internucleosomal and high molecular weight DNA fragmentation, as well as by the activation of the cysteine protease cascade of apoptosis. Differences in apoptosis in the two cell types was correlated with differences in the loss of cell viability as measured by the MTT (3-[3,5-dimethylthiazol-2-yl]-2,5-diphenyltetrasolium bromide) assay. Proximal steps in Ara-C metabolism including intracellular accumulation of Ara-CTP relative to dCTP, Ara-C DNA incorporation, Ara-C-induced DNA strand breaks (by the alkaline elution assay) and Ara-C-induced inhibition of DNA synthesis (by measurement of [³H]-TdR incorporation), were not significantly different between HL-60/neo and HL-60/Bcl-2 cells. Bcl-2 expression was studied in cells surviving over time after Ara-C treatment. Various clones of HL-60/Bcl-2 cells were generated by limiting dilution of transfected HL-60/Bcl-2 cells. Regardless of their endogenous Bcl-2 levels, following Ara-C treatment, the non-apoptotic (surviving) cells of various clones exhibited further transcriptional up-regulation of *bcl-2* mRNA and p26Bcl-2 levels detected by RNase protection assay, and Western blot analysis or flow cytometry, respectively. HL-60/neo cells that had survived the initial Ara-C treatment were exposed to a second dose of Ara-C, to determine whether the induction in the Bcl-2 levels in these cells were biologically relevant. This was confirmed by demonstrating a reduced

reduced cytotoxicity of the second dose of Ara-C by the MTT assay. Whether increased Bcl-2 levels in HL-60/Bcl-2 cells promote increased repair of non-lethal Ara-C-induced DNA damage was also addressed. Following Ara-C treatment, HL-60/neo as well as HL-60/Bcl-2 cells exhibited equivalent rates of repair of non-lethal DNA damage, as assessed by the comparisons of unscheduled DNA synthesis, and assessment by PCR of the repair of the damage of the *c-myc* genomic DNA template. Therefore, these data indicate that while Bcl-2 does not block early steps of Ara-C metabolism, Ara-C-induced DNA damage or its repair, it does block the induction of Ara-C-induced apoptosis by inhibiting the conversion of Ara-C-induced early and potentially repairable DNA damage into lethal DNA fragmentation characteristic of apoptosis.

ACKNOWLEDGEMENTS

I wish to wholeheartedly thank:

All those scientists and friends whose guidance helped me progress from the beginning to the end of this Ph.D. project.

- I extend my deepest appreciation to my mentor, **Dr. Kapil Bhalla**, for allowing me the opportunity and privilege of being a part of his laboratory, and for guiding me through my dissertation work. I thank Dr. Bhalla for providing me with his laboratory space and materials, funds for attendance to research meetings, and the opportunities to meet the experts in our field and to experience these incredible environments for learning. I also thank Dr. Bhalla for his acknowledgement of the potential for excellence in everyone, for striving toward its ultimate cultivation, and for instilling that quest for excellence in me. Dr. Bhalla has taught me many valuable life lessons from which I will benefit for the rest of my career.
- I am indebted to the members of my Advisory Committee, **Dr. Daniel Fernandes, Dr. James Norris, Dr. Clifford Schweinfest, Dr. Robert Stuart, Dr. Mark Willingham** for their advice, guidance, and support. I thank **Dr. Fernandes, Dr. Willingham, and Dr. Stuart, as well as Dr. Elena Tourkina, Dr. Anna Ludwicka Bradley, Dr. Richard Silver, Dr. Maria Buse, Mrs. Katherine Robinson, Mr. Jeffrey Koning, and Ms. Amy Feagin**, for providing me with additional laboratory space and materials with which to finish my experiments at MUSC.
- I wish to extend my appreciation to **Dr. Perry Halushka**, for his supportive and efficient direction of the Medical Scientist Training Program at the Medical University of South Carolina. I also extend my appreciation to **Mrs. Hester Young and Mrs. Susan Higerd** for all their assistance, dependability, and support given to myself and the students of this program.
- I thank all the members of **Dr. Bhalla's lab** with whom I have worked at MUSC in Charleston, and at Emory University in Atlanta: **Dr. Charles Holladay, Ms. Mary Ella Mahoney, Dr. Vidya Ponnathpur, Dr. Caroline Tang, Dr. Swapan Ray, Dr. Yue Huang, Mr. Amir Nawabi, Mr. GuoFu Fang, Ms. Linda Liu, Dr. Michelle Lyles, and Ms. Ana Maria Ibrado (dearest Ana Banana)**, for their expert assistance, support, and friendship.
- I thank **Dr. David Schwartz** for his abundant advice in molecular cloning techniques.
- I thank **Dr. Carlo Catapano** for his willingness and guidance in helping me set up the extensive DNA damage and repair techniques used in these studies.
- I thank **Dr. Shuli Li and Dr. Gian G. Re** for their time and assistance in teaching me an additional Rnase protection assay for my studies, as well as for providing the end-products of a labor-intensive cloning project for use in this assay.
- I acknowledge **Mrs. Carylee Wiggins** at MUSC, and **Mr. Robert Karaffa** at Emory University for their extensive expert technical assistance in the flow cytometric techniques used in these studies.
- I wish to thank **Drs. Beatrice Robinson, Garritt Lughthart, and Father James O'Brien** of the Biology Department at LeMoyne College, Syracuse, New York, for fostering my enthusiasm

toward this goal and giving me the foundation in Biology on which to build this progress. I also thank **Dr. William S. Kushner** of the Biology Department at Cicero-North Syracuse High School, Cicero, New York, who was my first teacher to ignite my enthusiasm for Biology.

Personal Acknowledgements:

- I am eternally grateful to **Dr. Elena Tourkina** for her constant support, friendship, and technical advice.
- I wish to thank **the Reverend Dr. James H. Shaud** of Faith Lutheran Church, Cicero, New York, for his constant support, concern, and sharing of his spiritual strength.
- I wish to thank as sufficiently as I can, **my wonderful parents, Dr. Charles and Marian Bullock**, and **my sister and best friend, Victoria**, for their unconditional love and tireless support throughout this, as well as all my endeavors in life; for constantly renewing my strength and my perseverance, for keeping God's Love with me, and for being the wind beneath my wings. I also thank **my parents** for providing me with an excellent education and with abundant opportunities to embrace and soar with. You all are the greatest gifts of my life.
- Most importantly, how can I adequately thank You, Lord? All this is Yours. (Romans 8:28)

LIST OF FIGURES AND TABLES:

A. List of Figures	Page
1. Schematic illustration of the <i>bcl-2</i> α transcript which encodes p26Bcl-2 α .	13
2. The Bcl-2/Bax “rheostat” death checkpoint which may govern susceptibility to apoptosis.	30
3. Extension of Oltvai and Korsmeyer’s Bcl-2:Bax “rheostat” model to include interaction of Bcl-2-related proteins.	31
4. Model of interactions between Bcl-2 and its related proteins.	32
5a. Alignment of Bcl-2-related proteins: Conserved homology in BH1 and BH2 domains.	33
5b. Alignment of Bcl-2-related proteins: Conserved homology in newly described BH3 domains.	34
6. The hematopoietic “tree”.	39
7. Illustration of Ara-C metabolism and known mechanisms of action.	48
8. Schematic diagram of Ara-C-induced DNA damage and regulation of the endpoints of apoptosis by various gene products.	49
9. Expression of Bcl-2 in AML cell lines.	57
10. Drug-induced DNA fragmentation in HL-60 and K562 cells.	58
11. Expression of Bcl-x _L in HL-60 and K562 cells.	59
12. The lactose operon in <i>E. coli</i> .	62
13. The LacSwitch inducible mammalian expression system.	63
14. Selection of HL-60 cells transfected with LacSwitch components and attempts toward induction of overexpression of p26Bcl-2.	72
15. Immunofluorescent and Western blot analyses of retrovirally-transfected HL-60/neo and HL-60/Bcl-2 cells.	80
16. Morphologic evidence of Ara-C-induced apoptosis in HL-60/neo versus HL-60/Bcl-2 cells.	81
17. Ara-C-induced internucleosomal and high molecular weight DNA fragmentation in HL-60/neo versus HL-60/Bcl-2 cells.	98
18. Profiles of alkaline elution of DNA from Ara-C-treated or irradiated HL-60/neo and HL-60/Bcl-2 cells.	102
19. Ara-C-induced internucleosomal and high molecular weight DNA fragmentation over time in HL-60/neo cells versus HL-60/Bcl-2 cells.	136
20. Flow cytometric determination of apoptosis in HL-60/neo cells versus HL-60/Bcl-2 clones after Ara-C treatment.	138
21. Assessment of cell viability after Ara-C treatment in HL-60/neo cells versus HL-60/Bcl-2 clones by MTT assay and trypan blue dye exclusion.	139
22. Western blot analyses for p26Bcl-2:p21Bax expressions in HL-60/neo cells versus HL-60/Bcl-2 clones over time after Ara-C treatment.	141
23. Immunofluorescent analyses of Bcl-2 levels in HL-60/neo cells versus HL-60/Bcl-2 clones over time after Ara-C treatment.	143
24. Ribonuclease protection assay for induction of <i>bcl-2</i> mRNA expression in HL-60/neo versus HL-60/Bcl-2 cells over time after Ara-C treatment.	146
24a. Induction of <i>bcl-2</i> mRNA assessed by RNase Protection Assay in HL-60/neo and HL-60/Bcl-2 cells after Ara-C treatment.	147
25. Flow cytometry determination of Bcl-2 levels by in HL-60/neo cells versus HL-60/Bcl-2 clones after Ara-C treatment: Effect of concomitant actinomycin D/ cycloheximide treatment.	150
26. Assessment of cell viability by MTT assay of HL-60/neo cells after first and second	

treatments with Ara-C.	151
27. Flow cytometric determination of apoptosis in HL-60/neo cells after first and second treatments with Ara-C.	152
27a. Assessment of cell viability by MTT assay and flow cytometric determination of apoptosis in HL-60/neo cells after first and second treatments with Ara-C.	153
28. [³ H]-thymidine incorporation in HL-60/neo and HL-60/Bcl-2 cells.	177
29. [³ H]-thymidine incorporation in HL-60/neo and HL-60/Bcl-2 cells after Ara-C treatment.	178
30. Alkaline Elution profiles for HL-60/neo and HL-60/Bcl-2 cells after Ara-C treatment.	180
31. Dose-response curves for amplification of <i>c-myc/tPA</i> products by PCR.	184
32. Determination of Ara-C- and UV-induced lesion frequency in the <i>c-myc</i> gene by PCR in genomic DNA templates from HL-60/neo and HL-60/Bcl-2 cells.	185
33. Flow cytometric confirmation of enrichment of HL-60/neo and HL-60/Bcl-2 cells for S-phase cells by centrifugal elutriation.	187
34. Flow cytometric analysis of bromodeoxyuridine incorporation in elutriated HL-60/neo versus HL-60/Bcl-2 cells after Ara-C treatment.	188
35. Preliminary illustration of Bcl-2-mediated blockade of the progression of apoptosis induced by DNA damage.	207
36. Preliminary illustration of possibilities for Bcl-2-mediated interference with known signalling events induced by Ara-C.	208
37. Hyperinduction of <i>c-jun</i> mRNA in HIDAC-treated HL-60/Bcl-2 cells as compared with HL-60/neo cells, and increased <i>c-myc</i> mRNA expression in HL-60/Bcl-2 cells.	209
38. Western blot analysis for Bcl-2-mediated inhibition of cleavage of pro-CPP32 β /Yama protease and degradation of its target PARP in the progression of Ara-C-induced apoptosis.	210
39. Proposed model for Bcl-2-mediated blockade of protease cascade(s) preceding the onset of apoptosis.	211
40. Proposed model for Bcl-2 function in blocking Ara-C-induced apoptosis in HL-60 cells.	212

<u>B. List of Tables</u>	<u>Page</u>
I. Characteristics of cell necrosis versus apoptosis.	6
II. Bcl-2 and related gene products.	35
III. Flow cytometric determination of p26Bcl-2 levels in apoptotic and non-apoptotic HL-60/neo versus HL-60/Bcl-2 cells following Ara-C treatment.	99
IV. Morphologic evidence of Ara-C-induced apoptosis and inhibition of viability in HL-60/neo versus HL-60/Bcl-2 cells.	100
V. Intracellular metabolism of Ara-C in HL-60/neo and HL-60/Bcl-2 cells.	101
VI. Alkaline Elution data from Ara-C treated or irradiated HL-60/neo and HL-60/Bcl-2 cells.	103
VII. Slopes of alkaline elution profiles of DNA from Ara-C-treated or irradiated HL-60/neo and HL-60/Bcl-2 cells.	104
VIII. Flow cytometric determination of apoptosis in HL-60/neo versus HL-60/Bcl-2 cells over time after Ara-C treatment.	137
IX. Assessment of cell viability by MTT assay and trypan blue dye exclusion in HL-60/neo cells versus HL-60/Bcl-2 clones over time after Ara-C treatment.	140
X. Calculations of p26Bcl-2:p21Bax ratios in HL-60/neo cells versus HL-60/Bcl-2 clones over time after Ara-C treatment as assessed by scanning densitometry of Western blots.	142
XI. Immunofluorescent analyses of Bcl-2 levels in HL-60/neo cells versus HL-60/Bcl-2 clones over time after Ara-C treatment.	144
XII. Flow cytometric determination of Bcl-2 levels in HL-60/neo versus HL-60/Bcl-2 clones over time after Ara-C treatment.	145
XIII. Induction of <i>bcl-2</i> mRNA assessed by RNase Protection Assay in HL-60/neo and HL-60/Bcl-2 cells after Ara-C treatment.	148
XIV. Flow cytometric determination of Bcl-2 levels in HL-60/neo cells versus HL-60/Bcl-2 clones after Ara-C treatment: Effect of concomitant actinomycin D/ cycloheximide treatment.	149
XV. Assessment of cell viability by MTT assay of HL-60/neo cells surviving after first and second treatments with Ara-C.	151
XVI. Flow cytometric determination of apoptosis in HL-60/neo cells surviving after first and second treatments with Ara-C.	152
XVII. [³ H]-thymidine incorporation in HL-60/neo versus HL-60/Bcl-2 cells after Ara-C treatment.	179
XVIII. Alkaline Elution profiles for HL-60/neo and HL-60/Bcl-2 cells after Ara-C treatment.	181
XIX. Alkaline Elution slopes for HL-60/neo and HL-60/Bcl-2 cells after Ara-C treatment.	182
XX. Lysis of apoptotic cells during alkaline elution of Ara-C-treated HL-60/neo and HL-60/Bcl-2 cells.	183
XXI. Determination of <i>c-myc</i> lesion frequency by PCR in HL-60/neo and HL-60/Bcl-2 genomic DNA templates after Ara-C treatment (or UV irradiation).	186
XXII. Flow cytometric analysis of bromodeoxyuridine incorporation in elutriated HL-60/neo versus HL-60/Bcl-2 cells after Ara-C treatment.	189

GLOSSARY OF TERMS AND ABBREVIATIONS USED:

AML: acute myeloid/ myelogenous leukemia

Ara-CDP: arabinoside cytosine diphosphate (a metabolite of Ara-C)

Ara-CMP: arabinoside cytosine monophosphate (a metabolite of Ara-C)

Ara-CTP: arabinoside cytosine triphosphate (lethal metabolite of Ara-C)

Ara-UMP: arabinoside uridine monophosphate (breakdown metabolite of Ara-C)

ATP: adenosine triphosphate

blast(s): immature blood cell(s) of the bone marrow which can exhibit deregulated proliferation of malignant.

blast crisis: severe accelerated (acute) phase of CML in which the proportion of blasts in the blood and bone marrow may exceed 50 to 90 percent of the cells (Williams' Hematology, 5th edition, 1996).

bp: base-pair size of nucleotide sequences

BrdU: bromodeoxyuridine

BSA: bovine serum albumin

BSO: buthionine sulfoxamine

CAT: chloramphenicol acetyltransferase, a gene used in recombinant DNA techniques as a reporter for gene promoter activity

CD: "cluster designation", indicating specific surface antigens on blood and bone marrow cells, usually given a numerical assignment

CFU-GEMM: hematopoietic colony-forming unit which has the potential to form granulocytic, erythroid, monocytic, and megakaryocytic populations (See Figure 6)

CML: chronic myeloid/ myelogenous leukemia

CPT: camptothecin

DAG: diacylglyceride

EDTA: ethylene diamine tetraacetic acid

ELISA: enzyme-linked immunosorbent assay

ER: endoplasmic reticulum

(Fab')₂: pair of antigen binding-sites in immunoglobulin light chains

Fc: easily crystallizable fragment of immunoglobulin heavy chains, which contains the antigenic markers for the heavy chain

FIGE: field-inversion gel electrophoresis

FITC: fluorescein isothiocyanate

5-FU: 5- fluorodeoxyuridine

G-CSF: granulocyte colony stimulating factor

GF: growth factor

GM-CSF: granulocyte-macrophage colony-stimulating factor

HCl: hydrochloride

HeLa: human epithelioid cervical carcinoma cell line

HIDAC: high-dose Ara-C = 100 μ M 1- β -D-arabinofuranosylcytosine treatment for 4 hours, which corresponds to clinically achievable doses and effective peak plasma concentrations of Ara-C for leukemia patients.

HPLC: high performance liquid chromatography

ICE: Interleukin-1 β -converting enzyme

IL: Interleukin family of cytokines, given numerical designations

JNK: Jun N-terminal kinase, related to MAPK

K562: human CML blast crisis cell line

kB: kilobase size of nucleotide sequences

KB: human oral epidermoid carcinoma cell line

kDa: kilodalton size/ molecular weight of protein

KG-1: human acute myeloid leukemia cell line

LTR: long terminal repeat sequence(s) of retroviruses which drive transcription of proviruses upon integration into host genome

lymphoid: term relating to those hematopoietic precursor cells whose final maturation takes place within lymph nodes and tissue prior to circulation in the peripheral blood. Includes precursors of, as well as, mature T- and B- lymphocytes. (See Figure 6.)

MAP(K): mitogen-activated protein kinases

M-CSF: macrophage colony-stimulating factor

mdr: multidrug resistance

ML-1: human myeloid leukemia cell line

MTT: 3-(3,5-dimethylthiazol-2-yl)-2,5-diphenyltetrazolium bromide, a colored salt used to detect viable mitochondrial enzymes in cells treated with cytotoxic drugs.

myeloid: term relating to those hematopoietic precursor cells whose final maturation takes place within bone marrow prior to circulation in the peripheral blood. Includes precursors of, as well as, mature granulocytes, monocytes, erythrocytes, megakaryocytes, and platelets. (See Figure 6.)

ND: "not determined" at present

neo: neomycin resistance gene

NPC: nuclear pore complex

NTP: nucleotide triphosphate

OVCAR-3: human ovarian carcinoma cell line

PCD: programmed cell death

PI: propidium iodide

PKC: protein kinase C

pol: (DNA) polymerase

pSFFV: useful recombinant plasmid containing components of the spleen focus-forming virus

rads: ionizing radiation unit corresponding to the absorption of energy of 100 ergs/g

RSV: Rous sarcoma virus

RT-PCR: reverse-transcription polymerase chain reaction

Σ : "sigma" = sum in statistical formulas

SAPK: stress-activated kinase, related to MAPK

SCID: severe combined immune deficiency

SEM: standard error of mean

TdR: thymidine

TPO: thrombopoietin, a stimulator of platelet formation

V: volts

SYMBOLS FOR AMINO ACIDS:

A = Alanine (Ala)

B = Asparagine/ Asparatic acid (Asx)

C = Cysteine (Cys)

D = Aspartic acid (Asp)

E = Glutamic acid (Glu)

F = Phenylalaine (Phe)

G = Glycine (Gly)

H = Histidine (His)

I = Isoleucine (Ile)

K = Lysine (Lys)

L = Leucine (Leu)

M = Methionine (Met)

N = Asparagine (Asn)

P = Proline (Pro)

Q = Glutamine (Gln)

R = Arginine (Arg)

S = Serine (Ser)

T = Threonine (Thr)

V = Valine (Val)

W = Tryptophan (Trp)

Y = Tyrosine (Tyr)

Z = Glutamine/ Glutamic acid (Glx)

(from Stryer L, *Biochemistry*, third edition. New York: WH Freeman, 1988)

CHAPTER I.

General Introduction.

CHAPTER I: INTRODUCTION:

A. Apoptosis.

The balance between cell proliferation and cell death is of critical importance in the biologic homeostasis of normal and cancerous tissues. The regulation of cell death is as complex as the regulation of cell proliferation. Apoptosis, or programmed cell death, is a distinctly active gene-directed form of physiological cell death which differs fundamentally and biochemically from the other form of cell death such as classically defined pathological process of cell necrosis (reviewed in 1).

1. Distinction from necrosis.

Cell necrosis has been described as an “accidental” cell death (2) which occurs in response to a wide variety of noxious stimuli, injury including hyperthermia, hypoxia, ischemia, complement attack, metabolic poisons, direct cell trauma, and exposure to toxins and highly toxic levels of drugs (reviewed in 2,3). A cell undergoing necrosis exhibits characteristic morphologic and biochemical changes which have been extensively described. Early abnormalities include gross swelling of the cytoplasm and organelles such as the endoplasmic reticulum and mitochondrial matrix (2-4). Nuclear chromatin initially condenses, becoming slightly pyknotic (3). However, as cell necrosis progresses, the nuclear, organelle, and plasma membranes rupture, causing cell contents to leak out into the extracellular space (2), and margined nuclear chromatin masses are eventually dispersed, leaving a nuclear “ghost” when stained (**karyolysis**) (3). Early loss in membrane integrity and ion-pumping capabilities may be responsible for the tremendous cellular swelling (2, 3), and further disruptions of membranes are caused by the resulting extreme Ca^{2+} and other ion imbalances (3, 5). During the late stages of necrosis, ruptured lysosomes release hydrolytic enzymes which cause rapid cellular disintegration (2, 3), as well as digestion of DNA into diffuse fragments of various sizes (6). Fluctuations in DNA, RNA, and protein levels rapidly occur (2, 4). Cell necrosis usually occurs in tracts of contiguous cells, and typically elicits an exudative inflammatory reaction in adjoining tissue (3). The released cellular debris is then ingested and degraded by phagocytosis (3).

2. Definition of programmed cell death, apoptosis and its characteristics.

In contrast, apoptosis is described as a morphologically distinct “spontaneous” form of cell death that occurs in many different tissues exposed to various conditions. Named from the ancient Greek word *αποπτωση*, describing the “falling off” as petals from flowers or leaves from trees, apoptosis characteristically occurs in scattered single cells (2, 3), and is a corollary of the concept of programmed cell death (7). Programmed cell death is defined as a functional state in development (7), or an internal suicide program which plays a crucial role in widespread physiological processes including embryogenesis, normal adult tissue turnover, organ atrophy, and the immune response (7). The type of cell death utilized in these important natural circumstances is virtually that of apoptosis. Apoptosis, however, can also be induced by external non-physiologic stimuli.

Table I summarizes the morphologic and biochemical differences between apoptosis and more disorganized cell necrosis. The early stages of apoptosis consist of cell shrinkage, chromatin condensation, nuclear disintegration, cell surface blebbing, and the appearance of membrane-bound apoptotic bodies (3, 8). The dilated endoplasmic reticulum forms vesicles which fuse with the plasma membrane, causing the cell’s outline to become deeply convoluted (2). Cell shrinkage is associated with the resulting loss of intracellular fluid and ions. Other detectable biochemical changes occurring in cells undergoing apoptosis include a rapid and sustained increase in intracellular Ca^{2+} levels (2). This increase has been measured in thymocytes induced to undergo apoptosis by the addition of glucocorticoids or Ca^{2+} ionophores (9), and has recently been attributed to gradual loss of Ca^{2+} from the endoplasmic reticulum and rise in Ca^{2+} amounts in the mitochondria associated with the onset of apoptosis in growth-factor dependent cells deprived of lymphokine (10). Most recently, another biochemical change associated with the induction of apoptosis in Interleukin (IL)-2-dependent cytotoxic T-lymphocytes is intracellular acidification as a result of a modulated set-point in an intact Na^+/H^+ -antiporter (11). Plasma membrane integrity persists, however, and the cell breaks up into several membrane-bound apoptotic bodies which enclose nuclear fragments and/or structurally intact cytoplasmic organelles (2, 3). These apoptotic bodies protrude from the cell and are typically phagocytosed by nearby cells such as macrophages in the absence of an exudative inflammatory reaction. It has been recently described that the stimulus for this

phagocytic process is the increased expression of vitronectin on the surface of the apoptotic bodies and its recognition by macrophages via the vitronectin receptor, CD36 (12).

In contrast to cell necrosis, the process of cellular fragmentation in apoptosis occurs extremely rapidly, within several minutes to hours after exposure to an apoptotic stimulus (2) and culminates in a distinct order of events. Once the apoptotic pathway is engaged, a significant manifestation of apoptosis first described by Wyllie (13) is the fragmentation of genomic DNA into integer multiples of nucleosome-sized (approximately 180-200 base pairs) units. In the early literature, this was reportedly accomplished by the activation of a putative non-lysosomal $\text{Ca}^{2+}/\text{Mg}^{2+}$ -dependent endonuclease which cleaves at the linker DNA between DNA-histone octamers (13). The generation of this specific “ladder” of internucleosomal DNA fragmentation has been historically described as the biochemical hallmark of apoptosis, and is easily appreciated by standard agarose gel electrophoresis of DNA. The putative endonuclease(s) responsible for this fragmentation, however, have not yet been unequivocally isolated, due to its attributed scarcity and lability (14). Recently, Peitsch *et al.* characterized this endonuclease extracted from isolated rat thymocyte nuclei as identical, functionally and immunohistochemically, to deoxyribonuclease I (DNase I) (14). However, Brown *et al.* first reported the additional cleavage of DNA in apoptotic thymocytes into high molecular weight fragments ranging from 50 to 300-kb in size; this type of fragmentation, resolved by pulsed-field and field-inversion gel electrophoresis techniques, and suggests that another key enzyme or endonuclease may also play a role in the induction of apoptosis (15-17). It is presently not yet clear whether high molecular weight fragmentation precedes induction of low molecular weight fragmentation in the progression of apoptosis, whether high molecular weight fragmentation is required in all situations, or which endonuclease(s) are universally responsible for either of these types of irreversible DNA fragmentation.

3. Occurrence and mediators of apoptosis.

Programmed cell death has been observed in diverse organisms from nematodes such *Caenorhabditis elegans* (18) to humans. In humans, apoptosis has been documented to be induced in embryonal development during mesonephric regression and interdigital web loss; in hormonal regulation in the endometrium, breast, and prostate; in the regulation of inflammation; in the regulation of immunity in the selection of mature immune cells, T cell effector mechanisms; in AIDS as the mechanism by which the human immunodeficiency virus (HIV)

depletes CD4⁺ cells; and in neoplasia in the regulation of tumor growth rate (reviewed in 19). Apoptosis is induced by growth-factor withdrawal in factor-dependent cells, as well as by loss of matrix attachment (20). Despite engagement of apoptosis as the mode of cell death in normal physiologic processes, this internal cell suicide program can be induced when cells become damaged (2, 19). Of note, clinically achievable doses of several anticancer drugs have been shown to induce apoptosis in target cells (21). In myeloid leukemia cells, Ara-C (to be described later) has been shown to induce internucleosomal DNA fragmentation and apoptosis (22, 23), as do taxol (24) and mitoxantrone (25), to name a few. How these chemotherapeutic agents may stimulate this cell death program is the focus of intense investigations of the physiologic mechanisms of apoptosis in normal and neoplastic cells.

TABLE I: CHARACTERISTICS OF CELL NECROSIS VERSUS APOPTOSIS: (refs 3, 7, 8)

<u>Characteristic:</u>	<u>CELL NECROSIS:</u>	<u>APOPTOSIS:</u>
Biochemical features	<ul style="list-style-type: none"> • Evoked by nonphysiological disturbances • Loss of regulation of ion homeostasis • No requirement for energy or macromolecular synthesis 	<ul style="list-style-type: none"> • Induced by physiological stimuli and mild injury • Tightly regulated process with activation step • Possible requirement for energy and/or macromolecular synthesis
Nuclear biochemical features	<ul style="list-style-type: none"> • Random diffuse degradation of DNA 	<ul style="list-style-type: none"> • Nonrandom high molecular weight DNA fragmentation (5-300 kB size) • Nonrandom internucleosomal fragmentation of DNA into 180-200-bp units
Membrane integrity	<ul style="list-style-type: none"> • Early loss of membrane integrity, early inclusion of dyes 	<ul style="list-style-type: none"> • Membrane blebbing, but no loss of integrity; early exclusion of dyes
Morphologic features	<ul style="list-style-type: none"> • Death of cell groups • Cytoplasmic and organelle swelling • Clumpy, ill-defined aggregation of chromatin, pyknosis • Lysosome leakage 	<ul style="list-style-type: none"> • Deletion of single cells • Cell shrinkage; formation of apoptotic bodies • Condensation of chromatin into dense masses • Lysosomes intact
Pathologic response	<ul style="list-style-type: none"> • Significant inflammatory • Phagocytosis by macrophages 	<ul style="list-style-type: none"> • No inflammatory response • Phagocytosis by adjacent normal cells and some macrophages

4. Genes which regulate apoptosis.

Several genes have been implicated in the regulation of apoptosis. Much of the current knowledge about specific cell death genes has been derived from genetic studies in the nematode *C. elegans* (18). Fourteen different genes have been isolated, in which mutations have been demonstrated to affect specific stages of programmed cell death in this organism (26). Three genes, *ced* (cell death defective)-3, *ced-4*, and *ced-9*, have been shown to affect the execution of the cell death program; *ced-3* and *ced-4* function to promote cell death, while *ced-9* functions to prevent cell death (26). The *ced-3* gene encodes a protein that is similar to the family of cysteine proteases in mammalian cells which convert some pro-enzymes to their active forms (26, 27), and includes interleukin-1 β -converting enzyme (ICE) (27, 28) and *nedd-2/Ich-1* (29). Overexpression of *ced-3*, ICE, or *Nedd-2/Ich-1* in mammalian cells causes apoptosis (30, 31). ICE specifically cleaves proteins at Asp-X bonds (X is any amino acid), similar to granzyme B, a serine protease responsible for apoptosis induced by cytotoxic T lymphocytes in target cells (27, 32), and suggests that, in some instances, proteolytic processing of inactive proteins to their active states may be required for the induction of apoptosis. However, it has also been shown by Kuida *et al.* that ICE-deficient (-/-) mice are not necessarily protected from apoptosis. Thymocytes from ICE (-/-) mice were found to still be sensitive to apoptosis induced by dexamethasone or ionizing radiation (33), suggesting that ICE itself may not be a universal regulator of apoptosis in mammalian cells. Instead, other newly discovered members of the ICE family may be involved in the apoptotic pathway engaged in lymphocytes as well as other bone marrow cells. These include ICE homolog CPP32/Yama and members of a putative irreversible protease cascade culminating in the activation of DNA fragmentation, as demonstrated in the most recent literature exploring the effectors of apoptosis (34). These possibilities will be discussed in greater detail in **Chapter Six** of this dissertation.

Other genes which promote apoptosis have also been identified in the immune system. The *Apo-1/Fas* gene encodes the Fas ligand (FasL), a cell surface molecule which is a member of the tumor necrosis factor family. When FasL, expressed predominantly in activated T cell, binds to its receptor Fas, it is capable of inducing apoptosis in various Fas-bearing target cells (35). The Fas-FasL system is involved in cytotoxic T lymphocyte (CTL)-mediated immunity, as well as down-regulation of immune responses (35). The cytoplasmic domain of FasL consists of 70 amino acids which are highly conserved with the TNF receptor R1, and are necessary and

sufficient for the transduction of the apoptotic signal (35, 36). The apoptotic pathway(s) induced by the Fas/FasL system remains to be elucidated. It is known that cell death induced by Fas does not require the presence of a nucleus, or DNA fragmentation (34); this process does not require macromolecular synthesis (37) and is independent of extracellular Ca^{2+} (38). And although Fas and TNF-R1 share conserved regions with each other, as well as with newly identified death effectors TRADD (39), FADD (40), and RIP (41, 42), there is evidence that Fas-induced death is not blocked by many inhibitors of TNF-R1-transduced apoptosis (35). Therefore Fas-mediated apoptosis is an intriguing system still under investigation.

Many important oncogenes are also reported to regulate apoptosis. The proto-oncogene *c-myc* encodes for a protein which contains many domains similar to known transcription factors (43). *c-myc* has been implicated in the control of proliferation of many cells, including normal and leukemic bone marrow progenitor cells (43). Expression of *c-myc* has been shown to decrease as cells terminally differentiate (44, 45). However, overexpression of *c-myc* in serum-starved fibroblasts has been shown to induced apoptosis in these growth limiting conditions (43), as well as in other specific settings which include growth-factor deprivation (46, 47). These data indicate that *c-myc* has a proliferative function as well as an apoptotic function, the balance of which is significant in cancer biology.

The tumor suppressor gene *p53* encodes a nuclear phosphoprotein, which in its wild-type form (wt-p53) can inhibit cell cycle progression (48, 49). wt-p53 is a sequence-specific transcription factor which functions at the G_1 checkpoint control of the cell cycle to inhibit progression of cells into S phase (48). wt-p53 is induced by a post-transcriptional mechanism after DNA damage by a wide variety of agents including ionizing radiation (48). wt-p53 can suppress growth of cells which have incurred DNA damage through the action of several transcriptionally-activated p53-responsive genes. These include *GADD45* (growth-arrest and DNA damage) (50), and *p21* (*WAF1/CIP1*, wild-type p53-activated fragment/cdk-interacting protein 1) (51). This gives cells the opportunity to repair damaged DNA templates before the resumption of proper DNA replication (48, 52). p53 also induces the *mdm2* gene, whose product conversely blocks p53 function in a feed-back loop which may govern the length of G_1 arrest in response to DNA damage (48, 53). For cells already in S-phase, however, the components of this global checkpoint may not be as necessary to induce S-phase arrest (54). Fibroblasts with

stable expression of mutant p53 do not show induction of p21^{WAF1/CIP1}, but still show reduction in rate of DNA synthesis in cells already in S in response to bleomycin or ionizing radiation (54). In addition, S phase arrest induced by cytosine arabinoside (Ara-C) in ML-1 myeloblastic leukemia cells is also not associated with changes in p53 protein levels themselves (55). p53 is frequently mutated in many human tumors (48, 56). wt-p53 also has the ability to induce apoptotic cell death, while mutant p53 fails to enhance apoptosis (57). Yonisch-Rouach *et al.* have demonstrated that when p53-defective hematopoietic cells were transfected with a temperature-sensitive p53 mutant (Val 135), that mutated p53 protects against apoptosis, but when p53 reverts to the wild-type conformation at the permissive temperature of 32°C, apoptosis is readily induced (48, 58). However, this wt-p53 apoptotic activity was not associated with G₁ arrest (59), and therefore represents two potentially separate pathways for p53 function in response to various stimuli. wt-p53-mediated apoptosis appears not to be required in normal development since p53-null mice develop normally (48). Instead, wt-p53-induced apoptosis may be utilized to delete cells which have sustained overwhelming DNA damage yet still retain the capacity for further proliferation (48), and has an important impact on drug-induced apoptosis (60, 61). wt-p53-mediated apoptosis has been shown to be mediated through the induction of the p53-responsive pro-apoptotic *bax* gene (62-64), to be described later.

Other oncogenes have been shown to inhibit apoptosis. The t(9;22) chromosomal translocation in chronic myelogenous leukemia (CML) yields a fusion gene consisting of the *bcr* (break-point cluster region) gene from chromosome 22 and the *c-abl* tyrosine kinase proto-oncogene from chromosome 9 (65). The resulting **bcr-abl** fusion protein possesses increased tyrosine kinase activity compared to the normal *c-abl* protein product, and is considered to be responsible for the pathogenesis of CML (66). Evans *et al.* have demonstrated that transfection of the *v-abl* oncogene suppresses apoptosis upon growth-factor withdrawal in an interleukin-3-dependent hematopoietic cell line (67). Recently, it has been shown that when antisense oligonucleotides down-regulate *bcr-abl* expression in hematopoietic cells, they become more sensitive to the induction of apoptosis by growth factor or serum withdrawal (68), as well as various chemotherapeutic agents (69), indicating that p210bcr-abl has the ability to inhibit apoptosis to a certain extent.

This inhibition of apoptosis by specific regulators is crucial to the understanding of normal and cancer cell biology. Inhibition of apoptosis by gene products is also seen in the nematode *C. elegans* by the *ced-9* gene product, which protects cells that should survive after programmed cell death takes place in the development of the nematode (26). It is not known exactly how the *ced-9* gene product inhibits PCD in nematodes. However, this gene encodes a protein that is homologous to the *bcl-2* gene product, one of the most significant regulators of cell death to be discovered in human cells to date.

B. Bcl-2.

The *bcl-2* (B-cell lymphoma/leukemia-2) gene was first discovered by virtue of its involvement in B-cell malignancies whereby t(14;18) chromosomal translocations in the majority of follicular non-Hodgkin's B-cell lymphomas juxtapose the normal *bcl-2* gene from chromosome 18 (at 18q21) with immunoglobulin heavy-chain (IgH) enhancer elements at 14q32 (70, 71). This results in deregulation of the normal *bcl-2* gene and overproduction of *bcl-2* mRNAs and protein products (70), and illustrates an explanation for malignant potential in these instances. The *bcl-2* gene encodes an integral membrane protein which has been localized to the nuclear envelope, the endoplasmic reticulum, and the outer mitochondrial membrane (72). Because of an alternative splicing mechanism and the utilization of alternative promoters, the *bcl-2* gene can potentially encode 26kD (p26Bcl-2 α) and 22kD (p22Bcl-2 β) proteins (73, 74).

1. The *bcl-2* gene structure.

The human *bcl-2* gene displays a complex gene structure and strategy for expression (for summary, please see illustration in **Figure 1**). The normal *bcl-2* gene has a 3-exon structure on chromosome 18 (74). As described by Seto *et al.*, the first exon has been found to be untranslated, similar to the organization of the *c-myc* oncogene, homeotic genes of *Drosophila*, and the insulin gene (74), and contains stop codons in all its open reading frames. There exist a facultative 220 bp intron I which is variably spliced and a 370-kb intron II. Initiation sites in exon II include TATA plus CAAT boxes, associated with classic promoter elements, and a decanucleotide ATGCAAAGCA homologous with immunoglobulin (Ig) variable region enhancers. In addition, multiple initiation sites are also found in a GC-rich region in exon I, very similar to that of other B-cell lineage active oncogenes *c-abl* and *c-myb*. However, the major

sites of transcription initiation have been demonstrated to be further upstream of exon I at -1457 to -1386 base pairs from the open reading frame (designated P1, for major promoter, with the former designated P2, for minor promoter), and contain multiple sites for the binding of Sp1 polymerase, a general eukaryotic transcription initiation factor (74). More recently, two smaller promoter regions have been discovered even farther upstream of the major promoter (P1) (at -1552 to -1534, and -1611 to -1552 base pairs upstream of the open reading frame, respectively), and were found to be responsive to binding by phosphorylated CREB proteins during B cell activation (75). As analyzed by Tsujimoto and Croce, the use of these alternate promoters result in the transcription of several overlapping mRNAs comprised of exons II/III or I/II/III. To date, the 5.5-kb and 3.5-kb mRNA transcripts are the most important, produced by transcription from the major promoter and splicing within the first exon and joining to the second exon. The 5.5-kb and 3.5-kb transcripts carry two overlapping reading frames, and the open reading frame is not interrupted by chromosomal translocation, since the breakpoints are located farther downstream at sites which bind helicase, Ku antigen, and ssDNA binding proteins (76). The 5.5-kb mRNA spans the 717 nucleotides, that codes for the 239-amino acid **Bcl-2 α** protein with molecular mass of 26 kD; the 3.5-kb mRNA is identical except at the carboxy-terminus, and codes for the 205-amino acid **Bcl-2 β** protein with molecular mass of 22 kD. Only the 26 kD Bcl-2 α protein possesses a 3' hydrophobic region typical of a membrane-spanning segment. In structure-function studies, this segment has been shown to be partially responsible for the ability of Bcl-2 α to block apoptosis (77). Bcl-2 β , however, has much less activity in blocking apoptosis (77). While the function of alternate splicing has significance in neurons and in immunoglobulin genes to generate diversity (78), this mechanism is unknown as to its significance in the *bcl-2* gene. The presence of dramatically different promoters and alternatively utilized exons suggests a role in lineage or stage-specific expression of the *bcl-2* gene (77).

Figure 1:

Schematic illustration of the *bcl-2* α transcript which encodes p26Bcl-2 α .

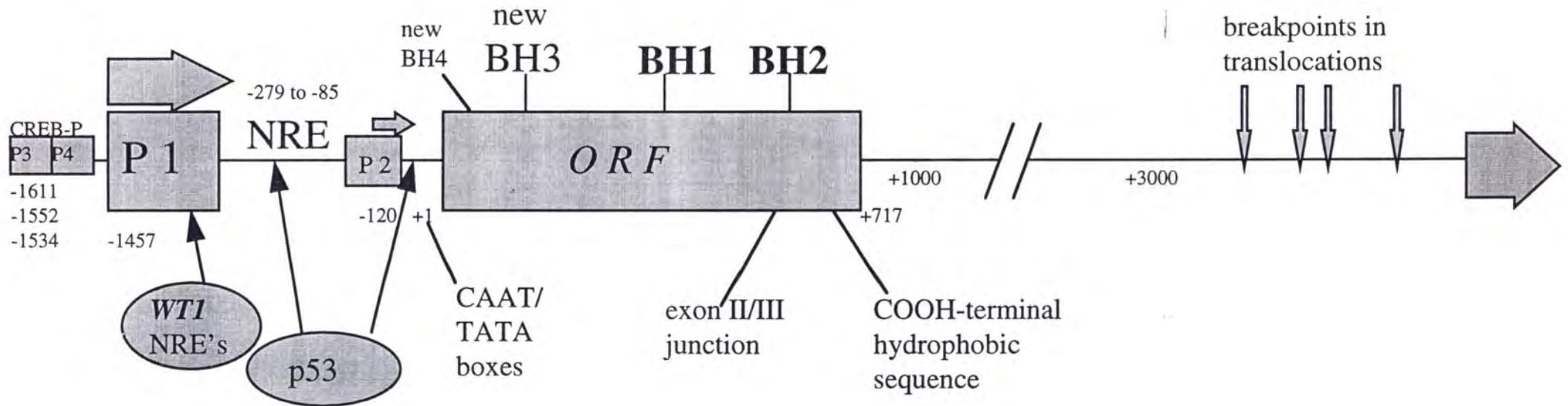
(Bullock, circa. December 1995, after refs 74-82)

Transcription of the *bcl-2* gene is usually initiated at the major promoter **P1**. Other promoters have been described to reside upstream of **P1** as well. Negative regulation of *bcl-2* transcription has been documented to be imposed by **WT1** at the **P1** region, by wild-type **p53** at sequences downstream of both the major promoter and the minor promoter **P2**, and another negative regulatory region has been described here as well. The open reading frame is 717 nucleotides in size and consists of the junction of exons II and III. The *bcl-2* α open reading frame (ORF) includes conserved sequences of the Bcl-2 homology domains **BH1**, **BH2**, and newly described **BH3**, and ends with a carboxy-terminal hydrophobic sequence which targets p26Bcl-2 α to its residence in the subcellular membranes described in the text. Chromosomal translocations in lymphomas include the normal *bcl-2* gene since the breakpoints lie further downstream of the open reading frame.

Figure 1.

bcl-2 α TRANSCRIPT:

(Bullock, circa. April 1996.)



2. Regulation of *bcl-2* gene expression: Indications for transcriptional or post-transcriptional/translational modifications.

Recently a negative regulatory element was identified in the *bcl-2* gene downstream of the major promoter at the -279 to -85 base-pair region (79, 80); this negative regulatory element was later found to be responsive to wt-p53, which reduces CAT (chloramphenicol acetyltransferase) expression and CAT activity from reporter gene constructs in co-transfection experiments (80). In addition, the Wilms' tumor gene *WT1* has been found to repress transcription of the *bcl-2* major promoter P1, with five potential WT1 binding motifs overlapping the Sp1-binding sites in the promoter region (81). Therefore, the loss of either of these tumor suppressor genes in malignant tissues may result in the deregulation of *bcl-2* expression by loss of transcriptional control. A shorter sequence within the negative regulatory element (-119 to -84), described as an upstream open reading frame (uORF) was additionally found to repress Bcl-2 expression at the translational level as well, since deletions of this uORF from CAT reporter gene constructs containing the *bcl-2* promoter increased CAT activity in various cell lines but not CAT mRNA levels (82). Possible mediators of translational control of Bcl-2 are under investigation.

Binding sites for several transcription factors are found in the *bcl-2 α* sequence by computer analysis. Transcription factor sites located upstream of *bcl-2 α* open reading frame includes sites for hsp70.2, Sp1, Ets-1, and Egr-1. Of further interest, a binding site for the Jun/AP-1 transcription factor (5'-TGA[G/C]TCA-3') lies downstream of the open reading frame of the *bcl-2 α* transcript at +1305, and two additional homologous sites lie further downstream (Bullock, observations).

Analyses of the *bcl-2* gene sequence fail to detect any sequence motifs such as known protein kinase sites (Bullock, observations). However, the Bcl-2 protein can be post-translationally modified, presumably through various protein kinases. May *et al.* have associated hyperphosphorylation of Bcl-2 α with suppression of apoptosis by hematopoietic growth factors (83, 84). Following protein kinase C activation in murine myeloid factor-dependent FDC-P1/ER cells by interleukin-3, erythropoietin, and the natural macrocyclic lactone product bryostatin-1, which stimulates protein kinase C (PKC), phosphorylation of Bcl-2 α occurs on a serine site in association with the inhibition of apoptosis by addition of these growth factors to cell culture

(84), despite the maintenance of Bcl-2 levels by these treatments. Haldar also reports phosphorylation of Bcl-2 on serine by okadaic acid (OKA) and by taxol in lymphoid cells (85). However, in contrast to May's findings, phosphorylated Bcl-2 in these conditions was rendered unable to suppress apoptosis itself or to prevent lipid peroxidation associated with OKA- or taxol-induced apoptosis. In addition, Haldar *et al.* have also found that taxol induces Bcl-2 phosphorylation and, subsequently, apoptosis in PC3 prostate carcinoma cells (86). Chen and Faller recently demonstrated that the phosphorylation state of Bcl-2 is modulated by inhibition of PKC as well as activated p21^{Ha-ras} in Jurkat cells. However, in this state and in this setting, Bcl-2 was found to be able to block Ras-specific cell death (87, 88). Further clarification of the significance of Bcl-2 phosphorylation status for the regulation of drug-induced apoptosis, or its relationship to specific pathways induced by different apoptotic stimuli, is therefore essential.

3. The *bcl-2* gene product blocks a final common pathway for apoptosis.

Vaux *et al.* first showed that overexpression of *bcl-2* prolongs survival of IL-3-dependent pre-B cells in vitro upon cytokine deprivation (89). This was then confirmed by Nunez *et al.* when deregulated *bcl-2* expression was demonstrated to extend short-term survival of IL-3-dependent FL5.12 pro-B lymphocytes, as well as IL-3-dependent 32D mast cells and FDC-P1 promyeloid cells upon growth factor withdrawal. In addition, Borzillo *et al.* demonstrated that Bcl-2 protects an IL-7-dependent pre-B-cell line against apoptosis associated with growth factor withdrawal (90). In these cases, Bcl-2 prevented cell death but did not affect cell-cycle progression (91). Microinjected *bcl-2* has also been demonstrated to selectively rescue neurotrophic factor-dependent embryonic neurons from apoptosis upon withdrawal of NGF, brain-derived neurotrophic factor, and neurotrophin-3 (92). Furthermore, Bcl-2 suppresses apoptosis yet still allows differentiation and development of a multipotent IL-3-dependent cell line in the absence of growth factors (93). In addition, Bcl-2 inhibits apoptosis associated with terminal differentiation of HL-60 myeloid leukemia cells (94). Also, Bcl-2 levels are regulated when neuroblastoma cells are induced to differentiate (95), with a relationship established between the level of Bcl-2 and the amount of differentiation of several types of neuroblastoma clones. These data are significant since once terminally differentiated from a multipotent state, hematopoietic cells proceed to die by apoptosis after the duration of their life span, and one

interesting question in the literature is whether the differentiation and apoptotic pathways overlap.

Significant studies demonstrate that Bcl-2 blocks glucocorticoid-induced apoptosis in human pre-B-leukemias (96), and apoptosis induced by multiple chemotherapeutic drugs including methotrexate, Ara-C and vincristine in murine lymphoid lines (97) and in pre-B leukemias (98). Transfection with a *bcl-2* expression vector protects transplanted murine bone marrow from adriamycin- and etoposide-induced myelosuppression (99). These studies examine low molecular weight internucleosomal DNA fragmentation associated with apoptosis and its inhibition by enforced *bcl-2* expression. In addition, Bcl-2 inhibits cisplatin- and etoposide-induced apoptosis in neuroblastoma, and also decreases the incidence of large molecular weight DNA fragmentation (5-300 kb) seen by pulsed-field gel electrophoresis also associated with apoptosis (100).

An important question to address, then, becomes which step in the progression of drug-induced apoptosis is it that Bcl-2 specifically blocks. Recent studies have examined proximal events in drug-induced apoptosis. Bcl-2 blocks nitrogen mustard- and camptothecin (CPT)-induced apoptosis, but still allows early events to occur at comparable intensity (101), including CPT-induced DNA single-strand break formation and resealing, as well as cell cycle perturbations. Resistance to thymidylate stress by Bcl-2 overexpression was demonstrated to be independent of previously established resistance pathways, such as cell cycle inhibition, and modulation of thymidylate synthase levels and activity, since early targets are still affected by 5-fluorodeoxyuridine (5-FU) treatment in control as well as Bcl-2-overexpressing human lymphoma cells (102). In addition, it was concluded that Bcl-2 protein inhibits etoposide-induced apoptosis through effects on events distal to topoisomerase-II-induced DNA strand breaks and their repair since parental and Bcl-2-overexpressing mouse B-cells showed little or no difference in etoposide-induced DNA damage and repair by alkali unwinding and alkaline elution assays (103). Furthermore, Tang *et al.* showed that Bcl-2 overexpression in 697 pre-B-leukemia cells blocks taxol-induced apoptosis and DNA fragmentation but still allows equivalent microtubular bundling due to taxol as compared to 697-*neo* cells (104).

Bcl-2 has also been documented to block cell death due to positive regulators of apoptosis, further suggesting that Bcl-2 interferes distally with a final common pathway culminating in apoptosis. Bcl-2 inhibits wt-p53-triggered apoptosis in a *v-myc*-induced T-cell lymphoma line (105). Bcl-2 blocks p53-dependent apoptosis by adenovirus E1A and diverts the activity of p53 from induction of apoptosis to induction of growth arrest (106). Apoptotic death induced by *c-myc* is inhibited by *bcl-2* (107), and it has been illustrated that *c-myc* and *bcl-2* proto-oncogenes can interact cooperatively in tumor progression (108). Another example of interacting anti-apoptotic oncogenes was recently shown in IL-3-dependent Ba/F3 and DoHH2 cells. When *bcr-abl* transfection induced *bcl-2* expression in these cells, both were demonstrated to cooperate in the inhibition of apoptotic cell death due to growth-factor withdrawal (109). In addition, *bcl-2* expression in mouse hemopoietic cells lines was demonstrated to cooperate with thermotolerance in promoting cell survival against heat-induced cell death, when heat-shock protein expression was simultaneously induced (110).

Bcl-2, therefore, is a central regulator in the suppression of apoptosis, and these diverse data suggest that Bcl-2 blocks an important final common pathway leading to apoptotic cell death. However, the exact mechanism of action by which Bcl-2 can prevent the progression to apoptosis by a variety of stimuli is still under intense investigation.

4. Speculations on the mechanism of action of Bcl-2.

4a. Motifs in the *bcl-2* sequence.

As mentioned previously, the biochemical action of Bcl-2 is unknown. Comparison of the *bcl-2* cDNA and protein sequences with known sequences in computer databases yield no significant homologies except for moderate homology with DNA binding viruses such as components of Epstein-Barr virus, Dengue virus, Herpes simplex virus, pseudorabies virus, and Varicella-Zoster virus. Early studies reported by Cleary *et al.* showed that Bcl-2 has weak homology with the open reading frame of Epstein-Barr virus (EBV) BHRF-1 component (111). The BHRF-1 protein also has a hydrophobic tail, resides in intracellular membranes, and has been shown, like Bcl-2, to block apoptosis induced in human and murine hematopoietic cells by growth factor deprivation (112, 113). These results suggest that Bcl-2 homologs could contribute to persistent and latent infections in a conducive cellular environment (70).

Furthermore, the EBV genome contains additional genes capable of upregulating the human *bcl-2* gene in B-cells (114, 115). Of additional interest, Neilan *et al.* have discovered that the LMW5-HL protein of the African Swine Fever virus shares homology with Bcl-2 (70, 116), demonstrating another virus which might use this potential mechanism to prevent host cell death while replication is attempted (70).

In addition, computer analysis of the *bcl-2* α sequence reveals various sequences which are homologous to motifs such as iron-sulfur binding region signatures found in ferredoxins, mammalian defensins, epidermal growth factor-like cysteine pattern domains, integrin beta chain cysteine-rich domain signatures, class I metallothioneins signatures, and a thiolase signature (Bullock, observations). Whether these motifs indicate predictions of Bcl-2 mechanism of action relating to these homologous functions remains to be addressed.

4b. Bcl-2 as an antioxidant.

Examination of the subcellular location of Bcl-2 has indeed provided some possible speculations as the function of Bcl-2. Bcl-2 was originally reported to reside in the inner mitochondrial membrane (117). However, as previously mentioned, confocal, laser, scanning, and electron microscopy, as well as subcellular fractionation studies prove that Bcl-2 resides in the **nuclear envelope**, parts of the **endoplasmic reticulum (ER)**, and **outer mitochondrial membrane**, but not in the plasma membrane (70, 72). These subcellular localizations have prompted studies examining the function of Bcl-2 with respect to these locations. For example, the localization of Bcl-2 to the mitochondria prompted studies to link Bcl-2 function to an influence on oxidative phosphorylation. However, Mah *et al.* reported that despite Bcl-2-mediated inhibition of apoptosis in PC12 rat pheochromocytoma cells induced by Ca^{2+} ionophores or serum deprivation, no difference was appreciated between control and Bcl-2 overexpressing cells with respect to rise in intracellular free calcium, oxygen consumption, or adenosine triphosphate (ATP) concentration (70, 118, 119). Suggestion that Bcl-2 may function as an antioxidant first came into the literature by Hockenbery *et al.*, who demonstrated that Bcl-2 can protect IL-3-dependent FL5.12 cells from hydrogen peroxide- and menadione-induced oxidative cell deaths by inhibiting apoptosis due to these agents (120). Bcl-2 overexpression in these cells does not prevent menadione-induced oxidative bursts in these cells but suppresses

lipid peroxidation in association with inhibition of apoptosis (120). In addition, Kane *et al.* found that when GT1-7 neural cells were treated with buthionine sulfoxamine (BSO) and were thus depleted of glutathione (GSH), a tripeptide thiol involved in the protection of cells from oxidative injury, intracellular levels of reactive oxygen species (ROS) and lipid peroxides rose rapidly (121). Most notably, however, this increase in ROS associated with the induction of apoptosis was not seen in identically treated GT1-7 cells previously transfected with *bcl-2*, nor was associated with inhibition of cell death by *bcl-2* (121). Recently, Bcl-2 overexpression in murine lymphoma cells was also shown to increase intracellular antioxidants such as GSH in response to inhibition of radiation-induced apoptosis (122). Furthermore, Kane *et al.* found that Bcl-2 overexpression in *Saccharomyces cerevesiae* mutants deficient in Mn^{2+} -superoxide dismutase (SOD) or Cu^{2+}/Zn^{2+} -SOD partially rescued the organisms when subjected to conditions which required respiratory metabolism (121). It was concluded that Bcl-2 may function to scavenge free radicals, bind metals, or ultimately decrease formation of superoxide by inhibiting transfer of electrons from complexes I-III through dioxygen in the inner mitochondrial membrane (121) or at other sites of superoxide generation, such as electron transport which can also occur to an extent in the ER and nuclear membranes (120).

However, Bcl-2 can also inhibit the induction of apoptosis by hypoxia in PC12 ad 7316A rat hepatoma cells, which does not generate reactive oxygen species (ROS or ROI) (123, 124), and also protects against cell death from anaerobic conditions in lymphoid cells (125). One surprising report has suggested that Bcl-2 may be a pro-oxidant instead of an anti-oxidant since in *E. coli*, Bcl-2 expression actually generates ROI and, in murine B-cells, increases SOD activity, yet still has the capability of inducing endogenous cellular antioxidants such as reduced GSH (126). Taken together, these data suggest that **Bcl-2-mediated inhibition of apoptosis may be downstream of the detection oxidative state of a cell, and in maintaining cell viability, instead indirectly provides cells with the capacity to mount these antioxidant responses.**

4c. Bcl-2 and regulation of Ca^{2+} flux.

Since the mitochondria, and to some extent, the ER, are also major sites for the intracellular storage of calcium, several other studies have examined a possible link between Bcl-2 function

and Ca^{2+} homeostasis. As previously mentioned, Bcl-2 has been shown to inhibit apoptosis induced by Ca^{2+} ionophores in thymocytes (70) as well as in PC12 neural cells (119). Baffy *et al.* reported that factor withdrawal in IL-3-dependent murine 32D hematopoietic cells induced apoptosis and was associated with an intracellular shift in Ca^{2+} levels from the ER to the mitochondria (10). This Ca^{2+} repartitioning associated with apoptosis was prevented by Bcl-2 overexpression in these cells (10), as well as in Bcl-2-overexpressing WEHI7.2 cells treated with the ER Ca^{2+} pump poison thapsigargin (TG) (127). These suggest that by virtue of its association with the mitochondrial membrane, Bcl-2 can directly or indirectly affect apoptosis-related Ca^{2+} flux, and perhaps, ultimately the putative Ca^{2+} -dependent endonuclease(s) involved in the fragmentation of DNA associated with apoptosis as well (70). Other recent studies by Distelhorst *et al.* indicate that while Bcl-2 overexpression in WEHI7.2 cells inhibits ER Ca^{2+} pool depletion associated with apoptosis induced by TG (but not dexamethasone) (128), and H_2O_2 (which generates ROI, and subsequently, intracellular Ca^{2+} flux) (129), that Bcl-2-mediated inhibition of apoptotic cell death is downstream from these events where different Ca^{2+} -dependent and -independent apoptotic pathways may converge (128). Furthermore, McCormick and Distelhorst have demonstrated that in inhibiting TG-induced apoptosis, Bcl-2 overexpression enables WEHI7.2 cells to elicit a stress response which includes up-regulation of GRP78, an ER calcium binding protein, and GRP94, of the heat shock protein family (130). These present studies serve as insights beginning to distinguish direct versus indirect results of intracellular Bcl-2 overexpression.

While several of the above studies seek to link Bcl-2 function to the implications from its subcellular residence, a previous finding that Bcl-2 is still capable of blocking staurosporine-induced apoptosis in cells lacking mitochondrial DNA (131) has negated the requirement for intact mitochondria for the ability of Bcl-2 to block apoptosis. However, a recent finding, that mutant U937 cells lacking mitochondrial DNA still exhibit loss in mitochondrial transmembrane potential concomitant with the progression of $\text{TNF}\alpha$ -induced apoptosis, does not negate contribution of mitochondria themselves in the apoptotic process (132). In addition, a study by Smets *et al.* has associated high Bcl-2 overexpression and subsequently high ATP content in leukemia and lymphoma cell lines with decreased sensitivity to glucocorticoid-induced apoptosis (133). These associations may not necessarily prove that Bcl-2 participates directly in these

effects. Taken together, these findings may instead suggest a distally operative role for Bcl-2-mediated inhibition of apoptosis, which **indirectly allows** for the mediation of various protective responses by the cell, which include metabolic, antioxidant, and Ca^{2+} -related stress responses.

4d. Bcl-2 and interaction with Ras.

Preliminary evidence also implicates Bcl-2 in a possible signal transduction pathway to regulate apoptosis by its association with R-*ras*. Fernandez-Sarabia and Bischoff demonstrated by using the yeast two-hybrid system, that Bcl-2 binds to R-*ras* p23, and that both can be co-immunoprecipitated in human cell extracts (134). The *ras* gene family are oncogenes which have the potential to induce transformation of cells and mediate cell cycle progression (88, 135). R-*ras*, as well as H-*ras*, belong to a small M_r G-protein group of signal transducers which possess GTP-binding activity (135). Early reports suggested that Bcl-2 itself was also a GTP-binding protein (135), but in subsequent experiments and under more stringent conditions, Bcl-2 was unable to bind GTP (134, 136), and this GTP-binding activity was probably due to R-*ras* p23 associated with Bcl-2 (134). Human R-*ras* encodes a 218-amino acid polypeptide which shares 55% identity with H-*ras* p21 (134), but does not share the oncogenic properties of other *ras* proteins (134). As summarized by Chen and Faller (88), activated p21^{Ras} , whose state is generated via guanine nucleotide exchange factors including Sos and GDP-releasing factor, targets the serine/threonine kinase Raf-1. Raf-1 kinase, in turn, stimulates a kinase cascade which includes the mitogen-activated protein kinases (MAPK), its precursors, and its PKC-dependent and -independent targets (88). Activation of Ras by inducible oncogenic Ras in IL-3-dependent hematopoietic cells has been shown to result in rapid up-regulation of *bcl-2* and *bcl-2* homolog *bcl-x_L*, to be described later, but does not affect *bcl-2* homolog *bax* expression, and may contribute to the mechanism by which IL-3 and granulocyte-macrophage colony-stimulating factor (GM-CSF) inhibit apoptosis as they stimulate the Ras pathway (136). As mentioned previously, Chen and Faller reported that Bcl-2 is phosphorylated by, yet still protects Jurkat cells from apoptosis induced by activated *ras* ($\text{p21}^{\text{Ha-ras}}$), and suppression of protein kinase C (87, 88). However, Wang *et al.* have shown that Bcl-2 can also be co-immunoprecipitated with the Ras target Raf-1 serine/threonine kinase in 32D.3 cells as well as Sf9 insect cells transfected with both Bcl-2 and Raf-1 kinase (137). Both proteins individually, when overexpressed, can delay onset of apoptosis due to IL-3 withdrawal in 32D.3 cells, and may demonstrate a

functional synergy when co-transfected (138). Raf-1 does not appear to phosphorylate Bcl-2 itself during their interaction, and reciprocally, Bcl-2 does not appear to alter the activity of Raf-1 kinase itself, suggesting that interaction of Bcl-2 with Raf-1-kinase may work to target Raf-1 to other substrates which regulate apoptosis (139). However, it has been recently demonstrated that taxol-induced apoptosis in MCF7 cells is dependent of the presence of Raf-1, and, conversely, is associated with cell death (140, 141). Clarification of the biologic significance and the universality of Bcl-2 association with the Ras pathway are thus still required.

4e. Bcl-2 and transport of nuclear proteins.

Bcl-2 has also been recently shown to affect subcellular trafficking of nuclear proteins which may be critical during apoptosis. Bcl-2 overexpression in HeLa cells has been shown to suppress apoptosis as well as the amount of cyclin-A-dependent kinases cdc2 and cdk2 translocated to the nuclei of these cells associated with the induction of apoptosis by staurosporine, caffeine, 6-dimethylaminopurine, and okadaic acid (142). In this case, however, as evidenced by histone H1 kinase assays, Bcl-2 did not prevent the activation of these cell cycle-dependent kinases (142), which are critical steps thought to be required for mitosis as well as the very similar chromosomal and cytoplasmic manifestations of apoptosis (142, 143). Bcl-2 overexpression did, however, reduce the abundance of cdc2 and cdk2 within the nucleus, and this reduction was associated with the inhibition of apoptotic chromatin condensation (142).

Similarly, Bcl-2 has been shown, by cooperating with *c-myc*, to inhibit wt-p53-induced apoptosis in murine erythroleukemia (MEL) cells, as well as cell cycle arrest, by altering the subcellular trafficking of p53 during the normal cell cycle from the cytoplasm to the nucleus (144). During a critical period in G₁, wt-p53 was shown to remain in the cytoplasm of cells co-transfected with *c-myc*, *bcl-2*, and *p53*, instead of normal translocation to the nucleus. These data confirm that Bcl-2 can protect cells from wt-p53-induced apoptosis, and suggest that addition of *c-myc* can overcome wt-p53-mediated cell cycle arrest (144). These findings are compatible with the localization of Bcl-2 near random pore structures of the outer nuclear membrane reminiscent of nuclear pore complexes (72), and indicate a possible role for Bcl-2 in the regulation of protein transport across cellular membranes (72, 144). However, Bcl-2 overexpression has also been shown to block cytoplasmic manifestations of apoptosis in the

absence of a nucleus (145), indicating that residence in the nuclear membrane is not an absolute requirement for the protective activity of Bcl-2. Bcl-2 may also have a protective function during mitosis after nuclear envelope breakdown, given its cytoplasmic residence. By fluorescent immunocytochemistry in KB and OV/CAR-3 cells, Willingham has demonstrated a concentration of Bcl-2 at the margins of condensed chromosomes during prophase, metaphase, and anaphase, and its disappearance from these locations at telophase when the nuclear envelope reforms (146).

Further critique of these theories of Bcl-2 mechanism of action in the context of this dissertation will be given in the final discussion **Chapter Six**.

5. *bcl-2*-Related Family of Genes.

In attempts to understand the function of Bcl-2, continued analysis of the *bcl-2* cDNA and protein structure has led to the cloning of several *bcl-2* related genes. *Bcl-x* is a recently identified *bcl-2*-related gene cloned from chicken lymphoid cells by differential hybridization and washing conditions (147). The *bcl-x* gene, like *bcl-2*, utilizes alternative splicing mechanisms to generate two distinct *bcl-x* mRNAs. The larger transcript *bcl-x_L*, codes for the 241-amino acid, 29-31 kD Bcl-x_L protein, which has 74% homology to Bcl-2 (70). When stably transfected into IL-3-dependent murine FL5.12 cells, Bcl-x_L was found to inhibit apoptosis due to growth factor withdrawal to an equal if not greater extent than Bcl-2 itself (147). Bcl-x_L overexpression was also demonstrated to block apoptosis in U937 cells due to ionizing radiation (148), and in neuroblastoma cells due to chemotherapeutic drugs such as cisplatin, 4-HC, and VP-16, respectively (149). *bcl-x_L*, but not *bcl-2*, expression in murine myeloma cells has been associated with their resistance to apoptosis (150). Similar to the ability of Bcl-2, however, Bcl-x_L overexpression has also been shown to rescue WEHI-231 B-lymphocytes from serum deprivation or oxidant-mediated cell death following diverse apoptotic stimuli including exposure to γ -irradiation, the sphingomyelin ceramide, and compounds which increased intracellular levels of oxidants (151). In contrast, the shorter *bcl-x* transcript, *bcl-x_S* encodes a shorter 178-amino acid, p20Bcl-x_S protein which lacks the 63-amino acid domain well-conserved among Bcl-2-related proteins (152). Bcl-x_S counteracts the protective function of Bcl-2 in growth-factor deprived cells (147), as well as in chemotherapy-treated breast cancer

cells (153). In addition, expression of *bcl-x_S* can induce apoptosis in solid MCF-7 tumors in nude mice (154), as well as in breast, colon, stomach carcinomas, and neuroblastoma cells (155). Bcl-x_S can also antagonize the effects of Bcl-x_L; however, since recent coimmunoprecipitation studies demonstrate that Bcl-x_S binds to Bcl-x_L only weakly, and does not inhibit the ability of Bax to heterodimerize with Bcl-x_L, Bcl-x_S may enhance apoptosis by a mechanism distinct from the formation of dimers like those of other Bcl-2 family members (156). It was found that *bcl-x_S* mRNA is expressed at high levels in cells such as developing lymphocytes, which experience high rates of cell turnover, whereas *bcl-x_L* mRNA is found to be expressed in long-lived postmitotic cells such as adult brain neurons (147, 157), and in primitive human hematopoietic precursors which express CD34 but lack maturation-linked surface antigens (158). An additional transcript, *bcl-x_β* (157) is still under investigation. Preliminary evidence shows that microinjection of *bcl-x_β* into primary sympathetic neurons can inhibit their death induced by NGF withdrawal similar to the activity of *bcl-x_L* (157). In addition, *bcl-x*-deficient mice are unable to survive and display massive apoptotic cell death in their developing neurons as well as hematopoietic cell systems (159). In contrast, Bcl-2 deficient mice are able to survive to birth; however, they exhibit extensive apoptosis in their lymphoid systems, polycystic kidney disease and hypopigmented hair (160). These data suggest roles for different Bcl-2-related proteins in different stages of development.

Another important Bcl-2-related protein simultaneously discovered is the Bcl-2 homolog Bax, which coimmunoprecipitates with Bcl-2, and was found to heterodimerize with Bcl-2 (161). The *bax* gene has a complex six exon structure. Alternative splicing produces three forms of Bax protein: the 21kD Bax α membrane protein, and the less abundant Bax β and 18kD Bax γ cytosolic proteins (161). Overexpression of *bax* was shown to accelerate apoptotic cell death in IL-3-dependent murine lymphoid progenitor FL5.12 cells upon growth factor withdrawal (161). Bax α is capable of both homodimerization, as well as heterodimerization with Bcl-2 (161). Historically, the domains in Bcl-2 responsible for this heterodimerization have been identified and designated **BH1** and **BH2 (Bcl-2 homology 1 and 2)**, and are well-conserved among the majority of members of the Bcl-2 family of proteins (162). Mutation analyses of BH1 and BH2 domains in Bcl-2 protein have demonstrated the absolute requirement for the integrity of these regions in order for Bcl-2 to heterodimerize with Bax as well as to inhibit apoptosis (162), suggesting that Bcl-2 must exert its function through heterodimerization with Bax (162, 163,

164). In addition, phosphorylation of Bcl-2 by taxol in prostate carcinoma cells was shown by immunoprecipitation to inhibit Bcl-2 binding to Bax in conjunction with taxol-induced cell death (86). Incidentally, recent studies show that while interaction with Bax is required for proper Bcl-2 functioning, interaction with Bax is not necessarily required for the functioning of the more potent Bcl-x_L protein, which still retains 70-80% of its anti-apoptotic activity when specific mutations disrupt its heterodimerization with Bax (165).

It has been suggested that the intracellular ratio of p26Bcl-2:p21Bax ratios govern the fate of the cell after exposure to apoptotic stimuli (161), with higher Bcl-2 levels promoting cell survival, and higher Bax levels promoting cell death. **Figure 2** is a drawing of the model for the interrelationship between Bcl-2 and Bax, and its affect on the regulation of apoptosis, as proposed by Oltvai and Korsmeyer (161). Because overexpression of Bax counters the activity of Bcl-2 in blocking apoptosis, this model was proposed in which a major death checkpoint occurs in the progression of apoptosis which is governed by a preset "rheostat" composed of the intracellular amounts of Bcl-2 and Bax proteins (161, 166): When Bcl-2 levels are higher, and more Bcl-2:Bax heterodimers form, cells are protected from death by apoptosis, whereas when Bax levels are higher and more Bax homodimers can form, cells may be more susceptible to the induction of apoptosis.

Bax has been determined to be expressed in a more widespread fashion than Bcl-2 itself, and found to be most intensely expressed in some areas associated with high rates of apoptosis. These include specific areas in crypts of small intestinal mucosa and gastric pits of the stomach, germinal centers of lymph nodes, and several different populations of neurons (167). Just as wt-p53 has been demonstrated to regulate *bcl-2* gene expression (80), analysis of the *bax* gene reveals that *bax* is also subject to regulation by p53, however, in a positive manner (62, 63). The *bax* gene promoter region has been found to contain four specific motifs which have homology to the p53 consensus DNA-binding sequence 5'-PuPuPuC(A/T)(T/A)GPyPyPy-3' (64), and suggests that *bax* may be involved in a p53-regulated pathway for the induction of apoptosis (64).

Additional members of the Bcl-2 family of related proteins have rapidly been identified. **Mcl-1** and **A1** were discovered through screening of cDNA libraries derived from myeloid

leukemia cells and normal cells induced to differentiate (70). When ML-1 human myeloid leukemia cells were induced to differentiate along the monocyte/macrophage pathway by phorbol esters, an increase in the expression of the novel *mcl-1* gene was detected (168). Mcl-1 has 95% sequence similarity to Bcl-2, and encodes a 37 kD protein whose differential expression has also been detected in germinal center lymphocytes of reactive lymph nodes, neoplastic follicles of follicular non-Hodgkin's lymphomas containing t(14;18) chromosomal translocations, and in Reed-Sternberg cells of Hodgkin's disease, but is absent in malignant mantle cell lymphomas (169). Recently, overexpression of *mcl-1* in Chinese hamster ovary (CHO) cells was demonstrated to delay internucleosomal DNA fragmentation and apoptosis induced by *c-myc* overexpression (170). Furthermore, Lomo *et al.* have correlated levels of expression of Mcl-1 with *in vitro* survival of peripheral blood B-lymphocytes exposed to apoptotic or survival stimuli (171). A1 encodes a hematopoietic-specific 20kD protein which shares 40% homology with Bcl-2 (172). A1 expression has been demonstrated to permit growth-factor-induced differentiation of myeloid cells, but delays apoptotic cell death due to growth factor withdrawal similar to Bcl-2 (173, 174).

The yeast two-hybrid and λ expression cloning systems were used by Yang *et al.* to screen for Bcl-2 interacting proteins in the FL5.12 cell line (175) and allowed the detection of another novel Bcl-2-interacting protein **Bad** (Bcl-2-associated death promoter) which is homologous to Bcl-2 in the BH1 and BH2 domains (175). Bad heterodimerizes with Bcl-x_L and Bcl-2, but not with Bax, Bcl-x_S, Mcl-1, or A1, and does not homodimerize (175). Interaction cloning demonstrated that Bad binds more strongly to Bcl-x_L than to Bcl-2. It was then found that when transfected and overexpressed in IL-3-dependent FL5.12 cells already overexpressing Bcl-2 or Bcl-x_L, Bad displaces the binding of Bax to Bcl-x_L and therefore allows apoptosis to proceed by virtue of free Bax proteins (175). A model proposed by Yang and Korsmeyer is summarized in **Figure 3**.

Protein interaction cloning has also identified **Bag-1**, a novel Bcl-2-binding protein which is unique in that it shares no homology with Bcl-2 (176). However, co-expression of Bag-1 and Bcl-2 in human Jurkat lymphoid cells, as well as Bag-1 transfection in 3T3 fibroblasts, provides markedly increased protection from apoptosis induced by staurosporine, anti-Fas antibody, and cytolytic T-cells (175).

Recently, three **Bak** (Bcl-2 homologous antagonist/killer) proteins were identified in Jurkat cells by virtue of their ability to bind to adenovirus E1B 19K protein, which inhibits apoptosis (177). *Bak*, *bak-2*, and *bak-3* represent pseudogenes which share 97% homology (178). They were found to have strong homology to Bcl-2 in the BH1 and BH2 domains (178). Overexpression of *bak* in sympathetic neurons accelerates apoptosis induced by NGF-deprivation (178), serum-deprived fibroblasts (179), and was also shown to block the protective effect of co-injected E1B 19K (178). Bak also binds to Bcl-x_L (178). *Bak* expression is demonstrated to be widespread in various tissues, with highest levels in heart and kidney (178).

Bfl-1 (Bcl-2-related gene expressed in fetal liver) is also a recent *bcl-2*-related gene to be cloned. Isolated from human embryonic liver (180), Bfl-1 has highest homology to the murine *A1* gene, and homology to other Bcl-2 family proteins only in the BH1 and BH2 domains. The *bfl-1* gene was found to be very strongly expressed in the bone marrow, and to a much lower level in cell lines, normal adult lung, spleen, and esophagus tissue, as well as Burkitt's lymphoma cells. Notably, *bfl-1* was found to be associated with the development of stomach cancer, with highest expressions in tissue samples from metastatic tumor nodules (180). Presently, it is hypothesized that Bfl-1 promotes cell survival.

In addition, ***nr-13*** is a *bcl-2*-related gene found to be activated in embryonic quail fibroblasts and neuroretina cells transformed by the Rous sarcoma virus (*v-src*) (181), and was isolated from a cDNA library. *Nr-13* encodes a 177-amino acid protein which shares homology with Bcl-2 in the BH1 and BH2 domains, and may contribute to the increased lifespan of RSV-transformed cells (181), However, its function remains to be confirmed.

The *C. elegans* cell death repressor **ced-9** has also been found to be homologous to Bcl-2, as previously mentioned (182). The sequence and function of its BH1 and BH2 domains were also demonstrated to be essential for the proper functioning of the *ced-9* protein as a death repressor. Hengartner and Horvitz showed that a glycine to glutamate amino-acid substitution in the BH1 and BH2 domains in *ced-9* caused a gain-of-function activation of mutant *ced-9* as an accelerator of apoptosis (183). This also demonstrates an extraordinary conservation of cell death regulator proteins through evolution.

Brag-1 (brain-related apoptosis gene) is a most recently identified *bcl-2*-related gene, specifically expressed in normal human brain but found to be rearranged and overexpressed as a truncated transcript in human glioma (184). The gene was identified by screening poly-A-enriched RNA preparations from glioma cDNA libraries with a *bcl-2* probe under low stringency conditions, and encodes a 31kD protein which also shares significant homology with Bcl-2 in the BH1 and BH2 domains (184). *In vitro*-translated BRAG-1 protein was found to cross-react with Bcl-2 monoclonal antibody (184). It is assumed that its activity is similar to that of Bcl-2 or Bcl-x_L in blocking apoptosis.

Finally, **bik** (Bcl-2-interacting killer, also known as **Bip1** for Bcl-2-interacting protein), is the latest *bcl-2*-related clone to be identified by the yeast two-hybrid method for Bcl-2-interacting proteins. Bik interacts with survival-promoting proteins Bcl-2 and Bcl-x_L, as well as Epstein-Barr virus BHRF1 and adenovirus E1B-19K (185). In co-transfection experiments, these survival-promoting proteins were shown to suppress the death-promoting activity which Bik overexpression exerts by itself. Like Bag-1, however, Bik does not show homology to the Bcl-2 family in their conserved BH1 and BH2 domains, but is unique in that it shares a new nine-amino acid **BH3** domain with Bax and Bak (185).

The newly identified BH3 domain is emerging in significance as playing a potential role in the pro-apoptotic activities of Bax, Bak, and now Bip. It has been observed that deletion of the BH3 stretch in Bik, Bak, and Bax alters their death-inducing activities as well as their ability to interact with Bcl-x_L (186). Zha *et al.* have recently found that while BH1 and BH2 are required in the Bcl-2 protein for its proper function and for heterodimerization with Bax, neither of these domains are exclusively required for binding of Bax to Bcl-2 or to Bax proteins themselves (187, 188). Instead the essential region in Bax for its dimerization has been mapped to its **BH3** domain (187, 188). In Bcl-2 this BH3 domain is upstream of the more widely established BH1 domain, but downstream of the amino-terminal domain identified by Borner *et al.* as another region crucial to proper Bcl-2 activity (163), now called **BH4**. A significant recent study by Hunter and Parslow identifies the BH3 peptide sequence in Bax as its “suicide domain”, and demonstrates that the substitution of this Bax BH3 stretch of amino acids into the corresponding BH3 domain of Bcl-2 converts Bcl-2 into an activator of apoptosis (189). They suggest that Bcl-

2 may block apoptosis by suppressing the activity of Bax (189). Just as Yang and Korsmeyer hypothesize that the Bad protein, which sequesters Bcl-xL and allows free Bax homodimers to promote apoptosis (175), **Bcl-2 may function in sequestering Bax through heterodimerization, and thereby neutralizing its activity.**

Amino acid substitution in the **BH4** domain in Bcl-2 affects its death-suppressing activity as well (163, 185). In addition, the BH4 domain localized to residues 10-30 has been recently discovered to be required for binding of Bag-1 to Bcl-2 (190). The BH3 and BH4 domains may also be necessary for Bcl-2 interaction with Raf-1 kinase (139, 190). Since not addressed in this thesis, it will be important to further clarify and establish the functions and significance of these domains in order to understand and eventually manipulate these complex protein interactions which may regulate cell death. Please see **Figures 5a and 5b**, and **Table II** for summaries on the homologies and interactions between Bcl-2 and its related proteins.

Figure 2: The Bcl-2/Bax “rheostat” death checkpoint which may govern susceptibility to apoptosis. Summarized from proposals by Oltvai and Korsmeyer (161, 166).

Figure 3: Extension of Oltvai and Korsmeyer’s Bcl-2:Bax “rheostat” model to include interaction of Bcl-2-related proteins with Bad: as proposed by Yang and Korsmeyer (175): Excess Bad most strongly sequesters Bcl-x_L proteins, rendering Bcl-x_L unable to bind free Bax. Levels of free Bax/Bax homodimers capable of promoting apoptosis can then increase, and may render cells more susceptible to the induction of apoptosis when exposed to apoptotic stimuli.

Figure 4: Model of Interactions Between Bcl-2 and its Related Proteins (Bullock, circa December 1995).

Figure 2.
After Oltvai and
Korsmeyer,
1993,1994.

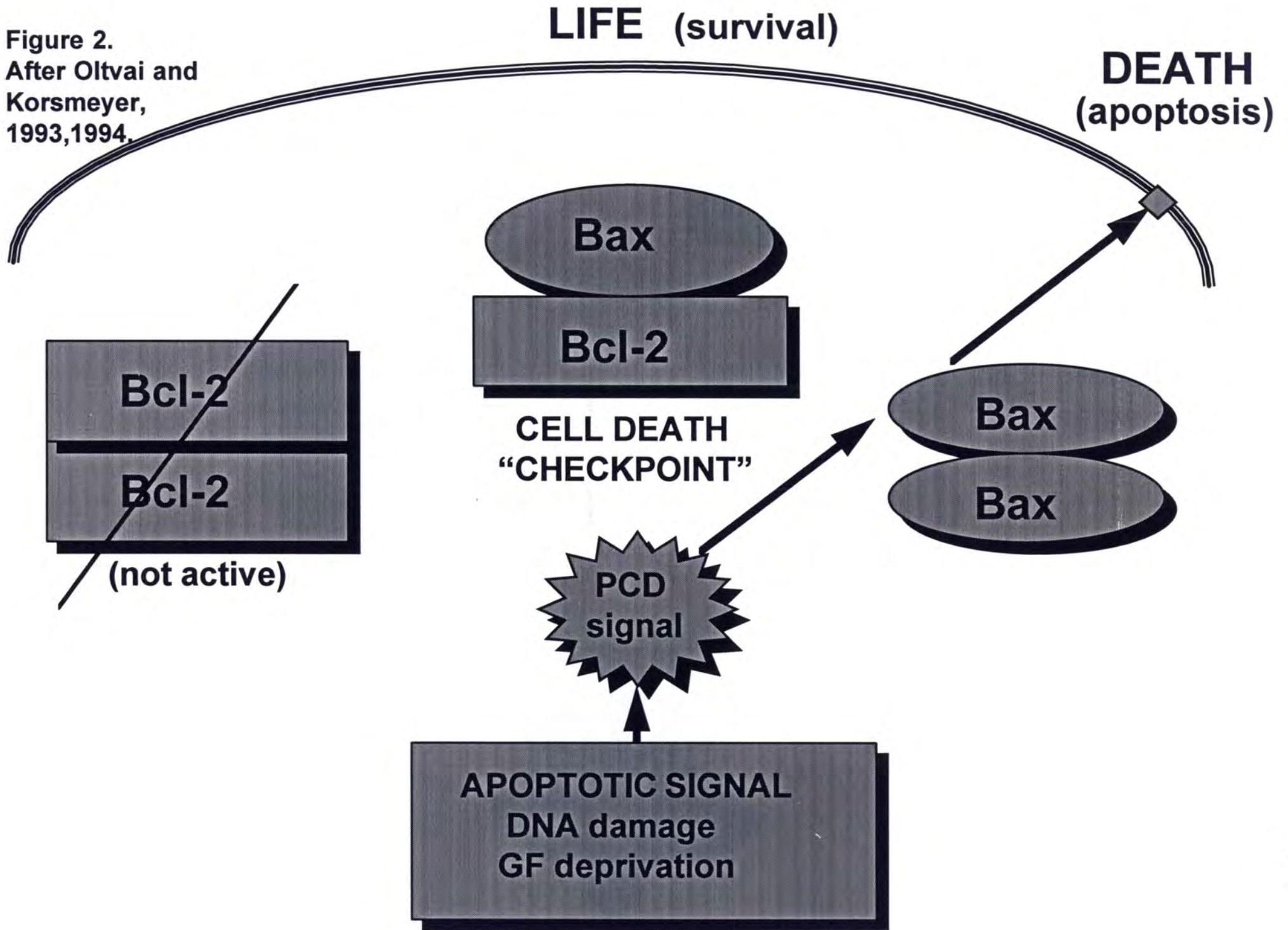


Figure 3.
After Yang and
Korsmeyer, 1995

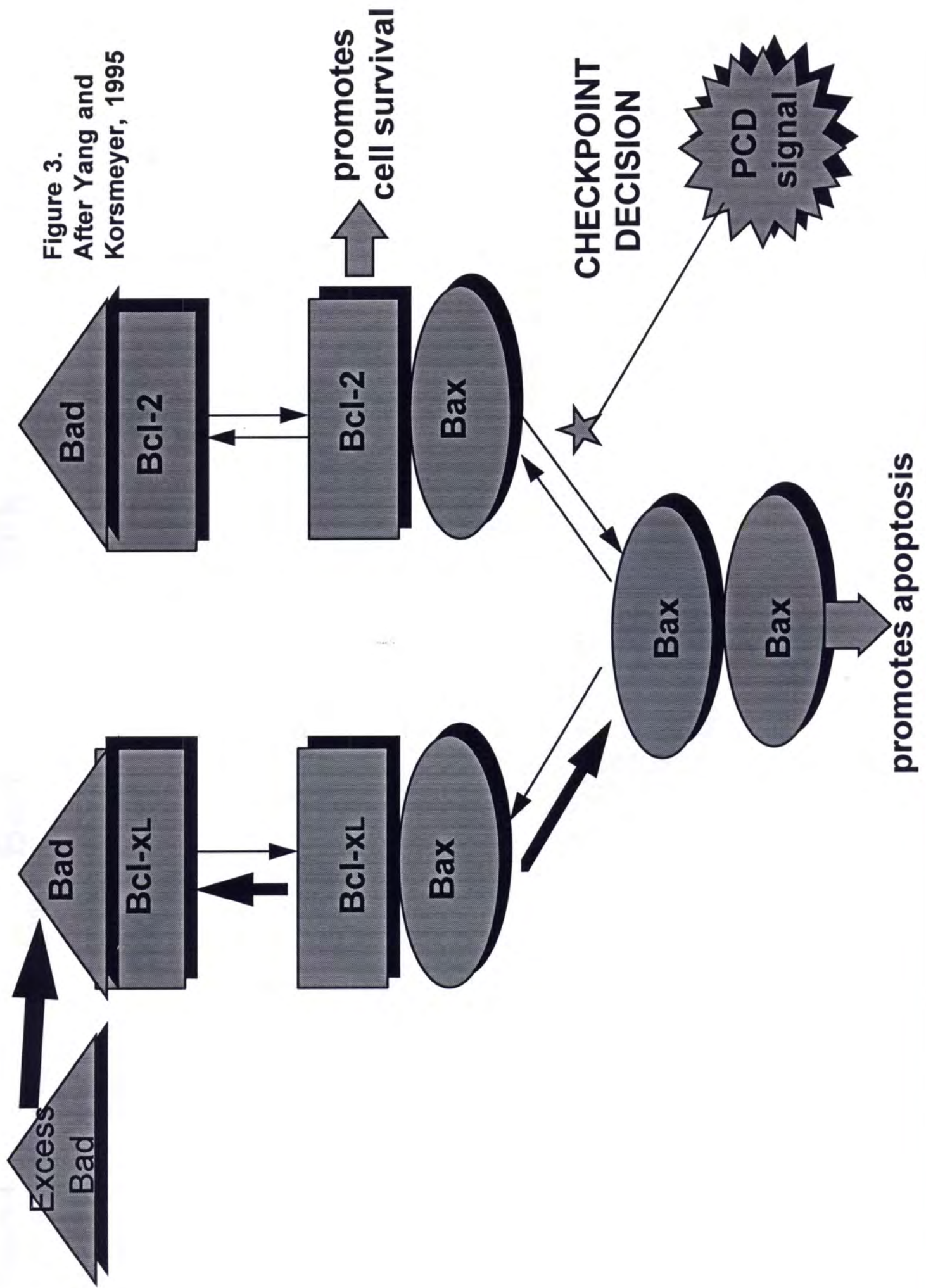


Figure 4.
(Bullock, circa December 1995)

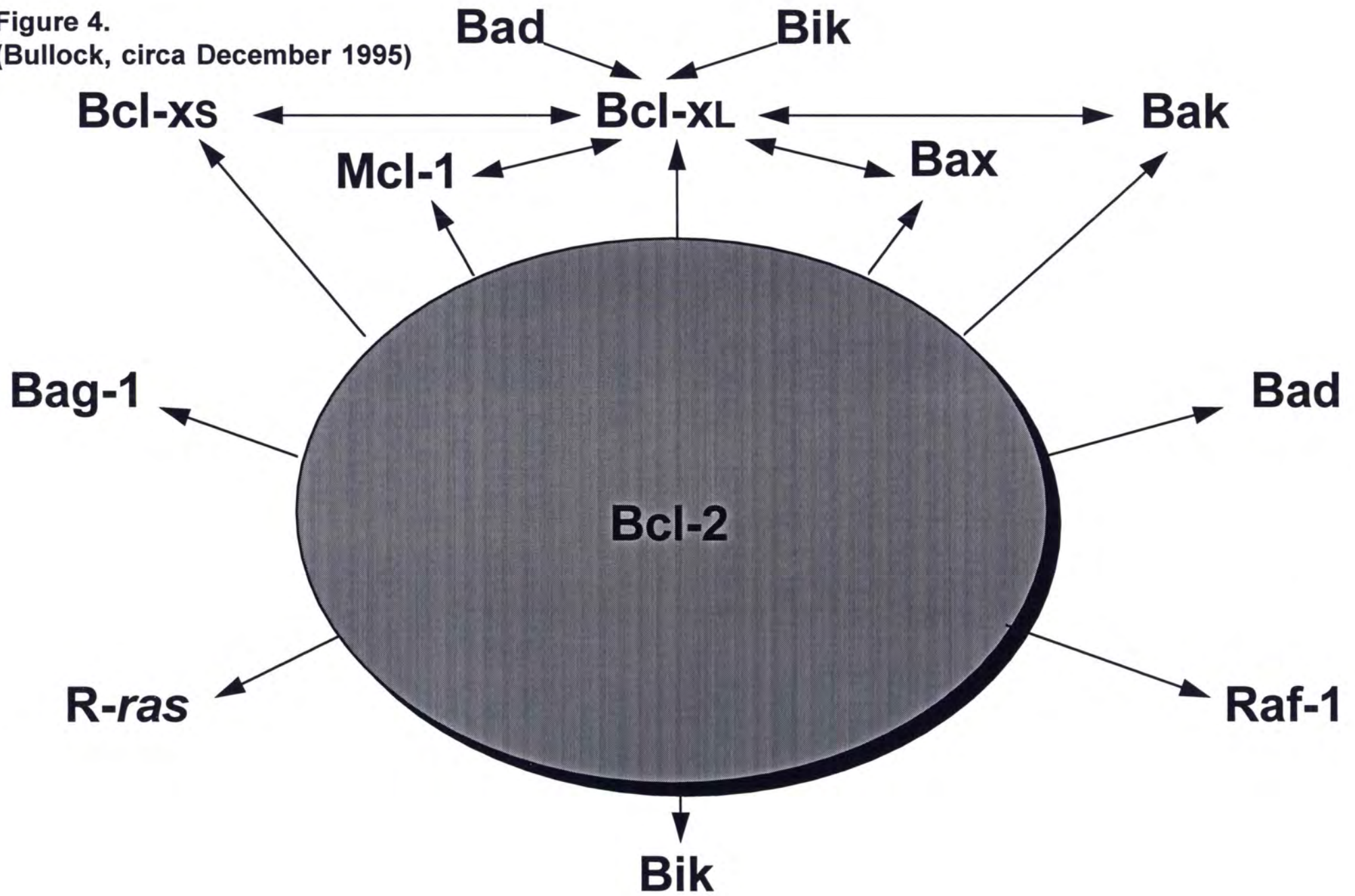


Figure 5a.

**ALIGNMENT OF Bcl-2-RELATED PROTEINS:
KNOWN CONSERVED HOMOMOLOGY IN
BH1 and BH2 DOMAINS**
(refs 173, 175, 177, 180, 181)
(Bullock, circa. April 1996)

BH1

Bcl-2 α	AA 132	VVEEL	FRDG_VNWGRIVA	FFFEFGVMCV	159
Bcl-x _L	125	VVNEL	FRDG_VNMGRIVA	FFSFGGALCV	152
Bax	95	VAADM	FSDGNFNSGRVVA	LFYFASKLVL	122
Mcl-1	249	VMIHV	FSDGVTNWGRIVT	LISFGAFVAK	276
A1	74	VMEKE	FEDGI INWGRIVT	IFAFGGVLLK	101
Bad	138	PP	NLWAAQRYGRELR	RMSDE F E G	160
Bak	117	SL	FES G_ INWGRVVA	LLGFGY	136
Bfl-1	86	VMEKE	FEDG I INWGRIVT	IFAFEGILIKKL	105
Nr-13	71	VAAOL	ETDGGLNWGRLLA	LVVFRGTLAA	98
ced-9	157	VGNAQ	TDQCPMSYGRLIG	LISFGGFVAM	85
BRAG-1	138	_A	SRVPPGSWG_VMP	IFSDRM	158
CONSENSUS		V__EL	F_DG__NWGRIVA	_F_FGG__	

BH2

				<u>3'CARBOXY</u>	<u>BH3</u>		
				<u>TAIL?</u>	<u>HOMOLOGY?</u>		
Bcl-2 α	176	NRHLHT_	WI_QDN_GGWD	AFVELYG	203	yes	yes
Bcl-x _L	170	NDHLEP_	WI_QEN_GGWD	TFVELYG	196	yes	yes
Bax	140	RERLLG_	WI_QDQ_GGWD	GLLSYFG	166	yes	yes
Mcl-1	295	VRTKRD_	WL_VKQR_GWD	GFVEFF_	320	yes	
A1	123	MNNTGE_	WI_RQN_GGWE	DG___F_	148	no	
Bad	182	G_	WT_RIIQSWWD	RN__LGK	197	unk	
Bak	168		WIAQR__GGWV	AALNLG	184	unk	yes
Bfl-1	128	MNNTGE_	WI_RQN_GGWE	NGFVKK	150	unk	
Nr-13	124	ACCQGE_	WMEE_HGGGWD	GFCR___	149	unk	
ced-9	207	KTRIRNN	WKEHN_RSWD	_FMTLGK	230	yes	
BRAG-1	198		CNLQQ I ADFS	NIHPXS	213	unk	
CONSENSUS		___L___	WI___N_GGWD	_FVELF_			

FIGURE 5b.

ALIGNMENT OF Bcl-2-RELATED PROTEINS:
KNOWN CONSERVED HOMOLOGY IN NEWLY-IDENTIFIED
BH3 DOMAIN (refs 185, 186, 188)
 (Bullock, circa. December 1995)

BH3

Bip1/Bik	AA 61	L A C I G D E M D	69
Bcl-2	97	L R Q A G D D F S	105
Bcl-x_L	90	L R E A G D E F E	98
Bax	63	L K R I G D E L D	71
Bak	78	L A I I G D D I N	86

TABLE II:**Bcl-2 AND RELATED GENE PRODUCTS:**

(refs 170, 180, 185, 191, 192)

(Bullock, circa. April 1996).

<u>Gene:</u>	<u>Protein:</u>	<u>Regulation of Apoptosis:</u>	<u>Interactions with:</u>	<u>Expression:</u>	<u>Subcellular location:</u>
<i>bcl-2</i>	Bcl-2α	blocks	Bcl-2, Bcl-x _L , Mcl-1 Bax, Bcl-x _S Raf-1	Wide embryonic tissues Some postnatal tissues	Outer mitochondrial, Endoplasmic reticulum, Nuclear membranes
<i>bcl-x</i>	Bcl-x_L	blocks	same as Bcl-2	same as Bcl-2	same as Bcl-2
	Bcl-x_S	promotes	Bcl-2, Bcl-x _L	thymus	
	Bcl-xβ	blocks	unknown	unknown	unknown
<i>bax</i>	Baxα	promotes	Bcl-2, Bcl-x _L	widespread	same as Bcl-2
<i>bad</i>	Bad	promotes	Bcl-x _L , Bcl-2 (sequesters)	unknown	unknown
<i>bag-1</i>	Bag-1	blocks	Bcl-2	unknown	unknown
<i>bak</i>	Bak	promotes	Bcl-x _L , Bcl-2	widespread	unknown
<i>bak-2</i>			E1B 19K		
<i>bak-3</i>					
<i>bfl-1</i>	Bfl-1	unknown	ND	bone marrow lung, spleen, esophagus stomach cancer	unknown
<i>A1</i>	A1	blocks		hematopoietic tissues	unknown
<i>mcl-1</i>	Mcl-1	blocks	Bcl-2, Bcl-x _L	myeloid cells	similar to Bcl-2
<i>nr-13</i>	NR-13	blocks	unknown	embryonic cells transformed by RSV	same as Bcl-2
<i>brag-1</i>	BRAG-1	unknown	unknown	brain, glioma	unknown
<i>bik</i>	Bik/Bip1	promotes	Bcl-2, Bcl-x _L EBV-BHRF1 E1B 19K	unknown	unknown

6. Expression of *bcl-2* and related genes in malignancies.

These discoveries represent a vast and rapidly-growing list of complex interactions by which the viability of cells at different stages of development are subjected to regulation. It will be crucial to learn how these interactions govern drug-induced apoptosis in the clinical setting. The expression of *bcl-2* and its related genes have significance in the treatment and prognoses of cancers. For example, Bcl-2 is expressed in the prostate and is associated with the emergence of androgen-independent prostate cancer (193). Bcl-2 is expressed in early lymphoid malignancies (194), and Bcl-2 expression in Burkitt's lymphoma cell lines can be induced by latent Epstein-Barr virus genes (115). Reed-Sternberg cells in Hodgkin's disease frequently express both *bcl-2* and *c-myc* oncogene products, suggesting that these oncogenes may act cooperatively in the pathogenesis of this disease (195).

The classic involvement of *bcl-2* in human malignancies is its participation in the t(14;18) chromosomal translocation of follicular non-Hodgkin's B-cell lymphomas, as previously mentioned (70). PCR (polymerase chain reaction) is an excellent tool in molecular medicine and can even detect point mutations in *bcl-2* genes of malignancies with t(14;18) (196). It has been reported that all advanced stage non-Hodgkin's lymphoma with a polymerase chain-reaction (PCR)-amplifiable breakpoint of *bcl-2* have residual cells which contain the *bcl-2* rearrangement at evaluation and after chemotherapy treatment, suggesting the contribution of *bcl-2* to and prediction of minimal residual disease (197).

Bcl-2 expression is not restricted to lymphomas carrying t(14;18), however. Bcl-2 is broadly expressed in various hematopoietic neoplasms (198). Kondo *et al.* report that Bcl-2 expression is detectable in early normal as well as neoplastic lymphoid precursors, and persists in B-cell blasts, T-cell blasts (198), as well as myeloma cells (198, 199). Bcl-2 is also expressed in normal plasma cells (199). In the myeloid lineage, however, they report that Bcl-2 expression is not seen in myeloid precursors, but is expressed in later myeloblasts. Bcl-2 expression was not detected in stem cells. These data are in agreement with studies by Park *et al.* (158), and suggest that the expression of *bcl-2* and its related genes is stage-specific. Bcl-2 expression is found in acute myeloid leukemia (AML) cells such as KG1 cells, but not in K562 cells (200). Instead, K562 represent an extremely resistant form of chronic myeloid leukemia blast crisis

cells which harbor not only the t(9;22) chromosomal translocation and resulting bcr-abl fusion protein, but also express the potent Bcl-2 homolog Bcl-x_L (201-203), both of which contribute to their resistance to drug-induced apoptosis, as will be described in **Chapter Two**.

Bcl-2 expression in malignancies can indeed impact on clinical outcome. Campos *et al.* have reported that high expression of Bcl-2 protein in patient-derived AML cells is associated with poor response to chemotherapy regimens which include Ara-C as well as daunorubicin and mitoxantrone (204). Furthermore, inhibition of Bcl-2 protein with antisense oligonucleotides induces apoptosis and increases the sensitivity of normal bone marrow progenitor cells (205) as well as patient-derived AML blasts to Ara-C (206). These data highlight the important impact of Bcl-2 levels in leukemias on patient outcome. The correlations suggest a clinical relationship between Bcl-2 function and drug-induced apoptosis worthy of further pursuit in order to improve treatment of AML, as well as other malignancies.

C. Acute Myeloid Leukemia.

1. Definition, history, and classification.

Acute myeloid leukemia (AML) is a clonal malignant disease of hematopoietic stem cells which normally have the capability of maturing into blood cells of the myeloid species including mature erythrocytes, megakaryocytes (and subsequently, platelets), monocytes, macrophages, neutrophils, eosinophils, and basophils. Please see **Figure 6** for an illustration. The myeloid lineage differs from cells committed to the lymphoid lineage, which give rise solely to B- and T-lymphocytes, and mature in the lymph tissue. AML is characterized by the proliferation of abnormal blast cells in the bone marrow incapable of normal maturation and differentiation, as well as suppression of the production of normal blood cells due to this crowding (207).

AML was first documented by Friedreich (208), first named by Ebstein in 1889 (209), and distinguished from chronic myeloid leukemia by Frankel in 1895 (210). Presently, the disease is subclassified into eight subgroups (M1-M8) by the French-American-British (FAB) classification which only distinguishes the lineage involvement of the leukemic blasts at diagnosis based on morphological, cytochemical, and cytogenetic criteria (207, 211): acute myeloblastic leukemia (AML)(M1,M2); acute promyelocytic leukemia (APL)(M3); acute myelomonocytic leukemia (AMML)(M4); acute monoblastic leukemia (AMoL)(M5); erythroleukemia (EL)(M6); megakaryocytic leukemia (ML)(M7); and rarely, eosinophilic leukemia (EoL)(M8). This classification is in the process of being updated based on molecular information.

Figure 6:

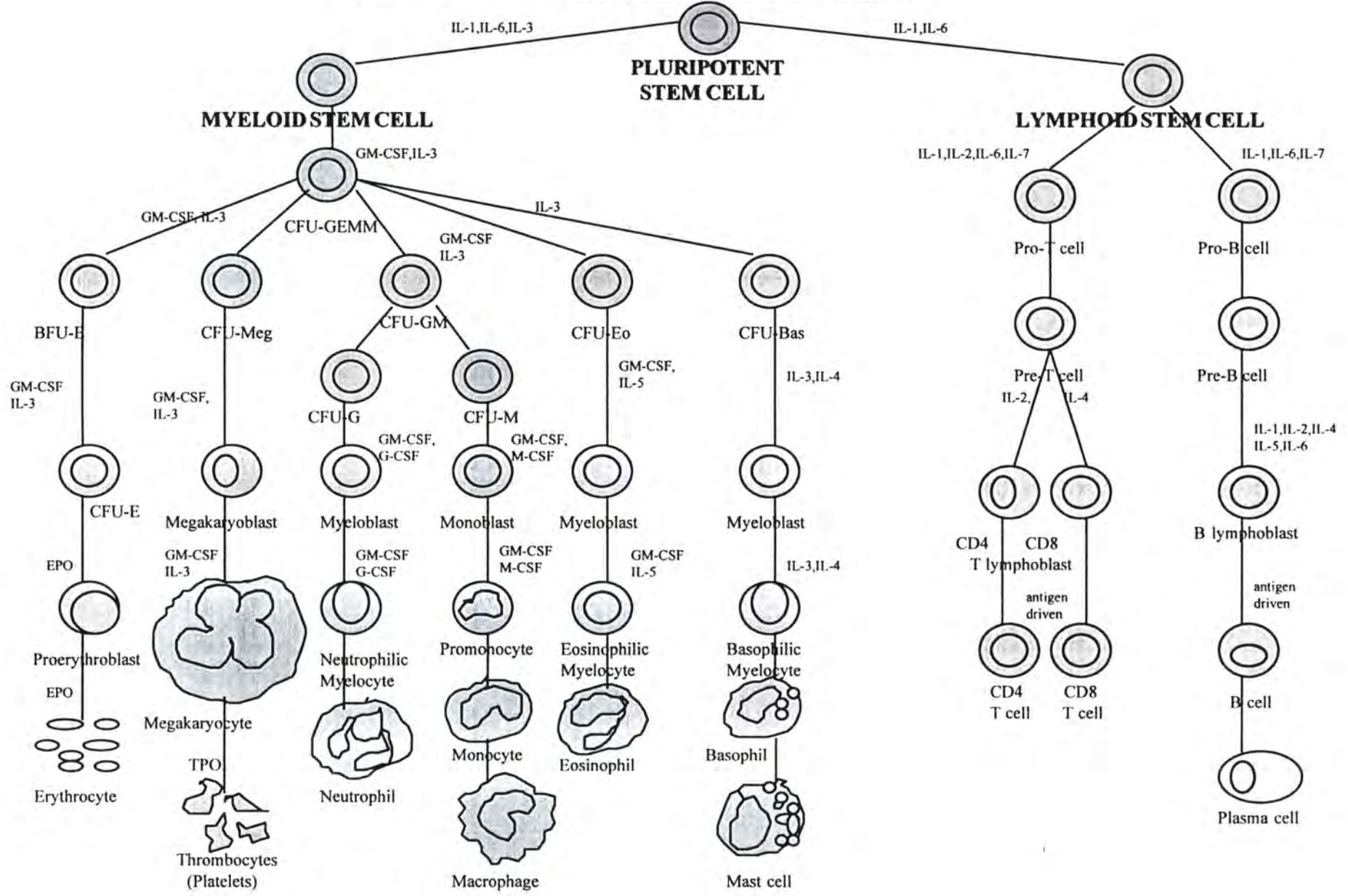
The hematopoietic “tree” is a hierarchical scheme illustrating the irreversible development of immature self-renewing stem cells in the bone marrow into progressively more differentiated progenitor cells prior to their ultimate terminal maturation. The functional cells in their final forms for each lineage are then capable of circulating from the bone marrow into the peripheral blood, and perform various actions, but are incapable of self-renewal.

CFU refers to a *colony-forming unit*, and **BFU** refers to a *burst forming unit*, which are among the first stages of commitment of progenitor cells to specific myeloid lineages. These terms refer to in vitro colonies which contain cells of several lineages.

Acute leukemias can develop from any of these early stages in maturation, as described in the text, and are characterized as such.

Sources of hematopoietic regulators such as humoral interleukins, include progenitor cells themselves, as well as activated T-lymphocytes, monocytes, marrow stromal cells, and some endothelial cells. (refs 207, 212)

Figure 6. HEMATOPOIETIC "TREE":



2. Presentation at diagnosis.

Leukemogenesis is considered to involve two steps (207): first, a critical mutation occurs in a single cell, usually in a proto-oncogene which is normally tightly regulated, and a second genetic change involving one or more oncogenes subsequently leads to the progression of AML (213). The etiology of AML is still largely unknown. Some conditions predisposing to the development of AML include environmental factors such as exposure to radiation, benzene, or alkylating agents; acquisition from pre-existing hematopoietic diseases; and some inherited conditions (207, 214). Usually seen in adults, general symptoms of AML include pallor, fatigue, weakness, palpitations, and dyspnea on exertion, reflective of anemia (207); signs of bone marrow failure include easy bruising, petechiae and hemorrhages, reflective thrombocytopenia, and infections reflective of neutropenia (207). Infiltration of leukemic cells in various organ systems including the skin, gastrointestinal tract, liver, lungs, heart, kidneys, spleen, and central nervous system, may occur as immature cells circulate through the bloodstream (207).

3. Treatment of AML.

The current standard treatment for AML is first, the attempted **induction** of remission with cytotoxic drugs, that is, eradication of the monoclonal leukemic population to a level at which the leukemic cells are no longer detected in bone marrow aspiration or biopsy. Clinical trials in AML have shown that drug regimens which include combinations of an anthracycline antibiotic or an anthraquinone and **cytarabine (1- β -D-arabinofuranosylcytosine) (Ara-C)** (207, 215-217), can achieve general remission rates of 50-90% in adults (218). Additional treatment with mitoxantrone or etoposide may be more effective for remission induction (207, 218). Furthermore, supplementation of chemotherapy regimens with hematopoietic growth factors such as G-CSF or GM-CSF (granulocyte- or granulocyte/macrophage colony-stimulating factors) can diminish myelosuppression and infections on a short-term basis (218). Long-term remission can occur in approximately 20% of patients treated (207). In order to prolong the duration of remission, **consolidation** or **postremission chemotherapy** with different doses of the same cytotoxic agents is necessary; autologous or allogeneic bone marrow transplantation of hematopoietic stem cells can supplement this treatment, and can prolong remission greater than two years.

However, relapse of the leukemia occurs in the majority of patients due to many factors; only 10 percent of adults between ages 15-60 who are treated with chemotherapy remain in

remission for over 5 years (207), and repeated chemotherapy often becomes less effective. The basis of this relapse is under intense investigation: explanations include drug resistance of leukemic clones by various mechanisms including down-regulation of enzymes critical for drug metabolism (219), as well as up-regulation of transmembrane drug-efflux pumps coded for by the *mdr* gene family (220), and now, the emergence of altered expression of oncogenes such as the *bcl-2* family which block drug-induced cell death (204-206). As previously mentioned, Campos *et al.* have reported that high expression of Bcl-2 protein in AML cells is also associated with poor response to remission induction chemotherapy treatment including an anthracycline drug or mitoxantrone plus Ara-C (204). In this study, high Bcl-2 expression was detected in immature forms of AML (M1 and M2) (204). Porwit-MacDonald *et al.* also found that mean Bcl-2 levels were higher by flow cytometry in AML with M1 and M2 features than more differentiated promyelocytic (M3) or myelo-monocytic (M4/M5) leukemias (221). In Campos' study, only 29% of cases which had 20% or more leukemic blasts positive for Bcl-2 expression achieved complete remission after intensive chemotherapy, whereas 85% of cases with less than 20% cells positive for Bcl-2 expression achieved complete remission. In addition, Deng *et al.* have found that Bcl-2 is expressed at high levels in patient-derived AML cells which possess monosomy 5 and 7, and are thus representative of cases with poor prognosis (222). Because AML blasts with high Bcl-2 expression are able to survive longer *in vitro* as well as *in vivo*, the expression of Bcl-2 in AML is associated with very poor prognosis (204).

Therefore it is essential to increase our understanding of not only how the treatments of choice for AML are effective, but how their efficiency may be hindered, in order to improve the achievement of remission of leukemia, and decrease the chances of relapse after treatment.

D. 1- β -D-Arabinofuranosylcytosine (Ara-C).

1- β -D-arabinofuranosylcytosine (Ara-C, cytarabine, cytosine arabinoside) is a nucleoside analogue. It is one of the most effective agents in the treatment of acute myeloid leukemia (AML) (223). Arabinose nucleosides are also antimetabolites, and were originally isolated from the sponge *Cryptothethya crypta*, but now are produced synthetically (224). Ara-C differs from normal deoxycytidine by the presence of a β -OH group in the 2' position of the normal sugar (224). Ara-C has a limited spectrum of activity, but is selective against rapidly dividing cells (223, 224). Ara-C therefore has little activity as a single agent in solid tumors which do not show progression through the cell cycle as rapidly at the cellular level. Ara-C is used primarily in combination with anthracycline antibiotics doxorubicin (adriamycin) or daunomycin for remission induction in AML (224). Ara-C is also useful in combination therapy for histiocytic lymphoma as well as for childhood acute lymphocytic leukemia (ALL) (224). The specific basis for the selectivity of action of Ara-C is largely unknown.

1. Intracellular metabolism of Ara-C.

Ara-C enters cells by a carrier-mediated process of facilitated diffusion via membrane nucleoside binding sites shared by normal deoxycytidine (224-227). The number of binding sites detected by incubation with nitrobenzylthioinosine (224, 225) have been demonstrated to be greater in AML cells than in ALL cells (226, 227). Intracellularly, Ara-C is phosphorylated by the sequential action of first, the rate-limiting deoxycytidine kinase, followed by deoxycytidylate kinase (dCMP) and nucleoside diphosphate (NDP) kinase, to be ultimately converted to its active metabolite, Ara-CTP (224, 225), as illustrated in **Figure 7**. Ara-CMP can be inactivated by dCMP deaminase to Ara-UMP. Ara-C is an S-phase-specific agent (228). The lethal metabolite Ara-CTP competes with normal dCTP for incorporation into actively replicating DNA by DNA polymerases α and β , but does not incorporate into RNA. While relationships have been drawn between the intracellular dCTP/Ara-CTP ratio and the cytotoxic effect of Ara-C (229), the extent of Ara-CTP incorporation has historically been correlated with inhibition of DNA synthesis, loss of clonogenic survival and cytotoxicity (223, 228, 230, 231).

2. Mechanism of action of Ara-C.

Ara-C has been previously described as a relative DNA chain terminator (223). Upon incorporation into DNA, Ara-C disrupts replicative DNA synthesis. Extension from the altered 3' terminus of Ara-C is inefficient, causing the subsequent stalling of DNA polymerases, and reinitiation of synthesis by DNA polymerase in previously replicated segments (endoreduplication) (223-225, 232, 233). Ara-C also causes aberrant synthesis of primer RNA by DNA primase, required for the extension of Okazaki fragments on the lagging strand of the DNA replication fork (rev. in 233). These effects of Ara-C inhibit the proper formation and continuity of replication forks (233, 234), and are described as resulting single-strand gaps or breaks in genomic DNA. In addition, if Ara-C is not removed by cellular repair processes (explained in more detail in **Chapter Five**), the residues accumulate in an internal position in the altered DNA chains, and contribute to the lethality of Ara-C (230, 231, 235-238).

High-dose Ara-C, in combination with other DNA damaging agents, is also a potent inhibitor of DNA repair synthesis. This is suggested by observations that Ara-C increases the frequency of DNA single-strand breaks, chromosomal aberrations and cytotoxicity induced by UV-irradiation (239), alkylating agents (240), and X-irradiation (241). It has been demonstrated by alkaline sucrose gradient analysis that Ara-C induces single-strand DNA breaks upon incorporation into fibroblast DNA undergoing repair of UV-induced damage (242). Evidence for formation of DNA strand breaks by Ara-C itself come from experiments by Fram and Kufe, which demonstrate DNA strand lesions in DNA from intact L1210 murine leukemia cells exposed to Ara-C, and detected by the alkaline elution technique for single-strand DNA breaks (243). Fram and Kufe suggest that these lesions are due to inhibition of DNA synthesis rather than incorporation into the DNA strand by virtue of the use of aphidicolin, a DNA polymerase inhibitor which does not incorporate into the DNA strand, but which produces similar elution results (243). Ross clarifies Ara-C-induced DNA damage by his demonstrations utilizing pH-step alkaline elution of nascent or newly synthesized DNA, in which accompanying alkaline sucrose density gradients prove that DNA with molecular weight nearest to Okazaki fragments elutes from filters at pH 11.0, nascent DNA (with relative molecular weight [M_r] of $8-12 \times 10^6$ bp) synthesized at replicon origins elutes at pH 11.3, and subgenomic DNA strands (M_r $20-30 \times 10^6$ bp) elute at pH 11.5 and 12.1. Ross *et al.* demonstrated that **Ara-C-induced DNA damage in HL-60 cells is appreciated at fixed pH 12.1**, indicating that Ara-C inhibits nascent chain

elongation and thus leaves single-strand breaks, but Ara-C does not decrease the production of smaller Okazaki fragments or other lower molecular weight nascent DNA species, evident by the failure of Ara-C to decrease [^3H]-thymidine incorporation into these fragments at low levels (237). Endoreduplication is suggested to contribute to the accumulation of these shorter DNA fragments (223, 232, 234). Studies have also shown, however, that Ara-C inhibits DNA ligase activity in HL-60 and K562 leukemic cell lines through inhibition of an intermediate ligase-adenylate complex during its action (244, 245), and may also explain accumulation of shorter DNA species.

Grem *et al.* have recently reviewed the chronology of Ara-C-induced DNA damage in a series of experiments which separate early events from later events (246). They demonstrate that immediately following a 24-hour exposure of HCT 116 and NCI-H630 human colon carcinoma cells to increasing concentrations of Ara-C, proportionate increases in Ara-CTP pools, as well as Ara-C DNA incorporation were observed. Increases in Ara-C-mediated strand breaks in higher molecular weight DNA templates were evidenced by shifts in fixed pH alkaline elution profiles of single-strand breaks at pH 12.1, in conjunction with decrease in overall DNA synthetic rate by [^{14}C]-thymidine incorporation. Proportionate increases in nascent or newly synthesized DNA, however, were evidenced during elution with pH steps 11.0, 11.3, and 11.5, indicating accumulation of lower molecular weight species reflective of DNA synthesis reinitiation and endoreduplication. Double-strand breaks or fragmentation in parental DNA, however, were most evident by ELISA for oligonucleosomal fragmentation 16 hours after removal of Ara-C from the cells, indicating a chronological progression of early to later events of DNA damage when cells are exposed to Ara-C. Ara-C-induced double-strand internucleosomal DNA fragmentation is associated with morphologic features characteristic of apoptosis (22, 98) in leukemic cell lines. **However, the precise mechanism(s) by which the observed molecular perturbations due to Ara-C contribute, either directly or indirectly, toward the engagement of the final common pathway leading to apoptosis remain to be elucidated.**

3. Other targets of Ara-C.

Ara-C has also been documented to affect various targets not necessarily contributing to its cytotoxicity, but possibly linked to intracellular signal transduction in the cellular response to Ara-C. For example, high doses of Ara-C can form a significant metabolite Ara-CDP choline, an analogue of cytidine 5'-diphospho-choline (CDP-choline). CDP-choline is involved in an enzymatic pathway for phosphatidylcholine biosynthesis, and is linked to protein kinase C (PKC) signalling (224, 225, 247). Ara-CDP can subsequently inhibit synthesis of membrane glycoproteins and glycolipids (224, 225, 248, 249), and represents a potential alternative pathway for Ara-C-induced cell perturbations independent of its effect on DNA synthesis. The contribution of Ara-CDP choline toward cell cytotoxicity remains uncertain. Ara-C treatment also results in increases in ceramide and diglycerides within 30 minutes in HL-60 cells, also the result of activation of phospholipid pathways and related second messengers (250). Notably, ceramide itself has been demonstrated to induce DNA fragmentation associated with apoptosis in HL-60 cells (251) by virtue of its implication in a signal transduction pathway utilized by tumor necrosis factor- α (TNF- α) (251-253). The ultimate inclusion of pro-apoptotic ceramide in the signal transduction of Ara-C-induced apoptosis is presently under investigation.

Other targets affected by Ara-C include the transcription factor *kB* (NF κ B), which has been shown to be activated within 30 minutes of Ara-C treatment in human KG-1 cells (254). Ara-C can also regulate H1 histone expression at both the transcriptional and posttranscriptional levels: Ara-C treatment of HL-60 cells for 15 minutes has been associated with inhibition of H1 histone gene transcription as well as decrease in stability of H1 histone transcript (255). These expressions, however, have not been related to Ara-C-induced apoptosis. The *c-jun* gene, which encodes a sequence-specific bZIP DNA-binding protein, is induced at the transcriptional level by Ara-C (256), as are *jun-B*, *jun-D*, and *c-fos* (257-259). The AP-1 transcription factor is activated in KG-1 cells by Ara-C, and its binding to the AP-1 site in the *c-jun* gene promoter is increased by Ara-C treatment (260). Ara-C-induced *c-jun* gene induction was also found to be mediated through PKC (261). However, *c-jun* induction may not necessarily be required for Ara-C-induced apoptosis. Abrogation of *c-jun* induction by concomitant treatment with the protein kinase inhibitor staurosporine was demonstrated to enhance Ara-C-induced apoptosis in HL-60 cells (262). In addition, U937 monoclonal leukemia cells expressing a mutant c-Jun protein

(TAM67) lacking the transactivation domain were shown to exhibit equivalent degrees of Ara-C-induced apoptosis (263).

Ara-C can activate MAP kinase through kinetics similar to those of protein kinase C (264). Most recently, however, Saleem *et al.* have demonstrated the activation of a stress-activated protein (SAP) kinase by Ara-C, as well as by other DNA-damaging agents (265). After 3-hour treatment of U-937 cells with HIDAC, activation of p54 SAP kinase (which is also known as JNK, and is related to MAP kinases) was also found to phosphorylate the amino terminus of c-Jun and thereby stimulate its transactivation function. In addition, the binding of SAP kinase to the SH3 domain of Grb2, an SH2/SH3-containing adapter protein, is also induced by Ara-C, and a complex with phosphatidylinositol 3-kinase (PI 3-kinase) at the Grb2 SH2 domain results. Saleem *et al.* have thus attempted to link the ultimate manifestation of Ara-C-induced internucleosomal DNA fragmentation with Ara-C-induced interaction between SAP kinase and PI 3-kinase. If Ara-C treatment increases ceramide levels in affected cells, the link may be in recently described initiation of SAPK/JNK signalling by ceramide itself (266). The link may also include the activation of the c-abl non-receptor tyrosine kinase by Ara-C, which was shown to be necessary for the stimulation of SAP kinase (267).

Short exposure (3 to 6 hours) of HL-52S myeloid leukemia cells to Ara-C has been demonstrated to induce Early growth response-1 mRNA transcription and activation of nuclear pp90^{rsk}, a kinase which functions early in the MAP kinase signal transduction pathway (259). Most recently, Ara-C was shown to activate tyrosine phosphorylation of the cell cycle regulator protein p34^{cdc2} by its association with the src-like p56/p53^{lyn} kinase, and subsequently inactivates p34^{cdc2} (268). It is suggested that Ara-C-induced cytotoxicity includes negative regulation of cell cycle progression, which is contrary to mechanisms demonstrated in cells undergoing apoptosis due to taxol, as well as the lymphocyte granule protease, which require activation of p34^{cdc2} (143, 269). The significance of these findings remains to be clarified since the precise and complex details of the signalling of apoptosis leading to the eventual generation of double-strand DNA breaks are also unclear (please see **Figure 8**).

Figure 7:

Illustration of Ara-C metabolism and known mechanisms of action (after Kufe, ref. 196, and Chabner, ref. 224, 225).

Upon entering leukemia cells via carrier-mediated diffusion at nucleoside binding sites, Ara-C is phosphorylated to its active metabolite Ara-CTP, which competes with normal dCTP for incorporation into genomic DNA undergoing active replication and repair. Incorporated Ara-C residues cause significant inhibition of activity of DNA polymerase, resulting in inefficient chain elongation, single-strand gaps in DNA, and attempted reduplication of DNA sequences. Ara-C subsequently causes both high molecular weight and low molecular internucleosomal double-stranded DNA fragmentation associated with the morphological features of apoptosis in leukemia cells, but the pathway by which single-strand damage is transduced to a signal which induces this fragmentation remains yet to be elucidated.

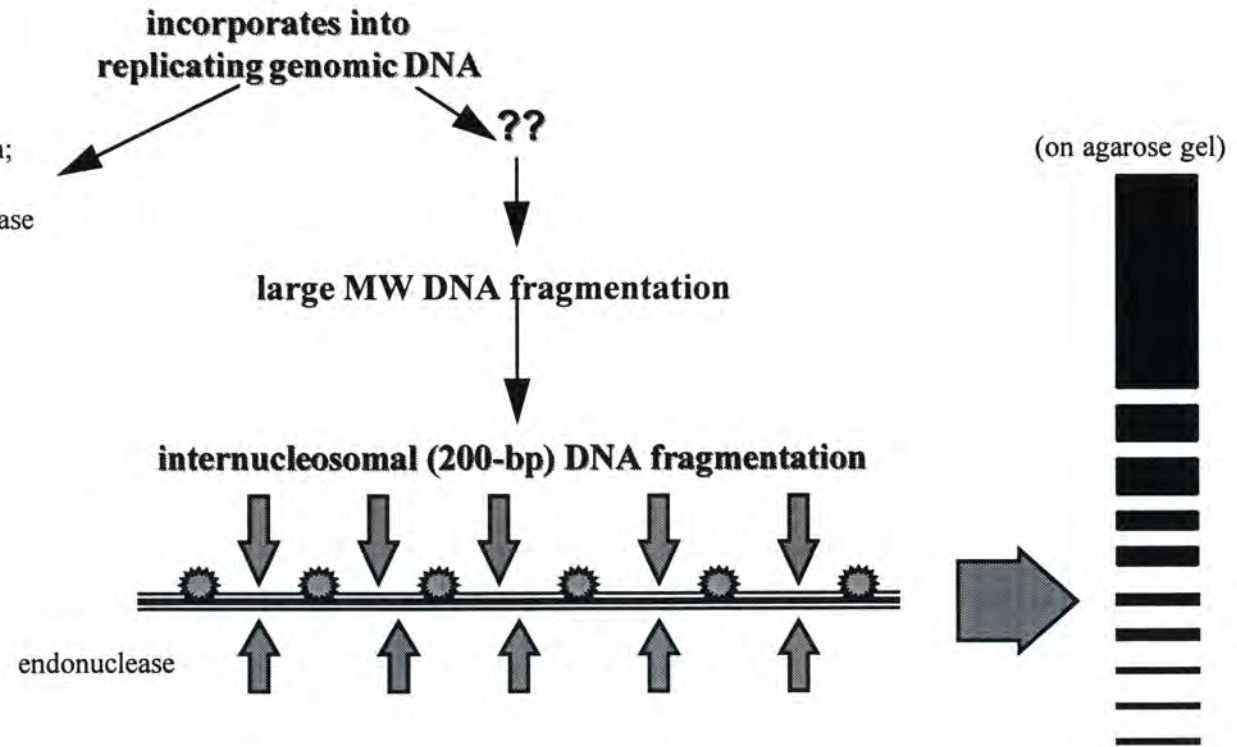
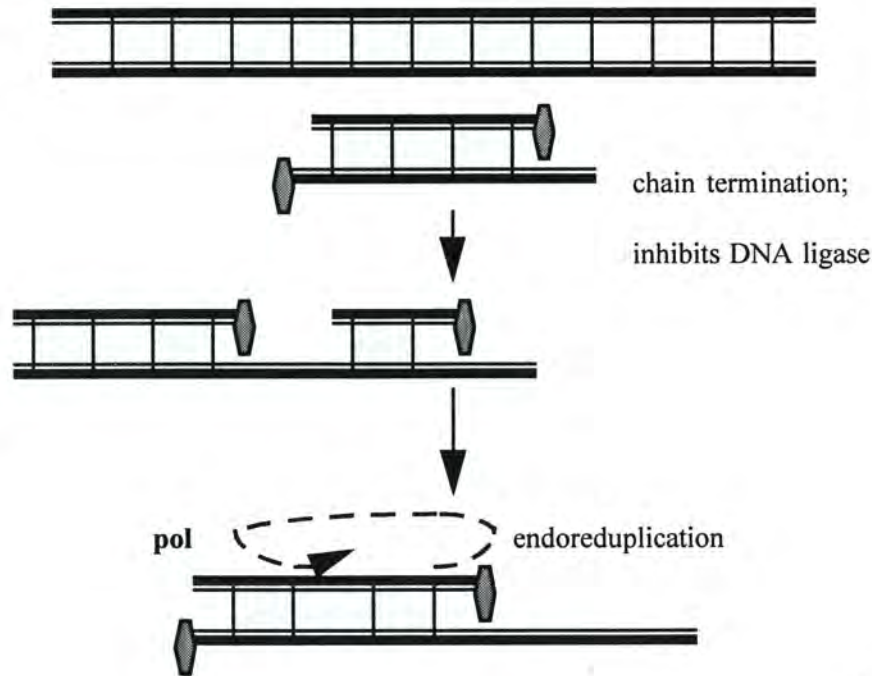
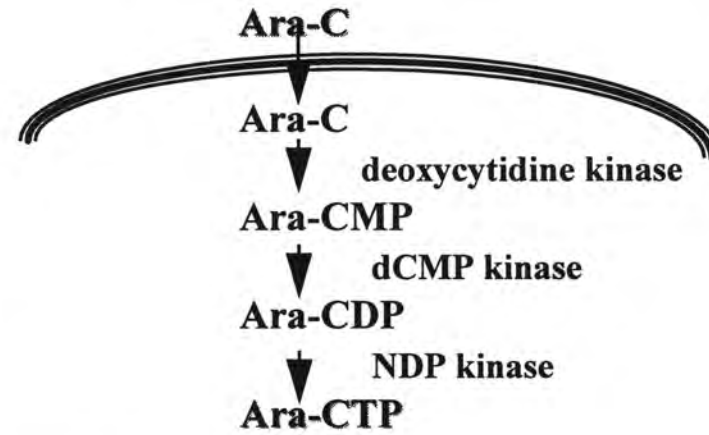
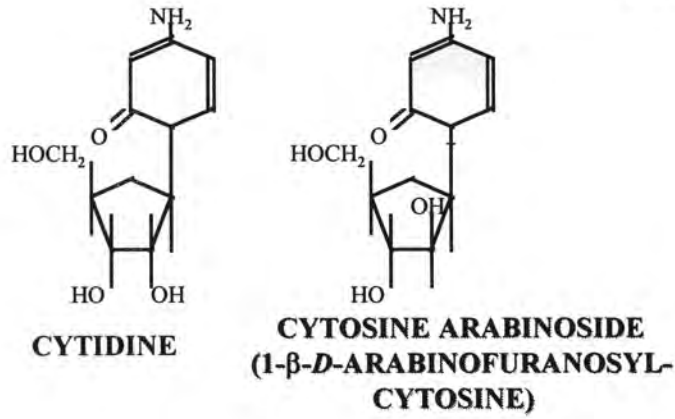
Figure 8:

Schematic diagram of Ara-C-induced DNA damage and regulation of the endpoints of apoptosis by various gene products.

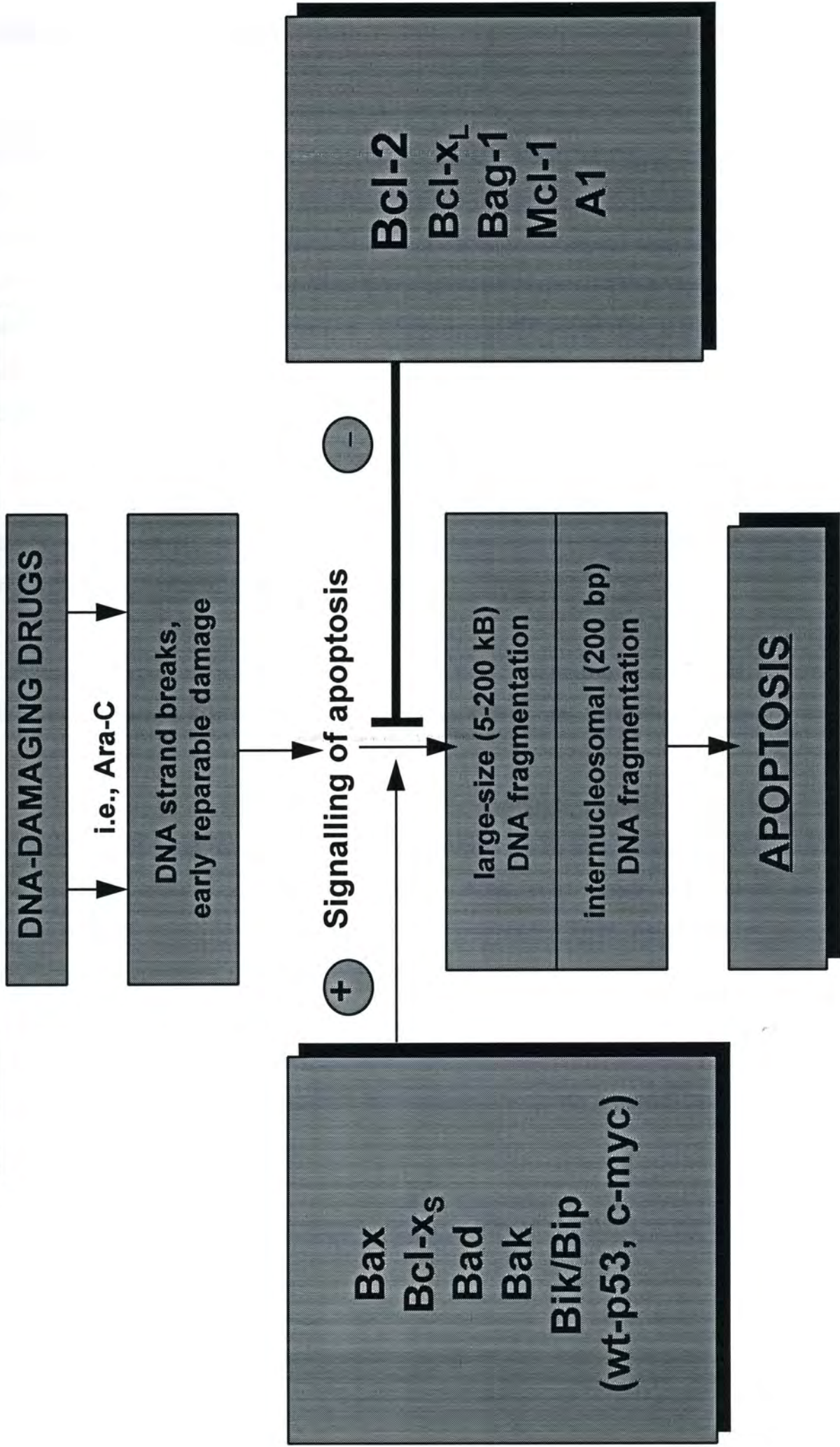
As mentioned in **Figure 7**, Ara-C causes single-strand damage to DNA upon incorporation into the DNA strand. How this single-strand DNA damage is translated into and progresses to the induction of double-stranded DNA damage associated with apoptosis, however, is unknown. The endonuclease(s) responsible for this double-stranded DNA damage are also controversial. The involvement of cysteine protease cascades in the progression of drug-induced apoptosis will be discussed later in this thesis.

Various gene products have substantial impact on the progression to drug-induced apoptosis, as listed above. However, how these gene products interplay in the signalling of apoptosis, and which types of DNA damage they affect is still under investigation.

Ara-C metabolism and mechanism of action
 After Kufe (1985) and Chabner (1990, 1996)



REGULATION OF APOPTOSIS:



E. Objectives of this dissertation.

Previous studies of Ara-C's mechanism of lethality in leukemia cells have only defined incorporation into DNA as the most important cytotoxic event, and have not defined the key lethally damaging event responsible for the induction of apoptosis by Ara-C. Likewise, since Bcl-2 is known to block double-strand DNA fragmentation associated with apoptosis, it would be worthwhile to further explore the other types of Ara-C-induced DNA damage which Bcl-2 can also potentially block as an explanation. The purpose of these studies is to further define the extent of Ara-C-induced cytotoxicity in AML cells, and to define the lethal events which occur with respect to relative Bcl-2 expression, since high Bcl-2 levels can affect treatment outcome (204). The overall objectives of this thesis are to use an *in vitro* human AML cell model to further examine the biochemical mechanisms underlying Ara-C-induced DNA damage, cytotoxicity, and apoptosis, as well as to examine how enforce high expression of p26Bcl-2 interferes with Ara-C-induced apoptosis.

The major hypothesis of these studies is that Bcl-2 overexpression in AML cells blocks total DNA fragmentation due to Ara-C. In this dissertation, the following hypotheses will be tested:

1. The metabolism of Ara-C to its lethal metabolite Ara-CTP, its incorporation into DNA and its ability to induced breaks in DNA, are similar in AML cells which overexpress Bcl-2 as compared to parental cells. However, the total double-stranded DNA fragmentation associated with Ara-C-induced apoptosis is blocked in AML cells which overexpress Bcl-2.
2. The intracellular p26Bcl-2 levels determines not only the initial amount of Ara-C-induced DNA damage but also the fate of residual DNA damage over time, which correlates with the survival of cells after Ara-C treatment.
3. Following Ara-C-induced DNA damage, unscheduled DNA repair synthesis will be higher in cells with higher Bcl-2 levels.

Hypotheses.

In **Chapter III (hypothesis #1)**, the metabolism of Ara-C is studied in AML cells with disparate levels of Bcl-2 expression, and the affectation of early targets of Ara-C are compared. In **Chapter IV (hypothesis #2)**, the level of Bcl-2 expression in AML cells is correlated with the fate of cells after Ara-C treatment. In **Chapter V (hypothesis #3)**, the possibility of increased repair of Ara-C-induced DNA damage in AML cells which overexpress Bcl-2 is examined in an attempt to explain the increased survival of these cells after Ara-C treatment. **The ultimate goal of these studies is to target specific sites in Bcl-2 mediated inhibition of Ara-C-induced apoptosis, in order to improve the antileukemic efficacy of Ara-C.**

CHAPTER II.

Development of an *in vitro* AML cell model.

CHAPTER II: DEVELOPMENT OF IN VITRO AML CELL MODEL:

A. Choice of a model cell line.

1. Expression of Bcl-2 and related proteins in AML cell lines.

The first goal for these studies was to transfect AML cells with the *bcl-2* cDNA and to achieve overexpression of p26Bcl-2. To select a suitable AML cell line for such a transfection, first *in vitro* AML cell lines were screened for their endogenous levels of expression of p26Bcl-2. One initial goal was to choose a cell line with the lowest endogenous Bcl-2 expression in order to facilitate overexpression. **Figure 9** shows a Western blot demonstrating p26Bcl-2 levels in several AML cell lines. For example, p26Bcl-2 was detectable in parental KG-1 (first lane), U937 (second lane), and HL-60 myeloid leukemia cells (fourth lane), but no p26Bcl-2 expression was detected in K562 chronic myeloid leukemia (CML) blast crisis cells (third lane). This suggested that K562 cells would be ideal for the transfection and overexpression of the *bcl-2* gene. However, despite undetectable p26Bcl-2 levels, K562 cells are extremely resistant to drug-induced apoptosis (201-203). **Figure 10** demonstrates that clinically achievable doses and schedules of Ara-C, taxol, and mitoxantrone readily induce internucleosomal DNA fragmentation and apoptosis in HL-60 cells, but not in K562 parental cells. To determine the mechanism underlying this, the expression of the *bcl-2* family of genes was examined in K562 cells. **Figure 11** shows that in contrast to HL-60 cells which are extremely sensitive to drug-induced apoptosis, K562 cells have high endogenous levels of *bcl-x_L* mRNA and p29Bcl-x_L protein (201-203, 270). The high expression of this *bcl-2* homolog, can suppress apoptosis to an equal if not greater extent than Bcl-2 (147). In addition, K562 cells contain the *bcr-abl* fusion gene from the t(9;22) translocation of CML. This has also been shown to suppress drug-induced apoptosis (67, 68). Therefore, overexpression of Bcl-x_L, together with *bcr-abl*, render K562 cells highly resistant to drug-induced apoptosis. Not being derived from CML, HL-60 cells do not possess p210*bcr-abl*. In addition, both HL-60 and K562 cells have deletions of the p53 tumor suppressor gene (271, 272). wt-p53 promotes, while mutated p53 confers resistance to apoptosis

(48-49, 57-59), and therefore p53 expressions would not interfere in subsequent apoptosis studies. Although U937 cells have less p26Bcl-2 expression than either KG-1 or HL-60 cells, however, unlike these two cell lines, they are also described by the American Tissue Culture Collection (ATCC) as histiocytic lymphoma cells. Thus they would not be considered as representative of AML cells. Therefore, HL-60 cells appeared to be the best overall candidate cells to use for the proposed studies. **To summarize, HL-60 cells have: a) detectable Bcl-2 levels; (b) absence of Bcl-x_L expression; (c) absence of p53; and (d) are sensitive to drug-induced apoptosis.**

2. HL-60 cell line.

HL-60 is a growth-factor independent immortal suspension culture cell line originally cultured by Collins *et al.* (273). The cells were derived from peripheral blood leukocytes obtained from a 36-year-old Caucasian female diagnosed with acute promyelocytic leukemia (274). HL-60 cells indeed have distinct myeloid characteristics, and are phenotyped as expressing CD33 and CD38, but not CD34, unlike more primitive CD34+ AML stem cells of FAB class M1 or M2, which are capable of engrafting after transplantation into SCID mice (275). In addition, HL-60 cells lack specific lymphoid markers but express surface receptors for Fc fragment and complement (261). Approximately 5-10% of cultured HL-60 cells spontaneously differentiate beyond the promyelocytic stages, to become morphologically mature myelocytes, metamyelocytes, banded or segmented neutrophils (271, 273), and therefore represent a more committed progenitor cell later in myeloid development than stem cells themselves (please refer to **Figure 6**). Differentiation into granulocytes is further enhanced in HL-60 by the addition of polar-planar compounds such as dimethylsulfoxide (DMSO) (271, 276) and retinoic acid (277). In addition, naturally occurring compounds such as 1,25 dihydroxyvitamin D₃ can induce differentiation of HL-60, as well as normal bone marrow cells, into cells which exhibit monocytic characteristics (278, 279). Macrophage-like characteristics can be induced in HL-60 cells primarily by the phorbol ester tumor promoter 12-*O*-tetradecanoylphorbol-13-acetate (TPA), which causes HL-60 cells to become more adherent than HL-60 monocytes (271, 280, 281). Granulocytic differentiation of HL-60 cells, however, appears to be associated with greater loss of proliferative capacity of the induced cells than does monocytic differentiation (271).

HL-60 cells exhibit genomic aberrations with regard to at least three cellular oncogenes: *c-myc*, *N-ras*, and *p53* (271). HL-60 cells exhibit a 15- to 30-fold amplification of the *c-myc* gene as compared to normal cells (271, 282, 283) and, in the undifferentiated state, exhibit high levels of steady-state *c-myc* RNA (271). The *N-ras* oncogene has been identified in HL-60 cells as having a point mutation involving the second nucleotide of *N-ras* codon 61 (271, 284). This mutated *ras* gene in HL-60 cells has the ability to malignantly transform NIH3T3 fibroblasts in transfection assays (285). The expression of the tumor suppressor gene *p53* is absent in HL-60 cells because the *p53* locus on the short arm of chromosome 17 is extensively deleted (271, 286, 287). It is suggested that because *c-myc* and *p53* may share some physiologic functions, populations of HL-60 progenitors may have selected for cells harboring amplified *c-myc* in order to compensate for the loss of *p53* (271, 286).

Recently, it has been documented that true promyelocytic leukemias harbor a characteristic reciprocal chromosomal translocation t(15;17) involving the *RAR α* (retinoic acid receptor α) and *PML* gene, which encodes a putative zinc finger transcription factor (288-292). The resulting fusion protein PML/RAR α contains a mutated RAR α which affects the survival of myeloid precursor cells. PML itself has been shown to be a promoter-specific transcriptional repressor (292). HL-60 cells do not harbor this translocation and are sensitive to retinoic acid. Transfection of HL-60 cells with the *PML/RAR α* fusion transcript, however, was shown to inhibit granulocytic differentiation due to retinoic acid (291). In addition, transfection of *PML/RAR α* into U937 myeloid precursor cells was shown to cause loss of their capacity to differentiate when induced by vitamin D₃, and showed a higher growth rate due to reduced apoptotic cell death associated with terminal differentiation (289). Therefore HL-60 cells do not possess this additional regulator of apoptosis in APL, and are more correctly termed acute myeloid leukemia (AML) cells.

Figure Legends:

Figure 9: Expression of Bcl-2 in AML cell lines.

KG-1, U937, K562, HL-60 cells were obtained from the American Type Culture Collection (Rockville, MD). Total protein was extracted from each of the logarithmically growing cell lines, and 10 μ g from each was subjected to Western blot analysis for p26Bcl-2 expression as described in the proceeding methods. Blot represents experiments repeated three times, each with similar results.

Figure 10: Drug-induced internucleosomal DNA fragmentation in HL-60 and K562 cells.

Logarithmically growing HL-60 and K562 cells were either untreated (lanes 1 and 5, respectively) or exposed to 100 μ M Ara-C for 4 hours (Lanes 2 and 6), 500 nM taxol for 24 hours (lanes 3 and 7), or 1 μ M mitoxantrone for 1 hour (Lanes 4 and 8). At the end of these incubations, total genomic DNA was extracted for **Panel A**, or DNA-agarose plugs prepared for **Panel B**, from each sample, as described in the methods in the proceeding **Chapter III**. For analysis of internucleosomal DNA fragmentation in **Panel A**, 1 μ g of each was electrophoresed in 1.8% agarose/1X TAE gels. For analysis of high molecular weight DNA fragmentation in **Panel B**, field-inversion gel electrophoresis (FIGE) was performed. Gels were stained with ethidium bromide and photographed utilizing UV transillumination, and the film negatives used for the Figure. M represent a 123-bp DNA ladder (**Panel A**) or previously digested lambda DNA (**Panel B**) as markers. Gel represents results of three experiments, each with similar results.

Figure 11. Expression of Bcl-x_L in HL-60 and K562 cells.

Logarithmically growing HL-60 and K562 cells were either untreated (lanes 1 and 3, respectively) or exposed to 100 μ M Ara-C for 4 hours (lanes 2 and 4, respectively). At the end of these incubations, total RNA was extracted from each sample for Northern blot analysis presented in **Panel A**, as described in the methods of the proceeding **Chapter Four**, or total protein was extracted from each sample for Western blot analysis presented in **Panel B**, as described in the proceeding methods of this chapter. In contrast with HL-60 cells (lanes 1,2), K562 cells exhibit high endogenous levels of *bcl-x_L* mRNA, as demonstrated in **Panel A** (lanes 3 and 4), and high endogenous levels of p29Bcl-x_L protein (**Panel B**, lanes 3 and 4), which are not significantly altered by Ara-C treatment.

The *bcl-x_L* cDNA probe is a 700-bp *EcoRI* fragment in pSFFV-neo, and was the kind gift of Dr. Gabriel Nunez (University of Michigan, Ann Arbor, MI). Anti-Bcl-x antibody is a rabbit polyclonal antiserum, and is the kind gift of Drs. Stanislaw Krajewski and John C. Reed (LaJolla Cancer Research Foundation, LaJolla, CA).

Figure 9. Expression of p26Bcl-2 in AML cell lines.

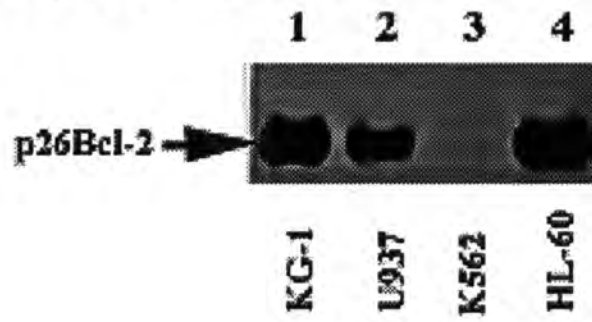
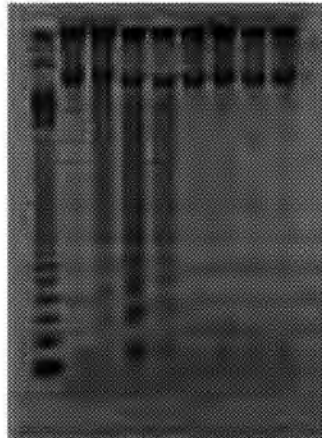


Figure 10.

A. HL-60 K562
M 1 2 3 4 5 6 7 8



B. HL-60 K562
M 1 2 3 4 5 6 7 8

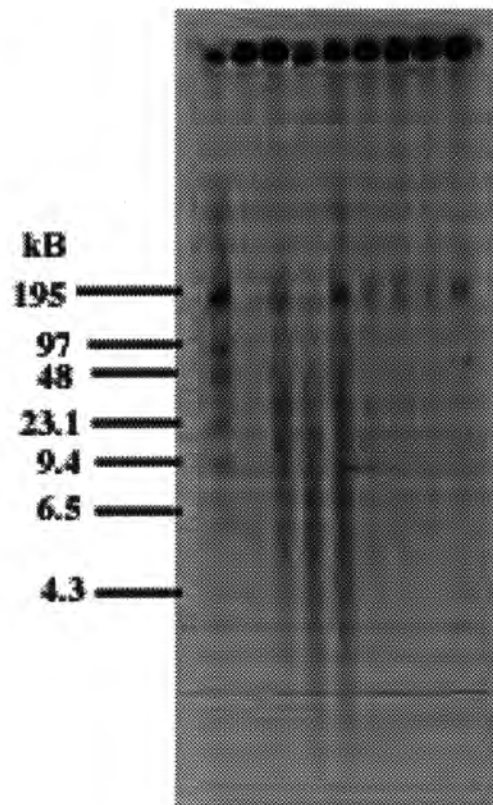
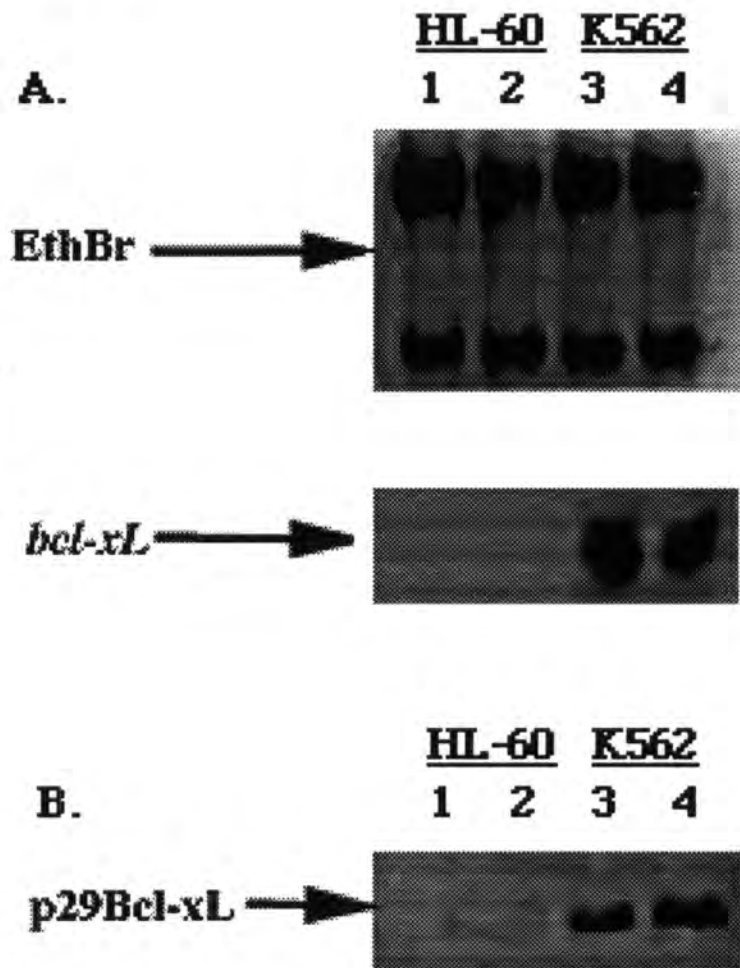


Figure 11.



B. The LacSwitch inducible mammalian expression system.

Introduction.

The first specific aim of these studies was to develop an AML cell model which stably overexpressed p26Bcl-2. To determine the direct effect of Bcl-2 overexpression on the biochemical and morphological features of Ara-C-induced apoptosis, a vector system of inducible *bcl-2* expression was originally chosen for this purpose.

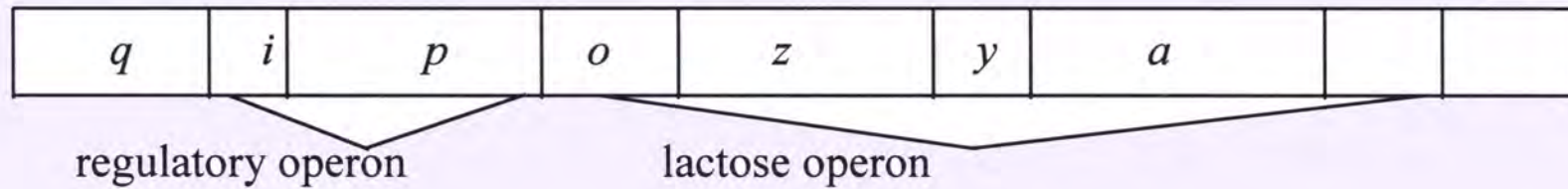
The Lac Switch Inducible Mammalian Expression System by Stratagene is a new vector system which has utilized elements of the specifically and elegantly regulated lactose operon from *E. coli*. In *E. coli*, the genes which govern the production of enzymes which metabolize sugars are under tight control. The lactose operon in *E. coli* consists of several genes in tandem, and include: three structural genes *lac Z*, *lac y*, and *lac a*, which code for enzymes involved in the transport and catabolism of lactose; a promoter gene *lac p*; an operator gene *lac o*; and a regulatory gene *lac i*, which codes for a lactose-operon repressor protein that binds to the operator gene (78, 293) (please see **Figure 12**). In the absence of extracellular lactose, the Lac repressor binds as a homotetramer to the lac operator, and therefore blocks transcription of the *lac Z*, *lac y*, and *lac a* genes, since no metabolism of lactose is necessary. When a physiologic inducer such as allolactose, or a synthetic inducer such as isopropyl- β -D-thiogalactoside (IPTG) bind to the Lac repressor, they cause a conformational change in the repressor and effectively decrease the affinity of the repressor for the operator. When the repressor is removed from the operator, transcription from the lactose operon resumes, the metabolizing enzymes are produced, and these sugars can be utilized by the *E. coli* cell (78, 293). This is a classic example of derepression as a mechanism for transcriptional regulation in biology.

In the vector system of Stratagene's LacSwitch Inducible Mammalian Expression System, the lactose operon elements have been modified, but the principle of "inducible" gene expression is unchanged. The gene of interest is inserted by cloning into either the eukaryotic pOPI3CAT or pOPRSVICAT vector, both of which contain the lac operator element. In addition, the separate eukaryotic vector p3'SS contains the Lac repressor element. The vectors each contain different antibiotic-resistant genes (please see **Figure 13**). Both vectors are transfected simultaneously, or sequentially (p3'SS followed by pOPI3 or pOPRSVI with the cDNA of interest into Lac repressor-positive cells) into a cultured cell line. The expression of the inserted

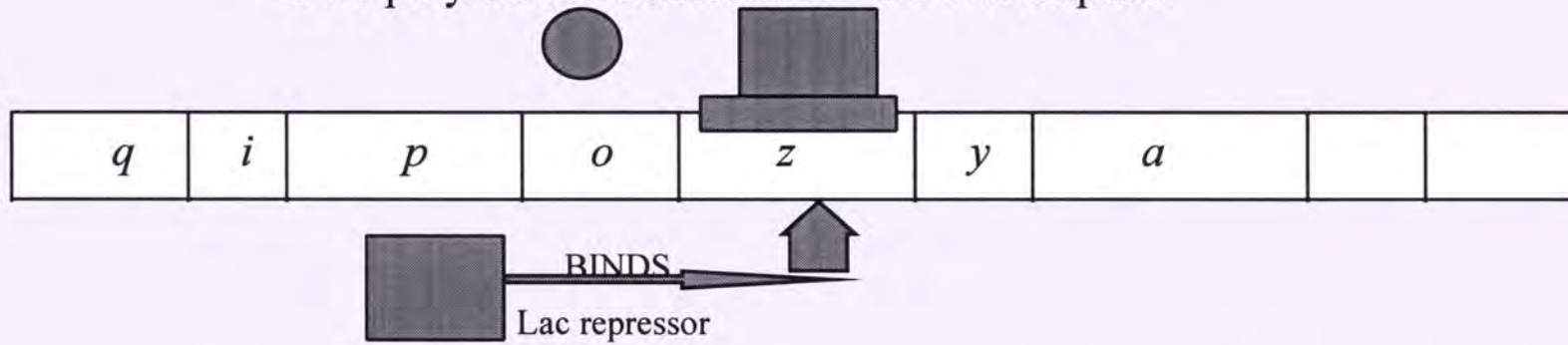
gene of interest is repressed until the nontoxic, rapidly transported and fast-acting inducer, IPTG, is added to the culture media. Upon induction, expression of the inserted gene should resume to a high level due to the relative strength of the RSV-LTR promoters present in the operator vectors. For use in the proposed studies, *bcl-2* cDNA was cloned into the pOPI3CAT vector. The p3'SS Lac repressor vector, and subsequently, the recombinant pOPI3-*bcl-2* vector were transfected into HL-60 cells. The resultant cells resistant to the individual selective antibiotics indicative of the presence of the vector system were tested for their usefulness as an AML cell model with sufficient overexpression of p26Bcl-2 to render the cells resistant to Ara-C-induced apoptosis.

Figure 12. **THE LACTOSE OPERON IN *E.coli*:**
after Cano and Colome' (ref 293)

1. The *lac* operon:



2. ABSENCE OF LACTOSE = REPRESSION OF LACTOSE OPERON:
RNA polymerase cannot bind = no transcription



3. PRESENCE OF LACTOSE = REPRESSOR CANNOT BIND = transcription proceeds

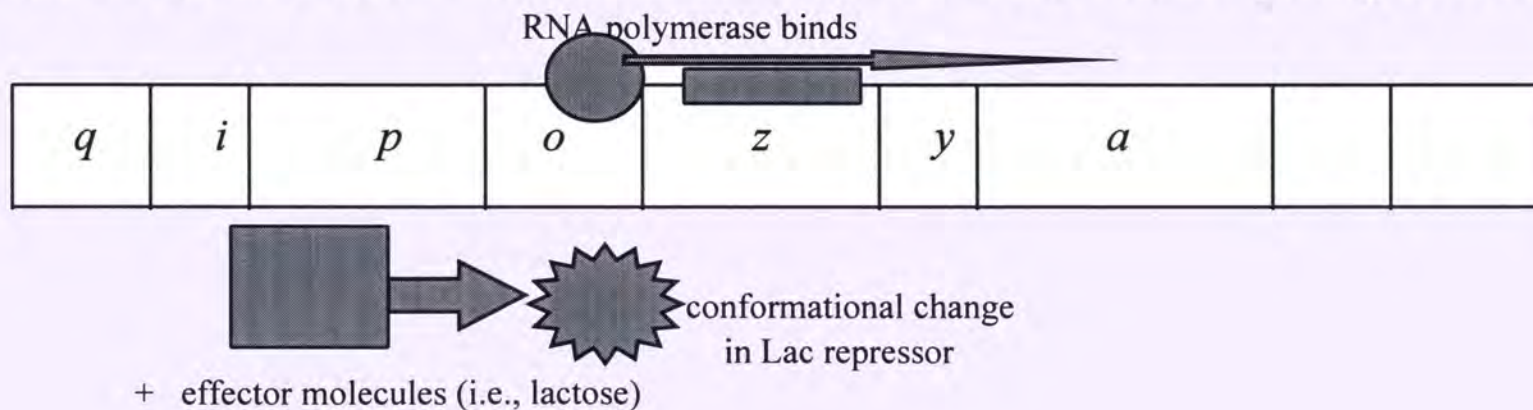
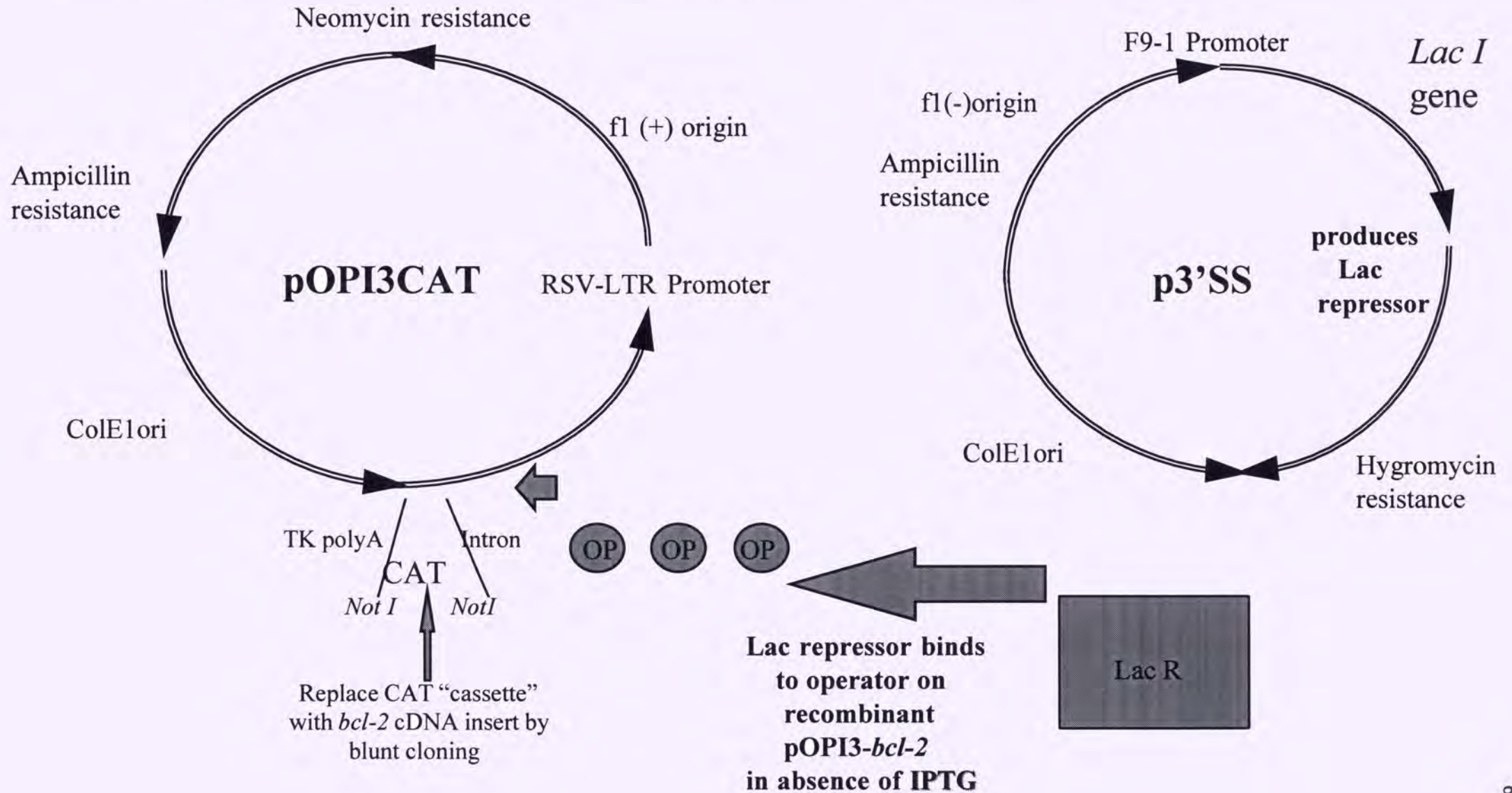


Figure 13.

LAC SWITCH INDUCIBLE MAMMALIAN EXPRESSION SYSTEM (Stratagene):



Materials and Methods:

•Cell line:

HL-60 cells were purchased from American Type Culture Collection (ATCC, Rockville, MD), and were continuously passaged in 1X RPMI 1640 media (GIBCO/BRL, Grand Island, NY) supplemented with 10% fetal bovine serum (Intergen). Logarithmically growing HL-60 cells were used for all proceeding transfections. Cell cultures were routinely tested for the absence of mycoplasma infection using fluorescent staining with 4',6-diamidine-2'-phenylindole dihydrochloride (DAPI, Boehringer Mannheim Corporation, Indianapolis, IN) and fluorescent microscopy.

•Cloning of *bcl-2* cDNA insert into pOPI3CAT vector:

The *bcl-2* cDNA was a 1.9 kb *EcoRI* insert in the pSFFV vector, and was a gift from Dr. Gabriel Nunez (University of Michigan, Ann Arbor, MI). The *bcl-2* cDNA insert was cloned into the *NotI* site of the pOPI3 vector after the CAT cassette was removed, and was ligated after the ends of both the insert and vector were rendered blunt by using the Klenow fragment of DNA polymerase I (New England Biolabs, Beverly, MA) and standard blunt cloning techniques (294). The blunt-cloning of the *bcl-2* cDNA insert into the pOPI3 vector was facilitated by the use of calf intestinal alkaline phosphatase (New England Biolabs, Beverly, MA) on the linearized pOPI3 vector and T4 polynucleotide kinase (New England Biolabs, Beverly, MA) on the *bcl-2* cDNA insert. Ligation reactions were transformed into Epicurian Coli competent cells (Stratagene, LaJolla, CA), and clones positive for a *bcl-2* signal upon colony hybridization as outlined in Maniatis' manual (295) were analyzed for proper orientation of the *bcl-2* insert.

•DNA sequencing of recombinant pOPI3-*bcl-2* vector:

Dideoxy-sequencing by the recombinant pOPI3-*bcl-2* vector was accomplished using the Sequenase T7 DNA polymerase Version 2.0 kit (United States Biochemical, Cleveland, Ohio). Purified plasmid DNA was made single-stranded by incubation with 2 N NaOH and 7.5 M ammonium acetate, pH 7.0 at room temperature. The ethanol-precipitated, single-stranded DNA was then incubated with DMSO, and the following sequencing primers from the pOPI3 vector flanking the insertion site for the *bcl-2* cDNA :

5' (+) primer for pOPI3-*bcl-2*: (17-mer): 5'-CAAAGAACTGCTCCTCA-3'

3' (-) primer for pOPI3-*bcl-2*: (15-mer): 5'-ATTGCCGTCATAGCG-3'

The primers were allowed to anneal to the single-stranded templates at 65°C for 5 minutes, and the reactions allowed to cool slowly to room temperature. To the annealed template-primer were added 0.1 M dithiothreitol (DTT), Labeling Nucleotide Mix, 5 µCi [α -³⁵S] dATP, and diluted Sequenase Version 2.0 enzyme. The labeling reaction was allowed to proceed for 4 minutes at room temperature, at which time, 2.5 µl of each template was added to each of four tubes (G,A,T, or C) containing the appropriate dideoxy termination mixture. The termination reaction was incubated at 37°C for 5 minutes, mixed with stop solution (Sequenase kit), and electrophoresed on a 6% non-denaturing polyacrylamide gel (Gel-Mix 6, GIBCO/BRL, Grand Island, NY). The gel was dried and exposed to Kodak X-Omat film for autoradiography.

•Electroporation of Lac Switch vectors:

Both p3'SS and pOPI3-*bcl-2* vectors were purified over cesium chloride density gradients as described in Maniatis' cloning manual (296). 50 µg of the Lac repressor p3'SS vector, linearized with *Nhe I* (New England Biolabs, Beverly, MA), was electroporated into 5×10^6 logarithmically growing HL-60 cells using a BioRad Gene Pulser (capacitance 500 µF, voltage 0.30 kV/cm). HL-60/p3'SS cells were selected in 300 µg/ml hygromycin (Boehringer Mannheim, Indianapolis, IN) in 1X RPMI 1640 media supplemented with 10% fetal bovine serum. Resultant hygromycin-resistant HL-60 cells were then electroporated with 50 µg of the purified recombinant pOPI3-*bcl-2* vector, linearized with *Nhe I* (capacitance 500 µF, voltage 0.30 kV/cm). HL-60/p3'SS/pOPI3-*bcl-2* cells were then selected in 300 µg/ml hygromycin as well as 500 µg/ml G418 (Geneticin, GIBCO/BRL, Grand Island, NY). Resultant antibiotic-resistant cells were then tested for induction and overexpression of Bcl-2.

•Plating of transfected cells to obtain monoclonal populations:

HL-60 cells electroporated with both p3'SS and pOPI3-*bcl-2* vectors and growing in selective antibiotics were further subcloned by two methods to obtain monoclonal populations with homogeneous expression of the components of the Lac Switch system. First, transfected HL-60/p3'SS/pOPI3-neo (HL-60/neo) and HL-60/p3'SS/pOPI3-*bcl-2* (HL-60/Bcl-2) cells were plated in soft agar containing 50% 1X Minimal Essential Medium (MEM, Sigma, St. Louis,

MO), 30% FBS, and 10% conditioned medium from 5637 bladder carcinoma cell cultures (5637-CM) in 0.3% agarose, as well as the appropriate concentrations of selective antibiotics. After incubation at 37°C with 5% CO₂ for two weeks, individual colonies were plucked with sterile pipet tips and grown in liquid 1X RPMI 1640 medium supplemented with 10% FBS and the appropriate selective antibiotics. In addition, HL-60/p3'SS/pOPI3-*bcl-2* cells were serially diluted in 96-well plates to concentration of one cell per well in 1X RPMI 1640 medium containing 10% FBS plus the appropriate selective antibiotics. After two to three weeks, populations of cells growing from one original cell were used to screen for induction of Bcl-2 expression.

•Genomic DNA dot blot hybridization for presence of *bcl-2* insert:

Total genomic DNA was isolated from numerous HL-60/neo and HL-60/Bcl-2 clones growing in selective antibiotics as outlined in QIAamp Blood Kit (QIAGEN, Chatsworth, CA). The DNA was rendered single-stranded by incubating with 2 M NaOH for 5 minutes at 65°C, and then 3 M Ammonium acetate was added. The DNA solution was then adsorbed to nitrocellulose membranes through a slot-blot manifold under low vacuum. The dried, UV-cross-linked dot blot was then hybridized with the same 1.9 kb *bcl-2* cDNA insert used in cloning into the pOPI3 vector, labelled with [α -³²P]dCTP by nick translation (GIBCO/BRL, Grand Island, NY). After hybridization in a 10% dextran sulfate/0.1% SDS/50% formamide mixture containing denatured salmon testes DNA (Sigma Chemical Co., St. Louis, MO) for 20 hours at 42°, the dot blots were washed with 0.2X SSC, 0.1% SDS solutions at 42°C, and then exposed to Kodak X-Omat films for autoradiography.

•Induction of p26Bcl-2 expression:

After selection of HL-60 clones in hygromycin and geneticin, cells were assayed for increased expression of p26Bcl-2 after addition of isopropylthiogalactoside (IPTG)(Stratagene) to the culture media. IPTG was used in increasing concentrations from 1 to 10 mM and for increasing durations ranging from 1 hour to 7 days continuous exposure.

• Western blot analysis for expression of Lac repressor and p26Bcl-2:

The expression of the Lac repressor as well as p26Bcl-2 were determined by Western blot analysis using specific antibodies, according to a previously described method (297). Total protein was extracted from HL-60/neo and HL-60/Bcl-2 cells with an extraction buffer containing 150 mM NaCl, 10 mM Tris-HCl, pH 7.4, 5 mM EDTA, 1.0% Triton X-100. Appropriate protein amounts (50 µg for p38Lac repressor, 10 µg for p26Bcl-2) were subjected to 10% sodium dodecyl-sulfate polyacrylamide gel electrophoresis. After electrophoresis, proteins were transferred to nitrocellulose sheets (0.5 A at 100 V, at room temperature) for 16 hours. The blots were blocked in 5% nonfat dry milk solution for 3 hours at room temperature with gentle shaking (5% nonfat milk [wt/vol]/phosphate-buffered saline [PBS]/0.2% sodium azide, pH 7.4). This was followed by incubation with the following specific antibodies for 3 hours at room temperature: 1:1000 dilution of polyclonal rabbit antiserum to the Lac repressor (Stratagene, LaJolla, Calif.); 1:260 dilution of a mouse monoclonal anti-Bcl-2 antibody (type #124, DAKO Corporation, Carpinteria, Calif.), described later. After washing with nonfat dry milk/PBS/sodium azide solution, the blots were further incubated with anti-rabbit or anti-mouse peroxidase-conjugated secondary IgG antibodies, respectively. Immune complexes were detected with an enhanced chemiluminescence detection method by immersing the blots for one minute in a 1:1 mixture of ECL chemiluminescence reagents A and B (Amersham, Amersham, UK) and then exposing to Kodak XCL film for a few seconds.

• **Drugs.** Ara-C was purchased from Sigma Chemical Co. (St.Louis, MO). Ara-C was stored as powder at 4°C, and freshly prepared by dissolving in medium and sterilizing through 0.22 µm syringe filter (Millipore, Cambridge, MA).

• **Morphology of Apoptotic Cells.** After treatment with or without Ara-C 50×10^3 HL-60/neo or HL-60/Bcl-2 cells were washed with PBS, pH 7.3 and resuspended in the same buffer. Cytopsin preparations of the cell suspensions were fixed and stained with Wright stain. Cell morphology was determined by light microscopy. Five different fields were randomly selected for counting at least five hundred cells. Percentage of apoptotic cells was calculated for each experiment. Cells designated as apoptotic were those which displayed the characteristic morphologic features of apoptosis including cell volume shrinkage, chromatin condensation, and the presence of membrane-bound apoptotic bodies (8).

Results:

The *bcl-2* cDNA insert was cloned into the lac-operator-containing pOPI3CAT vector by standard blunt cloning techniques, enhanced by dephosphorylating the linearized vector, and by phosphorylating the *bcl-2* insert. When the DNA of transformed bacterial clones positive for the presence of the *bcl-2* insert by colony hybridization was screened for the orientation of the *bcl-2* insert, restriction enzyme analysis confirmed the presence of the *bcl-2* insert in the pOPI3 vector by size when subjected to 1.8% agarose gel electrophoresis. Specific restriction enzyme tests were designed based on the cDNA sequence of *bcl-2* and the unique sites in the pOPI3 vector. After restriction enzyme digestion and electrophoresis, positive bacterial clones were chosen in which the fragments released from the candidate recombinant plasmids were of the predicted sizes for a recombinant plasmid containing the *bcl-2* insert in the proper sense, or forward, orientation. Sequence analysis of the positive recombinant plasmids with the *bcl-2* insert in the sense orientation further confirmed the presence of the *bcl-2* insert, the proper sense orientation, and in addition, that the open reading framed was intact.

These positive recombinant plasmids were transfected into HL-60/p3'SS cells positive for the expression of the 38 kD Lac repressor, as shown in **Figure 14, panel A**. Purified and linearized recombinant pOPI3-*bcl-2* vector was then transfected into these HL-60/p3'SS cells, and when the genomic DNA of several resultant antibiotic-resistant populations were screened for presence of the *bcl-2* insert, those with the highest intensity of signal (see **Figure 14, panel B**) were used for further induction studies. Western blots for p26Bcl-2 expression were performed after incubation of both HL-60/neo and HL-60/Bcl-2 cells after various incubations with 1 to 10 mM IPTG for several (1 to 8) hours to several (1 to 7) days. These IPTG inductions were attempted in clonal populations which had grown from total suspension cultures immediately after electroporation, as well as those plucked from soft agar culture and those grown from limiting dilution of suspension culture cells. Only slight if any increase in expression of p26Bcl-2 was observed in over 100 HL-60/Bcl-2 clones over that of HL-60/neo cells, as shown in a representative Western blot (**Figure 14, Panel C**). Of importance is the slight, if any, increase in p26Bcl-2 expression induced by IPTG in the last lane of this Western blot of HL-60/Bcl-2 clones. When this one clone exhibited an increase in p26Bcl-2 expression, the clone was tested for its resistance to Ara-C-induced apoptosis by incubating the clonal population with 100 μ M Ara-C for 4 hours at 37°C, after which time, microscope slides were

prepared of the drug-treated cells and stained with Wright-Geimsa stain. It was observed that despite this increase in p26Bcl-2 level, these HL-60/Bcl-2 were not resistant to Ara-C-induced apoptosis, and exhibited the morphologic features of apoptosis to the same extent as identically treated HL-60/neo cells.

Discussion:

In order to develop an AML cell model which stably overexpresses p26Bcl-2, the Lac Switch Inducible Mammalian Expression System was used to transfect HL-60 cells with the *bcl-2* cDNA. Attempts were made to induce p26Bcl-2 to a sufficiently high level to protect them from Ara-C-induced apoptosis. However, in over 100 HL-60/Bcl-2 positive clones incubated with various doses and exposures of IPTG, markedly higher expression of p26Bcl-2 was not achieved.

The Lac Switch inducible mammalian expression system is theoretically an ideal system to induce controlled expression of a gene of interest and has been previously used successfully (298). It is, theoretically, an invaluable tool for the study of a gene in comparison to a control model system which has little or no expression of the gene of interest, as is demonstrated in the studies by Lin and Lane. Utilizing this system, they showed that the expression of CCAAT/enhancer binding protein α was turned on or off in adipocytes. The system also has the potential to produce stable clones with induction levels of 20- to 95-fold over basal expression of the gene of interest, as documented by Stratagene. This, however, could not be achieved in HL-60 cells which had been transfected with p3'SS plus pOPI3-*bcl-2*.

The problems that were encountered with the Lac Switch Inducible Mammalian Expression System in HL-60 cells, can be summarized as follows: (a) The stability of expression and integration of the operator and/or the Lac repressor in AML model was variable, as evidenced by inconsistency of the *bcl-2* signal from one clone to another. This was seen when genomic DNA dot blots were probed. Also, an inconsistency of the expression of the Lac repressor was observed over time. (b) The concentrations of IPTG needed to optimally induce the expression of

the *bcl-2* gene in HL-60 cells could not be defined. (c) The ability of increasing IPTG concentrations to correspondingly increase p26Bcl-2 expression and, in turn, modulate apoptosis, could not be successfully determined. (d) The appropriate IPTG concentrations necessary to maintain high levels of p26Bcl-2 for prolonged intervals to demonstrate their biological effect was unsuccessful. (e) The number copies of the *bcl-2* cDNA of interest to be delivered by the operator vector into the target cells could not be ascertained.

In conclusion, several attempts to optimize the Lac Switch inducible mammalian expression system for the induction of graded overexpression of p26Bcl-2 were unsuccessful for the various reasons detailed above. In addition, the Lac Switch system was considered not suitable for the purpose of sufficiently overexpressing p26Bcl-2 levels above endogenous levels in HL-60 cells to protect these cells from Ara-C-induced apoptosis. Furthermore, the Lac Switch system was considered not suitable for the purpose of generating different levels of p26Bcl-2 expression in the same clones of HL-60 cells, by utilizing different levels of IPTG, in order to specifically study the effects on Ara-C metabolism, DNA damage and repair, and apoptosis. Hence, this avenue of research targeted to develop an inducible *bcl-2* expression in HL-60 cells was abandoned.

Figure Legend:

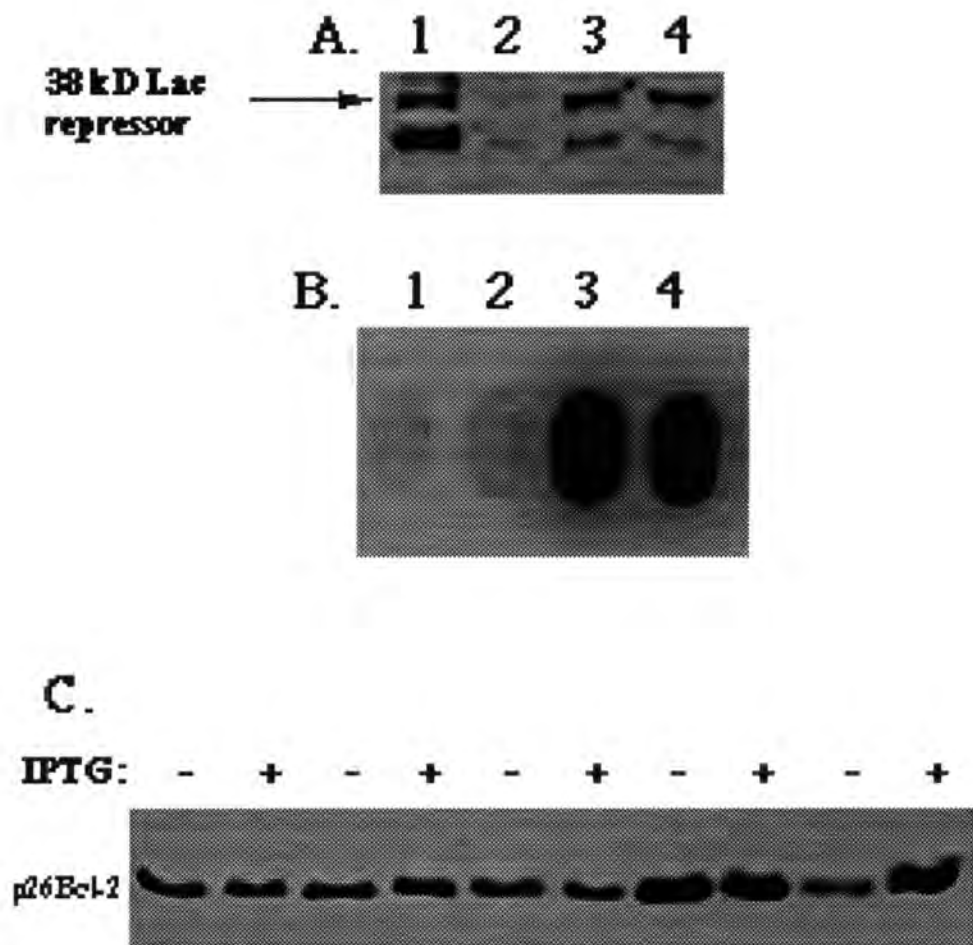
Figure 14: Selection of transfected HL-60 clones positive for expression of both components of the LacSwitch system and attempts toward induction of overexpression of p26Bcl-2.

Panel A shows Western blot analysis of HL-60 cells transfected with p3'SS utilizing rabbit polyclonal antiserum for the Lac repressor. In Lane 1 is 10 µg total protein from *E. coli* strain JM-110 as a positive control. In Lane 2 is 50 µg total protein from HL-60 parent cells. Lanes 3 and 4 contain 50 µg total protein from two populations transfected with p3'SS.

Panel B shows a genomic DNA dot blot hybridized with *bcl-2* cDNA to test for the presence of *bcl-2* after transfection of pOPI3-*bcl-2* into positive HL-60/p3'SS cells chosen from results in Panel A. 10 µg genomic DNA are probed from the following cell lines: HL-60 parental cells (lane 1); HL-60/p3'SS cells (lane 2); HL-60/p3'SS/pOPI3-*bcl-2* cells (lanes 3,4).

Panel C shows Western blot for p26Bcl-2 induction in positive HL-60/p3'SS/pOPI3-*bcl-2* transfectants chosen from results in Panel B. 5 µg total protein were analyzed from several recombinant clonal populations after incubations with 5 mM IPTG for 3 days.

Figure 14.



C. Retroviral-mediated transfer of *bcl-2* cDNA to HL-60 cells.

Introduction.

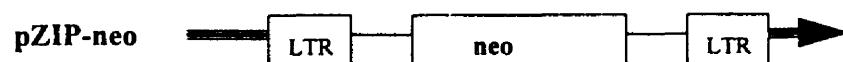
An alternative technique of retroviral-mediated transfection of HL-60 cells with *bcl-2* cDNA was found to be successful in producing a new HL-60 cell line which stably overexpresses p26Bcl-2.

Materials and Methods:

• **Retroviral Constructs and Transfection of HL-60 Cells.** HL-60 cells were maintained in suspension culture in RPMI 1640 medium (GIBCO/BRL, Grand Island, NY), supplemented with 10% fetal bovine serum, as described in Part One. As described below, HL-60 cells were transfected with cDNA of the *bcl-2* gene and/or neomycin resistance gene transduced from recombinant retroviruses. Recombinant expression plasmids pZIP-*bcl-2* and pZIP-*neo* were constructed and packaged as infectious amphotrophic retroviruses using PA317 cells, as previously reported (78, 98, 299), and were the kind gifts of Drs. Toshiyuki Miyashita and John C. Reed (LaJolla, CA). The pZIP constructs contain long-terminal repeats (LTR) from the murine Maloney leukemia virus, and the *gag*, *pol*, and *env* genes were replaced by cloning techniques with the neomycin resistance gene alone or in tandem with a 910-bp *bcl-2* cDNA (98) corresponding to the open reading frame of the *bcl-2* α cDNA sequence from -57 to +800 relative to the ATG start site (300).

Retroviral constructs contained in PA317 packaging cells used to transfect HL-60 cells:

pZIP-*neo* construct



pZIP-*bcl-2* construct



• summarized from Miyashita and Reed (98)

1×10^5 /ml HL-60 cells were incubated with fresh filtered supernatant from confluent high titer producing PA317 cells containing either pZIP-*bcl-2* or pZIP-*neo* recombinant retroviruses for 3 days at 37°C, 5% CO₂. The fresh supernatant was replenished every 12 hours, and retroviral transfer was theoretically enhanced by further supplementation of the cultures with 20% FBS to enhance cell cycling and 6 μ g/ml polybrene (Sigma) to provide electrostatic “bridges” across the

target cell membranes (301). HL-60/neo and HL-60/Bcl-2 cells were then selected by growth for two weeks in fresh medium containing 500 $\mu\text{g/ml}$ G418 (Geneticin, GIBCO/BRL).

HL-60/Bcl-2 cells were further subcloned to homogeneity of expression by serially diluting 100,000 logarithmically growing transfected cells in 96-well plates to a concentration of one cell per well in RPMI 160 medium containing 10% FBS plus 500 $\mu\text{g/ml}$ G418. After two to three weeks, populations of cells growing from one original cells were screened for homogeneity of p26Bcl-2 expression utilizing immunofluorescence microscopy as described.

• **Immunofluorescent Analysis of Bcl-2 Expression.** Immunofluorescent analysis of p26Bcl-2 in HL-60/neo and HL-60/Bcl-2 cells was performed as previously described (146). HL-60/neo and HL-60/Bcl-2 cells were attached to 35-mm-diameter sterile culture dishes with poly-L-lysine (Sigma). After fixation in 3.7% formaldehyde/PBS, the cells were incubated with a 1:260 dilution of DAKO type #124 mouse monoclonal anti-Bcl-2 antibody in 1% BSA/0.1% saponin/PBS, and the signal amplified by incubations with goat anti-mouse secondary IgG followed by rabbit anti-goat secondary IgG antibodies, both conjugated to rhodamine (Jackson Immuno Laboratories, West Grove, PA) (1:1000 dilutions in 1% BSA/0.1% saponin/ PBS). The specific anti-Bcl-2 antibody was raised against Bcl-2 amino acids 41-54, an epitope common to both Bcl-2 α and Bcl-2 β , as previously described (146, 302, 303). Dishes of stained cells were examined for Bcl-2 expression by using a Zeiss Axioplan microscope equipped with an MC-100 camera exposure system, a 63x planapochromat objective lens (N.A. 1.4), an EMI photomultiplier (Model 9658R, EMI Gencom, Plainview, NY) operated at 1 kV, and a Keithley Model 480 picoameter (304).

• **Western Blot Analysis of p26Bcl-2, p21Bax, and p29Bcl-x_L Oncoprotein Expressions.** The expression of p26Bcl-2, p21Bax, and p29Bcl-x_L oncoproteins in untreated and Ara-C-treated HL-60/neo and HL-60/Bcl-2 cells were determined by Western blot analyses according to previously described method (Part B). A mouse monoclonal antibody to human Bcl-2 was used (type #124, DAKO Corporation, Carpinteria, CA), described above. Rabbit anti-Bax as well as anti-human Bcl-x antisera were also utilized, the kind gifts of Drs. Stanislaw Krajewski and John C. Reed (LaJolla, CA) (61, 151, 166). Briefly, for immunoblot analyses, total protein was extracted from cells with a buffer containing 150 mM NaCl, 10 mM Tris-HCl (pH 7.4), 5 mM EDTA, 1% Triton X-100. Appropriate amounts (10 μg for p26Bcl-2, 50 μg for p21Bax and

p29Bcl-x_L) were mixed with electrophoresis dye (100 mM Tris-HCl, pH 6.8, 0.2% SDS, β-mercaptoethanol, glycerol), subjected to sodium dodecyl sulfate-polyacrylamide gel electrophoresis (12.5% gel). After electrophoresis, proteins were transferred to nitrocellulose sheets (0.5 A at 320 V, at 4°C) for 3 hours. The blots were blocked in 5% nonfat dry milk solution for 3 hours at room temperature with gentle shaking (5% nonfat milk [wt/vol]/phosphate-buffered saline [PBS]/0.02% sodium azide, pH 7.4). This was followed by incubation with the respective antibody (anti-Bcl-2, 1:260 dilution; anti-Bax, anti-Bcl-x, 1:1000 dilution) at room temperature for 3 hours with gentle shaking, and then with anti-rabbit or anti-mouse peroxidase-conjugated secondary IgG antibodies. Immune complexes were detected with an enhanced chemiluminescence detection method by immersing the blot for one minute in a 1:1 mixture of chemiluminescence reagents A and B (Amersham, Amersham, UK), and then exposing to Kodak XCL film for a few seconds.

- **Ara-C.** Ara-C was purchased from Sigma Chemical Co. (St.Louis, MO). Ara-C was stored as powder at 4°C, and freshly prepared by dissolving in medium and sterilizing through 0.22 μm syringe filter (Millipore, Cambridge, MA).

- **Morphology of Apoptotic Cells.** After treatment with or without Ara-C 50 x 10³ HL-60/neo or HL-60/Bcl-2 cells were washed with PBS, pH 7.3 and resuspended in the same buffer. Cytospin preparations of the cell suspensions were fixed and stained with Wright stain. Cell morphology was determined by light microscopy, as previously mentioned. Cells designated as apoptotic were those which displayed the characteristic morphologic features of apoptosis including cell volume shrinkage, chromatin condensation, and the presence of membrane-bound apoptotic bodies (8).

Results:

Figure 15, Panel A, shows by immunofluorescence, subcellular distribution of Bcl-2 in HL-60/neo cells to be membranous in location, reflecting the reported distribution of Bcl-2 in the outer nuclear, endoplasmic reticulum, and outer mitochondrial membranes (72, 146, 303). **Panel B** shows immunofluorescent analysis for Bcl-2 expression in HL-60/Bcl-2 cells, in which the subcellular distribution of Bcl-2 is the same as in HL-60/neo cells, however, the intensity is approximately 6.3 times higher, as measured by the photographic apparatus on the fluorescent microscope. **Panel C** shows Western blot analyses for p26Bcl-2 and p21Bax expressions in HL-60/neo (lanes 1 and 2) and HL-60/Bcl-2 cells (lanes 3 and 4), either untreated (lanes 1 and 3) or exposed to 100 μ M Ara-C for 4 hours (lanes 2 and 4). These Western blot analyses demonstrate that Bcl-2 overexpression in HL-60/Bcl-2 cells is approximately 5- to 10-fold greater than that in HL-60/neo cells, and does not impact on the barely detectable levels of endogenous p21Bax expression. Although not shown, immunoblot analyses utilizing polyclonal anti-Bcl-x antibodies did not demonstrate any difference in p29Bcl-x_L or p20Bcl-x_S levels in HL-60/neo versus HL-60/Bcl-2 cells. In addition, both p26Bcl-2 and p21 Bax levels remain unchanged immediately following Ara-C treatment.

The preliminary test for sufficient protection of HL-60/Bcl-2 cells from the effects of Ara-C-induced apoptosis given the above mentioned level of p26Bcl-2 overexpression, was analysis of cellular morphology by light microscopy and Wright-Geimsa staining of Cytospin preparations. **Figure 16** clearly demonstrates that exposure of HL-60/neo cells to 100 μ M Ara-C, for 4 hours readily induces morphologic features of apoptosis (**Panel B**), including chromatin condensation and the budding of apoptotic bodies. However, the overexpression of Bcl-2 to approximately 6.3 times higher than the level in HL-60/neo cells indeed rendered HL-60/Bcl-2 cells resistant to the induction of morphologic features of apoptosis after the same Ara-C exposure (**Panel D**), and represents the successful generation of an in vitro AML model cell line which overexpresses intact and biologically functional p26Bcl-2. This population of HL-60/Bcl-2 cells was then utilized for the studies presented in this thesis, and the stable homogeneous overexpression of p26Bcl-2 in HL-60/Bcl-2 cells has remained consistent for well over one year.

Discussion:

Retroviruses are RNA viruses whose viral genes are converted into double-stranded DNA molecules by reverse transcription after penetration into a target host cell. This viral DNA then integrates into the host genome as an obligatory part of the viral replication process, and, as a result, the viral DNA becomes indistinguishable from other cellular genes (305). Retroviral gene transfer, therefore, has been optimized as a tool for introducing genes into cells. While electroporation or lipofection methods are reported to be among the most efficient and convenient methods of stable transfection of immortalized cell lines (306), it was found that biological infection of HL-60 cells with recombinant retroviruses, containing the neomycin-resistance gene with or without *bcl-2* cDNA, was superior for this particular cell line. This method, which increased the probability of stable integration of *bcl-2* cDNA into the genome of HL-60 cells by virtue of highly active LTR components of murine Moloney leukemia virus within the recombinant constructs (98, 307-309), generated a reliable and consistent cell model to use for all the studies presented in this thesis and beyond. While the manipulation of a retroviral vector to include the gene of interest is labor-intensive, the use of retroviral-mediated gene transfer to HL-60 cells proved to be, in this case, the most valuable and efficient tool toward generating the desired AML cell model which stably overexpresses p26Bcl-2 to high, biologically significant levels. Retroviral-mediated gene transfer to HL-60 cells has also been found to be successful by Collins *et al.* (310) and Naumovski and Cleary (94).

The use of retroviral-mediated gene transfer has great significance as a powerful tool in medicine. For example, cycling self-renewing bone marrow cells are important targets towards which therapeutic genes are delivered via retroviruses, because of the efficiency and broad host range of retroviruses (305). Retroviral-mediated *ex vivo* transfer of the adenosine deaminase (ADA) gene to bone marrow cells has been successful, and is one of the classic therapies of a severe clinical immunodeficiency by gene transfer and subsequent transplantation (305, 311, 312). The transfer of clotting Factor IX gene and its production in skin fibroblasts by retroviruses has been proposed as potential gene replacement therapy for hemophilia B (313). Peripheral blood lymphocytes are also important targets for potential gene therapy, and have been studied as preclinical models for CD18- leukocyte adhesion deficiency (LAD), severe combined immunodeficiency (SCID), and acquired immunodeficiency syndrome (AIDS) (314).

Retroviral transfer of the human *mdr-1* (multidrug resistance 1 gene) has been demonstrated in murine bone marrow cells, and can confer drug resistance to populations of cells desired for enrichment (315, 316).

Most recently, transplantation of bone marrow cells transfected with *bcl-2* from retroviral constructs was demonstrated to enable recovery of myelopoiesis after etoposide-induced myelosuppression, and may provide an alternative to the supplemental administration of G-CSF (granulocyte colony stimulating factor) (99). The transfer of *bcl-2* to HL-60 AML cells presented in this dissertation represents a model by which retroviral-mediated transfer of *bcl-2* can also produce powerful protection against chemotherapy-induced cell death.

Figure Legends:

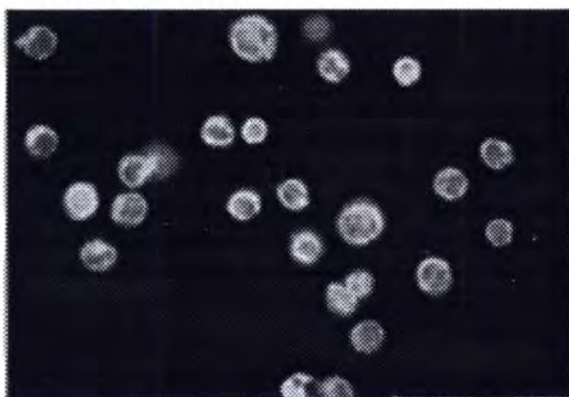
Figure 15. Immunofluorescent and Western blot analysis of retrovirally-transfected HL-60/neo and HL-60/Bcl-2 cells.

HL-60/neo (**Panel A**) and *bcl-2*-transfected HL-60/Bcl-2 cells (**Panel B**) were fixed and labelled for immunofluorescence using anti-Bcl-2 monoclonal antibody, as described in Materials and Methods. A significantly brighter and homogeneous cytoplasmic pattern of Bcl-2 localization can be seen in the cells in **Panel B** as compared to **Panel A**. **Panel C** shows Western analysis of p26Bcl-2 (upper panel) and p21Bax expressions (lower panel) in HL-60/neo (lane 1 and 2) and HL-60/Bcl-2 cells (lanes 3 and 4). Proteins in lanes 1 and 3 are from untreated control cells, while those in lanes 2 and 4 are from cells treated with 100 μ M Ara-C. 50 μ g total protein was used for both Western blots, and ECL exposure was 30 seconds. Data is representative of two individual experiments which yielded equivalent results.

Figure 16: Morphologic evidence of Ara-C-induced apoptosis in HL-60/neo versus HL-60/Bcl-2 cells. Microscope slides of HL-60/neo (**Panels A and B**) and HL-60/Bcl-2 (**Panels C and D**) were prepared as described in the methods section. **Panels A and C** represent non-apoptotic morphology in untreated HL-60/neo and HL-60/Bcl-2 cells, respectively. **Panel B** demonstrates the induction of apoptotic morphology, including nuclear condensation and apoptotic bodies in HL-60/neo cells treated with 100 μ M Ara-C for 4 hours (HIDAC). **Panel D** demonstrates that the induction of these features is blocked in HL-60/Bcl-2 cells exposed to the same dose and schedule of Ara-C.

Figure 1.

A. HL-60/neo CELLS: Control:



B. HL-60/Bcl-2 CELLS: Control:

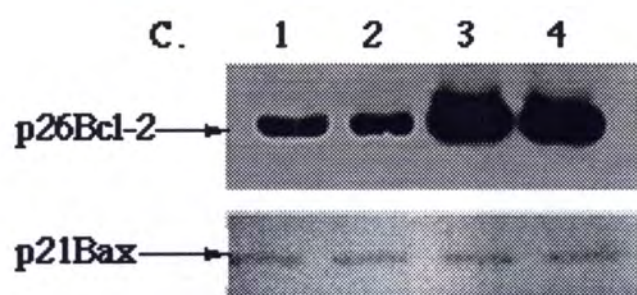
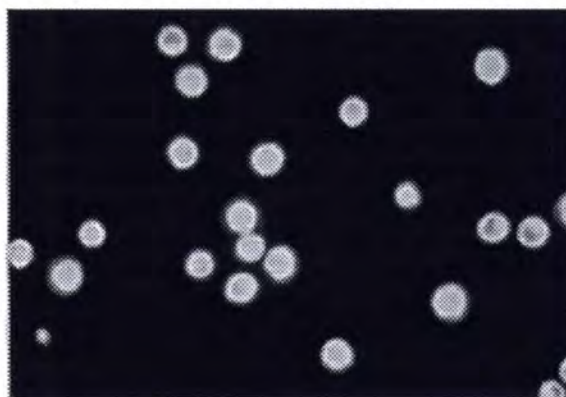
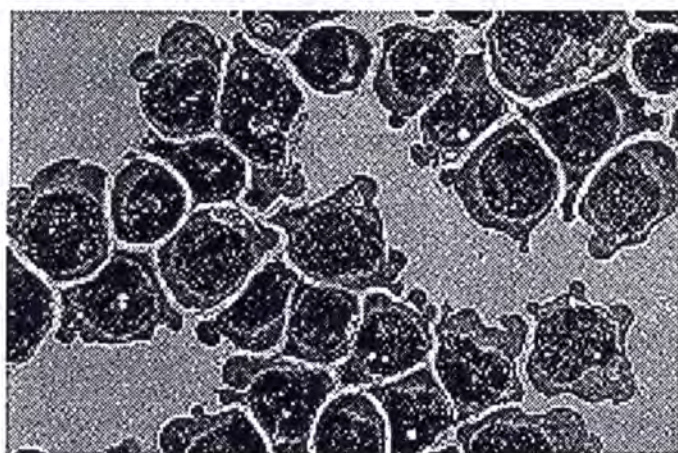
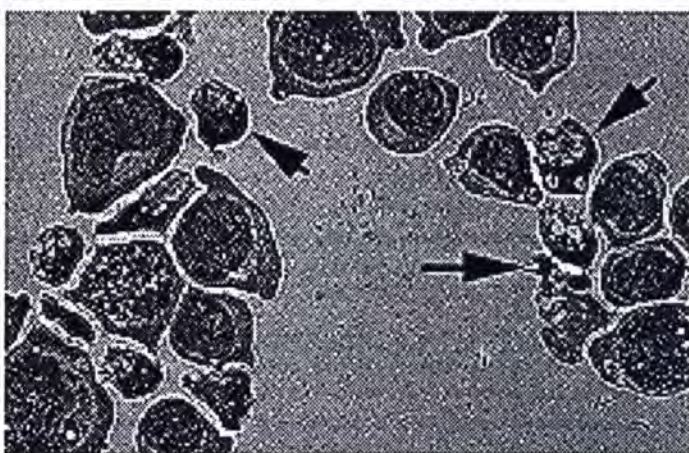


Figure 16.

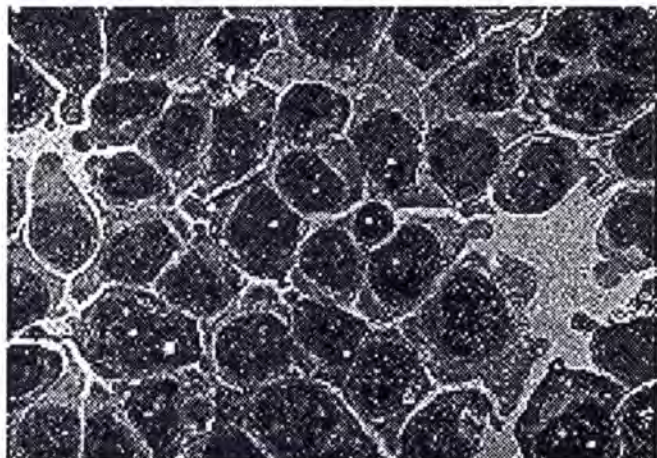
A. HL-60/neo control



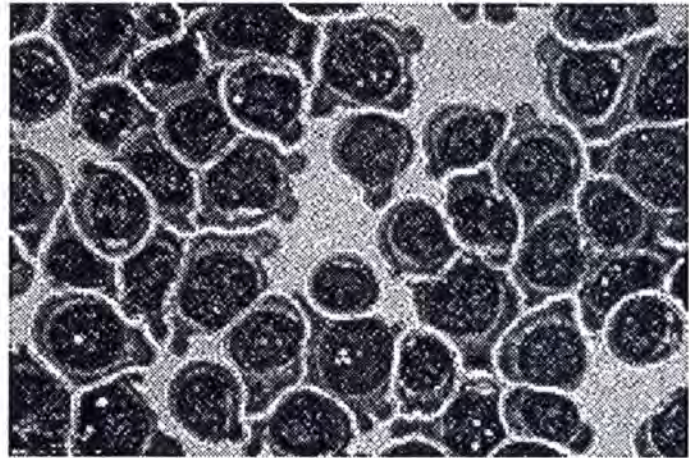
B. HL-60/neo + HIDAC



C. HL-60/Bcl-2 control



D. HL-60/Bcl-2 + HIDAC



CHAPTER III.

**Bcl-2 blocks Ara-C-induced DNA fragmentation
associated with apoptosis, but not early events
of intracellular Ara-C metabolism.**

CHAPTER III: Bcl-2 BLOCKS ARA-C-INDUCED DNA FRAGMENTATION ASSOCIATED WITH APOPTOSIS BUT NOT EARLY EVENTS OF INTRACELLULAR ARA-C METABOLISM.

Abstract

The effect of high intracellular levels of p26Bcl-2 in AML cells on the metabolism of high dose Ara-C (HIDAC) and Ara-C-induced strand breaks in genomic DNA, as well as the generation of large sized (5-300 kilobase) and internucleosomal DNA fragmentation associated with apoptotic cell death, were examined. For these studies, HL-60/Bcl-2 and HL-60/neo cells were created by retrovirally transfecting the human AML HL-60 cells with the pZIP-*bcl-2* and pZIP-*neo* plasmids, respectively. Western blot and immunofluorescent analyses demonstrated that, as compare to HL-60/neo, HL-60/Bcl-2 cells contained significantly higher (approximately 10 fold) p26Bcl-2 but equivalent and barely detectable levels of p21Bax and p29Bcl-x_L proteins. Exposure to HIDAC (10 to 100 μM for 4 hours) produced the lethal, kilobase-size, double-stranded DNA fragments and internucleosomal DNA fragmentation associated with apoptosis in HL-60/neo but not in HL-60/Bcl-2 cells. This was correlated with significantly greater loss of survival (by MTT assay), as well as flow cytometrically detectable and morphologically recognizable apoptosis of HL-60/neo cells. However, these effects were not accompanied by significant alterations in p26Bcl-2 levels in either of the cell types immediately following HIDAC treatment. Despite a striking reduction in apoptosis and the associated lethal DNA fragmentation, the intracellular accumulation of Ara-CTP relative to dCTP, Ara-C DNA incorporation and Ara-C-induced DNA strand breaks (by alkaline elution assay) were not significantly different between HL-60/neo and HL-60/Bcl-2 cells following exposure to HIDAC. These results indicate that in the presence of high intracellular levels of p26Bcl-2, neither the intracellular metabolism and DNA incorporation of HIDAC, nor the HIDAC-induced potentially reparable single strand DNA breaks are significantly prevented or impaired in HL-60/Bcl-2 cells. In contrast, the initiation of the final apoptotic cell death pathway associated with lethal, large-sized and internucleosomal DNA fragmentation is significantly inhibited in HL-60/Bcl-2 cells. This indicates a distally operative protective role of p26Bcl-2 in preventing the conversion of Ara-C-induced early DNA damage into lethal DNA fragmentation associated with apoptosis.

Introduction

Previous reports have demonstrated that following intracellular interaction with their molecular targets, anticancer drugs with diverse mechanisms of action engage the final common pathway of drug-induced apoptotic cell death (21, 23). A growing list of genes have been implicated in the regulation of drug-induced apoptosis, including *bcl-2*, *bcl-x*, *bax*, *bad*, and *p53* (60, 107, 147, 148, 170, 175, 317). The *bcl-2* gene, in particular, encodes for the p26Bcl-2 protein which is localized to the outer mitochondria membrane, endoplasmic reticulum, and nuclear envelope (72, 146, 303). High intracellular levels of p26Bcl-2 have been shown to suppress apoptosis due a variety of antileukemic drugs including cytosine arabinoside (Ara-C) (98, 100). The clinical relevance of these observations is further supported by the recent evidence that high levels of p26Bcl-2 in patient-derived AML blasts correlate with poor outcome following Ara-C based chemotherapy regimens (204). Furthermore, *in vitro* data indicate that the inhibition of *bcl-2* expression by antisense oligonucleotides results in improved antileukemic activity of Ara-C (205, 206).

Ara-C is the most commonly used agent in the treatment of AML (223). Intracellularly, Ara-C is phosphorylated to Ara-C triphosphate (Ara-CTP) which competes with normal dCTP for incorporation into DNA, and leads to the inhibition of DNA chain elongation and synthesis (223). However, previous studies have only correlated incorporation of Ara-C into DNA with the extent of its cytotoxicity in AML cells (231, 318). It is not clear how Ara-C DNA incorporation, which produces potentially reparable DNA strand breaks, triggers the generation of lethal double-stranded high molecular weight (5-300 kilobase) and internucleosomal DNA fragmentation associated with apoptosis (16, 22). Recently, Huang and Plunkett demonstrated that incorporation of nucleoside analogues into DNA is a critical event in fludarabine- and gemcitabine-induced apoptosis, when inhibition of incorporation into DNA by polymerase inhibitor aphidicolin blocked both fludarabine- and gemcitabine-induced high molecular weight and internucleosomal DNA fragmentation as well as apoptotic morphology in human T lymphoblastoid CEM cells (319). The studies presented in this thesis address whether Bcl-2 overexpression in HL-60 cells also blocks the ability of Ara-C to incorporate into and to affect its DNA target, and interferes in the metabolism of Ara-C leading up to early strand breaks which precede apoptotic cell death. In addition, in human pre-B leukemia 697 cells that had been retrovirally transfected with the cDNA of the *bcl-2* gene and over-expressed p26Bcl-2

(697/Bcl-2) cells, Ara-C-induced apoptosis was markedly inhibited, but the inhibition of cellular proliferation was not affected (98). However, in this study neither the expressions of other genes which regulate apoptosis, nor the intracellular metabolism of Ara-C was determined in 697/neo versus 697/Bcl-2 cells (98). Utilizing for the first time human myeloid leukemia HL-60 cells which have been retrovirally transfected with either the pZIP-*bcl-2* or pZIP-*neo* plasmids, the present studies examine the intracellular Ara-CTP accumulation relative to dCTP levels, Ara-C DNA incorporation, Ara-C-induced DNA strand breaks, and Ara-C-induced DNA fragmentation and apoptosis following treatment with high-dose Ara-C (HIDAC, 100 μ M Ara-C for 4 hours mimics clinically achievable doses of Ara-C). The aim of these studies is to define which of the known steps in Ara-C metabolism and DNA damage may be inhibited by Bcl-2 overexpression. An additional aim of these studies is to correlate the differences in Ara-C-induced apoptosis of HL-60/Bcl-2 versus HL-60/neo cells with the expression of other genes that are known to regulate drug-induced apoptosis.

Materials and Methods:

• **Drugs and Antibodies.** Ara-C was purchased from Sigma Chemical Co. (St.Louis, MO). Ara-C was stored as powder at 4°C, and freshly prepared by dissolving in medium and sterilizing through 0.22 μ m syringe filter (Millipore, Cambridge, MA), as described in **Chapter Two**. Mouse monoclonal antibody anti-Bcl-2 (type #124) was obtained from DAKO (Carpinteria, CA), and was previously described (146, 300, 301). Polyclonal rabbit antisera to human Bax and human Bcl-x proteins were the kind gifts of Drs. Stanislaw Krajewski and John C. Reed (LaJolla, CA).

• **Transfection of HL-60 Cells.** HL-60/neo and HL-60/Bcl-2 cells were generated by retroviral-mediated transfection of HL-60 parental cells with the neomycin resistance gene alone or in combination with *bcl-2* cDNA as described in **Chapter Two**. Subcloning of HL-60/Bcl-2 cells by limiting dilution generated various clones with disparate levels of homogeneous overexpression of p26Bcl-2, as described in **Chapter Four**. Clonal population B, which exhibited p26Bcl-2 expression 6.3 times greater than HL-60/neo cells by immunofluorescence (described in **Chapter Two**), was used for the studies presented in this chapter.

• **Detection of Internucleosomal Fragmentation of Genomic DNA by Agarose Gel Electrophoresis.**

Following incubations with Ara-C, total genomic DNA was extracted as described by Ray *et al.* (23). 1×10^6 control and Ara-C-treated HL-60/neo and HL-60/Bcl-2 cells were washed twice in warm phosphate-buffered saline and the cell pellets incubated with 200 mM NaCl, 10 mM Tris-HCl, pH 8.0, 40 mM EDTA, pH 8.0, 0.5% SDS, containing 200 ng/ μ l RNase A (Sigma), 10 U/ μ l RNase T1 (Sigma), for one hour at 37°C. This was followed by incubation with 200 mM NaCl, 10 mM Tris-HCl, pH 8.0 0.5% SDS, containing 125 ng/ml Proteinase K (Boehringer Mannheim, Indianapolis, IN), for 3 hours at 50°C. DNA was then extracted twice with phenol:chloroform (1:1) and precipitated with 10 mM MgCl₂, and two volumes of ethanol. Pelleted and dried genomic DNA was dissolved in 10 mM Tris-HCl, pH 8.0, 1 mM EDTA at 4° C for four days before spectrophotometric quantitation. 1 μ g genomic DNA for each condition was subjected to electrophoresis in 1.8% agarose at 30 V/cm. After electrophoresis, the gel was stained with 0.5 μ g/ml ethidium bromide, destained with distilled water, and photographed on a UV transilluminator. Subsequently, the negative was developed for the DNA profile.

• **Preparation of DNA Plugs and Field Inversion Gel Electrophoresis.**

Formation of large-sized DNA fragments was determined by a modification of previously described methods. (16, 320). Intact genomic DNA-agarose plugs were prepared from control and Ara-C-treated HL-60/neo and HL-60/Bcl-2 cells by gently mixing 2×10^5 cells in warm phosphate-buffered saline (PBS) with an equal volume of 1.5% InCert agarose (FMC BioProducts, Rockland, Maine) in prepared in L-buffer (0.1 M EDTA, pH 8.0, 0.01 M Tris-HCl. pH 7.6, 0.02 M NaCl). This mixture was used to prepare 10 μ l plugs on pre-labelled 35-mm petri dishes on ice, and allowed to solidify over 30 minutes. The solidified DNA-agarose plugs were incubated for 96 hours at 42°C with slow shaking in two changes of lysis solution containing 10 μ g Proteinase K/0.2% Sarkosyl in L-buffer. The lysis solution was then removed, and the plugs were incubated with 200 μ M phenylmethylsulfonylfluoride (PMSF, Sigma) in TE buffer twice for 1 hour each at 50°C, and equilibrated with TE buffer (321). The plugs were then inserted into the wells of a 1% (w/v) agarose gel (pulsed field certified, BioRad, Hercules, CA), sealed with molten agarose, and subjected to horizontal field-inversion gel electrophoresis (FIGE, a type of pulsed-field gel electrophoresis) in a BioRad apparatus. A FIGE program was specifically optimized to resolve

fragments 5-300 kilobase in size, employing 180 V forward/ 120 V backward pulses at increasing intervals from 0.4 to 3.5 seconds over 6 hours. Two set of marker DNA were used: lambda ladder for FIGE (BioRad) and lambda DNA digested with *Hind III* (Stratagene). After electrophoresis, the gel was stained with 0.5 µg/ml ethidium bromide, destained with distilled water, and photographed on a UV transilluminator. Subsequently, the negative was developed for the DNA profile.

• **Flow Cytometric Analysis of Apoptosis and Bcl-2 Levels.** The flow cytometric evaluation of Bcl-2 levels and apoptosis was performed according to a modification of a previously described method (322-324). Briefly, $2-3 \times 10^6$ untreated or drug-treated HL-60/neo and HL-60/Bcl-2 cells were centrifuged, washed in Hank's Balanced Salt Solution (HBSS) and fixed in 70% ethanol. The tubes containing the cell pellets were stored in -20°C for at least 24 hours. Following this, the cells were centrifuged at $800 \times g$ for 5 minutes to completely remove ethanol, and pellets were resuspended in 40 µl of Phosphate-Citrate (PC) buffer at room temperature for 30 minutes followed by washing with 1 ml 1.5% bovine serum albumin (BSA) in PBS. Subsequently, the pellets were incubated in 100 µl of diluted mouse anti-human Bcl-2 antibody (DAKO, type #124) (diluted 1:100 in 1% BSA/PBS) at 4°C overnight. On the following day, 4-5 mls of 1% BSA/PBS were added, the cells centrifuged and the resulting pellets resuspended in 100 µl goat anti-mouse FITC conjugated (Fab')₂ antibody fragment diluted 1:30 in 1% BSA/PBS and incubated for 30 minutes at room temperature in the dark. Following this incubation, the cells were washed with 4-5 mls of 1% BSA/PBS and stained with propidium iodide (20 µg/ml PI + 20 µg/ml RNase A) for 30 minutes. The samples were read on a Coulter Elite flow-cytometer using Elite Software program 4.0 for two-color detection. Bcl-2 expression was measured as mean fluorescence intensity and the percentage of cells in the apoptotic sub-G₁, as well as G₁, S, G₂/M phases of the cell cycle were calculated using Multicycle Software (Phoenix Flow Systems, San Diego, CA).

• **Morphology of Apoptotic Cells.** After treatment with or without Ara-C 50×10^3 HL-60/neo or HL-60/Bcl-2 cells were washed with PBS, pH 7.3 and resuspended in the same buffer. Cytopsin preparations of the cell suspensions were fixed and stained with Wright stain. Cell morphology was determined by light microscopy. Five different fields were randomly selected for counting at least five hundred cells. Percentage of apoptotic cells was calculated for each

experiment. Cells designated as apoptotic were those which displayed the characteristic morphologic features of apoptosis including cell volume shrinkage, chromatin condensation, and the presence of membrane-bound apoptotic bodies (8).

• **Assessment of Cytotoxicity by the MTT Assay.** The MTT assay for cell cytotoxicity was used as previously described (325, 326). The assay is based on the conversion of the yellow tetrazolium salt, 3-(3,5-dimethylthiazol-2-yl)-2,5-diphenyltetrasolium bromide (MTT) to a colored formazan product by mitochondrial enzymes in the viable cells. HL-60/neo and HL-60/Bcl-2 cells were incubated with or without Ara-C for 4 hours at 37°C. Subsequently, the control and drug-treated cells were washed, resuspended in drug-free medium, and 100 μ l aliquots of 40,000 cells per condition were dispensed into 96-well flat-bottomed microtiter plates (Costar) and incubated at 37°C for an additional 20 hours. At the end of this incubation, 50 μ l of a 5 mg/ml solution of MTT (Sigma, St. Louis, MO) was added to each well and the plates incubated for another 5 hours at 37°C. Next, the plates were centrifuged for 10 minutes at 500 x g. After removing the supernatants, the formazan crystals were dissolved with 150 μ l of a 1:1 DMSO/ethanol solution. The absorbance, A, of the wells was measured with a Titertek multiscan plate reader (Flow Laboratories, Finland) at 540 nm. The percentage of cell survival was defined as:

$$\text{mean A of treated wells/ mean A of untreated control wells} \times 100\%$$

• **Intracellular Ara-CTP and dCTP Level Determination by HPLC.** In extracts of 20×10^6 untreated and Ara-C-treated HL-60/neo and HL-60/Bcl-2 cells, the intracellular Ara-CTP and dCTP levels were determined by a High Performance Liquid Chromatography (HPLC) method as previously described (327, 328). Cell pellets were washed with ice-cold PBS, and resuspended in 10 μ l 25% perchloric acid. After incubation on ice and centrifugation for 10 minutes at 4000 rpm, the supernatants were mixed with 2 μ l phenol red and neutralized with 4 M KOH. Salts were precipitated from the extracts by centrifugation. Ribonucleotides were removed by periodation by the addition of an equal volume of NaIO₄, and 4 M methylamine. After mixing, the reactions were incubated at 37°C for 30 minutes. 3 μ l 1 M rhamnose was added to remove remaining IO₄⁻, and the samples were immediately put on ice. 100 μ M each of dCTP, Ara-CTP, and dTTP standards (Sigma, St. Louis, MO) were also prepared in distilled water for injection prior to sample analysis.

The Ara-C and deoxyribonucleotide triphosphates (AraCTP and dNTPs) were analyzed by an HPLC system (Waters Associates, Inc., Milford, MA). This was equipped with two model 6000A pumps, a Parsitil-10 SAX (Whatman Chromatography) anion-ion exchange column (250 x 4 mm), model 490 UV detector, and a Hewlett-Packard model 1084 data and chromatography control system. Cellular dNTPs and Ara-CTP were separated by injecting 250 μ l aliquots of standards or periodate-treated samples onto the column and run over 75 minutes at a flow rate of 3 ml/min. Elution was started with an initial buffer composition of 65% buffer A (0.005 M $\text{NH}_4\text{H}_2\text{PO}_4$, pH 2.8) and 35% buffer B (0.75M $\text{NH}_4\text{H}_2\text{PO}_4$, pH 3.7, Fisher Scientific Corp.) and ending at 100% buffer B. Retention times of nucleoside triphosphates were dCTP, 21.69 minutes; Ara-CTP 24.75 minutes; dTTP, 29.33 minutes, as derived from analysis of standards. The intracellular NTP concentration was calculated by dividing the NTP amount, reflected in the area counts under each NTP peak, by the number of cells analyzed and the mean cell volume, and was expressed as picomoles NTP per million cells.

• **[^3H] Ara-C DNA Incorporation.** Following treatment of HL-60/neo and HL-60/Bcl-2 cells with [^3H] Ara-C, extent of incorporation into DNA was determined as previously described (329). HL-60/neo and HL-60/Bcl-2 cells were incubated with 100 μM Ara-C (Sigma) plus 20 nM (0.5 Ci/ml) [5- ^3H] cytosine- β -D-arabinoside (specific activity 25 Ci/mmol, Moravек Biochemicals, Inc., Brea, CA). After incubation for 4 hours at 37°C, total genomic DNA was extracted for both HL-60/neo and HL-60/Bcl-2 cells as described above. 1 μg genomic DNA from each condition was measured in a scintillation counter for [^3H] signal, and the counts converted to molarity by comparison with levels of [^3H] counted in the original culture.

• **Measurement of DNA Damage by Alkaline Elution.** Ara-C-induced single-strand breaks in parental DNA were measured using the alkaline elution technique, described by Kohn *et al.* (330) and previously modified for the study of drug-induced DNA damage (242, 331). Logarithmically growing HL-60/neo and HL-60/Bcl-2 cells were co-incubated with 0.1 $\mu\text{Ci/ml}$ [methyl- ^3H] thymidine (specific activity 65.6 Ci/mmol, Moravек Biochemicals, Brea, CA) and 1.0 μM thymidine (Sigma, St. Louis, Mo) for 24 hours. Subsequently, the cells were washed and incubated in fresh medium (RPMI 1640 supplemented with 10% fetal bovine serum) for an additional 24 hours to chase the radioactive label into high molecular weight DNA. A 2-hour

incubation with 100 μM Ara-C was employed to optimize for the induction of single-strand DNA breaks and to avoid induction of double-strand DNA breaks associated with apoptosis (23), or the cells were irradiated for 50 seconds with 500 rads in a ^{125}Cs blood product γ -irradiator, to be used as positive controls for DNA damage. Control and Ara-C-treated cells were washed with cold media, and 10^6 cells were layered onto polycarbonate filters (0.2 μm -pore size, 47-mm diameter, Costar), placed on a Swinnex funnel apparatus. Cells were then lysed in the dark with 5 mls of a lysis solution containing 2% sodium dodecyl sulfate, 0.02 M Na_2EDTA , 0.1 M glycine, pH 10.0, allowed to flow through by gravity. After connecting the filters with tubing to the pump system, 5 mls of a Proteinase K solution (0.5 mg/ml in lysis solution, Boehringer Mannheim, Indianapolis, IN) were added to the funnels and allowed to contact the cells for 15 minutes. DNA was then eluted from the filters by pumping an elution solution (0.02 M EDTA solution adjusted to pH 12.1 with tetrapropylammonium hydroxide [Sigma, St. Louis, MO]) containing 0.1% sodium dodecyl sulfate through the filters at approximately 2 ml/hr using a Rabbit-Plus peristaltic pump (Rainin Instrument Co., Emeryville, CA). These conditions are optimized to assess single-strand DNA breaks in drug-treated cells. Three-hour fractions were collected in glass test tubes and processed as described (330). Filters were removed from the apparatus and incubated in scintillation vials with 1 ml 1.0 N HCl for one hour at 60°C, and then with an additional 6.25 ml 0.4 M NaOH for one hour at room temperature after vigorous shaking. Simultaneously, the elution apparatus was washed through with 10 mls 0.4 M NaOH in order to collect remaining uneluted DNA prior to the disassembly of the apparatus. One ml aliquots of each fraction, the NaOH wash, and the entire filters were mixed with 10 ml complete scintillation cocktail (Research Products International Corp., Mount Prospect, Illinois), and taken for counting in a liquid scintillation counter. The percentage of DNA remaining on the filter for each time point was plotted on a semilogarithmic scale and expressed as:

$$1 - \frac{\text{fraction counts accumulated for each point}}{\text{total accumulation} + \text{counts on filter} + \text{counts in NaOH wash of fraction counts}}$$

Analysis of the elution plots included determination of the differences in retention values between earliest and latest points in the elution plots (expressed as Δ), suggested by Kohn (332). In addition, slopes of the elution curves were calculated using Microsoft Excel as follows (333, 334):

$$\text{slope} = \frac{\sum (x - \bar{x})(y - \bar{y})}{\sum (x - \bar{x})^2}$$

where x is the number of hours at which a fraction was collected, and \bar{x} is the average time of all fractions collected; y is the % DNA remaining on the filters at a given time point, and \bar{y} is the average of % DNA remaining on the filters at all time points.

• **Statistical Analysis.** Sample means, standard error of means, as well as significant differences in values obtained between populations of leukemic cells treated with identical experimental conditions (determined by unpaired t-test analyses) were obtained by using the StatView Student program (Macintosh).

Results:

• **Creation and Characterization of HL-60/Bcl-2 and HL-60/neo Cells.** HL-60 cells were stably infected with recombinant amphotropic retroviruses carrying either neomycin (G418) antibiotic resistance gene alone, or in combination with cDNA of the *bcl-2* gene. Thus, HL-60/neo and HL-60/Bcl-2 cell lines were established and sub-cloned by limiting dilution in suspension culture, as described in **Chapter Two, Part C.** **Figure 14, Panel C,** also demonstrated that treatment of HL-60/neo or HL-60/Bcl-2 cells with 100 μ M Ara-C for 4 hours did not result in any significant alteration in p26Bcl-2 or p21 Bax levels in the two cell types (HL-60/neo: lane 2 versus lane 1; HL-60/Bcl-2: lane 4 versus lane 3).

• **Apoptosis and the Associated DNA Fragmentation in Ara-C Treated HL-60/neo versus HL-60/Bcl-2 cells.** HIDAC (high-dose Ara-C) is an optimized dosage and schedule of Ara-C which has been used successfully clinically to overcome classical resistance to conventional doses of Ara-C, including decreased intracellular Ara-CTP generation and incorporation into DNA (223, 335-337). Pharmacokinetic studies in patient-derived serum samples as well as in bone marrow cells have demonstrated that peak plasma concentrations achieved in AML patients

given infusions of $3\text{g}/\text{m}^2$ (high-dose), range from $52.25 \pm 32.01 \mu\text{M}$ (338) to $160 \pm 119 \mu\text{M}$ (339, 340). Previous studies in our laboratory have documented 10 to $100 \mu\text{M}$ Ara-C as high doses which are sufficient to induce internucleosomal DNA fragmentation in HL-60 parental cells (23) before reaching a plateau in its effect. Similarly, **Figure 17, Panel A** demonstrates that exposure to 1.0, 10.0, or $100 \mu\text{M}$ Ara-C produced internucleosomal DNA fragmentation in the genomic DNA extracted from HL-60/neo (lanes 2, 3 and 4, respectively) but not in the genomic DNA of HL-60/Bcl-2 cells (lanes 6, 7, and 8, respectively). **Figure 17, panel B**, shows the results of the field inversion gel electrophoresis of DNA plugs derived from untreated HL-60/neo (lane 1) or HL-60/Bcl-2 cells (lane 4), or from the two cell types treated with 10 or $100 \mu\text{M}$ Ara-C (HL-60/neo: lanes 2 and 3; HL-60/Bcl-2: lanes 5 and 6, respectively). **Panel B** demonstrates that DNA fragments ranging from approximately 4 to 300 kilobase in size were observed more in HL-60/neo cells treated with 100 versus $10 \mu\text{M}$ Ara-C, but no significant DNA fragmentation was observed in Ara-C treated HL-60/Bcl-2 cells. Incidentally, in HL-60/neo cells, internucleosomal DNA fragmentation did not increase when the cells were exposed to 100 versus $10.0 \mu\text{M}$ Ara-C (**Figure 17, Panel A**, lanes 4 versus 3), demonstrating a possible plateau in response to increasing concentrations of Ara-C in HL-60 cells.

Table III shows the results of flow cytometric evaluation of Bcl-2 levels, measure as the mean fluorescence intensity of FITC, as well as the evaluation of apoptosis detected as the percentage of cells in the sub- G_1 phase in untreated and Ara-C treated HL-60/neo and HL-60/Bcl-2 cells, although apoptosis was not higher in cells treated with 100 versus $10 \mu\text{M}$ Ara-C. Flow cytometric evaluation showed markedly higher Bcl-2 expression in the untreated HL-60/Bcl-2 versus HL-60/neo cells, which did not significantly change following treatment with 1.0, 10.0, or $100 \mu\text{M}$ Ara-C. **Table III** clearly demonstrates that these doses of Ara-C produce significantly higher percentages of HL-60/neo cells exhibiting reduction in DNA content below 2C or diploid level on flow cytometric histograms, indicative of apoptosis (341, 342) than in HL-60/Bcl-2 cells. **Table III** also highlights that immediately following the induction of apoptosis in HL-60/neo cells, neither the apoptotic (sub- G_1) nor the non-apoptotic population of $G_1 + S + G_2/M$ phases) showed a change in Bcl-2 expression. In HL-60/neo versus HL-60/Bcl-2 cells, Ara-C-induced apoptosis was also determined by light microscopy by estimating the percentage of cells demonstrating the characteristic morphologic features of apoptosis. **Table IV** shows that following treatment with 1.0 to $100 \mu\text{M}$ of Ara-C for 4 hours, a significantly greater percentage

of morphologically recognizable apoptotic cells were observed in HL-60/neo versus HL-60/Bcl-2 cells. However, **Table IV** also demonstrates that this exposure to Ara-C produced significantly greater cytotoxicity in HL-60/neo versus HL-60/Bcl-2 cells, although the difference in cytotoxicity, as determined by the MTT assay, was much less than the difference in apoptosis of HL-60/neo versus HL-60/Bcl-2 cells. This may reflect the difference in the effect of the Ara-C treatment on the two disparate biologic fates being assessed by the two separate assays.

• Intracellular Metabolism of Ara-C and Alkaline Elution Profile of DNA in HL-60/neo

versus HL-60/Bcl-2 Cells. As compared to HL-60/neo, the resistance of HL-60/Bcl-2 cells to Ara-C-induced lethal DNA fragmentation and apoptosis raises the question whether these cells, following exposure to Ara-C have decreased accumulation of Ara-CTP, Ara-C DNA incorporation of Ara-C-induced DNA strand breaks. **Table V** shows that following treatment of HL-60/Bcl-2 cells with 100 μ M Ara-C for 4 hours, Ara-CTP accumulation, the decline in dCTP levels and Ara-C DNA incorporation were not significantly different from HL-60/neo cells. These data indicate that the initial, or proximal, steps of Ara-C metabolism are unimpaired in those cells that possess high intracellular levels of p26Bcl-2. **Figure 18** demonstrates the alkaline elution profile of DNA of HL-60/neo or HL-60/Bcl-2 cells which had been treated with 100 μ M Ara-C for 2 hours, with irradiated cells (500 rads over 50 seconds) serving as the positive controls. This dose and exposure interval to Ara-C were chosen because they had previously been demonstrate to not induced double-stranded DNA fragmentation associated with apoptosis (32). In addition, in the present studies, the conditions for alkaline elution had been optimized for the detection of single-strand breaks. As shown in **Figure 18**, neither the total eluted DNA at pH 12.1 over 18 hours, represented as the percent of DNA remaining on the filter, nor the slope of elution of DNA, nor calculations from the difference in percent DNA remaining on the filter between the earliest and the latest 3-hourly time-points, were significantly different in HL-60/Bcl-2 versus HL-60/neo cells ($p > 0.05$) (see data in **Tables VI and VII**). It is noteworthy that significantly more DNA with strand breaks ($p < 0.01$) could be eluted from the filters from irradiated versus Ara-C treated cells. This has also been previously noted (243). However, there was no significant difference in the total amount of eluted DNA at 12 hours or the slope of the elution of DNA from the irradiated HL-60/neo versus HL-60/Bcl-2 cells ($p > 0.05$).

Discussion:

In human myeloid leukemia cells, the cytotoxic effects of Ara-C have been correlated with the intracellular accumulation of its lethal metabolite Ara-CTP and its incorporation into DNA, which causes slowing of nascent DNA chain elongation, inhibition of DNA synthesis, resulting in DNA strand breaks (223, 237, 243, 246), as well as endoreduplication leading to chromosomal abnormalities (225, 232-234). Exposure to clinically achievable doses of Ara-C (10 or 100 μ M for approximately 4 hours) ultimately results in lethal, large size, double-stranded or internucleosomal DNA fragmentation associated with apoptosis (22, 23). As discussed above, previous studies had documented that high intracellular levels of p26Bcl-2 block Ara-C-induced internucleosomal DNA fragmentation and other features of apoptosis (98). In the present studies, these findings are confirmed with respect to the treatment of human AML cells with high-dose Ara-C (see **Figure 17**). In addition, the presence of high p26Bcl-2 levels are demonstrated to have no significant effect on the intracellular accumulation of Ara-CTP relative to dCTP, Ara-C DNA formation and Ara-C-induced DNA strand breaks detectable by alkaline elution analyses.

To examine the effect of overexpression of p26Bcl-2 on Ara-C metabolism, Ara-C-mediated perturbations in genomic DNA and subsequent Ara-C-induced apoptosis, HL-60/Bcl-2 and HL-60/neo cells were created by retroviral transfection of HL-60 cells with the pZIP-*bcl-2* or pZIP/neo plasmids (87). In addition, clonal populations of HL-60/Bcl-2 cells that homogeneously overexpressed p26Bcl-2 approximately 5- to 10-fold greater by Western blot than the level of expression in HL-60/neo were isolated by subcloning by limiting dilution. Compared to p26Bcl-2, these cells possessed significantly lower p21Bax levels, although its expression was similar in the two cell types. Therefore, consistent with a previous hypothesis, HL-60/Bcl-2 cells containing significantly higher p26Bcl-2 to p21Bax levels, were resistant to HIDAC-induced apoptosis (32). Coincident with HIDAC-induced apoptosis, p26Bcl-2 to p21Bax levels did not significantly change in HL-60/neo cells immediately following HIDAC exposure. In addition, immediately after HIDAC treatment flow cytometric analysis of the surviving population of HL-60/neo cells did not demonstrate a statistically significant rise in Bcl-2 (**Table III**). These findings are novel with respect to Ara-C-induced apoptosis of human

leukemic cells. However, in the present studies, the expression of Bad or other recently described Bcl-2-related gene products have not yet been examined (175, 178).

The demonstration that in HL-60/Bcl-2 versus HL-60/neo cells, HIDAC-induced apoptosis was blocked despite similar accumulation of Ara-CTP to dCTP and incorporation of Ara-C into DNA, suggests that high p26Bcl-2 levels may interfere in the subsequent HIDAC-induced DNA perturbations that culminate into lethal, double-stranded and endonucleolytic DNA fragmentation. This is despite the finding that the alkaline elution profiles at pH 12.1 of DNA of HL-60/Bcl-2 versus HL-60/neo cells following a two-hour treatment with HIDAC, conditions optimized to detect the potentially repairable single-strand DNA breaks, did not reveal significant differences in either the total eluate or the slope of the DNA elution curves generated in either cell line. This suggests that following the incorporation of Ara-C into DNA and the subsequent generation of DNA strand breaks, further step(s) involving the activation of the endonuclease(s) take place, resulting in lethal double-strand DNA damage, and it is these step(s) that are inhibited by high p26Bcl-2 levels. Therefore, it could be hypothesized that the cascade of events leading to HIDAC-induced apoptosis may be separated into proximal, potentially separable events which are unaffected by, and distal steps resulting in lethal DNA damage that are regulated by the intracellular p26Bcl-2 levels. Notably, this also occurs in HL-60 cells overexpressing p29Bcl-x_L (343). In previous reports, similar observations were made with respect to p26Bcl-2-mediated inhibition of 5-fluorodeoxyuridine (102), etoposide- (103), or taxol-induced apoptosis (104) which have also supported this hypothesis that Bcl-2 still allows drugs to affect their targets, yet inhibits only the late manifestations of apoptosis. While Grem *et al.* have established a chronology in DNA damage events induced by Ara-C and manifesting in double-strand DNA fragmentation (246), an alternative hypothesis might be that the accumulation of Ara-CTP initiates a death pathway separate from Ara-C DNA incorporation and DNA single-strand breaks, and indirectly promotes apoptosis. This pathway that still results in endonucleolytic DNA degradation and apoptosis, may involve protein kinases which have been shown to be activated by Ara-C treatment, and may be the target of the anti-apoptotic action of p26Bcl-2 (259, 261), as described in the Introduction, **Chapter One** of this dissertation.

During the preparation of this chapter, Huang *et al.* further defined high molecular weight DNA fragmentation (50-kb size assessed by pulsed-field gel electrophoresis) as a critical event in fludarabine- and gemcitabine-induced apoptosis in human leukemia CEM cells (344). They reported that high molecular weight DNA fragmentation could be distinguished from low molecular weight internucleosomal DNA fragmentation by their differential requirements for calcium. In their studies, drug-treated cells still exhibited morphologic features of apoptosis even when only low molecular weight internucleosomal DNA fragmentation was inhibited by Ca^{2+} chelation (344). However, when nucleoside analogue incorporation into DNA was inhibited by aphidicolin as previously reported, neither high molecular weight DNA fragmentation or low molecular weight internucleosomal DNA fragmentation or morphologic features of fludarabine- and gemcitabine-induced apoptosis occurred (319), further suggesting that DNA incorporation itself is a critical event for apoptosis (and cytotoxicity), and consistent with previous literature (231, 232). In the present studies in the HL-60/neo versus HL-60/Bcl-2 cell models described here, **the lethal DNA damage due to Ara-C has been defined as double-strand DNA fragmentation of high molecular weight (5 to 300 kilobase) and low molecular weight internucleosomal sizes, distal to single strand breaks generated upon incorporation of Ara-C into DNA.** Furthermore, while neither the essential incorporation of Ara-C into DNA nor generation of single-strand breaks by Ara-C are affected by p26Bcl-2 overexpression, **it is only this eventual double-stranded DNA damage which is inhibited by Bcl-2.** Although these findings help in providing a better understanding of the steps in the cascade of HIDAC metabolism and DNA perturbations that are not influenced and those that are inhibited by the anti-apoptotic action of p26Bcl-2, they do not specify the precise steps that are the targets for this activity. As mentioned in the Introduction in **Chapter One**, several reports have presented evidence to demonstrate one or the other biochemical mechanism underlying the anti-apoptotic effect of p26Bcl-2 (70). These have included (a) an anti-oxidant effect (120, 121); (b) inhibition of the intracellular calcium flux from the endoplasmic reticulum to mitochondria (10, 127); (c) the association with important R-ras and Raf-mediated signal transduction pathway(s) (134, 137); and (d) blocking nuclear localization of transcription factors that may promote apoptosis (142, 144). It remains to be elucidated whether one or more of these mechanisms are operative distally in the HIDAC-induced steps leading to the lethal DNA fragmentation and apoptosis of AML cells. It will also be interesting to study the fate of this Ara-C-induced damage over time given a cell population's relative level of p26Bcl-2, and to study whether p26Bcl-2 allows

increased repair of Ara-C-induced DNA breaks to take place, as addressed in **Chapters Four and Five**, respectively, of this dissertation. A clear understanding of these aspects may provide insights into developing more targeted and selective anti-AML treatments involving HIDAC.

Figure Legends:

Figure 17: Ara-C-induced internucleosomal and high molecular weight DNA fragmentation in HL-60/neo versus HL-60/Bcl-2 cells. For **Panel A**, HL-60/neo (lanes 1 to 4) and HL-60/Bcl-2 cells (lanes 5 to 8) were treated with 1.0, 10.0, or 100.0 μM Ara-C for 4 hours. Following these treatments, equal amounts (1.0 μg) of purified genomic DNA was electrophoresed in a 1.8% agarose gel (**Panel A**) to determine internucleosomal DNA fragmentation. DNA fragments in each of these lanes are from cells treated as follows: lanes 1 and 5, untreated cells; lanes 2 and 6, 1.0 μM Ara-C; lanes 3 and 7, 10.0 μM Ara-C; lanes 4 and 8, 100.0 μM Ara-C. For **Panel B**, HL-60/neo (lanes 1 to 3) and HL-60/Bcl-2 cells (lanes 4 to 6) were treated with 10 or 100 μM Ara-C for 4 hours. Subsequently, field inversion gel electrophoresis of the DNA plugs was performed to determine large-size DNA fragments (**Panel B**). DNA fragments in each lane are from cells treated as follows: lanes 1 and 4, untreated cells; lanes 2 and 5, 10.0 μM Ara-C; lanes 3 and 6, 100 μM Ara-C. M represents marker DNA in both panels. Data is representative of three separate experiments, each with similar results.

Figure 18: The profiles of alkaline elution of DNA from Ara-C treated or irradiated (positive control) HL-60/neo (top) and HL-60/Bcl-2 (bottom) cells expressed as the percent DNA remaining on the polycarbonate filters (for the methods, see text). Data points on the curves represent the means of eluted DNA in three-hourly fractions collected over 18 hours (mean of three experiments, with standard error of mean [SEM] tabulated in **Table VI**). The results demonstrate that there is no significant difference in the amounts or the slope of the elution of DNA in Ara-C treated HL-60/neo versus HL-60/Bcl-2 cells (see data in **Tables VI and VII**).

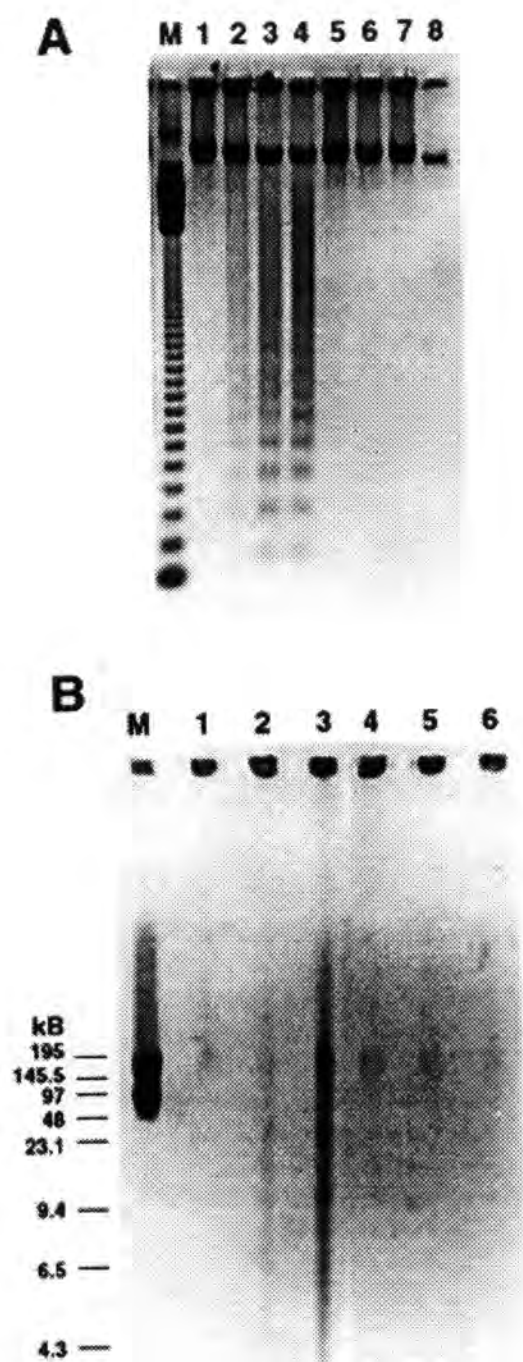
Figure 19.

TABLE III.**FLOW CYTOMETRIC DETERMINATION OF Bcl-2 LEVELS IN APOPTOTIC AND NON-APOPTOTIC HL-60/neo VERSUS HL-60/Bcl-2 CELLS FOLLOWING ARA-C TREATMENT:***

<u>Condition:</u>	<u>% Apoptotic cells:</u> (sub-G ₁ -phase)	<u>FITC-Bcl-2:</u>	<u>% Non-Apoptotic cells:</u> (G ₁ + S + G ₂)	<u>FITC-Bcl-2:</u>
<u>I. HL-60/neo cells:</u>				
control	1.08 ± 0.27	6.39 ± 0.63	95.62 ± 5.67	18.61 ± 3.80
1 μM Ara-C, 4 hr	8.54 ± 2.53	6.48 ± 1.28	90.10 ± 5.19	22.67 ± 4.18
10 μM Ara-C, 4 hr	24.68 ± 3.65	7.87 ± 0.80	73.57 ± 6.69	23.09 ± 3.98
100 μM Ara-C, 4 hr	17.44 ± 3.39	7.40 ± 0.68	82.47 ± 7.76	22.04 ± 3.44
<u>II. HL-60/Bcl-2 cells:</u>				
control	1.48 ± 0.25	49.28 ± 3.69**	99.07 ± 0.51	158.42 ± 26.01**
1 μM Ara-C, 4 hr	2.00 ± 0.21**	54.28 ± 3.17**	98.70 ± 0.97**	169.55 ± 22.70**
10 μM Ara-C, 4 hr	1.72 ± 0.19**	51.74 ± 3.95**	98.95 ± 1.22**	165.52 ± 24.26**
100 μM Ara-C, 4 hr	1.80 ± 0.21**	51.16 ± 3.79**	99.05 ± 1.26**	161.75 ± 27.62**

* Values represent means ± S.E.M. for n=4 experiments.

** Values obtained in identically treated HL-60/neo and HL-60/Bcl-2 cells are significantly different (p < 0.001).

TABLE IV.

**MORPHOLOGIC EVIDENCE OF ARA-C-INDUCED APOPTOSIS
AND INHIBITION OF VIABILITY IN
HL-60/neo VERSUS HL-60/Bcl-2 CELLS:**

Condition:	<u>% APOPTOTIC CELLS:*</u> (morphology)		<u>% INHIBITION OF VIABILITY:*</u> (by MTT assay)	
	<u>HL-60/neo:</u>	<u>HL-60/Bcl-2:</u>	<u>HL-60/neo:</u>	<u>HL-60-/Bcl-2:**</u>
control	0.33 ± 0.13	0.08 ± 0.08	--	--
1 μM Ara-C, 4 hr	10.48 ± 1.81	0.33 ± 0.13**	33.70 ± 7.40	15.70 ± 2.40
5 μM Ara-C, 4 hr	ND	ND	46.00 ± 6.60	17.00 ± 2.60
10 μM Ara-C, 4 hr	26.26 ± 4.48	0.50 ± 0.16**	51.70 ± 6.50	33.70 ± 4.33
50 μM Ara-C, 4 hr	ND	ND	59.30 ± 0.70	42.60 ± 4.80
100 μM Ara-C, 4 hr	19.33 ± 4.74	0.82 ± 0.21**	68.30 ± 3.20	46.30 ± 6.40

* Values represent mean ± S.E.M. for n=4 experiments.

** Values obtained for identically treated HL-60/neo versus HL-60/Bcl-2 cells are significantly different (p < 0.01).

TABLE V.

INTRACELLULAR METABOLISM OF ARA-C
IN HL-60/neo AND HL-60/Bcl-2 CELLS:*

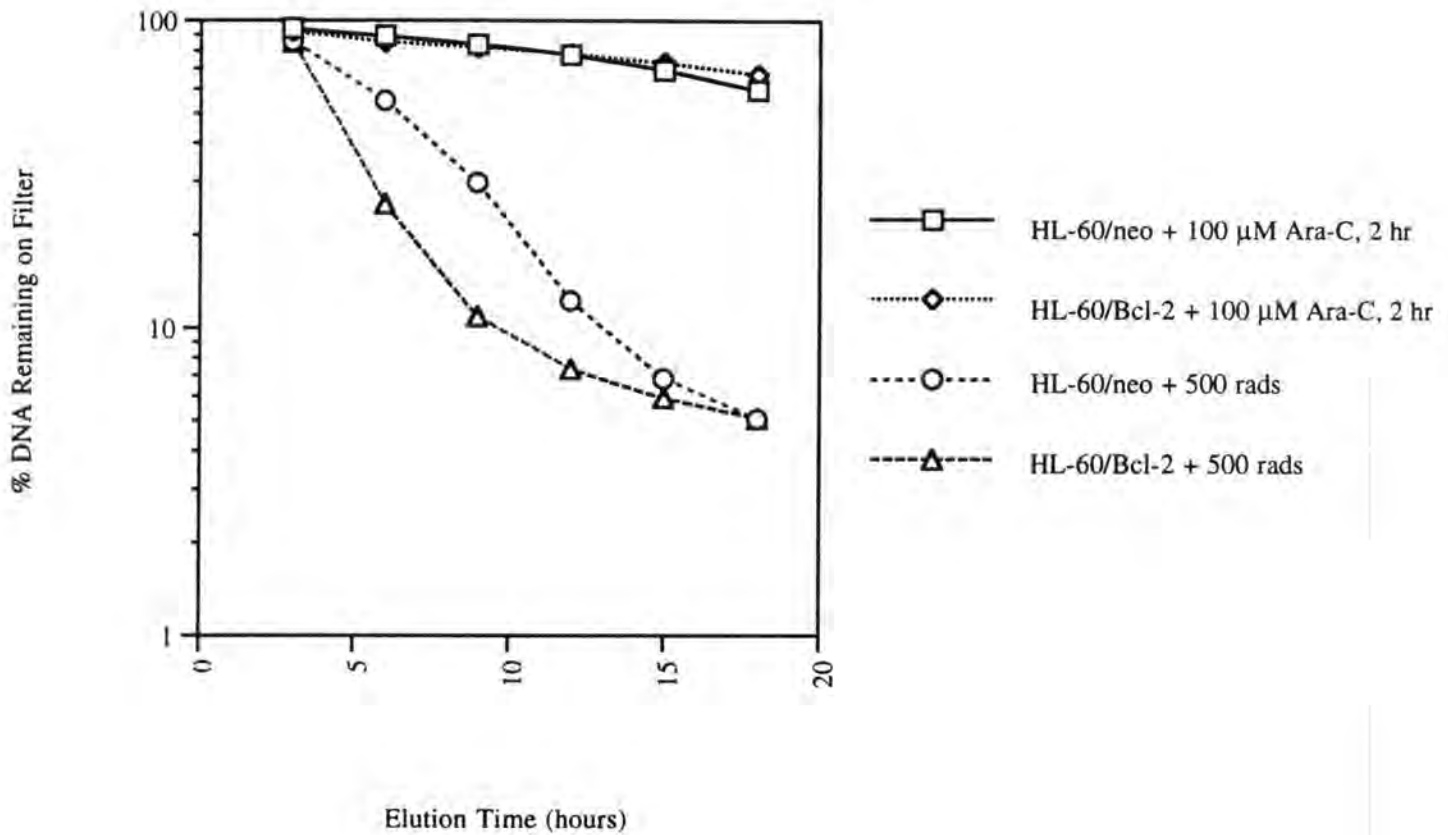
	<u>HL-60/neo:</u>		<u>HL-60/Bcl-2:**</u>	
	<u>Control:</u>	<u>+ HIDAC:</u>	<u>Control:</u>	<u>+ HIDAC:</u>
dCTP (pmols/10 ⁶ cells)	4.97 ± 0.45	3.12 ± 0.52	3.63 ± 0.46	3.41 ± 1.44
Ara-CTP (pmols/10 ⁶ cells)	--	31.29 ± 2.11	--	36.21 ± 6.18
Ara-C DNA (pmols/μg DNA)	--	2.70 ± 0.82	--	3.08 ± 0.52

* For the above Table, HL-60/neo and HL-60/Bcl-2 cells were incubated with or without 100 μM Ara-C for 4 hours = **HIDAC**, neutralized, periodated, and acid-soluble cell extracts were analyzed by HPLC for intracellular dCTP and/or Ara-CTP levels. Alternatively, following incubation with 100 μM [³H] Ara-C for 4 hours, cells were pelleted, DNA purified as described in Materials and Methods, and [³H] Ara-C DNA incorporation was determined and expressed as pmols/μg DNA.

** Values obtained in identically treated HL-60/neo and HL-60/Bcl-2 cells are not significantly different (p > 0.05).

Figure 18.

ALKALINE ELUTION IN HL-60/neo VERSUS HL-60/Bcl-2 CELLS



ALKALINE ELUTION IN HL-60/neo VERSUS HL-60/Bcl-2 CELLS

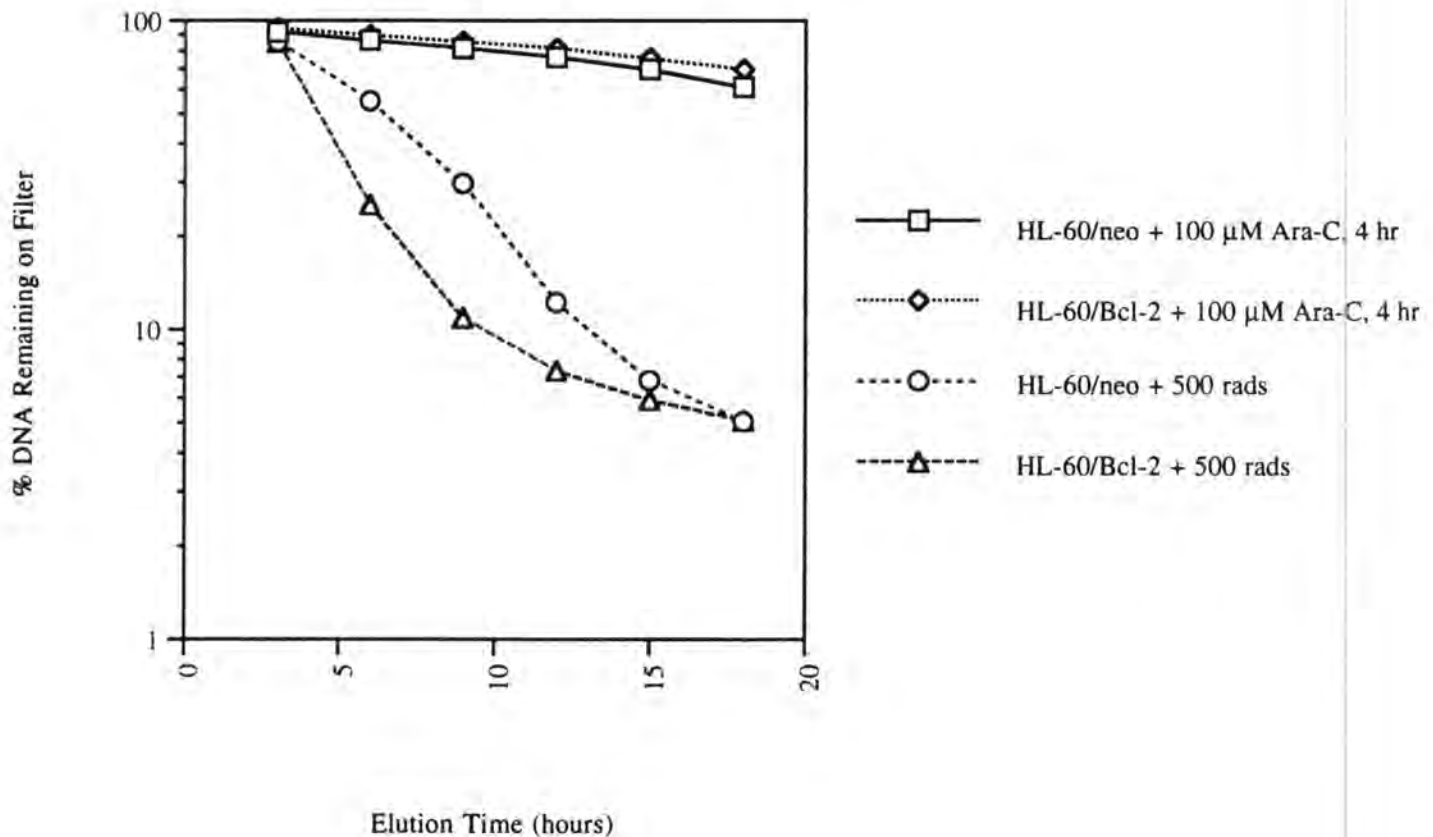


TABLE VI.**ALKALINE ELUTION IN HL-60/neo VERSUS HL-60/Bcl-2 CELLS:**

Condition:	<u>% DNA Remaining on Filter:</u>	
	<u>HL-60/neo:</u>	<u>HL-60/Bcl-2:</u>
<u>Control:* _</u>		
3 hr fraction	96.20 ± 0.36	94.92 ± 0.76
6 hr fraction	91.07 ± 0.32	90.70 ± 1.36
9 hr fraction	85.96 ± 0.36	86.99 ± 1.61
12 hr fraction	79.07 ± 0.09	82.02 ± 1.84
15 hr fraction	72.09 ± 0.18	75.67 ± 2.49
18 hr fraction	62.59 ± 0.93	70.70 ± 1.64
<u>100 μM Ara-C, 2 hrs:*</u>		
3 hr fraction	93.75 ± 0.42	95.67 ± 0.15
6 hr fraction	87.08 ± 1.71	89.91 ± 2.42
9 hr fraction	80.68 ± 0.98	83.86 ± 5.12
12 hr fraction	73.36 ± 1.62	77.82 ± 7.34
15 hr fraction	63.52 ± 3.92	69.50 ± 1.04
18 hr fraction	53.80 ± 5.75	60.89 ± 1.34
<u>500 rads, 0.8 min:**</u>		
3 hr fraction	98.07	98.99
6 hr fraction	54.21	43.99
9 hr fraction	22.70	12.33
12 hr fraction	13.12	6.14
15 hr fraction	8.49	4.44
18 hr fraction	5.64	3.31

* Values represent mean ± S.E.M. for n = 3 experiments.

** Values represent mean of 2 experiments.

TABLE VII.**ALKALINE ELUTION IN HL-60/neo VERSUS HL-60/Bcl-2 CELLS:**

<u>Condition:</u>	<u>HL-60/neo:</u>		<u>HL-60/Bcl-2:</u>	
	<u>Δ:*</u>	<u>Slope of Elution Curve:</u>	<u>Δ:*</u>	<u>Slope of Elution Curve:</u>
100 μM Ara-C, 2 hrs:**	34.73% ± 0.95	-2.12 ± 0.05	34.77% ± 1.33	-1.97 ± 0.35
500 rads, 0.8 min:***	81.17%	-7.79	80.27%	-6.09

* Δ (delta) represents the range of the percentage of DNA eluted from the filter under alkaline conditions between the earliest time point (3-hr fraction) and the latest time point (18-hr fraction), and represents the total amount of DNA eluted.

** Values represent mean ± S.E.M. for n = 3 experiments. Values obtained in identically treated HL-60/neo and HL-60/Bcl-2 cells are not significantly different (p > 0.05).

*** Values represent mean of 2 experiments. Δ values obtained in identically treated HL-60/neo and HL-60/Bcl-2 cells are not significantly different (p > 0.05).

CHAPTER IV.

**A. Disparate levels of overexpression of p26Bcl-2 govern
the response to Ara-C-induced apoptosis
and cytotoxicity over time.**

**B. *bcl-2* expression is induced in human AML cells
which survive treatment with high-dose Ara-C.**

CHAPTER IV:

A. DISPARATE LEVELS OF OVEREXPRESSION OF p26Bcl-2 GOVERN THE RESPONSE TO ARA-C-INDUCED APOPTOSIS AND CYTOTOXICITY OVER TIME:

B. *bcl-2* EXPRESSION IS INDUCED IN HUMAN AML CELLS WHICH SURVIVE TREATMENT WITH HIGH-DOSE ARA-C.

Abstract:

The effect of the level of endogenous p26Bcl-2 expression in three disparate clonal populations of retrovirally-transfected HL-60/Bcl-2 cells on the fate on Ara-C-induced DNA damage was examined and compared with identically treated HL-60/neo cells. HL-60/Bcl-2 clones with approximately two-fold, four-fold, and six-fold greater p26Bcl-2 expression, by immunofluorescence, as compared to HL-60/neo cells were demonstrated to be resistant to Ara-C-induced high molecular weight DNA fragmentation, low molecular weight internucleosomal DNA fragmentation, morphologic features of apoptosis, and inhibition of cell viability after HIDAC treatment. However, clones with four-fold and six-fold greater p26Bcl-2 expression remained resistant up to 48 hours after Ara-C treatment, while clones with only two-fold greater p26Bcl-2 expression showed indications of the induction of Ara-C-induced apoptosis and significant inhibition of cell viability by 12 hours after HIDAC treatment. The ability of Ara-C to inhibit cell viability was found to be inversely correlated to the amount of p26Bcl-2 overexpression, as assessed by the MTT assay. In the second part of this chapter, Bcl-2 expression itself was examined in cells surviving HIDAC treatment. By Western blot, p26Bcl-2:p21Bax ratios were demonstrated to increase over time after HIDAC treatment in all cell lines examined, by virtue of increase in p26Bcl-2 levels but no significant modulation of p21Bax levels. In all cell lines presented, increased Bcl-2 levels were confirmed by immunofluorescence and flow cytometry. To determine the molecular level at which this increase in Bcl-2 in surviving cells occurs, the ribonuclease protection assay (RPA) was utilized. While not readily detectable in HL-60/neo cells, *bcl-2* mRNA was found to be induced in HL-60/Bcl-2 cells beginning at 2 hours after cells were first exposed to Ara-C. Concomitant treatment with RNA synthesis inhibitor actinomycin D abrogated Ara-C-mediated increases in *bcl-2* mRNA as well as increased Bcl-2 protein levels by flow cytometry, suggesting that this increase occurs at the level of transcription. These increases in Bcl-2 levels in surviving cells were also found to be

biologically relevant in previously treated and surviving HL-60/neo cells, which exhibited lower Ara-C-mediated inhibition of viability by MTT assay and lower amounts of Ara-C-mediated total DNA breaks by the TUNEL assay upon second treatment with various concentrations of Ara-C.

Taken together, these data indicate that a threshold level for p26Bcl-2 expression exists which can extend protection of HL-60 cells against the eventual induction of Ara-C-induced apoptosis. These data demonstrate that following HIDAC treatment, AML cells which survive and do not exhibit features of Ara-C-induced apoptosis acquire increased Bcl-2 levels regardless of endogenous levels in untreated control cells. This increase in Bcl-2 is induced at the level of transcription and represents a biologically significant modulation in anti-apoptotic gene expressions. These studies simulate clinical treatment regimens in AML and illustrate potential for the acquisition of drug-resistance through the up-regulation of *bcl-2* during treatment schedules.

Introduction:

In **Chapter Three**, it was demonstrated that Bcl-2 overexpression in HL-60 AML cells blocks the late manifestations of Ara-C-induced apoptosis including high molecular weight DNA fragmentation and low molecular weight internucleosomal DNA fragmentation, as well as morphologic features of apoptosis. Because Bcl-2 overexpression in patient-derived AML blasts has been correlated with poor response to chemotherapy regimens (204), it is important to define the level of Bcl-2 which is responsible for this hindrance. The HL-60/Bcl-2 cell model used for the studies in Chapter Three expressed p26Bcl-2 at a level 5- to 10-fold higher than HL-60/neo. The studies in this Chapter Four examine the effect of disparate levels of Bcl-2 expression on the fate of residual DNA damage induced by high-dose Ara-C (HIDAC) in an attempt to identify a threshold level for protection against Ara-C-induced apoptosis by intracellular p26Bcl-2 protein. The other HL-60/Bcl-2 clonal populations utilized here have been characterized according to level of homogeneous overexpression of Bcl-2, have intermediate levels of Bcl-2 protein less than that in the HL-60/Bcl-2 cells used for the studies in Chapter Three.

In addition, the **acquisition** of drug resistance in residual cancer cells **after** chemotherapy treatment has also been documented to play a significant role in the relapse of cancers and the

failure of treatment. Historically, increased drug resistance has been thought to be due to selection of drug-resistant cells among the cancerous population, but recently has also been documented to be due to induction and up-regulation of drug-resistance genes (345). These drug-resistance genes include the *mdr-1* gene which encodes for a classical P-glycoprotein transmembrane, energy-dependent drug-efflux pump which decreases the intracellular accumulation in human cancers of several common hydrophobic anticancer drugs including anthracycline antibiotics such as adriamycin, vinca alkaloids such as vinblastine, and epipodophyllotoxin derivatives, as well as colchicine (346-348). Chaudhary and Roninson have demonstrated by reverse transcription-PCR the increased expression of *mdr-1* in human tissues 3 to 5 days following chemotherapeutic drug treatment (349). Hu *et al.* have most recently demonstrated that the rapid up-regulation of *mdr-1* RNA expression by short treatment with anthracyclines, VP-16, and vinca alkaloids in a variant human *mdr+* cell line CEM/A7R (345). In addition, Zhao *et al.* found that *mdr-1* RNA levels were elevated in mouse hepatoma cells after dexamethasone treatment by transcriptional control demonstrated by nuclear run-on experiments (350). These studies lend credence to the suggestion that induction of the expression of drug resistance genes may be responsible for the further development of drug-resistant tumors and unresponsive disease.

Since HL-60 cells themselves exhibit Bcl-2 expression, it is therefore worthwhile to study the effects of disparate levels of Bcl-2 on drug-induced DNA damage, and conversely, the effects of Ara-C on the levels of Bcl-2 after treatment. It has not been extensively studied whether Bcl-2 levels are modulated after drug treatment and whether their induction leads to the acquisition of drug-resistance over time against drugs which do not affect *mdr* activity. The present studies examine the late manifestations of Ara-C-induced apoptosis in three HL-60/Bcl-2 clonal populations over time after HIDAC treatment as compare to HL-60/neo, and examine the effects of this treatment on the expression of Bcl-2-related proteins over time. These studies test the hypothesis that the level of Bcl-2 overexpression in HL-60/Bcl-2 cells governs the fate of Ara-C-induced DNA damage over time after treatment. An additional question whether any increases in intracellular Bcl-2 levels in cells surviving after Ara-C treatment are due to selection of cells which exhibit higher Bcl-2 expression in any of the populations, and/or due to actual induction of *bcl-2*, will also be addressed.

Materials and Methods:

•**Drugs and Antibodies.** Ara-C (Sigma, St. Louis, MO) was prepared as described in **Chapter Two**. Actinomycin D was also purchased from Sigma, and a 5 mg/ml stock was made in DMSO. Cycloheximide (Sigma) was prepared as a 5 mg/ml stock in deionized water. Antibodies for Bcl-2-related oncoproteins were obtained from the sources listed in **Chapter Two**.

•**Retroviral Constructs and Transfection of HL-60 cells.** HL-60/neo and HL-60/Bcl-2 clonal populations were generated by retroviral-mediated transfection and subcloning by limiting dilution as described in Chapter Two.

•**Detection of Internucleosomal Fragmentation of Genomic DNA by Agarose Gel Electrophoresis.**

•**Preparation of DNA Plugs and Field Inversion Gel Electrophoresis.** DNA fragmentation analysis was performed as previously described (22, **Chapter Three**).

•**Flow Cytometric Analysis of Apoptosis and p26Bcl-2 Levels.** Flow cytometric evaluation for apoptotic cells and Bcl-2 levels was performed as described in **Chapter Three**. Additional flow cytometric data was obtained at the Winship Cancer Center, Emory University, Atlanta, GA, utilizing a Becton Dickinson FACSort flow cytometer using LYSYS II software program (Version 2.0) for two-color (PI, red, and fluorescein, green) detection of fluorescent emissions (Becton Dickinson Immunocytometry Systems, San Jose, CA).

•**Assessment of Cytotoxicity by the MTT Assay.** The MTT assay for cell cytotoxicity was performed as previously described (325, 326, **Chapter Three**).

•**Western Blot Analysis of p26Bcl-2, p21Bax, and p29Bcl-x₁ Oncoprotein Expressions.** Western blot analyses for Bcl-2-related proteins in HL-60/neo and HL-60/Bcl-2 clones after Ara-C treatment were performed as described in **Chapter Two**. Horizontal scanning densitometry of protein bands was performed on Western blots by utilizing acquisition into Adobe PhotoShop and analyses with NIH Image Version 1.57 programs (Macintosh).

•Immunofluorescent Analysis of p26Bcl-2 Expression and Up-Regulation of p26Bcl-2 Expression. Immunofluorescent analysis of Bcl-2 levels in HL-60/neo and HL-60/Bcl-2 clones was performed as previously described (146, **Chapter Two**). After Ara-C treatment, non-apoptotic cells were first identified by virtue of their morphologic features by paired-field fluorescence/phase-contrast microscopy on a Zeiss Axioplan microscope. Subsequently, mean p26Bcl-2 fluorescent intensity per non-apoptotic cell was measured as a function of the reciprocal of exposure time to the attached camera at film speed setting ASA 6400 set maximal sensitivity, on a Model MC100 automatic camera exposure system, using a 63x planapochromat objective lens (N.A. 1.4) on the fluorescent microscope. Levels of Bcl-2 intensity were expressed as percent of control.

•Ribonuclease Protection Assay for *bcl-2* and β -actin mRNA Expression. Total RNA was prepared by using the RNeasy Total RNA Isolation Kit (QIAGEN, Chatsworth, CA). To construct human *bcl-2* probes, the 850-bp *EcoRI* fragment of pB4, encoding the open reading frame of *bcl-2* α cDNA sequence (originally obtained from Drs. Emad S. Alnemri and Carlo S. Croce, 300) was digested with *SacII* to generate 302- and 620-bp *bcl-2* cDNA fragments, which were subsequently cloned in to the *SacII/EcoRI* sites of pBluescript SKII(+) (Stratagene, LaJolla, California) by Dr. Shuli Li, and were the kind gifts of Dr. Gian G. Re (Medical University of South Carolina, Charleston, SC). Recombinant plasmids were purified by ultracentrifugation over cesium chloride gradients (296). In order to transcribed antisense *bcl-2* RNA probes, T3 RNA polymerase was utilized for the *bcl-2* 302-bp cDNA segment in SKII(+) linearized with *EcoRI*, and T7 RNA polymerase was utilized for the *bcl-2* 620-bp cDNA segment in SKII(+) linearized with *SacII*. Sp6 RNA polymerase was utilized to transcribed a 125-bp antisense *b-actin* RNA probe from the linearized pTRI- β -actin human plasmid (Ambion, Inc., Austin, Texas). In vitro transcription of antisense RNA probes was achieved by utilizing the MAXIscript in vitro RNA transcription kit (Ambion, Austin, Texas), and by incubating 1 μ g linearized DNA template, 1X transcription buffer, 10 mM DTT, 500 mM ATP, 500 mM CTP, 500 mM GTP, 20 mM CTP, 50 μ Ci/ml [α -³²P]UTP (specific activity 3000 Ci/mmol, ICN Radiochemicals, Costa Mesa, CA), 12.5 U human placental RNase inhibitor, and 10 U of designated RNA polymerase, for 1 hour in a 37°C water bath. After heat-inactivation of RNA polymerase, DNA templates were then degraded by the addition of 4 U RNase-free DNase I (Ambion, Inc., Austin, TX) and additional incubation at 37°C for 20 minutes. RNA probes were

mixed with an equal volume of 2X gel loading buffer (80% formamide, 0.1% xylene cyanol, 0.1% bromophenol blue, 2 mM EDTA, Ambion, Inc.) and heated at 95°C for 3 minutes just prior to loading on and electrophoresis in a 4% polyacrylamide/8 M urea gel. After electrophoresis, the gel was exposed briefly to X-ray film for localization of the gel-purified full-length RNA probes, which were subsequently excised from the gel and eluted by incubation in 350 µl elution buffer (Ambion, Inc., Austin, TX) at 34°C with gentle shaking overnight.

The following day, elution supernatant was measured in a scintillation counter (Beckman, Columbia, MD) for radioactive ^{32}P signal, and approximately $2-8 \times 10^4$ cpm of each probe was co-precipitated with 50 µg total RNA samples by adding 0.5M sodium acetate (NaOAc) and 100% ethanol, and incubating at -20°C for 1 hour. Total RNA plus antisense RNA probes were pelleted by centrifugation, resuspended in 20 µl solution A (hybridization buffer: 80% deionized formamide, 100 mM sodium citrate pH 6.4, 300 mM sodium acetate pH 6.4, 1 mM EDTA; Ribonuclease Assay Kit, Ambion, Inc.), and allowed to hybridize at 42°C overnight with gentle shaking.

The following day, non-hybridized RNA sequences remaining single-stranded were digested by the addition of 0.5 U RNase A and 20 U RNase T1 (Ambion, Inc.) incubation at 37 C for 45 minutes after vigorous mixing. RNases were inactivated by addition of equal volume of solution Dx (Ambion, Inc.), and RNA-RNA hybrids were precipitated for 1 hour at -20°C with 0.5 M NaOAc and 2.5 volumes of 100% ethanol. RNA-RNA hybrids were pelleted by centrifugation, resuspended in 5 ml gel loading buffer (95% formamide, 0.025% xylene cyanol, 0.025% bromophenol blue, 0.5 mM EDTA, 0.025% SDS), heated at 95°C for 3 minutes, and electrophoresed on a 5% polyacrylamide/8M urea gel. The gel was dried at 85°C for 45 minutes in a BioRad Slab Gel Dryer apparatus (Brea, CA) and exposed to X-ray film at -80°C overnight. Horizontal scanning densitometry of *bcl-2* and β -*actin* bands was performed on the X-ray films by utilizing acquisition in Adobe Photoshop and analyses with NIH Image Version 1.57 programs (Macintosh).

•Flow cytometric determination of DNA strand breaks in apoptotic cells by *in situ* TUNEL (terminal deoxynucleotidyl transferase-mediated dUTP nick-end labelling) assay. After first and second exposures of HL-60/neo or HL-60/Bcl-2 cells to Ara-C, cells were fixed, and DNA was labelled by the addition of fluorescein dUTP at Ara-C-induced strand breaks by terminal deoxynucleotidyl transferase (TdT), utilizing the *in situ* Cell Death Detection Kit

(Boehringer Mannheim, Indianapolis, Indiana). This procedure was optimized from that originally described by Gorczyca and Darzynkiewicz (351). Briefly, following drug removal by centrifugation, 1×10^6 cells were washed in 3 mls PBS and resuspended in 70% ice-cold ethanol for storage at -20°C overnight. The next day, cells were washed 2 times in 1% BSA/PBS at 4°C , adjusted to $1-2 \times 10^7$ cells/ml and transferred to a flat-bottomed 96-well microtiter plate ($100\mu\text{l}/\text{well}$) for further processing. After centrifugation and removal of 1% BSA/PBS, the cells were resuspended in $100\mu\text{l}/\text{well}$ permeabilization solution (0.1% Triton X-100 in 0.1% sodium citrate) and incubated 2 minutes on ice. The cells were washed twice with 1% BSA/PBS and resuspended in $50\mu\text{l}/\text{well}$ TUNEL reaction mixture (TdT enzyme plus labelling solution consisting of nucleotides plus fluoresceinated dUTP), and incubated for 60 minutes at 37°C in a humidified incubator in the dark. After washing with 1% BSA/PBS, the cells were transferred to microcentrifuge tubes after resuspension in $5\mu\text{g}/\text{ml}$ propidium iodide (Sigma) containing 0.1% RNase A (Sigma). After incubation for 30 minutes at room temperature in the dark, flow cytometry was performed on a Becton Dickinson FACSort flow cytometer using LYSYS II Software program version 2.0 for two-color (PI, red, and fluorescein, green) detection of fluorescent emissions. DNA strand breaks in apoptotic cells (sub-G1 phase of the cell cycle) were measured as mean fluorescence intensity of biotin-dUTP labelling, and were analyzed also using LYSYS II software (Becton Dickinson, Immunocytometry Systems, San Jose, CA).

•Statistical Analysis. Statistical analyses were performed as described in **Chapter Three**. For Part A, unpaired t-test was used to compare values obtained between cell lines. For Part B, paired t-test was used to compare values within cell lines (control versus 48-hour values).

Results:

A. Disparate levels of overexpression of p26Bcl-2 govern the response to Ara-C-induced apoptosis and cytotoxicity in human AML HL-60 cells.

•**Creation and Characterization of HL-60/neo and HL-60/Bcl-2 cells:** HL-60 cells were stably infected with recombinant amphotrophic retroviruses carrying either the neomycin (G418) resistance gene alone, or in combination with *bcl-2* cDNA, as described in **Chapter Two**. Subcloning of HL-60/Bcl-2 cells by limiting dilution yielded several monoclonal populations, 15 of which were subsequently screened for homogeneity and level of Bcl-2 expression by immunofluorescence microscopy. By measuring the intensity of Bcl-2 staining as a reciprocal of the brightness level transduced to the camera attached, levels of Bcl2 overexpression compared to HL-60/neo were calculated. Three clonal populations of HL-60/Bcl-2 cells were chosen for their disparate levels of overexpression: HL-60/Bcl-2 clonal population F exhibited homogeneous Bcl-2 expression 2 times higher than HL-60/neo, and was designated as “low overexpression”; HL-60/Bcl-2 clonal population D exhibited homogeneous Bcl-2 expression 4 times higher than HL-60/neo, and was designated as “intermediate overexpression”; and HL-60/Bcl-2 clonal population B exhibited homogeneous Bcl-2 expression 6.3 times higher than HL-60/neo, and was designated as “high overexpression”. [Population B was used for studies presented in **Chapters Three and Five** of this dissertation.] As presented in **Chapter Two**, low endogenous levels of p21Bax and p29Bcl-x_L proteins were unchanged by p26Bcl-2 overexpression in HL-60 cells.

•**Ara-C-induced apoptosis, associated DNA fragmentation, and inhibition of viability in HL-60/neo versus HL-60/Bcl-2 clones:** HL-60/neo and HL-60/Bcl-2 clonal populations B, D, and F were treated with HIDAC (100 μM Ara-C for 4 hours), washed, and resuspended in fresh drug-free culture media to be monitored over time. **Figure 19, panel A** demonstrates that genomic DNA extracted from HL-60/neo cells immediately and 4 hours after HIDAC treatment (lanes 2 and 3, respectively) exhibits the characteristic pattern of internucleosomal DNA fragmentation in 1.0% agarose gel electrophoresis. By 24 and 48 hours after HIDAC treatment this fragmentation pattern is not as sharp and includes smearing indicative of necrosis. By contrast, Ara-C-induced internucleosomal DNA fragmentation is reduced in the lowest, and

blocked in the intermediate, and highest overexpressing HL-60/Bcl-2 clonal populations (HL-60/Bcl-2 clone F, lanes 7 to 10; HL-60/Bcl-2 clone D, lanes 12 to 15; HL-60/Bcl-2 clone B, lanes 17-20, respectively). Similarly, **Figure 19, panel B** demonstrates that higher molecular weight DNA fragments ranging from approximately 5 to 300 kilobase in size were observed more intensely in HL-60/neo cells immediately after HIDAC, 4, 24, and 48 hours after HIDAC treatment (lanes 2 to 5, respectively), than in HL-60/Bcl-2 clonal populations at the same time points when genomic DNA-agarose plugs were subjected to field inversion gel electrophoresis (HL-60/Bcl-2 clone F, Lanes 7 to 10; HL-60/Bcl-2 clone D, lanes 12 to 15; HL-60/Bcl-2 clone B, lanes 17 to 20). It is important to note, however, that beginning at 4 hours after HIDAC treatment and resuspension in drug-free media, genomic DNA extracted from the lowest overexpressing HL-60/Bcl-2 clone F exhibited internucleosomal DNA fragmentation at low intensity. In addition, field-inversion gel electrophoresed DNA-agarose plugs from HL-60/Bcl-2 clone F at 4 hours after HIDAC-treatment also exhibited faintly detectable levels of higher molecular weight DNA fragmentation. Later, in both HL-60/Bcl-2 clones D and B, this fragmentation was slightly detectable at 24 and 48 hours after HIDAC treatment in several experiments.

Table VIII, Part I shows the results of flow cytometric evaluation of apoptosis detected as the percentage of cells in the sub-G₁ phase of the cell cycle in propidium iodide-stained HL-60/neo and HL-60/Bcl-2 clonal populations, either untreated or at various time points after HIDAC treatment, with graphical representation of the data underneath the table. This table highlights that a significantly greater percentage of HL-60/neo cells are detected in the sub-G₁ phase of the cell cycle immediately following HIDAC treatment, as illustrated in the propidium iodide histograms in (see **arrow in Figure 20**, pointing to increased percentage of sub-G₁ phase cells in the HL-60/neo population), as well as 4, 24, and 48 hours after HIDAC treatment than any of the HL-60/Bcl-2 clonal populations assessed immediately following HIDAC treatment. The percentages of apoptotic HL-60/neo cells increase and reach a plateau over time. While the percentages of apoptotic HL-60/Bcl-2 cells in all three clonal populations increase over time, as well, these percentages are significantly lower than in HL-60/neo cells. However, this table demonstrates that as time progresses after HIDAC treatment, a greater percentage of apoptotic HL-60/Bcl-2 cells are detected in lowest overexpressing clonal population F than in intermediate or highest overexpressing clonal populations D and B.

As demonstrated in **Chapter Three**, Bcl-2 levels are directly correlated to increased cell viability after Ara-C treatment, and in this Chapter are demonstrated to extend this correlation over time after Ara-C treatment. **Figure 21, top graph**, shows assessment of cell viability by the MTT assay at various time points after Ara-C treatment in HL-60/neo versus HL-60/Bcl-2 clonal populations, as tabulated in **Table IX, Part I**. Overall, exposure to HIDAC produced significantly greater cytotoxicity in HL-60/neo versus HL-60/Bcl-2 clonal populations for up to 24 hours after HIDAC treatment. For up to 12 hours after HIDAC treatment, inhibition of viability was significantly less ($p < 0.05$) in lowest, intermediate, and highest overexpressing populations HL-60/Bcl-2 F, D, and B, as compared to HL-60/neo, and despite disparate endogenous levels of p26Bcl-2, inhibition of viability in HIDAC-treated HL-60/Bcl-2 F, D, and B were not found to be significantly different ($p > 0.05$) from each other during these time points. However, after 12 hours following HIDAC treatment, while inhibition of viability was consistently and significantly less in HIDAC-treated intermediate-overexpressing HL-60/Bcl-2 D and highest-overexpressing HL-60/Bcl-2 B clonal populations as compared to HL-60/neo cells, the inhibition of viability in the lowest overexpressing HL-60/Bcl-2 F clonal population increased to levels which were not significantly different ($p > 0.05$) from that demonstrated in HL-60/neo cells up to 48 hours following HIDAC. Therefore, at 24 and 48 hours after HIDAC treatment, the highest and intermediate overexpressing HL-60/Bcl-2 clonal populations D and B exhibit significantly less inhibition of viability by the MTT assay than lowest overexpressing HL-60/Bcl-2 clonal population F or HL-60/neo cells. These results are consistent with assessment of cell viability by trypan blue exclusion, a late manifestation of cytotoxicity characterized by loss of membrane permeability. **Figure 21, bottom panel** demonstrates that up to 24 hours after HIDAC treatment, all HL-60/Bcl-2 clonal populations show significantly less inhibition of viability by Ara-C treatment by virtue of higher percentages of viable cells, which are still able to exclude trypan blue from their membranes. This data in Figure 21 is tabulated in **Table IX, Part II**. At 48 hours, the membrane integrity assayed for by trypan blue dye exclusion is maintained significantly only in the highest overexpression HL-60/Bcl-2 clonal population B. As compared to the data obtained by the MTT assay, this discrepancy reflects the different endpoints tested for by the two assays.

B. *bcl-2* expression is induced in human AML HL-60 cells which survive treatment with high-dose Ara-C.

•**Western blot analyses for p26Bcl-2 and p21Bax expressions in HL-60/neo versus HL-60/Bcl-2 clonal populations.** Figure 22 displays Western blot analyses showing disparate endogenous levels of p26Bcl-2 expression in HL-60/neo (lane 1), lowest overexpressing HL-60/Bcl-2 clonal population F (lane 6), intermediate overexpressing HL-60/Bcl-2 clonal population D (lane 11), and highest overexpressing HL-60/Bcl-2 clonal population B (lane 16). In addition, these Western blots demonstrate that endogenous levels of Bcl-2 homolog p21Bax are similar in all four cell populations studied (same lanes). Immediately following HIDAC treatment, as well as 4, 24, and 48 hours following HIDAC treatment, total protein was extracted from all 4 cell lines for immunoblot analyses. 10 µg total protein was assessed for p26Bcl-2 levels and 50 µg assessed for p21Bax levels. When scanning densitometry was performed, levels obtained for p26Bcl-2 expression were multiplied by 5 to equalize with p21Bax amount and divided by the intensity level for p21Bax in order to obtain a ratio for p26Bcl-2:p21Bax expression. Table X shows results of calculations of p26Bcl-2:p21Bax ratios in HL-60/neo cells as compared to HL-60/Bcl-2 clonal populations F, D, and B for up to 48 hours following HIDAC treatment. While p21Bax levels remained the same in all populations studied, despite disparate endogenous levels of p26Bcl-2, p26Bcl-2:p21Bax ratios increased from control to 48 hours after HIDAC treatment in all four cell lines studied (corresponding to lanes 2 to 5 for HL-60/neo; lanes 7 to 10 for lowest overexpressing HL-60/Bcl-2 clonal population F; lanes 12 to 15 for intermediate overexpressing HL-60/Bcl-2 clonal population D; lanes 17 to 20 for highest overexpressing HL-60/Bcl-2 clonal population B, respectively, in Figure 22, with graphical representations in Figure 22a). Statistical analyses including paired t-test showed that these increases were significant in HL-60/neo cells ($p < 0.05$), in HL-60/Bcl-2 clonal populations F and D ($p < 0.01$), but not statistically significant in HL-60/Bcl-2 clonal population B, whose intensity of p26Bcl-2 expression by Western blot is already extremely high.

•**Flow cytometric and immunofluorescent analyses for increases in p26Bcl-2 expression in HIDAC-treated HL-60/neo and HL-60/Bcl-2 clonal populations:** Because scanning densitometry results are susceptible to variable subjectivity in determining the area and density of protein bands, and because the high intensity of signals may saturate the imaging films to

inaccuracy, two additional methods were employed to confirm the increases in Bcl-2 expression detected in all four cell populations studied after Ara-C treatment. Immunofluorescent staining and fluorescent microscopy was used also to detect increases in Bcl-2 intensity over time after HIDAC treatment in HL-60/neo and HL-60/Bcl-2 F, D, and B cells. As described in the methods section, after immunostaining fixed and permeabilized cells from various conditions, non-apoptotic cells surviving immediately after, 24, or 48 hours after HIDAC treatment were identified first by paired-field phase contrast microscopy, and Bcl-2 intensity level subsequently assessed as a function of the brightness sent to the attached camera when the fluorescence wavelength was activated. **Figure 23** is a graphical representation of the data presented in **Table XI**, which demonstrates that compared to untreated control cells, and despite disparate endogenous Bcl-2 levels in control cells, HL-60/neo as well as lowest, intermediate, and highest overexpressing HL-60/Bcl-2 F, D, and B clonal populations, respectively, exhibit statistically significant ($p < 0.05$) increases in Bcl-2 intensity in surviving, non-apoptotic cells up to 48 hours following HIDAC treatment. Taken together, these data represent confirmed increases in Bcl-2 protein levels in HL-60 cells which survive after Ara-C treatment despite disparate endogenous levels in parental versus transfected clonal populations. Increase in p26Bcl-2 levels over time in all cell lines presented was confirmed by flow cytometry. **Table XII** shows results of assessment of Bcl-2 levels by flow cytometry utilizing double staining by anti-Bcl-2 antibody and propidium iodide staining for DNA content in HL-60/neo cells and HL-60/Bcl-2 F, D, and B clonal populations with graphical representation underneath. Mean fluorescent p26Bcl-2 levels were tabulated in non-apoptotic (G_1 , S, and G_2 phase) cells by Elite multicycle software. At various time points over 48 hours after HIDAC treatment, non-apoptotic HL-60/neo cells as well as non-apoptotic HL-60/Bcl-2 F, D, and B clonal populations demonstrate statistically significant increases ($p < 0.05$) in Bcl-2 expression as compared with untreated HL-60/neo, HL-60/Bcl-2 F, D, and B cells.

• Ribonuclease protection assay for induction of *bcl-2* mRNA expression in HL-60/neo versus HL-60/Bcl-2 clonal populations after HIDAC treatment, and flow cytometric determination of effect of RNA synthesis and protein synthesis inhibitors on increased p26Bcl-2 levels: To address the question whether the mechanism by which the above demonstrated increase in Bcl-2 levels among surviving cells is due to selection of populations of cells which overexpress Bcl-2 or due to up-regulation of *bcl-2* mRNA expression, ribonuclease

protection assay for *bcl-2* mRNA expression relative to β -*actin* mRNA expression was performed on 50 μ g total RNA extracted from 100×10^6 HL-60/neo or HL-60/Bcl-2 B cells at various time points after HIDAC treatment. After double hybridization with human *bcl-2* and β -*actin* antisense RNA probes, *bcl-2* expression relative to β -*actin* expression levels were compared, utilizing horizontal scanning densitometry, and expressed as percent of control. **Figure 24** shows *bcl-2* mRNA expressions in HL-60/neo cells as compared to HL-60/Bcl-2 B cells at various time intervals following HIDAC treatment. **Panel A** shows that while *bcl-2* mRNA is barely detectable in HL-60/neo cells at this exposure and hybridization level, higher *bcl-2* mRNA levels in HL-60/Bcl-2 cells increased further to statistically significant values over control values beginning at 2 hours of Ara-C treatment and continuing up to 24 hours after Ara-C treatment (lanes 8-12 in HL-60/Bcl-2 versus lanes 2-6 in HL-60/neo cells). **Panel B** shows graphical representation of these values, shown in **Table XIII**, expressed as percentage of induction over *bcl-2*: β -*actin* ratio in control cells. (The left graph shows that induction of *bcl-2* mRNA was not detected in HL-60/neo cells, but indeed detected in HL-60/Bcl-2 cells on the right graph. Larger views of the graphs are provided in **Figure 24a**). To further determine whether these increases in *bcl-2* levels were due to increased RNA synthesis, the effect of concomitant exposure to 5 μ g/ml RNA synthesis inhibitor actinomycin D (as used previously in refs. 255, 352) was determined, both during Ara-C exposure, and then replaced when Ara-C was washed from the cells at the end of the 4-hour exposure. **Panel C** of **Figure 24** shows that in HL-60/Bcl-2 cells, increases in *bcl-2* mRNA levels after 2 and 4 hours of 100 μ M Ara-C treatment (lanes 2 and 3) as well as 4, 8, and 24 hours after Ara-C treatment (lanes 4, 5, and 6, respectively), were abrogated by concomitant actinomycin D exposure. The graph in **Panel D** (with larger view in **Figure 24a**) depicts that Actinomycin D treatment causes the *bcl-2*: β -*actin* levels to return to approximately that of control values, as listed in **Table XIII** (for example, 121.01% of control \pm 8.39 at 4 hours of Ara-C treatment versus 97.96% of control \pm 4.46 at 4 hours of Ara-C plus concomitant actinomycin D treatment), and suggests that new *bcl-2* mRNA synthesis is induced by Ara-C treatment in surviving cells of various populations. In addition, both concomitant treatments with actinomycin D as well as 10 μ g/ml cycloheximide (255) similarly abrogated Ara-C-mediated increases in p26Bcl-2 expression in all cell lines as detected by flow cytometry. **Table XIV** shows that, statistically significant increases in p26Bcl-2 levels up to 48 hours after Ara-C treatment (similar to the results in **Table XII**) are also abrogated by continuous exposure to 5 μ g/ml actinomycin D or 10 μ g/ml cycloheximide, which inhibit *de*

novo bcl-2 induction. Each inhibitor returns p26Bcl-2 levels to approximately equivalent to control levels in each cell line studied, as illustrated in the graphs in **Figure 25**. These data indicate that induction of *bcl-2* occurs at the RNA level after exposure to Ara-C, irrespective of endogenous level of p26Bcl-2.

•Effect of second HIDAC treatment of surviving HL-60/neo or HL-60/Bcl-2 on cell viability assessed by MTT assay, as indication of biological significance of increased Bcl-2 expression.

The above results demonstrate a statistically significant increase in Bcl-2 expression in HL-60/neo, HL-60/Bcl-2 F, D, or B cells surviving after HIDAC treatment, despite disparate endogenous p26Bcl-2 levels. To address the question whether this statistically significant difference in Bcl-2 expression over time is indeed biologically significant, HL-60/neo cells, which most readily show evidence of HIDAC-induced apoptosis, were pre-treated with HIDAC, washed 5 to 6 times with sterile PBS, and resuspended in fresh drug-free media. During three days' growth in drug-free media, the surviving cells in both populations were separated from dead or apoptotic cells and debris by daily centrifugation over Histopaque density gradient, and were re-exposed to various concentrations of Ara-C. After 4 hours of second treatment with different doses of Ara-C, cells were washed, resuspended in fresh, drug-free media for 20 hours and subsequently assessed for cell viability by the tetrazolium dye MTT assay. **Figure 26** shows results of assessment of viability after first and second Ara-C treatment of HL-60/neo cells. **The top panel** is an image of a 96-well plate showing the end result of a representative MTT assay in which HL-60/neo cells which have survived initial HIDAC treatment show higher viability by virtue of darker intensity of soluble mitochondrial enzymes precipitated in MTT and dissolved in DMSO/ethanol (as described in **Materials and Methods**) than original HL-60/neo cells exposed to the same concentrations of Ara-C. The following **Table XV** and **Figure 27a, top graph**, show that for various concentrations, Ara-C was less capable of inhibiting cell viability in pre-treated HL-60/neo cells as compared to previously untreated HL-60/neo cells. In addition, further evidence for increase in viability in surviving pre-treated HL-60/neo cells was also found by decreased percentages of apoptotic cells and total DNA breaks as detected by fluorescein-conjugated dUTP labelling (TUNEL assay), propidium iodide staining for DNA content, and subsequent flow cytometry. **Figure 27** is merged with **Table XVI**, and depicts propidium iodide histograms for the induction of apoptosis in previously untreated HL-60/neo cells exposed to increasing concentrations of Ara-C (100 nM to 100 μ M for 4 hours), and compares the height of

the sub-G₁ (apoptotic) peak with that seen in pre-treated HL-60/neo cells exposed to the same concentrations of Ara-C. **Table XVI** underneath each histogram shows that the percentage of apoptotic cells detected either flow cytometrically or visually for morphologic evidence of apoptosis in pre-treated HL-60/neo cells are significantly less for 1 and 10 μ M Ara-C than for previously untreated HL-60/neo cells (presented in **Figure 27a, bottom graph**), as are total DNA breaks labelled by TUNEL assay and detected flow cytometrically.

These results correlate increased Bcl-2 levels over time after HIDAC treatment with increased survival advantage upon re-exposure to Ara-C, especially at low dosages, by virtue of increased viability and significantly less manifestation of Ara-C-induced apoptosis.

Discussion:

Immediately following treatment with HIDAC (100 μ M Ara-C for 4 hours), it can be consistently demonstrated that high levels of p26Bcl-2 overexpression block the late manifestations of Ara-C-induced apoptosis, including Ara-C-induced internucleosomal DNA fragmentation, high molecular weight DNA fragmentation, and the morphologic features of apoptosis, and decreases Ara-C-induced inhibition of cell viability in HL-60 AML cells. The studies presented in **Chapter Two** demonstrated that although p26Bcl-2 blocks Ara-C-induced double-strand DNA damage, early steps in Ara-C metabolism, including the generation of early DNA damage manifested as strand breaks, are not affected by p26Bcl-2 overexpression. The studies presented in this chapter address the question as to what extent disparate levels of p26Bcl-2 overexpression in HL-60 cells affect the fate of residual Ara-C-induced DNA damage over time after Ara-C is removed from the culture media and cells either survive or engage the apoptotic pathway. As an explanation for cell survival, an additional question addressed in this chapter is whether Bcl-2 levels themselves are modulated

To attempt to answer these questions, HL-60/neo and HL-60/Bcl-2 cells generated for the studies in **Chapters Two and Three** were further characterized by virtue of the disparate levels of p26Bcl-2 overexpression in HL-60 parental cells transfected with retroviral constructs containing *bcl-2* cDNA. The original total population of HL-60 cells stably infected with *bcl-2*-

containing retroviruses was heterogeneous for its overexpression of p26Bcl-2, with individual cells exhibiting disparate levels of Bcl-2 overexpression, as assessed by immunofluorescent staining (data not shown). Because stable transfection results in random integration of the cDNA of interest into the genome (307-309), it is possible that *bcl-2*-containing retroviruses which infected HL-60 cells integrated at various sites which differed in their contributions toward favorable environments for *bcl-2* expression to high levels. Subcloning of HL-60/Bcl-2 cells by limiting dilution produced several clonal populations, which, since generated from an original population heterogeneous for Bcl-2 expression, exhibited homogeneous overexpression of Bcl-2 to different levels, but consistently low endogenous expression of p21Bax and p29Bcl-x_L by Western blot. Specifically, HL-60/Bcl-2 clonal populations F, D, and B were chosen, with levels of Bcl-2 overexpression approximately 2, 4, and 6.3 times higher than in HL-60/neo cells as determined by levels of intensity of Bcl-2 staining detected by a fluorescence microscope and photography apparatus described in the Methods section. Since HL-60/Bcl-2 clonal population B exhibited the highest level of overexpression, these cells were used for the studies in **Chapters Two and Three**. The studies presented in this chapter utilize clonal population B, as well as the intermediate overexpressing population D and the lowest overexpressing population F in order to identify a **potential threshold level** for p26Bcl-2-mediated blockade of Ara-C-induced apoptosis and protection of HL-60 cells after HIDAC treatment.

A. Disparate levels of overexpression of p26Bcl-2 govern the response to Ara-C-induced apoptosis and cytotoxicity in human AML HL-60 cells.

Analysis of genomic DNA for internucleosomal DNA fragmentation and DNA-agarose plugs for high molecular weight DNA fragmentation demonstrated that high and intermediate levels of overexpression of p26Bcl-2 protected HL-60 cells from HIDAC-induced double-stranded DNA fragmentation for up to 24 hours following Ara-C treatment. Only in HL-60/Bcl-2 clone F, with the lowest levels of overexpression (2 times greater than that exhibited by HL-60/neo cells), was double-strand DNA of both large size and low molecular weight size detected beginning at 4 hours after Ara-C treatment. Similarly, as detected by flow cytometry, Ara-C is prevented from inducing apoptotic fractions in the lowest, intermediate, and highest overexpressing fractions of HL-60/Bcl-2 cells for several hours. However, the lower the level of p26Bcl-2 overexpression, however, the more apoptotic cells are increasingly detected after

HIDAC treatment, illustrating a dose-response of Bcl-2 level to amounts of apoptosis inhibited.

In addition, as evident by the result from the MTT assay, which is specific for viable mitochondrial enzymes still functional after drug treatment, HL-60/Bcl-2 with highest levels of Bcl-2 overexpression (clonal populations D and B) exhibit significantly less inhibition of cell viability up to 48 hours after Ara-C treatment, while cells with lowest (two times higher) overexpression of Bcl-2 lose the ability to block inhibition of cell viability, similar to HL-60/neo cells, by 24 hours after Ara-C treatment. Trypan blue dye exclusion studies in these various clones also demonstrate that higher levels of Bcl-2 overexpression protect against loss of cell viability due to Ara-C, better than cells which have lower expression of Bcl-2. The different features of cell viability measured by the two assays may reflect the disparity in timing of protection against the loss of viability in HL-60/Bcl-2 clone F. The data presented may indicate that loss of membrane permeability occurs later than inhibition of mitochondrial enzymes, thereby explaining differences in viability levels in lower overexpressing HL-60/Bcl-2 F cells by the two methods.

Taken together, these data indicate that progressively greater levels of Bcl-2 confer HL-60 cells with a progressively greater survival advantage following treatment with Ara-C. Bcl-2 expression and the degree of protection it confers may be subject to interpretation based on the individual assays used to evaluate specific features of viability. When used, they demonstrate that even a two-fold level of overexpression of Bcl-2 does confer a distinct survival advantage.

While these data demonstrate that Bcl-2 can dampen the manifestations of apoptosis, an explanation is therefore required, however, as to the delayed induction of this double-strand DNA fragmentation. Tang *et al.* demonstrated that despite initial blockade of taxol-induced apoptosis by p26Bcl-2 overexpression, 697/Bcl-2 cells still exhibited taxol-induced microtubular bundling, and when monitored over time after taxol treatment, a small percentage of cells eventually escaped this blockade and exhibited internucleosomal DNA fragmentation associated with apoptosis (101). Here, an alternative pathway for taxol-induced cell death was suggested as an explanation for the eventual induction of apoptosis in a percentage of 697/Bcl-2 over time.

Manome *et al.* found that when U937 myeloid leukemia cells transfected with *bcl-2* were exposed to various doses of Ara-C (1 nM to 10 mM for 3 hours) and monitored for up to 24 hours after treatment, that protection from apoptosis by p26Bcl-2 was an operative mechanism only at low doses of Ara-C (353). They argue that because there was no associated increase in DNA fragmentation in *bcl-2*-transfectants with disparate levels of Bcl-2 given a fixed dose of Ara-C, and that because higher doses of Ara-C caused more cell death in U937/Bcl-2 cells than low doses of Ara-C, that apoptosis is probably a less relevant mechanism for Ara-C-induced cytotoxicity at higher doses than is diffuse DNA degradation associated with Ara-C-induced DNA strand breaks (353). This also suggests an alternative mechanism induced by Ara-C-mediated DNA damage in AML cells independent of the target(s) of Bcl-2-mediated blockade of cell death, with higher doses of Ara-C inducing more cytotoxicity beyond the scope of frank apoptosis. In addition, Yin and Schimke have recently reported that Bcl-2 overexpression in HeLa S3 cells delays aphidicolin- or colcemid-induced apoptosis and DNA fragmentation for up to 36 hours of treatment, yet does not increase clonogenic survival in drug-treated transfected cells (354). However, they report that Bcl-2 did increase clonogenic survival in HeLa S3 cells exposed to short treatment with a different apoptotic stimulus, trimetrexate (354). They suggest that aphidicolin treatment itself induced commitment to apoptosis upstream of Bcl-2-mediated blockade in these cells distinct from that of trimetrexate (354), and therefore also illustrate that Bcl-2-independent and Bcl-2-dependent pathways of apoptosis exist. Cuende *et al.* further support this suggestion by demonstrating that Bcl-2 overexpression in B lymphoma cells selectively protects against cell death due to withdrawal of only specific growth factors (355). **Therefore, alternate apoptotic signals independent of the initial Bcl-2-mediated blockade may account for the inevitable induction of apoptosis in a small percentage of cells irrespective of endogenous Bcl-2 levels.**

As mentioned in the introduction of **Chapter One** and the discussion of **Chapter Three**, Ara-C may also induce an additional pathway not affected by Bcl-2, including the modulation of protein kinases and/or transcription factors, and the stimulation of signal transduction pathways which affect targets distinct from genomic DNA. This concept may account for the delayed but eventual induction of apoptosis seen here even in cells overexpressing Bcl-2, by a pathway(s) which is independent of, and may override, Bcl-2 activity in a small percentage of cells. Conversely, this eventual induction of apoptosis in a small percentage of cells may be due to an

inherent or acquired heterogeneity of Bcl-2 expression in the populations studied, and is examined. Another question to be addressed is the mechanism by which the surviving cells maintain their blockade of the induction of the apoptotic pathway, despite the demonstration of equivalent extents Ara-C-induced early DNA damage in the studies presented in **Chapter Three**, and despite evidence for eventual engagement of the apoptotic pathway in a small percentage of cells presented in this chapter.

Part B. *bcl-2* expression is induced in human AML HL-60 cells which survive treatment with high-dose Ara-C.

When Tang *et al.* reported delayed onset of taxol-induced apoptosis in 697/Bcl-2 cells instead of complete blockade up to 4 days after taxol treatment, they demonstrated that this eventual demise in a percentage of the cell population, although less than in identically treated 697/neo cells, was not accompanied by decreases in p26Bcl-2 levels by Western blot analysis (104). Similarly, Tang *et al.* demonstrated that while combined treatment of HL-60 parental cells with GM-CSF/IL-3 fusion protein p1XY321 plus Ara-C enhanced apoptosis, this increase in cytotoxicity was not accompanied by decrease in p26Bcl-2 levels (356). The studies presented in this Chapter Four also examine p26Bcl-2 levels themselves as monitored over time after Ara-C treatment in HL-60/neo versus HL-60/Bcl-2 clonal populations, first in the total population by Western blot, and then specifically in non-apoptotic surviving cells distinguished by immunofluorescent microscopy and flow cytometry, as a potential explanation for the ability of surviving cells to avoid the induction of HIDAC-induced apoptosis. The Western blots in **Figure 22** display moderate increases p26Bcl-2 levels in HL-60/neo as well as HL-60/Bcl-2 clonal populations up to 48 hours after Ara-C treatment. Furthermore, p21Bax levels did not change by Western blot analysis, even as percentages of cells undergoing apoptosis, increased to various degrees in all cell lines examined, as detected by propidium iodide staining and flow cytometry. In the Western blots presented here, p21Bax levels represent total Bax levels, and were the only form of Bax detected in these cell lines with this method of protein extraction. Here, total Bax levels were not distinguished as being unbound or bound as homodimers or heterodimers with Bcl-2 or other Bcl-2 family members. Other newly described Bcl-2-related proteins which complex with Bcl-2 in various interactions, including bad, bag-1, and bak were also not yet examined (175-179). The increases in Bcl-2 levels over time after Ara-C treatment, however, were indeed confirmed by immunofluorescence and flow cytometry in HL-60/neo as

well as HL-60/Bcl-2 clonal populations. Furthermore, these confirmatory techniques allowed the distinction between apoptotic and non-apoptotic cells, and demonstrated that Bcl-2 levels indeed increased in surviving intact cells of all 4 cell lines up to $170.80\% \pm 26.89$ of control (or 1.7-fold increase) up to 48 hours after Ara-C treatment (as seen in HL-60/Bcl-2 clone F in **Table XII**). This is consistent with the recent findings by Andreeff *et al.* in leukemic CD34+ cells derived from patients who failed to achieve complete remission after 3 to 4 days of receiving induction chemotherapy, in which Bcl-2 levels increased by 185%, as detected by flow cytometry (357). Whether Ara-C treatment, Ara-C-induced transcription factors or protein kinases, or the apoptotic process may alter Bcl-2 conformation such that the epitope recognized by the anti-Bcl-2 antibody used is actually made more accessible, yielding a higher fluorescence at the protein level, is one cautioned possibility worthy of further confirmation (146). However, by Western blot, no other higher molecular weight species of Bcl-2 were observed after Ara-C treatment in any of the cell populations tested, as seen by Willingham in taxol-treated KB cells (146), or by Haldar *et al.* in taxol-treated prostatic carcinoma cells, indicative of phosphorylation of Bcl-2 (85). Only smaller bands are slightly detectable, which have also been previously noted using this antibody, and suggested to represent either breakdown products of Bcl-2 or products of alternatively spliced transcripts of *bcl-2* (94).

These data which show increased Bcl-2 at the protein level after Ara-C treatment only partially support the Bcl-2:Bax “rheostat” theory proposed by Oltvai and Korsmeyer, which hypothesizes that the levels of opposing proteins Bcl-2 and Bax govern the fate of cells exposed to apoptotic stimuli (161, 166). Oltvai and Korsmeyer predict that cells which possess higher Bcl-2 levels are protected from apoptosis, while cells which possess higher Bax levels are more susceptible to apoptosis (161, 166). Chresta *et al.* demonstrate that human testicular tumors with high Bax:Bcl-2 ratios are more susceptible to drug-induced apoptosis (358). In addition, Thomas *et al.* also demonstrate by Western blot analysis that B-cell chronic lymphocytic leukemia (B-CLL) cells with low Bcl-2:Bax ratios were sensitive to apoptosis induced by a camptothecin analogue, while cells with intermediate to high Bcl-2:Bax ratios were drug resistant (359). In addition, they showed the up-regulation of various Bax complexes in drug sensitive B-CLL cells undergoing apoptosis (359). The data presented in this chapter demonstrate indeed that HL-60 cells which possess high levels of p26Bcl-2 are protected from the induction of Ara-C-induced apoptosis. However, the consistently low levels of p21Bax

detected by Western blot in both HL-60/neo and HL-60/Bcl-2 cells do not illustrate any modulation in total p21Bax levels by this method, despite disparate apoptotic outcomes in these various cell lines after HIDAC treatment. If these data were to be consistent with Oltvai and Korsmeyer's model, it would be predicted that as HL-60 cells with disparate levels of overexpression of p26Bcl-2 undergo apoptosis, either immediately in a large percentage of HL-60/neo cells, or eventually in a small percentage of HL-60/Bcl-2 cells, the levels of p21Bax might rise and contribute to an explanation for their variable susceptibilities to drug-induced apoptosis. Further detailed studies examining absolute free Bax levels in apoptotic cells are presently underway in our laboratory. In addition, as mentioned in the introduction of this thesis, Miyashita *et al.* have recently demonstrated that the wild-type tumor suppressor p53 can regulate *bcl-2* and *bax* expressions (62) *in vitro* and *in vivo*, and may utilize the modulations of these genes as a mechanism of its ability to stimulate apoptosis. wt-p53 down-regulates *bcl-2* expression by virtue of its binding to a p53-dependent negative response element downstream of the major promoter utilized in the transcription of the *bcl-2* gene (62, 75). Conversely, the *bax* gene contains a consensus sequence for p53 binding, and is up-regulated by wt-p53 (63). HL-60 cells, however, have deletions of *p53* (285). The data presented here illustrate that p53 expression is not necessarily required for the induction of apoptosis by Ara-C in HL-60 cells, or for the modulation of *bcl-2* expression.

1. Induction of *bcl-2* versus selection for Bcl-2.

Whether increases in total Bcl-2 levels were also due to **selection** of populations of cells with higher Bcl-2 levels, or due to induction of *bcl-2*, was considered. In order to address the question whether the demonstrated increases in *bcl-2* levels take place at the transcriptional level, the ribonuclease protection assay (RPA) was then used. Previously, Bhalla *et al.* reported that in HL-60 cells subjected to a prolonged exposure to 100 μ M Ara-C (for 24 hours), *bcl-2* mRNA levels decreased as increasing percentages of cells underwent apoptosis, as demonstrated by Northern blot (360). However, this level of *bcl-2* mRNA was not quantitated relative to β -*actin* mRNA expression, and represents expression in the total cell population. The *bcl-2* RNA analysis presented in this chapter is the result of the more sensitive RPA, and the signals were quantitated using scanning densitometry. Furthermore, these results are obtained from total RNA from intact non-apoptotic HL-60/neo or HL-60/Bcl-2 cells separated from apoptotic cells after HIDAC treatment by Histopaque density gradient centrifugation. The studies presented

here in this chapter demonstrate the induction of *bcl-2* mRNA as detected by RPA most appreciably in Bcl-2-overexpressing cells exposed to and recovering from HIDAC treatment. Increases in steady-state *bcl-2* mRNA levels above that in untreated HL-60/Bcl-2 cells were abrogated by concomitant exposure to RNA synthesis inhibitor actinomycin D as previously used (255, 352), further indicating that this induction occurs at the level of transcription. While *bcl-2* mRNA levels in HL-60 parental and HL-60/neo cells are low, moderate levels of Bcl-2 protein are still detectable (Figures 14, 16, 22). This has been also noted by Delia *et al.* and attributed to the long half-life of the Bcl-2 protein (200). Thus a modest increase in *bcl-2* expression at the mRNA level (only approximately 120% of control in HL-60/Bcl-2 B clones, or 1.2-fold increase) may lead to a significant up-regulation of Bcl-2 at the protein level. When the final Bcl-2 protein product was re-examined by flow cytometry, concomitant actinomycin D, as well as protein synthesis inhibitor cycloheximide also abrogated *de novo* increases in Bcl-2 levels after Ara-C treatment. Similar results have been noted by Perreault and Lemieux when *de novo* expression of *c-myc* was inhibited to the same extent by either inhibition of transcription with Actinomycin D or inhibition of protein synthesis by cycloheximide, and links cycloheximide to the inhibition of gene expression in general (361). These similar results obtained in this Chapter with both types of synthesis inhibitors further suggest that the induction of *bcl-2* occurs at the transcriptional level because they interfere (at different steps) with the ultimate translation of *bcl-2* message into higher levels of Bcl-2 protein.

Selection is also a possible explanation for the mechanism for increased Bcl-2 levels detected by the above presented experiments. The proportion of cells in any population which succumbs to apoptosis may be that proportion with lower levels of Bcl-2, while those that survive may represent a new population of cells with higher Bcl-2, and which withstand a selective pressure. Andreef *et al.* suggest selection as the means of up-regulation of Bcl-2 levels in patient-derived CD34+ cells which survive after chemotherapy treatment because induction of *bcl-2* by PCR was not detected (356). In this Chapter, histopaque centrifugation to study RNA induction in only non-apoptotic cells may represent an artificial selection process in a population harvested for extraction. In this dissertation, however, the actual movement toward selection of cells with higher Bcl-2 levels from the total population of cells after Ara-C treatment does not seem as likely in the originally homogeneous clonal populations of HL-60/Bcl-2 cells presented here, as in HL-60/neo cells, which were not subcloned by limiting dilution and exhibit slight

heterogeneity of endogenous Bcl-2 intensity (seen previously by immunofluorescence in **Figure 15, Chapter Two**). Although selection from a population of cells which contain slightly higher levels of Bcl-2 may still be a possibility for all cell lines studied, it is not supported by the homogeneous overexpression of Bcl-2 maintained in the HL-60/Bcl-2 clones both at 10 and 19 months after original isolation, as visualized by immunofluorescence microscopy. **The modest induction of *bcl-2* is concluded to at least contribute to the up-regulation of Bcl-2 detected in cells which survive Ara-C treatment.** While induction of *bcl-2* mRNA was not detectable in HL-60/neo cells by the optimizations used in the RPAs presented here, higher Bcl-2 protein levels after Ara-C treatment were still detected in HL-60/neo cells as well, and abrogated by concomitant exposure to actinomycin D or cycloheximide, indicating that induction of *bcl-2* can occur in HL-60/neo cells as well.

How Ara-C treatment affects Bcl-2 levels is an important issue to address in understanding the mechanism for this up-regulation. Further in-depth studies to elucidate the molecular mechanism of regulation of *bcl-2* RNA transcription would include nuclear run-on assay to determine whether the mechanism of increased *bcl-2* RNA levels is due to increased rates of transcription or to increased stability of the *bcl-2* mRNA transcripts themselves. At the RNA level, further studies would be to examine the effect of Ara-C-induced transcription factors or protein kinases on the *bcl-2* promoter region by CAT (chloramphenicol acetyltransferase) assays. Also, because the *bcl-2* gene sequence contains two AP-1 binding sites downstream of its ORF, for example, another possibility to be examined is the regulation of *bcl-2* expression in *trans* by Ara-C-induced alternate targets. The existence of a positive feedback loop to up-regulate *bcl-2* expression when cells are exposed to an apoptotic signal may be yet another possibility. However, specific positive response elements in the *bcl-2* promoter sequence have yet to be identified. Whether the induction of *bcl-2* levels occurs after treatment of AML cells with drugs other than Ara-C is yet another important further study, and would give an important indication toward the mechanisms by which leukemic cells may launch a survival response after exposure to apoptotic stimuli.

The results presented in this part of Chapter Four are consistent with previous studies in the literature which have demonstrated up-regulation of drug resistance genes after drug treatment in various cell systems. *mdr-1* mRNA expression was induced after drug treatment in

mdr⁺ cell line CEM/A7R, as reported by Hu *et al.* (345), in mouse hepatoma cells after dexamethasone treatment, as reported by Zhao *et al.* (350), and by quantitative RT-PCR in K562 cells after treatment with various chemotherapeutic agents by Chaudhary and Roninson (349). Among the few instances in the literature of up-regulation of members of the Bcl-2-related protein family is a report by Schwarze and Hawley in which Interleukin-6 (IL-6)-mediated suppression of apoptosis in B9 myeloma cells was associated with up-regulation of *bcl-x* mRNA and Bcl-x_L protein, but not induction of *bcl-2* expression (362). Han *et al.* report the isolation of an HL-60 cell line resistant to 8-Cl-cAMP, after growth in concentrations of 10-100 μM for 4 weeks, which exhibits up-regulation of *bcl-x_L* mRNA as well as Bcl-x_L protein (363). Datta *et al.* also report that U937 cells selected for acquired resistance to doxorubicin and vincristine were found to eventually overexpress *bcl-x_L* mRNA and Bcl-x_L protein, and not Bcl-2 to biologically significant levels (148). These cell lines, however, were continually exposed to low (up to 20 ng/ml final) concentrations of these cytotoxic drugs in order to generate doxorubicin- and vincristine-resistant cell lines, and it is controversial whether the up-regulation is due to induction or to selection. In addition, these particular studies did not examine Bcl-2 or Bcl-x_L expression in cells previously treated with high doses of chemotherapeutic drugs or monitored after the drugs were removed from the cells. Recently, however, Lee *et al.* have detected by flow cytometry a 3-fold increase in Bcl-x_L protein in a surviving sub-population of L1210 murine leukemia cells 24 hours after etoposide treatment (364). This suggests an up-regulation in the non-apoptotic population as compared with apoptotic cells which showed no increase in Bcl-x_L (364). Furthermore, Yin and Schimke report that HeLa S3 cells which were transfected with and overexpress Bcl-2, also show an increased frequency of *DHFR* gene amplification when the transfectants were selected and grown in trimetrexate (354). Although not an up-regulation of a *bcl-2*-related gene itself, Yin and Schimke suggest Bcl-2 is capable of governing the emergence of drug resistance by other effects on the genome as well (365).

2. Biologic relevance.

Chaudhary and Roninson's documentation of up-regulation of *mdr-1* mRNA by quantitative RT-PCR in K562, KG1, and H9 leukemia cells after Ara-C, adriamycin, and methotrexate treatments (349) is a particularly important demonstration of biologically relevant acquisition of a drug-resistance gene occurring specifically at the RNA level. By flow cytometry they demonstrated, however, that only 3-17% of K562 cells exposed to different

chemotherapeutic drugs exhibited increased *mdr-1* levels, yet the contribution from this percentage was indeed responsible for the level of increase in *mdr-1* RNA detected by PCR (349). The demonstrations that induction of a drug resistance gene may occur in only a small percentage of cells, and that lower percentages of HL-60/neo cells remain viable after Ara-C treatment as compared with HL-60/Bcl-2 cells, may explain why induction of *bcl-2* mRNA in HL-60/neo cells presented in these RPAs presented in this Chapter was not readily detectable by this method. In addition, while Chaudhary and Roninson demonstrated that although only a small percentage of previously treated K562 cells showed up-regulation of *mdr-1*, the effect was indeed biologically relevant since K562 cells that survived Ara-C treatment (exposure to 10 μ M for 3 days, then cultured without Ara-C for 6 weeks), showed increased resistance to subsequent vinblastine treatment by virtue of a shift in the dose-response curve to vinblastine as compared to previously untreated K562 cells (349). Similarly, as presented in this Chapter, assessment of cell viability by the MTT assay in previously treated HL-60/neo cells exposed to a second round of Ara-C treatment was attempted in order to test the hypothesis that increased Bcl-2 expression over time after first HIDAC exposure is biologically relevant as well. HL-60/neo and not HL-60/Bcl-2 cells were used because differences in apoptosis would be better appreciated. Acquired increases in Bcl-2 levels render AML HL-60/neo cells more resistant to inhibition of viability by various concentrations of Ara-C in a second treatment, as illustrated by a lower percentage of inhibition of viability by the MTT assay, lower percentages of cells detected as apoptotic, and lower amounts of total DNA breaks detected by the TUNEL assay as compared to previously untreated HL-60/neo cells. While the first dose of Ara-C was highest (100 μ M Ara-C for 4 hours), the biological significance of increased Bcl-2 levels correlating with increased survival capacity is best appreciated when the second treatment of Ara-C is at lower dosage, and further reiterates the findings by Manome *et al.* that Bcl-2-mediated increase in cell survival is more effective at lower doses where the observed cytotoxicity may be more likely due to the process of frank apoptosis (353). The 1.5-fold increase in Bcl-2 levels in surviving HL-60 cells by 48 hours following Ara-C treatment is not sufficient to completely inhibit apoptosis, reminiscent of the unsuccessful attempts in Chapter Two to produce sufficient overexpression of p26Bcl-2 in HL-60 using the LacSwitch inducible mammalian expression system. (For this, the 4-fold higher level of homogeneous Bcl-2 overexpression retrovirally-transfected in HL-60/Bcl-2 clonal population D was identified as a threshold for maintenance of protection against apoptosis in HL-60 cells in Part A of this chapter.) Nevertheless, the acquired increase in Bcl-2 levels seen

even in HL-60/neo cells impact on the extent of Ara-C-induced apoptosis during a second exposure to this drug.

Typical treatment schedules for AML vary, and include rounds or repeated doses of Ara-C for over several days for induction of remission (207). The experiments presented in this Chapter examine AML cell viability upon re-administration of Ara-C, in the context of up-regulation of Bcl-2 after HIDAC is withdrawn from the cell culture. This mimics clinical infusion of a fixed schedule of Ara-C and physiologic removal of the drug after its metabolism. This experiment has then become an *in vitro* simulation of a problematic clinical scenario in which acquired increase of the level of an oncogene which blocks antileukemic drug-induced apoptosis may explain the worsening of the response to chemotherapy in leukemia patients. While these *in vitro* experiments demonstrate the statistically significant increases, these increases in Bcl-2 levels may obviously be more biologically relevant *in vivo* where cooperation with other oncogenes and factors in the bone marrow environment may further contribute to the danger of acquired drug resistance by surviving leukemic cells. Inductions of other gene expressions, however, in HL-60/neo cells which survived initial HIDAC treatment and were cultivated in culture, cannot be excluded as possible contributors in the increased resistance of these cells, since they were not further examined. Nevertheless, this remains an example of acquired drug resistance after chemotherapy treatment relevant at biologically significant levels.

C. Summary.

The studies in this chapter demonstrate several aspects of Bcl-2-mediated inhibition of Ara-C-induced apoptosis over time. Not only is a correlation of the level of Bcl-2 expression to the degree of protection of HL-60 cells against Ara-C-induced cytotoxicity identified, but modulations of Bcl-2 levels in cells which survive Ara-C treatment over time are examined in detail. **In summary, a) the eventual induction of apoptosis in a small percentage of cells overexpressing Bcl-2 is not due to increases in total Bax levels, but due to a possible alternative Bcl-2 independent mechanism of Ara-C signalling. b) In addition, cells surviving Ara-C-induced apoptosis display modest increases in Bcl-2 expression, which are: (i) accrued by the contribution of modest induction of *bcl-2* at the RNA level, consistent with other studies reporting induction of *bcl-2* family members, as well as *mdr-1*, after chemotherapy treatment. (ii) This increase in expression of Bcl-2 may also be due to**

selection of a population of cells that have slightly higher endogenous expression of Bcl-2. However, the inability to show heterogeneity of Bcl-2 expression in individual cells of the various clonal populations militates against this latter possibility. (iii) Regardless of the dominant mechanism underlying the higher Bcl-2 expression observed in the surviving cells, this clearly confers a detectable and biologically significant survival advantage against subsequent treatment with Ara-C. Furthermore, increases in Bcl-2 levels in surviving cells following Ara-C treatment are: (iv) independent of p53 expression in HL-60 cells since HL-60 cells lack *p53*; (v) not indicative of phosphorylation of Bcl-2 by Ara-C, and therefore may not be due to a resulting alteration of the amino acid epitopes that are detected by the anti-Bcl-2 antibody used in the Western blotting, immunofluorescence, or flow cytometric studies presented.

In **Chapter Three** it was demonstrated that Ara-C caused early DNA strand breaks even in Bcl-2-overexpressing HL-60 cells. If Ara-CTP accumulates even in cells which are not in S phase and are not immediately affected (364), an important question then arises as to the outcome of Ara-C-induced DNA damage in cells with high Bcl-2 levels which do survive initial Ara-C treatment. The hypothesis that surviving cells with high Bcl-2 levels exhibit greater capacity for repair of Ara-C-induced DNA strand breaks will be tested in the next chapter.

Figure Legends:

Figure 19: Ara-C-induced internucleosomal and high molecular weight DNA fragmentation over time in HL-60/neo cells versus HL-60/Bcl-2 clones.

For **Panel A**, HL-60/neo (lanes 1 to 5), HL-60/Bcl-2 clonal population F (lanes 6 to 10), HL-60/Bcl-2 clonal population D (lanes 11 to 15), and HL-60/Bcl-2 clonal population B (lanes 16 to 20) were treated with HIDAC (100 μ M Ara-C for 4 hours). Cells were washed, resuspended in fresh drug-free media, and genomic DNA was purified from 10^6 cells at various time points after Ara-C treatment. Equal amounts (1.0 μ g) of purified genomic DNA was electrophoresed on 1.0% agarose gel to determine **internucleosomal DNA fragmentation (Panel A)**. Assessment of DNA fragments in each of the lanes are from cells treated as follows: lanes 1, 6, 11, 16: untreated cells; lanes 2, 7, 12, 17: immediately following 4-hour Ara-C treatment; lanes 3, 8, 13, 18: 4 hours following 4-hour Ara-C treatment; lanes 4, 9, 14, 19: 24 hours following 4-hour Ara-C treatment; lanes 5, 10, 15, 20: 48 hours following 4-hour Ara-C treatment. M represents 123-bp ladder as marker.

For **Panel B**, HL-60/neo (lanes 1 to 5), HL-60/Bcl-2 clonal population F (lanes 6 to 10), HL-60/Bcl-2 clonal population D (lanes 11 to 15), HL-60/Bcl-2 clonal population B (lanes 16 to 20) were treated with HIDAC, washed resuspended in fresh drug-free media as described above, and DNA-agarose plugs were prepared from 10^6 cells, extracted at various time points after Ara-C treatment. DNA plugs were subjected to **FIGE** to determine **high molecular weight DNA fragmentation** (4 to 300 kb size). DNA fragments in each lane are from cells treated as follows: lanes 1, 6, 11, 16: untreated cells; lanes 7, 12, 17: immediately following Ara-C treatment; lanes 3, 8, 13, 18: 4 hours following 4-hour Ara-C treatment; lanes 4, 9, 14, 19: 24 hours following 4-hour Ara-C treatment; lanes 5, 10, 15, 20: 48 hours following 4-hour Ara-C treatment.

Data are representative of 3 separate experiments, each with similar results.

Figure 20: Flow cytometric determination of apoptosis in HL-60/neo cells versus HL-60/Bcl-2 clonal populations after Ara-C treatment. HL-60/neo or HL-60/Bcl-2 clonal populations F, D, or B were treated with HIDAC, washed, resuspended in drug-free media. At various time points after HIDAC treatment, cells were fixed for flow cytometric analysis as described in Materials and Methods. The panel represents flow cytometry histograms generated after propidium iodide staining of each cell population for their DNA content. Markers M1-M4 were drawn over each region corresponding to sub- G_1 (apoptotic), G_1 , S, or G_2 phase. Arrow points to significantly larger sub- G_1 peak in HIDAC-treated HL-60/neo cells than HL-60/Bcl-2 cells. Histograms are representative of 5 separate experiments, each with similar results.

Figure 21: Assessment of cell viability after Ara-C treatment in HL-60/neo cells versus HL-60/Bcl-2 clones by MTT assay and trypan blue dye exclusion. Graphical representation of the data presented in Table IX. Data represent mean \pm S.E.M. for $n = 5$ experiments.

Figure 22: Western blots were analyzed for p26Bcl-2 and p21Bax expression in total protein extracted from HL-60/neo cells (lanes 1 to 5), HL-60/Bcl-2 clonal population F (lanes 6 to 10), HL-60/Bcl-2 clonal population D (lanes 11 to 15), and HL-60/Bcl-2 clonal population B (lanes 16 to 20). Cells were treated with HIDAC (100 μ M Ara-C for 4 hours), washed resuspended in fresh drug-free media, and total protein extracted at various time points after Ara-C treatment. 10 μ g total protein for p26Bcl-2 immunoblots and 50 μ g total protein for p21Bax immunoblots

are from cells treated as follows: lanes 1, 6, 11, 16: untreated cells; lanes 2, 7, 12, 17: immediately following Ara-C treatment; lanes 3, 8, 13, 18: 4 hours following 4-hour Ara-C treatment; lanes 4, 9, 14, 19: 24 hours following 4-hour Ara-C treatment; lanes 5, 10, 15, 20: 48 hours following 4-hour Ara-C treatment. ECL exposure time was 2 minutes.

Data are representative of 3 separate experiments, each with similar results.

Figure 23: Immunofluorescent analysis of Bcl-2 levels in non-apoptotic HL-60/neo and HL-60/Bcl-2 cells surviving immediately, 24 and 48 hours after HIDAC treatment, is expressed as mean fluorescent intensity per non-apoptotic cell (top graph) and as percent of control (bottom graph) for each of 4 cell lines assessed. Cells were fixed, permeabilized, and stained for p26Bcl-2 as described in the text, and intensity of Bcl-2 staining was measured in at least 30 cells per condition. Bars represent mean \pm SEM for 3 individual experiments.

Figure 24: Results of ribonuclease protection assay for *bcl-2* mRNA expression relative to β -actin mRNA expression in HL-60/neo and HL-60/Bcl-2 clonal population B cells treated with Ara-

C for various time intervals. Total RNA was extracted and 50 μ g per condition was hybridized with RNA probes prepared and in vitro transcribed as described in the Materials and Methods section of the text.

Panel A shows *bcl-2* and β -actin mRNA signals from the same X-ray film from HL-60/neo (lanes 1-6) and HL-60/Bcl-2 cells (lanes 7-12) either untreated (lanes 1,7) or treated with 100 μ M Ara-C for 2 hours (lanes 2, 8), 4 hours (lanes 3, 9), and also examined 4, 8, and 24 hours after removal of Ara-C from the culture medium (lanes 4 and 10, 5 and 11, and 6 and 12, respectively).

Horizontal scanning densitometry generated values for *bcl-2*: β -actin mRNA levels expressed in the graphs in **Panel B**, and demonstrates that only in HL-60/Bcl-2 cells (right graph) was induction of *bcl-2* mRNA seen to reach over 100% as compared to untreated cells.

Panel C shows *bcl-2*: β -actin mRNA signals from the same X-ray film when HL-60/Bcl-2 cells were either untreated (lane 1) or treated with 100 μ M Ara-C for various intervals (lane 2, 7: 2 hours; lanes 3,8: 4 hours; lanes 4, 5, 6 and 9, 10, 11: 4, 8, and 24 hours after removal of Ara-C) in the absence (lanes 1-6) or presence (lanes 7-11) of 5 μ g/ml actinomycin D.

Similarly, horizontal scanning densitometry generated values for relative *bcl-2*: β -actin mRNA levels, expressed in **Panel D**, and demonstrates that induction of *bcl-2* mRNA above 100% of control was abrogated by concomitant actinomycin D treatment. These data are represented in **Table XIII**. Data are representative of 3 separate experiments, each with similar results.

Figure 25. The effect of concomitant actinomycin D and cycloheximide exposures on the induction of Bcl-2 levels. Flow cytometric analysis of Bcl-2 levels in HL-60/neo (top graph), HL-60/Bcl-2 F (middle graph) and HL-60/Bcl-2 B (bottom graph) cells surviving after Ara-C treatment is expressed as percent increase over control, and tabulated in **Table XIV**. Bars represent mean \pm S.E.M. for n = 3 experiments.

Figure 26. Top panel represents final results in 96-well plates of MTT assay for cell viability in HL-60/neo cells either previously untreated (left side of plate) or previously pre-treated with 100 μ M Ara-C for 4 hours (HIDAC) (right side of plate), surviving washed 5-6 times with sterile

PBS and spun over a histopaque gradient daily to remove dead cells for 3 days. On day 3, pre-treated cells as well as previously untreated cells were exposed to various concentrations of Ara-C (100 nM to 100 μ M for 4 hours), washed, cells plated in replicates of 5 wells per condition, and viability assessed by the MTT assay as described in Materials and Methods. The image in Panel A demonstrates well with viable cells as those containing higher amounts of extractable mitochondrial enzymes and thus having darker hue. Quantitative analysis of the absorbance of each well from a Anthos plate reader is tabulated in **Table XV** below. Image in the top panel is representative of 3 separate experiments, each with similar results.

Figure 27. Flow cytometric determination of Ara-C-induced apoptosis in previously untreated HL-60/neo cells (top row) versus HL-60/neo cells previously treated with HIDAC and cultivated as previously described (bottom row) are illustrated by histograms generated after propidium iodide staining for DNA content when both populations were exposed to increasing concentrations of Ara-C. Marker M1 represents the sub/G1 (apoptotic) population in each condition. The figure is merged with **Table XVI**, which shows percentages of cells detected as apoptotic by both flow cytometric and microscopic determinations underneath each histogram for the given condition. Total DNA breaks detected by the TUNEL assay (described in Materials and Methods) is expressed as mean fluorescent intensity of fluorescein-labelled DNA breaks. Data are representative of 4 separate experiments.

Figure 27a. Assessment of cell viability by MTT assay and flow cytometric determination of apoptosis in HL-60/neo cells after first and second treatments with Ara-C. Graphical representation of the data presented in **Figure 27/ Table XVI**. Data are representative of mean \pm S.E.M. for n = 4 experiments.

Figure 19.

Figure 19.

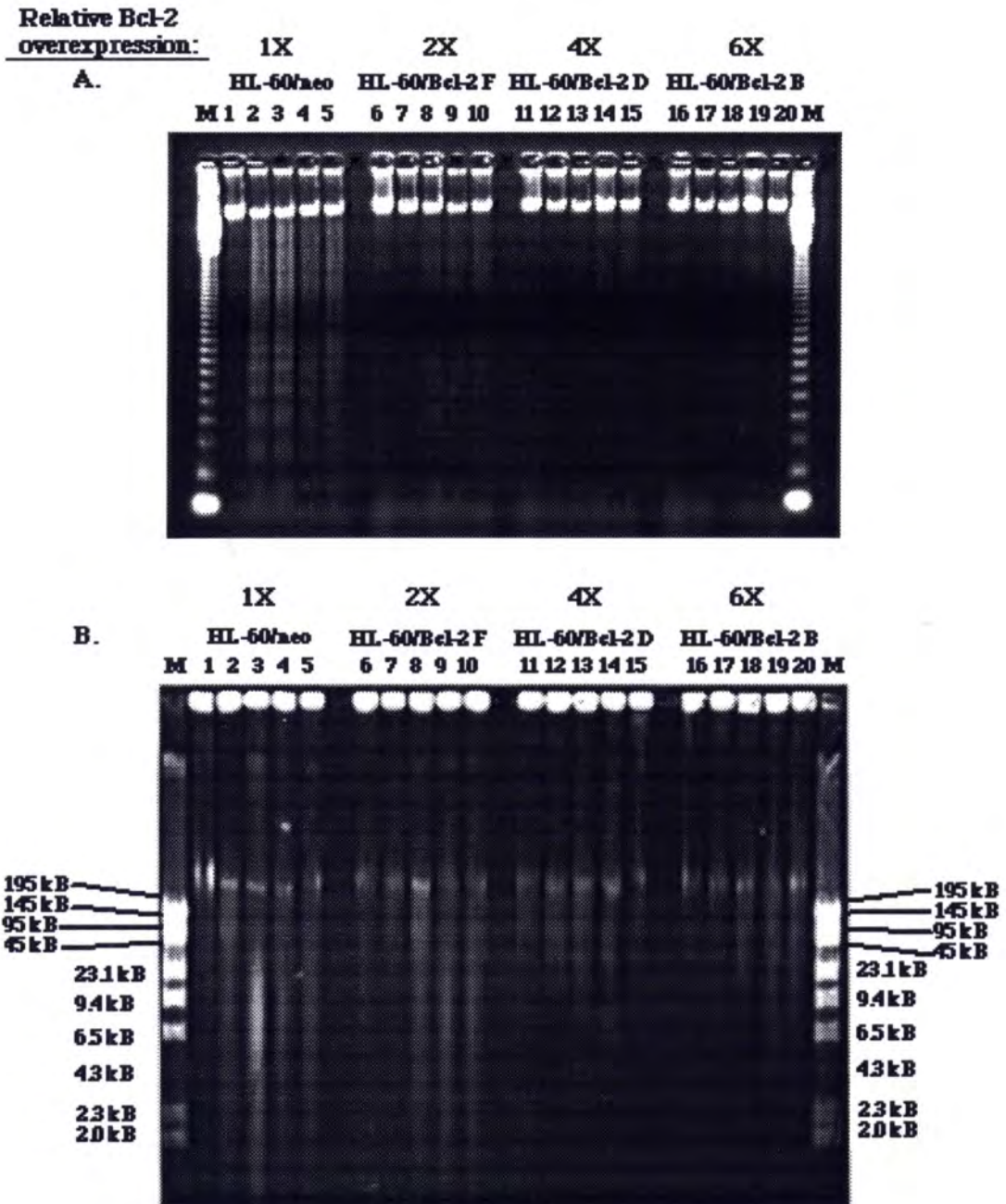


Table VIII.

**FLOW CYTOMETRIC DETERMINATION OF APOPTOSIS IN
HL-60/neo CELLS VERSUS HL-60/Bcl-2 CLONES AFTER ARA-C TREATMENT:***

% APOPTOTIC CELLS:

<u>Condition:</u>	<u>HL-60/neo:</u>	<u>HL-60/Bcl-2 F:</u>	<u>HL-60/Bcl-2 D:</u>	<u>HL-60/Bcl-2 B:</u>
control	3.27 ± 2.67	2.13 ± 0.88	1.57 ± 0.18	1.97 ± 0.52
0 hr post Ara-C	36.93 ± 6.96	2.75 ± 1.20	1.60 ± 0.10	1.70 ± 0.38
4 hrs post Ara-C	40.73 ± 4.99	14.00 ± 3.70	7.20 ± 2.80	6.43 ± 1.97
24 hrs post Ara-C	40.27 ± 8.23	17.55 ± 0.65	15.50 ± 3.40	7.63 ± 2.10
48 hrs post Ara-C	30.00 ± 9.96	19.85 ± 3.25	19.03 ± 1.77	11.53 ± 2.42

* Values represent mean ± S.E.M. for n = 5 experiments. Values obtained between identically treated HL-60/neo and HL-60/Bcl-2 F, D, B clones are significantly different (p < 0.01) for each condition after Ara-C treatment.

**FLOW CYTOMETRIC DETERMINATION OF APOPTOSIS
IN HL-60/neo CELLS VERSUS HL-60/Bcl-2 CLONES
AFTER ARA-C TREATMENT:**

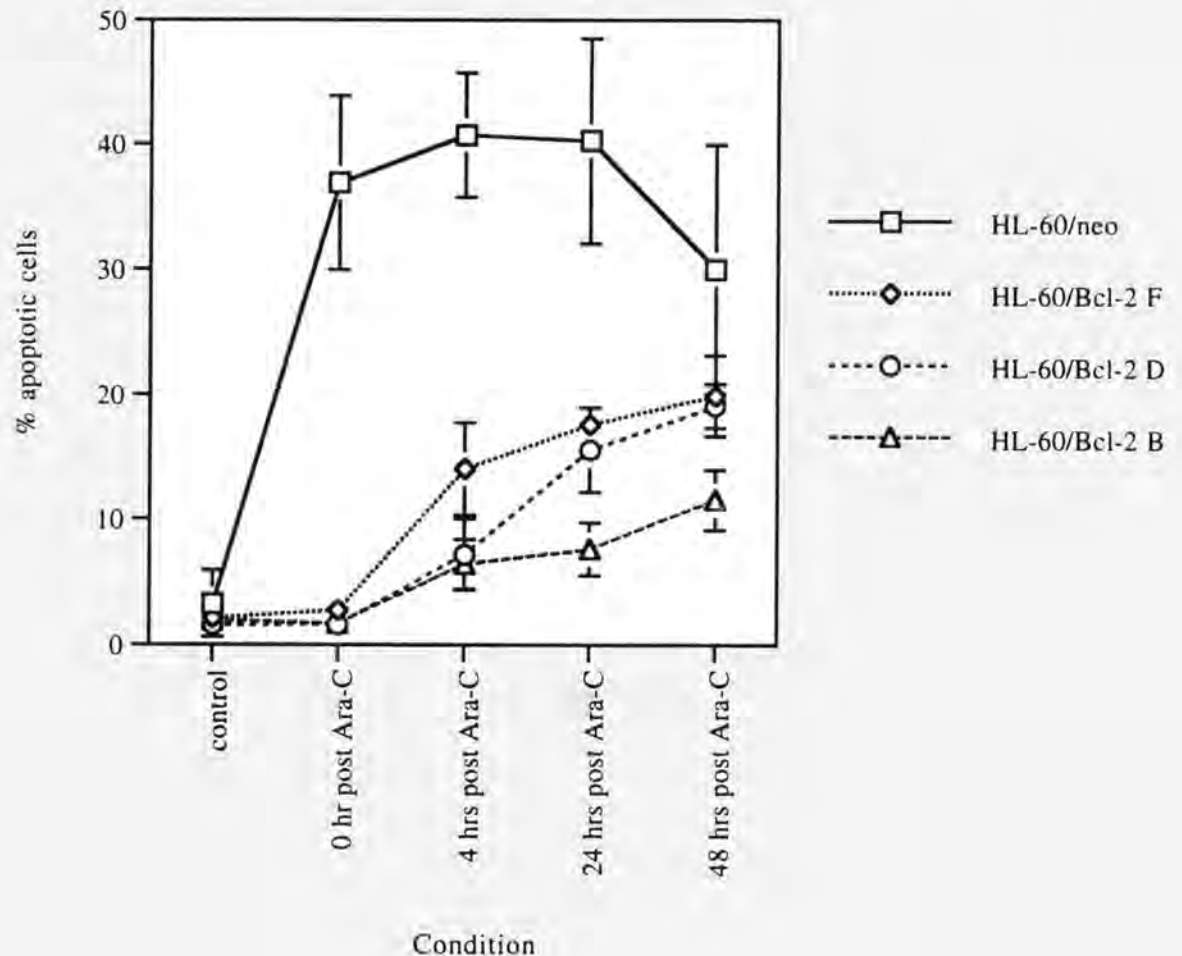


Figure 20: FLOW CYTOMETRIC DETERMINATION OF APOPTOSIS IN
 HL-60/neo CELLS VERSUS HL-60/Bcl-2 CLONES AFTER ARA-C TREATMENT:

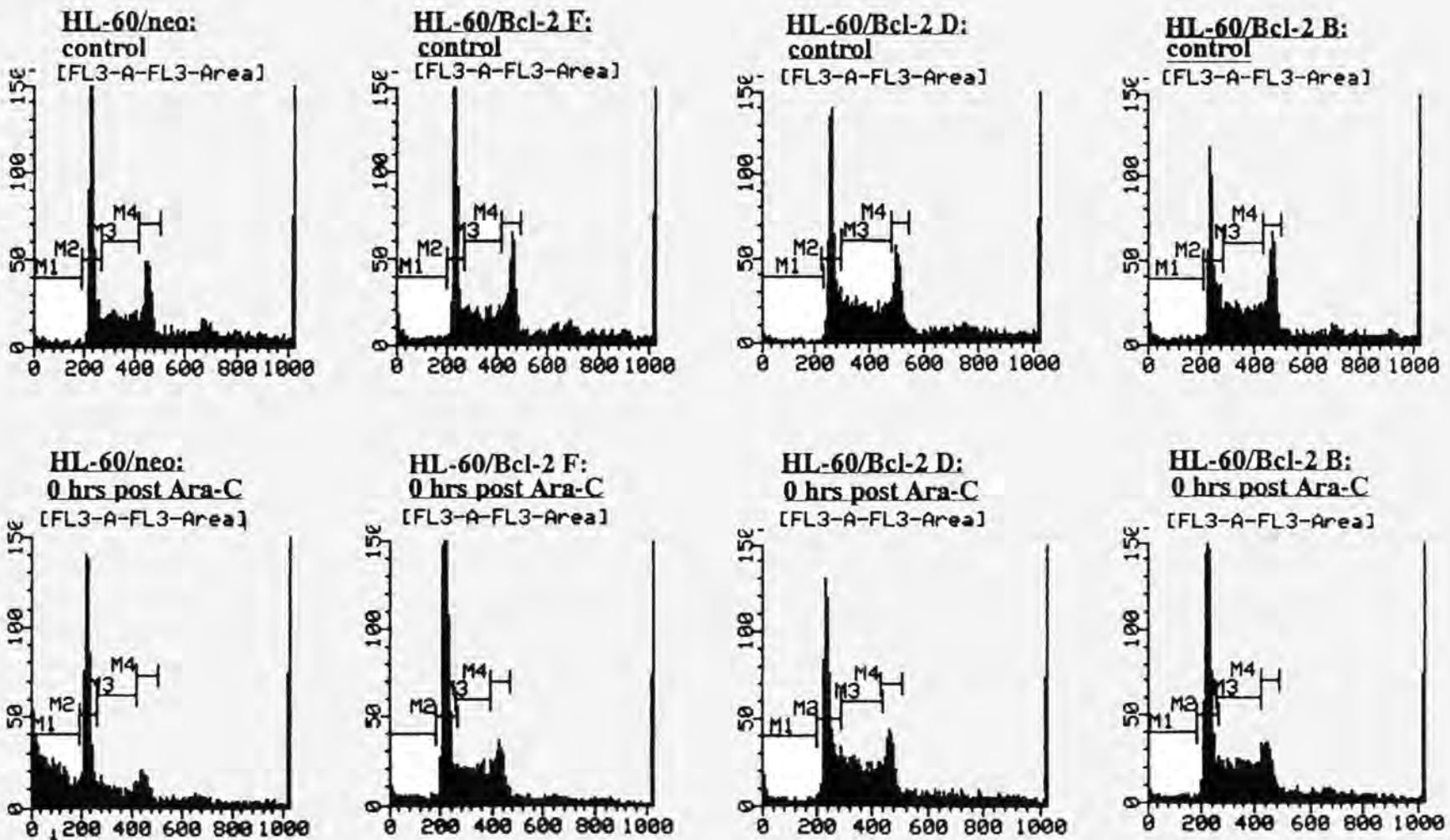
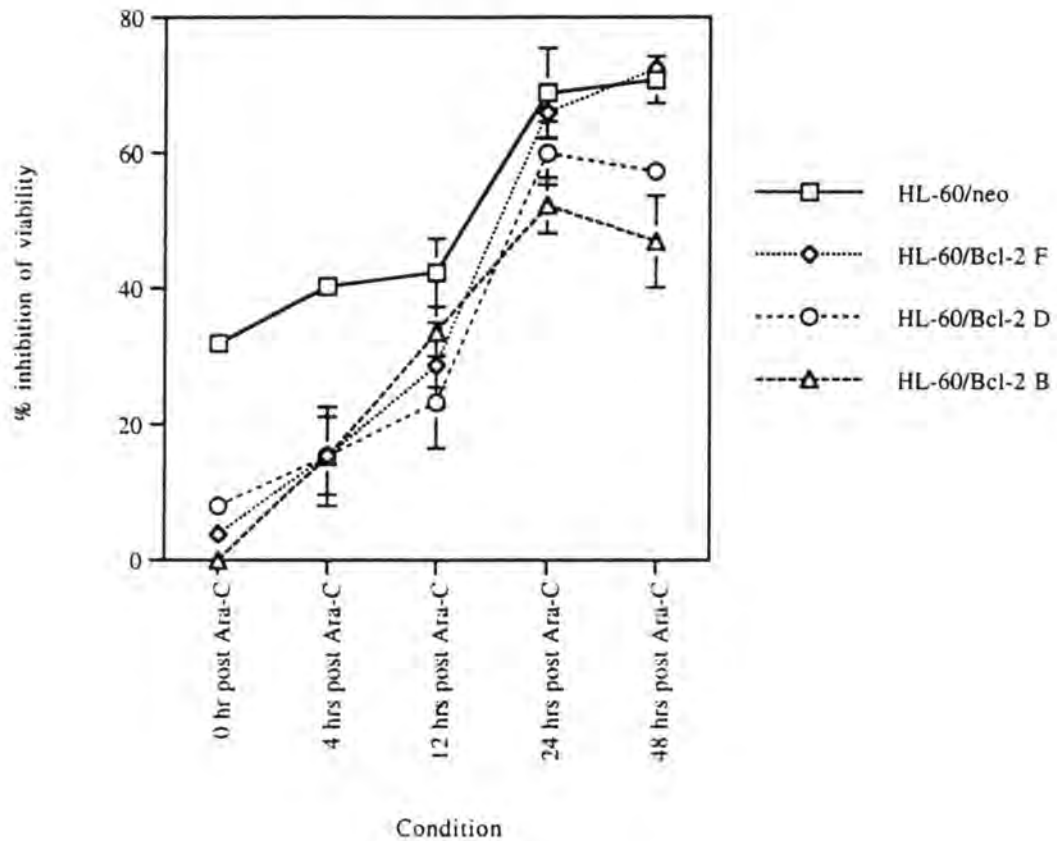


Figure 21:

**ASSESSMENT OF CELL VIABILITY AFTER ARA-C TREATMENT
IN HL-60/neo CELLS VERSUS HL-60/Bcl-2 CLONES
BY MTT ASSAY:**



**ASSESSMENT OF CELL VIABILITY AFTER ARA-C TREATMENT
IN HL-60/neo VERSUS HL-60/Bcl-2 CLONES
BY TRYPAN BLUE DYE EXCLUSION:**

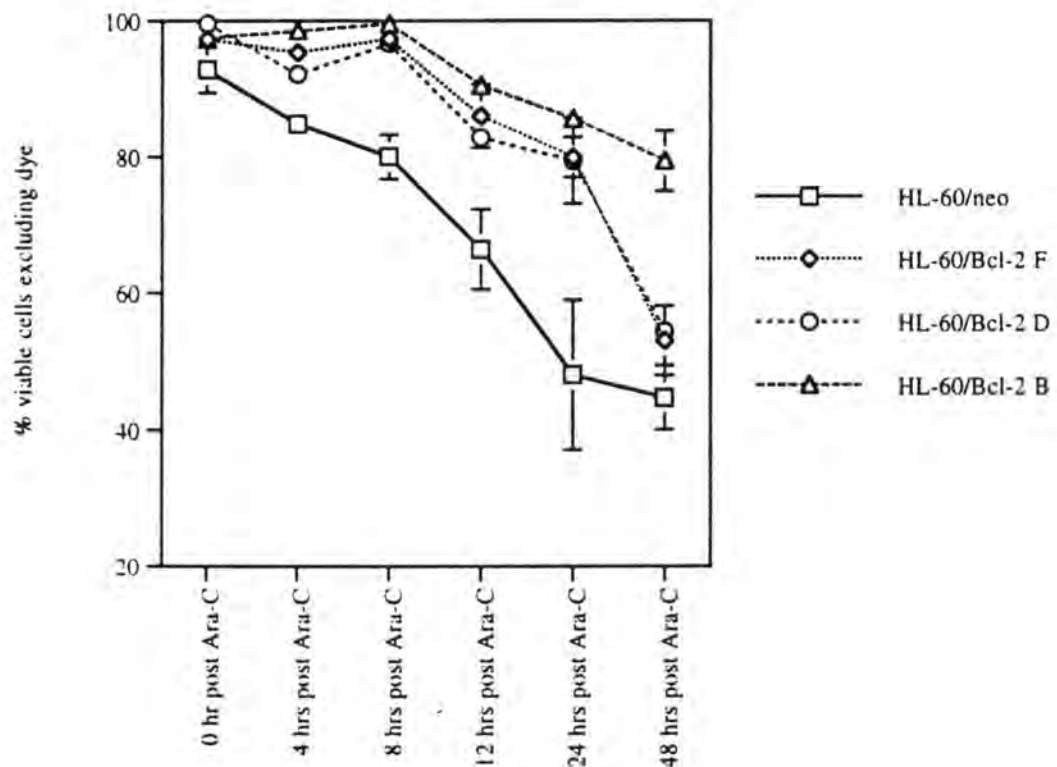


TABLE IX.

**Part I. ASSESSMENT OF CELL VIABILITY AFTER ARA-C TREATMENT
IN HL-60/neo CELLS VERSUS HL-60/Bcl-2 CLONES BY MTT ASSAY:**

<u>Condition:</u>	<u>% INHIBITION OF VIABILITY:</u>			
	<u>HL-60/neo:</u> *	<u>HL-60/Bcl-2 F:</u> **	<u>HL-60/Bcl-2 D:</u> ***	<u>HL-60/Bcl-2 B:</u> ****
0 hrs post Ara-C	31.90	3.75	7.89	0.00
4 hrs post Ara-C	40.32 ± 0.42	15.38 ± 5.76	15.27 ± 7.33	15.22 ± 0.56
12 hrs post Ara-C	42.32 ± 5.04	28.69 ± 6.25	23.23 ± 6.86	33.60 ± 8.17
20 hrs post Ara-C	68.30 ± 3.20	ND	57.41 ± 2.16	46.30 ± 6.40
24 hrs post Ara-C	68.85 ± 6.60	65.93 ± 3.79	59.95 ± 4.65	52.23 ± 4.14
48 hrs post Ara-C	70.71 ± 3.46	72.42 ± 1.12	57.25 ± 1.50	46.93 ± 6.78

Values represent means ± S.E.M. for n = 5 experiments.

* Values obtained in identically treated HL-60/neo cells versus HL-60/Bcl-2 D or B clones are significantly different from each other (p < 0.05).

** Values obtained in identically treated HL-60/neo cells versus HL-60/Bcl-2 F clones are significantly different (p < 0.05) for only 0, 4, 12 hrs post Ara-C. Values are not significantly different from each other (p > 0.05) for 24, 48 hrs post Ara-C.

*** Values obtained in identically treated HL-60/Bcl-2 D clones versus HL-60/Bcl-2 B clones are not significantly different (p > 0.05).

**** Likewise, values obtained in identically treated HL-60/Bcl-2 D or B clones versus HL-60/Bcl-2 F clones are not significantly different (p > 0.05) for only 0, 4, 12 hrs post Ara-C. values are significantly different (p < 0.05) for 24, 48 hrs post Ara-C.

**Part II. ASSESSMENT OF CELL VIABILITY AFTER ARA-C TREATMENT IN
HL-60/neo CELLS VERSUS HL-60/Bcl-2 CLONES BY TRYPAN BLUE DYE EXCLUSION*:**

<u>Condition:</u>	<u>% VIABLE CELLS EXCLUDING DYE:</u>			
	<u>HL-60/neo:</u>	<u>HL-60/Bcl-2 F:</u>	<u>HL-60/Bcl-2 D:</u>	<u>HL-60/Bcl-2 B:</u>
0 hrs post Ara-C	97.24 ± 3.34	97.26 ± 0.90	99.50 ± 0.41	97.39 ± 2.29
4 hrs post Ara-C	84.86 ± 1.04	95.34 ± 3.06	92.13 ± 2.22	98.54 ± 0.72
8 hrs post Ara-C	80.04 ± 3.27	97.33 ± 0.53	96.62 ± 0.38	99.50 ± 0.33
12 hrs post Ara-C	66.43 ± 5.89	85.96 ± 4.66	82.83 ± 1.10	90.53 ± 1.44
24 hrs post Ara-C	48.06 ± 10.93	79.95 ± 2.94	79.42 ± 6.23	85.61 ± 1.28
48 hrs post Ara-C	44.74 ± 4.70	53.05 ± 5.06	54.44 ± 0.62	79.43 ± 4.44

* Values represent means ± S.E.M. for n = 5 experiments.

Values obtained for identically treated HL-60/neo cells versus HL-60/Bcl-2 clones are significantly different (p < 0.05) up to 24 hrs post Ara-C.

Figure 22.

Figure 22.

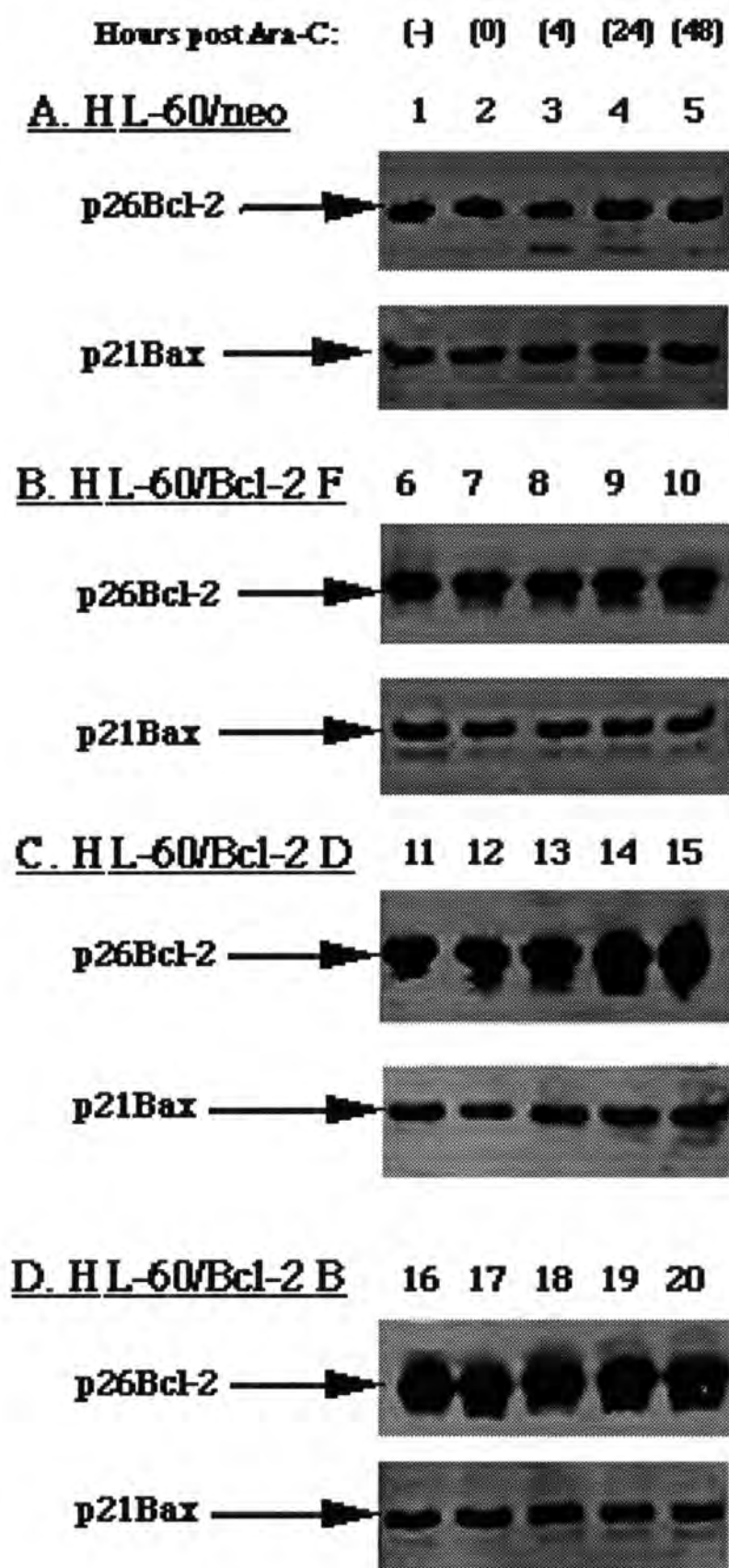


TABLE X. ASSESSMENT OF p26Bcl-2:p21Bax RATIOS BY WESTERN BLOT IN HL-60/neo CELLS VERSUS HL-60/Bcl-2 CLONES AFTER ARA-C TREATMENT:

RELATIVE RATIO OF p26Bcl-2:p21Bax BANDS AFTER DENSITOMETRY*:

<u>Condition:</u>	<u>HL-60/neo:</u>	<u>HL-60/Bcl-2 F:</u>	<u>HL-60/Bcl-2 D:</u>	<u>HL-60/Bcl-2 B:</u>
control	2.47 ± 0.42	6.33 ± 0.96	7.04 ± 0.87	10.11 ± 1.67
0 hrs post Ara-C	2.85 ± 0.49	7.42 ± 0.79	8.47 ± 1.35	10.87 ± 1.75
4 hrs post Ara-C	2.54 ± 0.34	7.96 ± 1.13	8.29 ± 1.53	10.71 ± 1.58
24 hrs post Ara-C	3.17 ± 0.50	9.53 ± 0.87	9.98 ± 1.86	11.36 ± 1.70
48 hrs post Ara-C	3.49 ± 0.66	9.45 ± 1.13	11.29 ± 1.81	12.36 ± 0.68

* Values represent mean ± SEM for n = 3 experiments. Values obtained for identically treated HL-60/neo, HL-60/Bcl-2 F and D clones are significantly different (p < 0.05) by paired t-test for control versus 48 hrs post Ara-C samples within each population.

ASSESSMENT OF p26Bcl-2:p21Bax RATIOS BY WESTERN BLOT IN HL-60/neo CELLS VERSUS HL-60/Bcl-2 CLONES AFTER ARA-C TREATMENT:

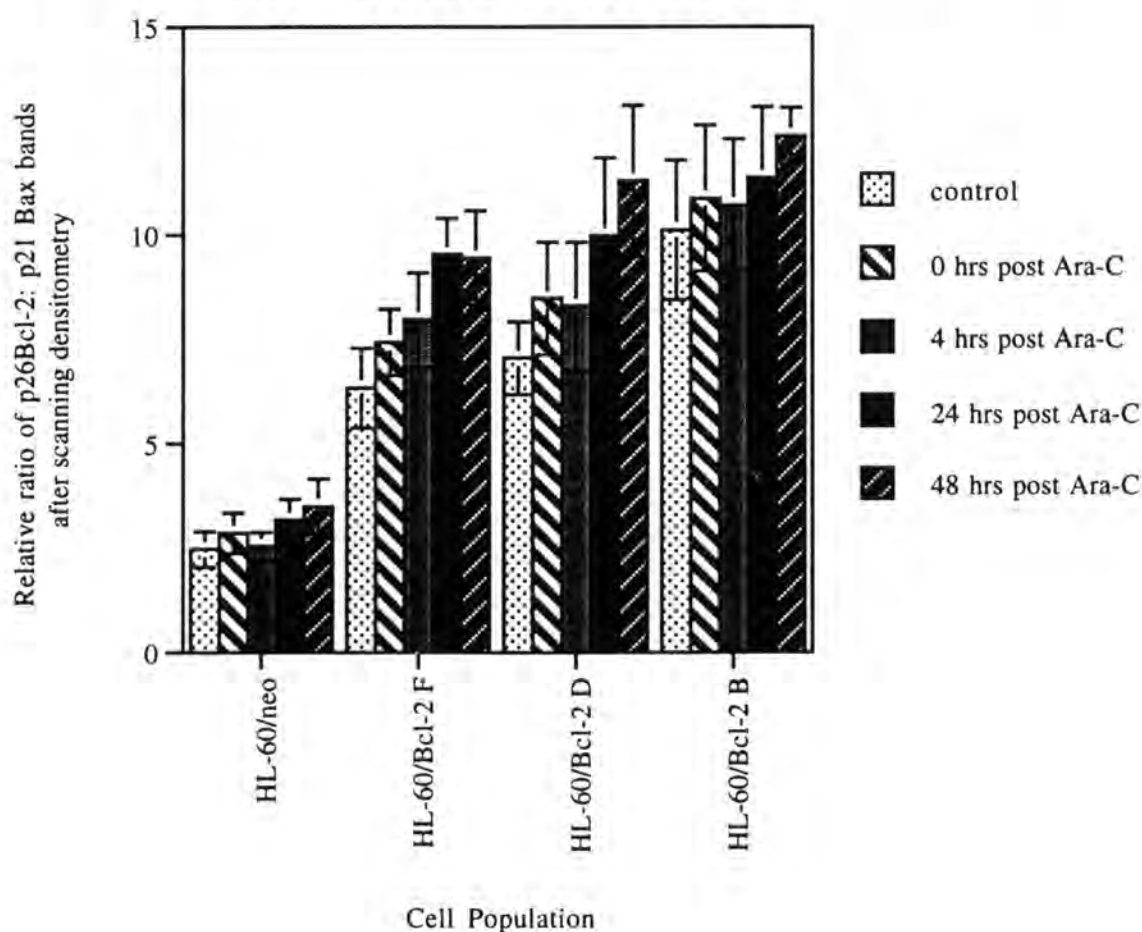
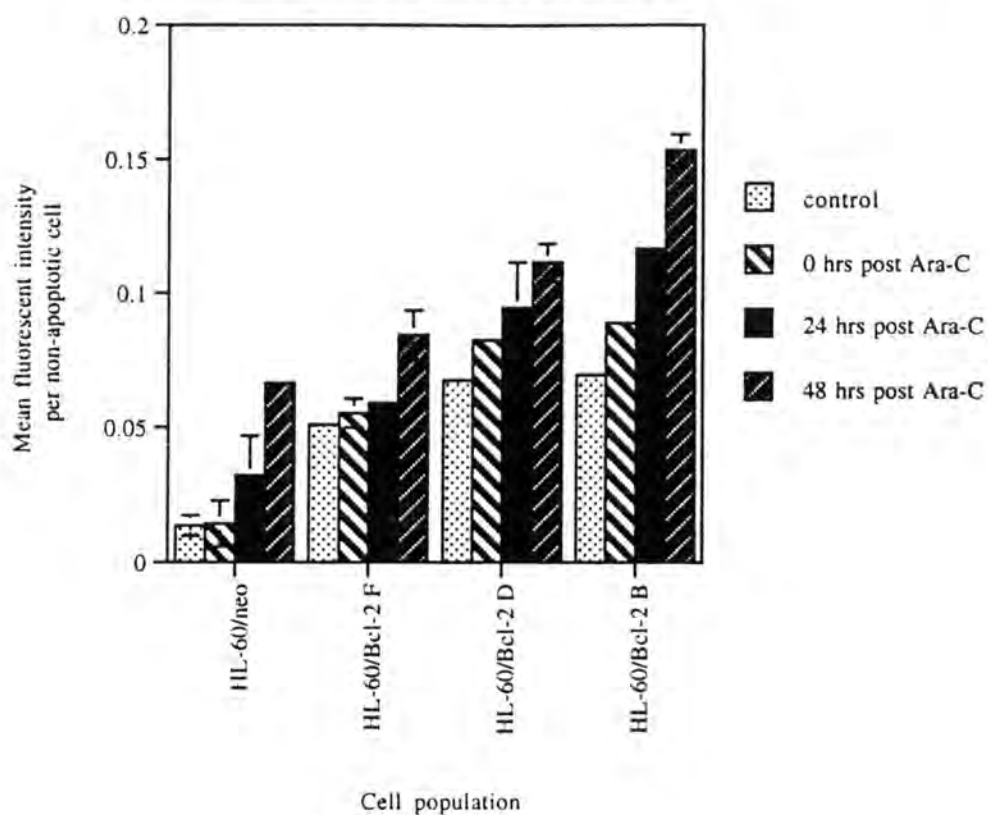


Figure 23.

**IMMUNOFLUORESCENT ANALYSIS OF p26Bcl-2 LEVELS
IN HL-60/neo CELLS VERSUS HL-60/Bcl-2 CLONES
AFTER ARA-C TREATMENT**



**IMMUNOFLUORESCENT ANALYSIS OF Bcl-2 LEVELS
IN HL-60/neo CELLS VERSUS HL-60/Bcl-2 CLONES
AFTER ARA-C TREATMENT:**

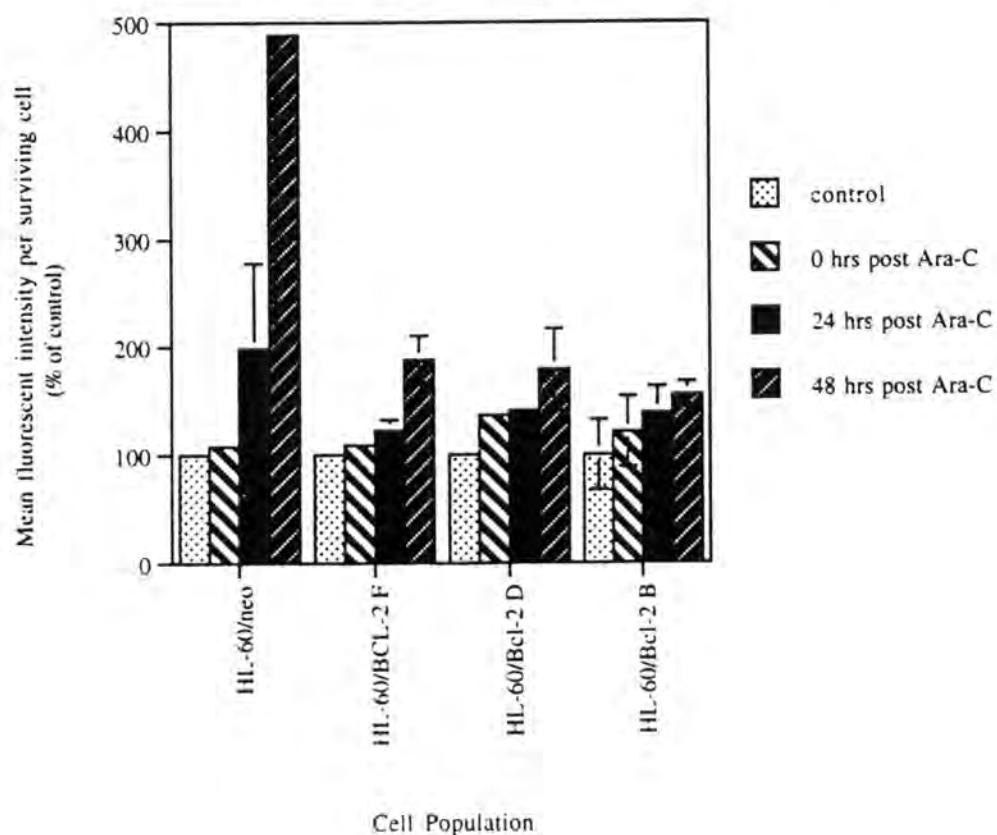


TABLE XI.

**ASSESSMENT OF Bcl-2 LEVELS BY IMMUNOFLUORESCENCE MICROSCOPY
IN NON-APOPTOTIC HL-60/neo CELLS VERSUS HL-60/Bcl-2 CLONES
AFTER ARA-C TREATMENT:***

MEAN FLUORESCENT INTENSITY PER NON-APOPTOTIC CELL:

<u>Condition:</u>	<u>HL-60/neo:</u>	<u>HL-60/Bcl-2 F:</u>	<u>HL-60/Bcl-2 D:</u>	<u>HL-60/Bcl-2 B:</u>
control	0.0137 ± 0.0038	0.0510 ± 0.0022	0.0677 ± 0.0013	0.0698 ± 0.0027
0 hrs post Ara-C	0.0144 ± 0.0087	0.0555 ± 0.0054	0.0825 ± 0.0025	0.0891 ± 0.0028
24 hrs post Ara-C	0.0323 ± 0.0146	0.0593 ± 0.0027	0.0946 ± 0.0170	0.1166 ± 0.0026
48 hrs post Ara-C	0.0666 ± 0.0013	0.0845 ± 0.0091	0.1115 ± 0.0069	0.1534 ± 0.0059

* Values represent mean ± S.E.M. for n = 3 experiments. Values obtained for identically treated HL-60/neo and HL-60/Bcl-2 F, D, B clones are significantly different (p < 0.05) for control versus 48 hrs post Ara-C samples within each population.

**ASSESSMENT OF Bcl-2 LEVELS BY IMMUNOFLUORESCENCE MICROSCOPY
IN NON-APOPTOTIC HL-60/neo CELLS VERSUS HL-60/Bcl-2 CLONES
AFTER ARA-C TREATMENT:***

**MEAN FLUORESCENT INTENSITY PER NON-APOPTOTIC CELL:
(% control)**

<u>Condition:</u>	<u>HL-60/neo:</u>	<u>HL-60/Bcl-2 F:</u>	<u>HL-60/Bcl-2 D:</u>	<u>HL-60/Bcl-2 B:</u>
control	100.00	100.00	100.00	100.00
0 hrs post Ara-C	107.91 ± 2.68	121.20 ± 32.65	136.59 ± 6.29	108.81 ± 2.89
24 hrs post Ara-C	198.51 ± 7.93	138.59 ± 24.58	140.77 ± 6.01	122.43 ± 10.12
48 hrs post Ara-C	488.89 ± 4.19	155.44 ± 11.55	178.68 ± 37.93	187.74 ± 22.08

* Values represent mean ± S.E.M. for n = 3 experiments. Values obtained for identically treated HL-60/neo and HL-60/Bcl-2 F, D, B clones are significantly different (p < 0.05) for control versus 48 hrs post Ara-C samples within each population.

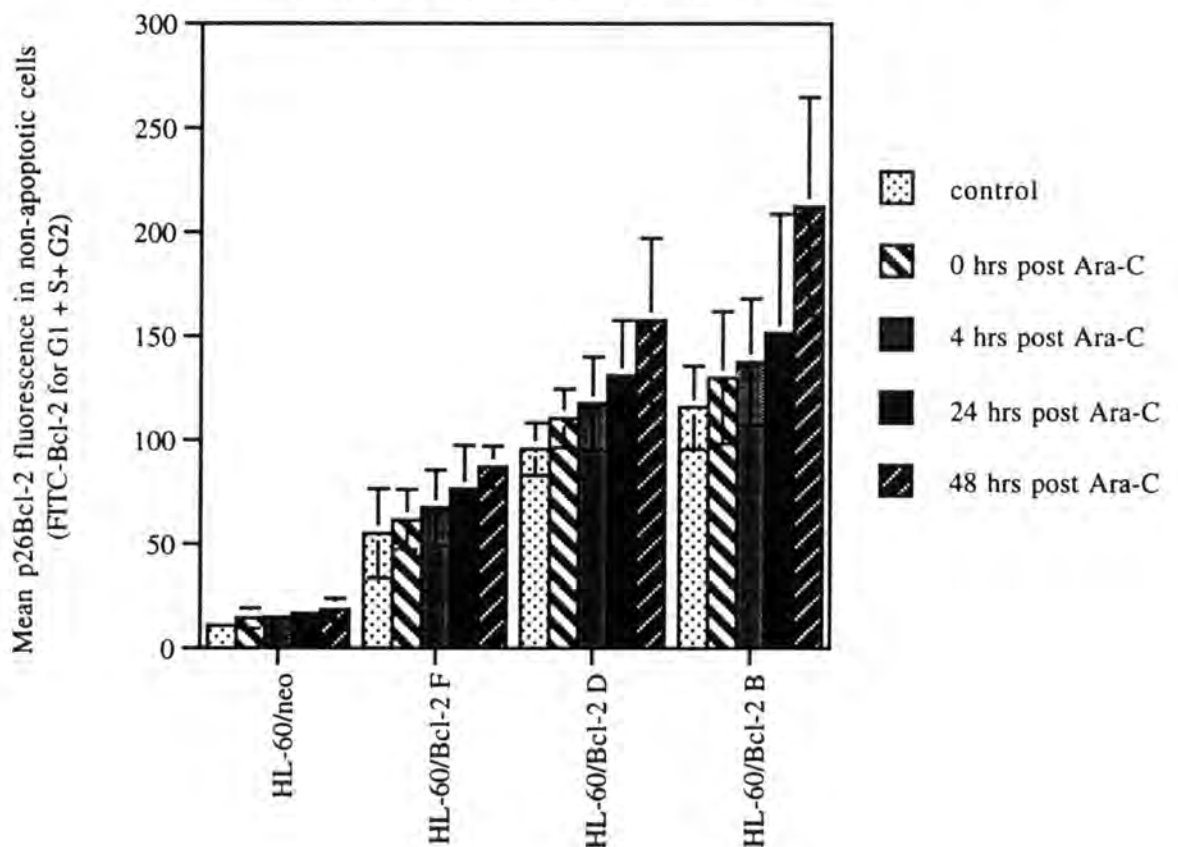
**TABLE XII. FLOW CYTOMETRIC DETERMINATION OF Bcl-2 LEVELS
IN HL-60/neo CELLS VERSUS HL-60/Bcl-2 CLONES AFTER ARA-C TREATMENT:**

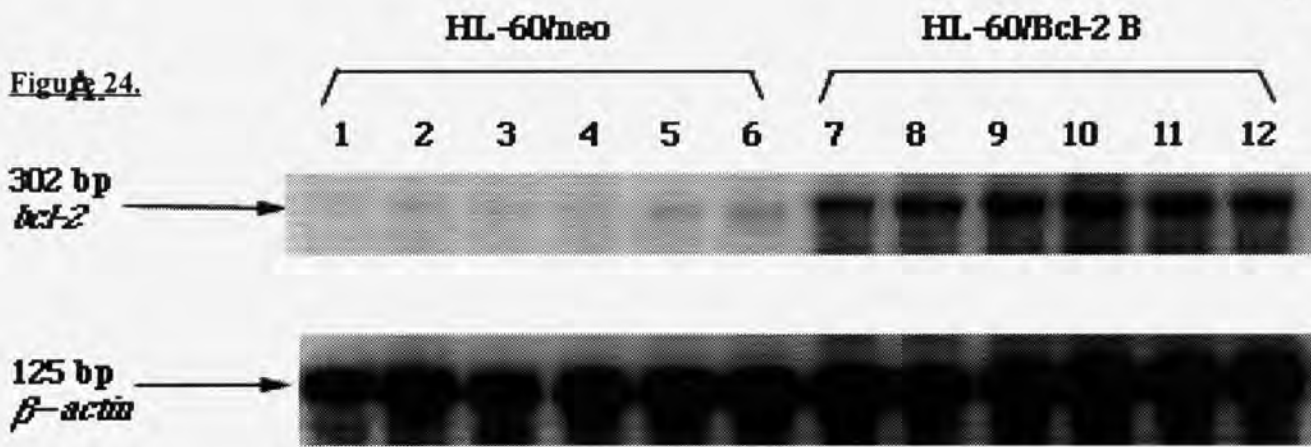
**TOTAL Bcl-2 FLUORESCENCE IN NON-APOPTOTIC CELLS
(FITC-Bcl-2 G1 + S + G2) (with % of control)*:**

<u>Condition:</u>	<u>HL-60/neo:</u>	<u>HL-60/Bcl-2 F:</u>	<u>HL-60/Bcl-2 D:</u>	<u>HL-60/Bcl-2 B:</u>
control	10.67 ± 4.29	55.01 ± 21.64	95.67 ± 12.54	115.60 ± 19.93
0 hrs post Ara-C	14.20 ± 4.87 (111.82 ± 10.60)	61.56 ± 14.56 (105.00 ± 12.71)	110.50 ± 14.03 (115.64 ± 5.72)	129.90 ± 31.90 (113.32 ± 7.47)
4 hrs post Ara-C	14.47 ± 3.95 (124.90 ± 14.12)	67.53 ± 17.96 (116.40 ± 10.44)	117.55 ± 22.37 (121.40 ± 7.52)	137.50 ± 30.47 (122.60 ± 13.68)
24 hrs post Ara-C	16.40 ± 3.98 (144.38 ± 14.77)	76.48 ± 20.91 (154.41 ± 25.74)	130.80 ± 26.57 (134.99 ± 13.40)	151.40 ± 57.21 (150.59 ± 6.41)
48 hrs post Ara-C	18.29 ± 5.45 (150.43 ± 18.61)	87.03 ± 10.07 (170.80 ± 26.89)	157.62 ± 39.57 (157.16 ± 19.87)	212.37 ± 52.46 (161.58 ± 19.28)

* Values represent mean ± SEM for n = 5 experiments. Values obtained for identically treated HL-60/neo and HL-60/Bcl-2 F, D, B clones are significantly different (p < 0.05) for control versus 48 hrs post Ara-C samples within each population.

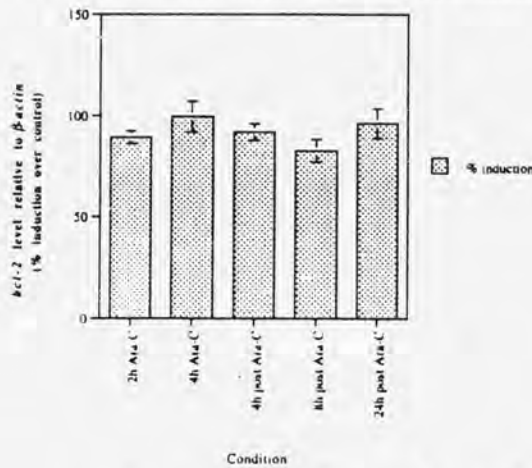
**FLOW CYTOMETRIC DETERMINATION OF Bcl-2 LEVELS
IN HL-60/neo CELLS VERSUS HL-60/Bcl-2 CLONES
AFTER ARA-C TREATMENT:**



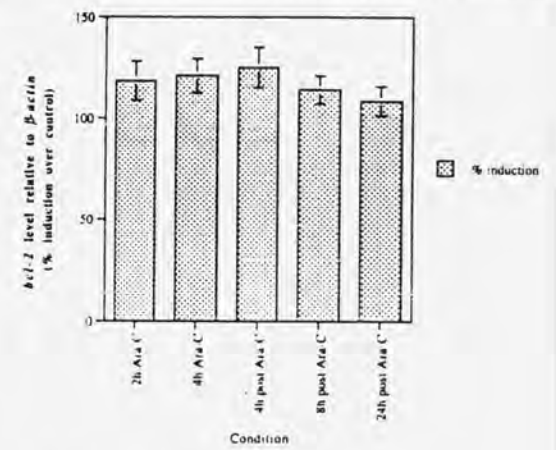


bcl-2 INDUCTION IN HL-60/neo CELLS AFTER ARA-C TREATMENT:

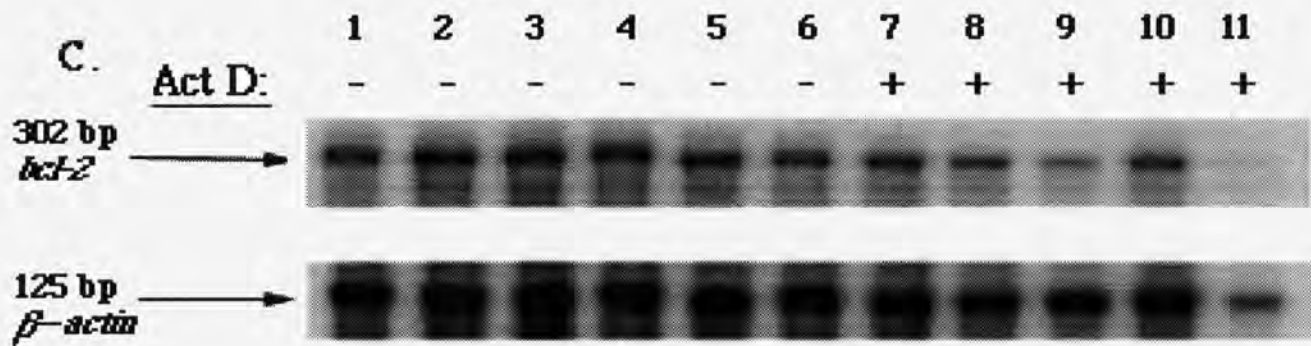
B.



bcl-2 INDUCTION IN HL-60/Bcl-2 CELLS AFTER ARA-C TREATMENT:



C.



D.

bcl-2 INDUCTION IN HL-60/Bcl-2 CELLS AFTER ARA-C TREATMENT:

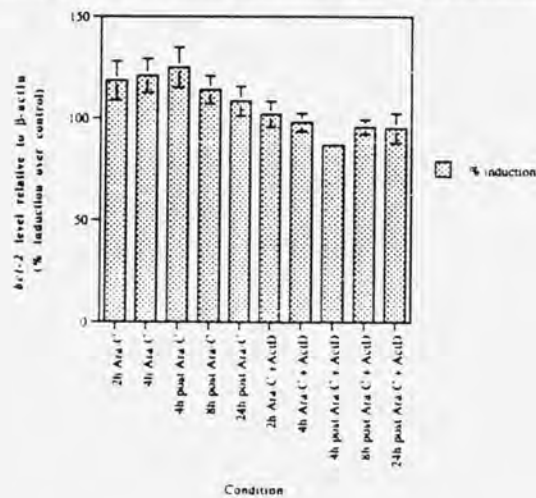
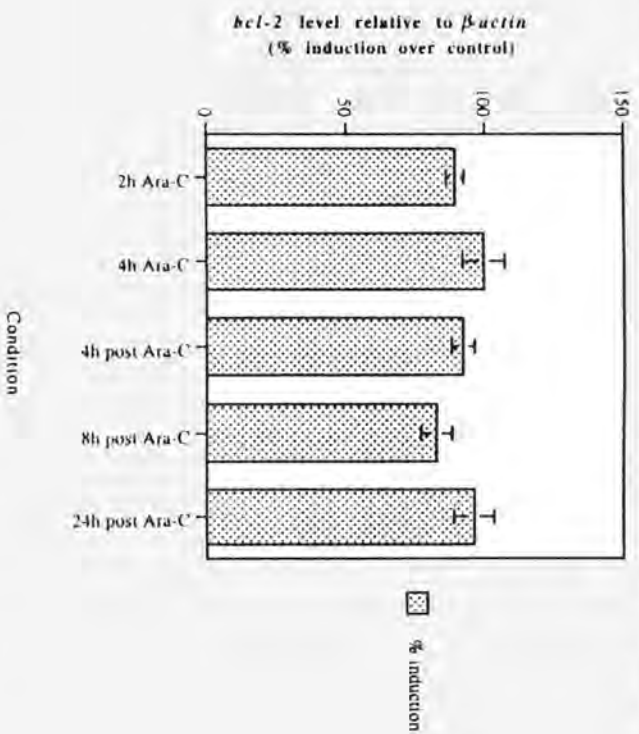
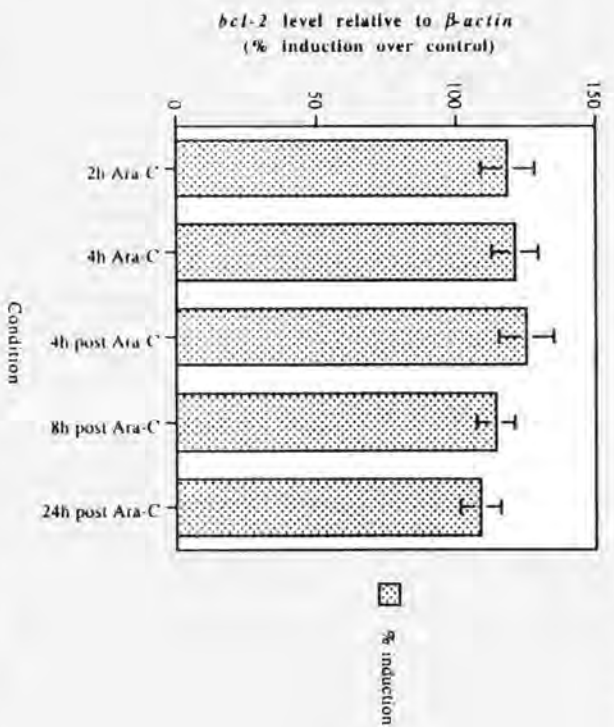


Figure 24a.



bcl-2 INDUCTION IN HL-60/Bcl-2 CELLS AFTER ARA-C TREATMENT:



bcl-2 INDUCTION IN HL-60/Bcl-2 CELLS AFTER ARA-C TREATMENT:

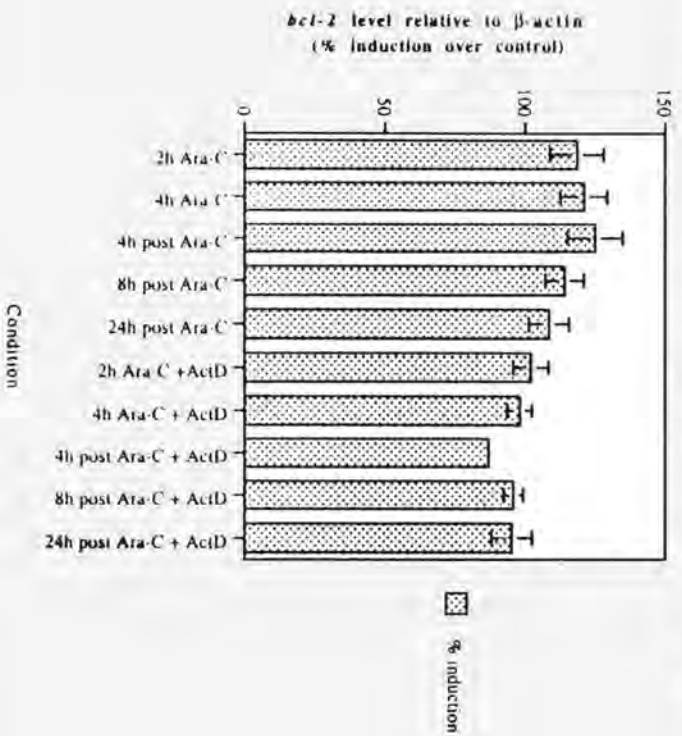


TABLE XIII.

**INDUCTION OF *bcl-2* mRNA ASSESSED BY
RIBONUCLEASE PROTECTION ASSAY IN
HL-60/neo AND HL-60/Bcl-2 CELLS FOLLOWING ARA-C TREATMENT*:**

(Ratio *bcl-2*: β -actin mRNA levels expressed as % control):

<u>Condition:</u>	<u>HL-60/neo:</u>	<u>HL-60/Bcl-2:</u>
2hr HIDAC**	89.29 \pm 3.08	118.45 \pm 9.64
4hr HIDAC	99.56 \pm 7.62	121.01 \pm 8.39
4hr post-HIDAC	91.89 \pm 4.19	125.04 \pm 9.94
8hr post-HIDAC	82.52 \pm 5.64	114.01 \pm 6.87
24hr post-HIDAC	96.20 \pm 7.28	108.45 \pm 7.26
2hr HIDAC + Act D [#]	ND	101.94 \pm 6.28
4hr HIDAC + Act D	ND	97.96 \pm 4.46
4hr post-HIDAC + Act D	ND	86.78 \pm 1.30
8hr post-HIDAC + Act D	ND	95.75 \pm 3.58
24hr post-HIDAC + Act D	ND	95.16 \pm 7.17

* Values represent mean \pm S.E.M. for horizontal scanning densitometry values of *bcl-2*: β -actin mRNA bands on X-ray films from n = 4 experiments.

** HIDAC indicates treatment with 100 μ M Ara-C for the designated exposure interval.

[#] Act D indicates usage of 5 μ g/ml actinomycin D as an inhibitor of RNA transcription.

**TABLE XIV. FLOW CYTOMETRIC DETERMINATION OF Bcl-2 LEVELS
IN HL-60/neo CELLS VERSUS HL-60/Bcl-2 CELLS AFTER ARA-C TREATMENT:
Effect of concomitant actinomycin D/ cycloheximide incubations:
TOTAL Bcl-2 FLUORESCENCE IN NON-APOPTOTIC CELLS
(FITC-Bcl-2 G₁+S+G₂) (% control):#**

Condition:	HL-60/neo:	HL-60/Bcl-2 F:	HL-60/Bcl-2 B:
0 hrs post Ara-C	111.82 ± 10.60	105.00 ± 12.71	113.32 ± 7.47
+ actinomycin D*	98.54 ± 6.41	111.42 ± 11.83	106.98 ± 15.06
+ cycloheximide**	105.14 ± 3.33	108.75 ± 9.79	96.07 ± 13.95
24 hrs post Ara-C	144.38 ± 14.77	154.41 ± 25.74	150.59 ± 6.41
+ actinomycin D*	113.68 ± 21.16	116.03 ± 4.00	105.21 ± 6.66
+ cycloheximide**	103.53 ± 14.46	111.06 ± 8.28	102.11 ± 7.84
48 hrs post Ara-C	150.43 ± 18.61	170.80 ± 26.89	161.58 ± 19.28
+ actinomycin D*	92.02 ± 11.30	98.36 ± 12.91	90.01 ± 13.49
+ cycloheximide**	107.83 ± 7.62	96.65 ± 5.44	99.91 ± 10.67

Values represent mean ± S.E.M. for n = 3 experiments.

* 5 µg/ml actinomycin D, prepared as listed in Materials and Methods.

** 10 µg/ml cycloheximide, prepared as listed in Materials and Methods.

Figure 25. **FLOW CYTOMETRIC DETERMINATION OF Bcl-2 LEVELS**
IN HL-60/neo CELLS VERSUS HL-60/Bcl-2 CLONES AFTER ARA-C TREATMENT:
Effect of concomitant Actinomycin D/ Cycloheximide treatment.

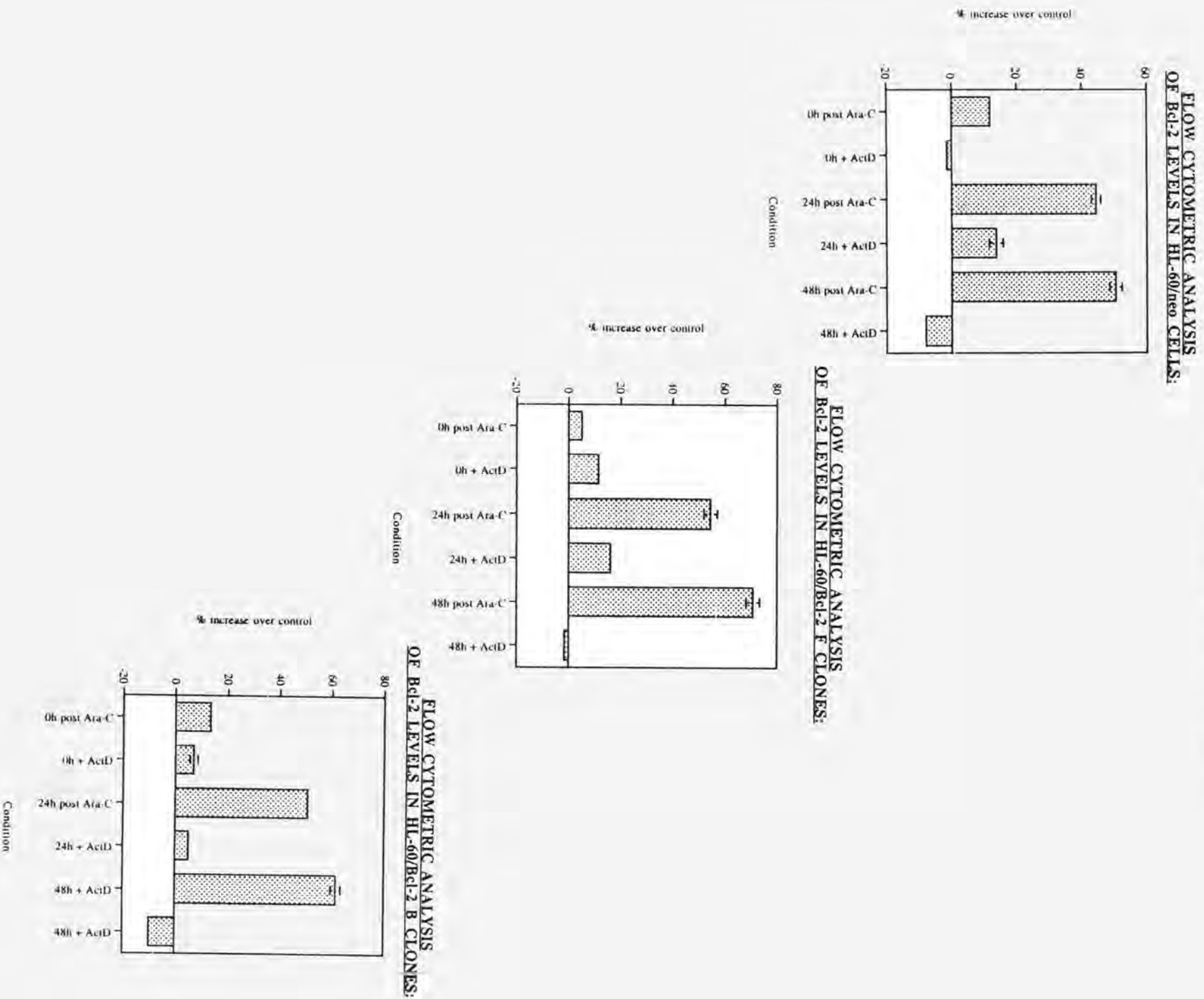


Figure 26.

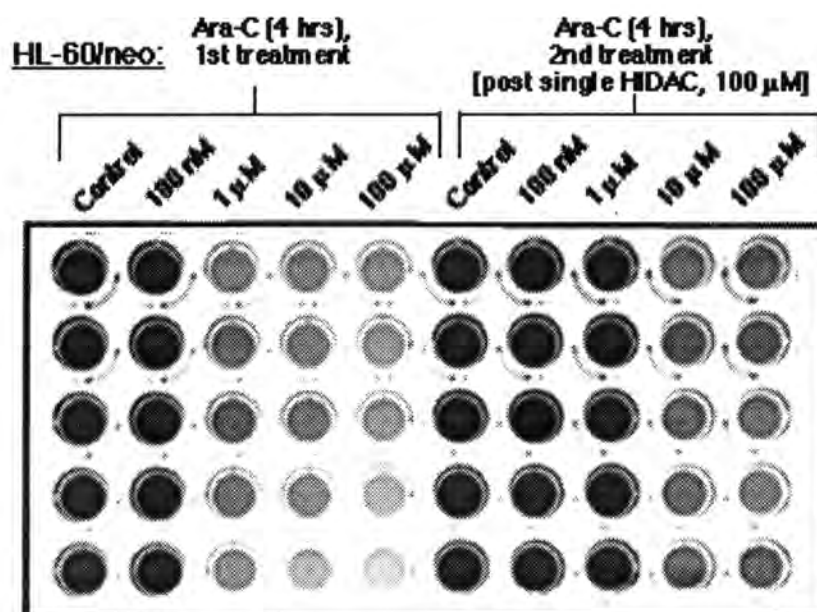


TABLE XV. ASSESSMENT OF CELL VIABILITY BY MTT ASSAY OF HL-60/neo CELLS SURVIVING AFTER FIRST AND SECOND TREATMENTS WITH ARA-C:

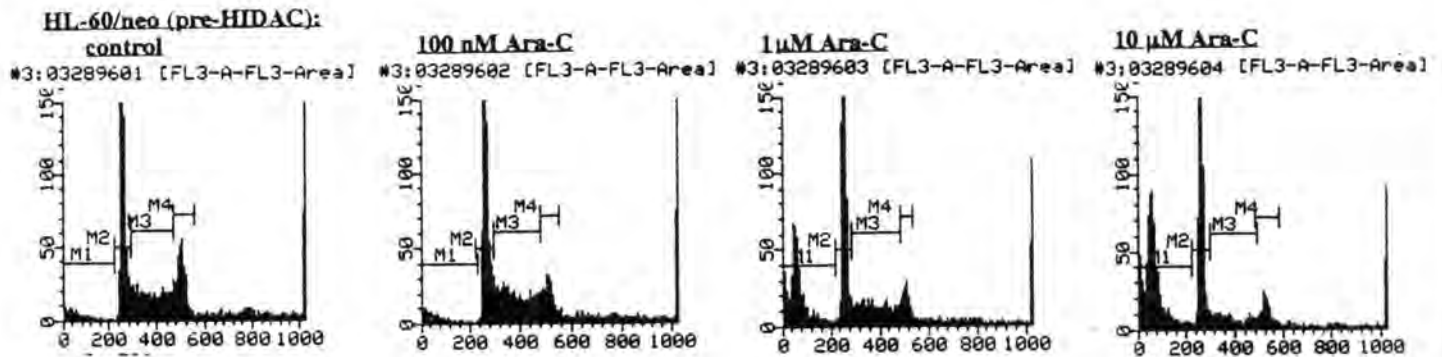
<u>Condition:</u>	<u>Inhibition of cell viability</u> <u>(compared to untreated control)*:</u>	
	<u>First treatment:</u>	<u>Post-HIDAC**:</u>
100 nM Ara-C, 4 hrs	10.41 ± 5.46	0.00 ± 0.00
1 μM Ara-C, 4 hrs	33.84 ± 12.63	3.27 ± 3.78
10 μM Ara-C, 4 hrs	58.85 ± 4.43	40.27 ± 11.77
100 μM Ara-C, 4 hrs	59.11 ± 2.44	52.04 ± 5.11

* Values represent mean ± S.E.M. for n = 3 experiments.

** HL-60/neo cells were treated with high-dose Ara-C (HIDAC=100 μM Ara-C, 4 hrs), washed 5 times with warm sterile PBS, histopaqued daily for three days to remove dead cells, and returned to fresh RPMI 1640 medium containing 10% FBS, prior to re-treatment with increasing concentrations of Ara-C.

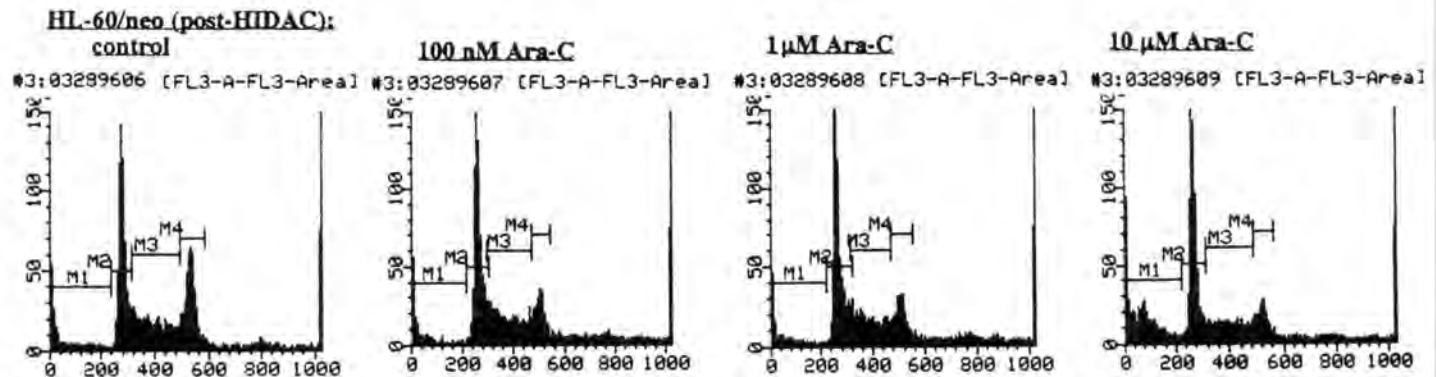
Figure 27/ Table XVI.

**FLOW CYTOMETRIC DETERMINATION OF APOPTOSIS IN HL-60/neo CELLS
AFTER FIRST AND SECOND TREATMENTS WITH ARA-C:***

**I. Pre-HIDAC**:**

Condition:	Control	100nM Ara-C	1μM Ara-C	10μM Ara-C
------------	---------	-------------	-----------	------------

% apoptosis (PI flow cytometry):		5.15 ± 2.18	34.29 ± 2.28	54.93 ± 2.67
% apoptosis (morphology):		0.66 ± 0.33	23.94 ± 0.18	39.21 ± 3.05
Intensity of total DNA breaks (TUNEL assay):		13.55 ± 2.92	15.83 ± 3.97	21.44 ± 12.06

**II. Post-HIDAC:**

Condition:	Control	100nM Ara-C	1μM Ara-C	10μM Ara-C
------------	---------	-------------	-----------	------------

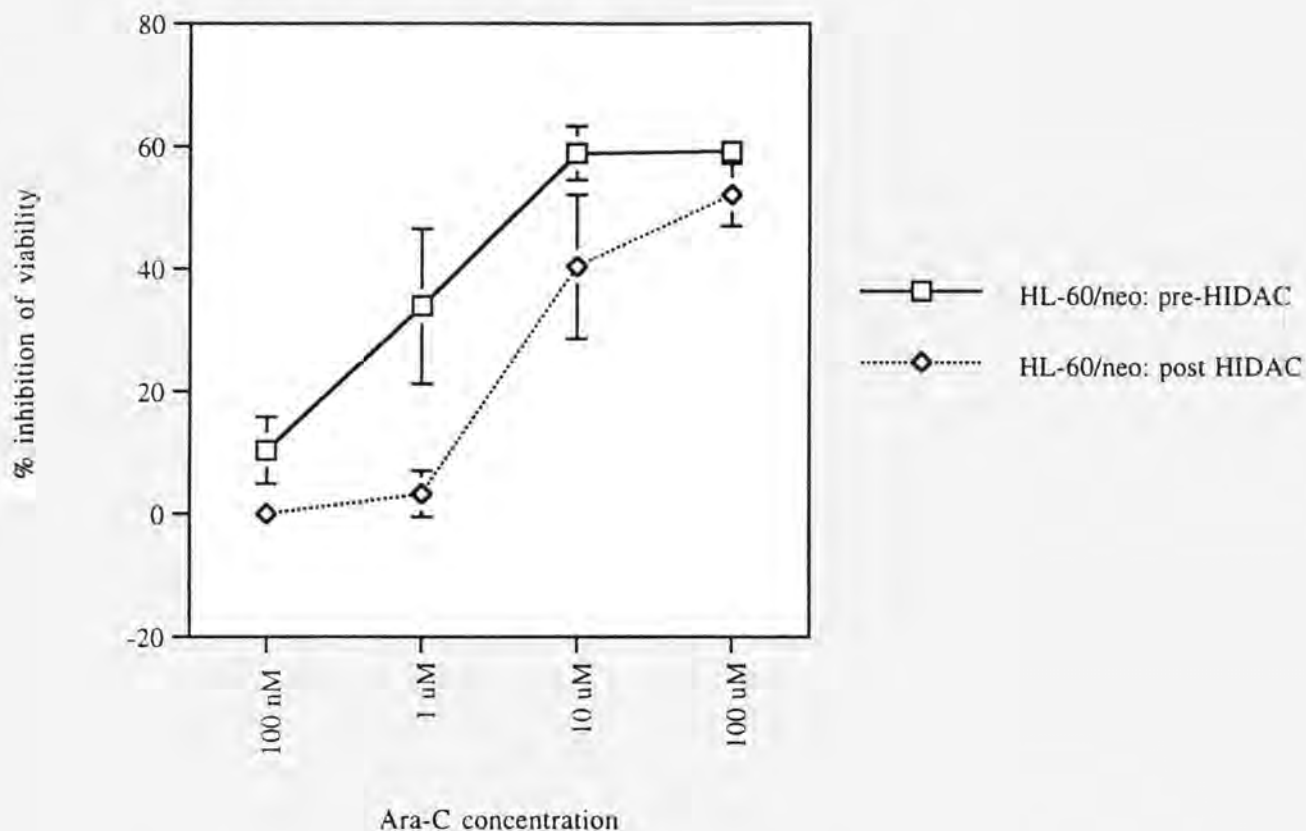
% apoptosis (PI flow cytometry):		6.04 ± 2.81	13.16 ± 3.40	36.34 ± 3.75
% apoptosis (morphology):		7.64 ± 1.13	8.74 ± 0.28	21.23 ± 1.92
Intensity of total DNA breaks (TUNEL assay):		12.75 ± 1.07	13.28 ± 1.28	14.78 ± 1.94

* Values represent mean ± S.E.M. for n=4 experiments, where HL-60/neo cells were exposed to various concentrations of Ara-C either prior or following initial HIDAC treatment and subsequent cultivation of surviving cells for 72 hours as described in Materials and Methods. Values obtained for HL-60/neo cells upon second HIDAC treatment are significantly different (p<0.05) than those obtained for HL-60/neo cells upon first HIDAC treatment.

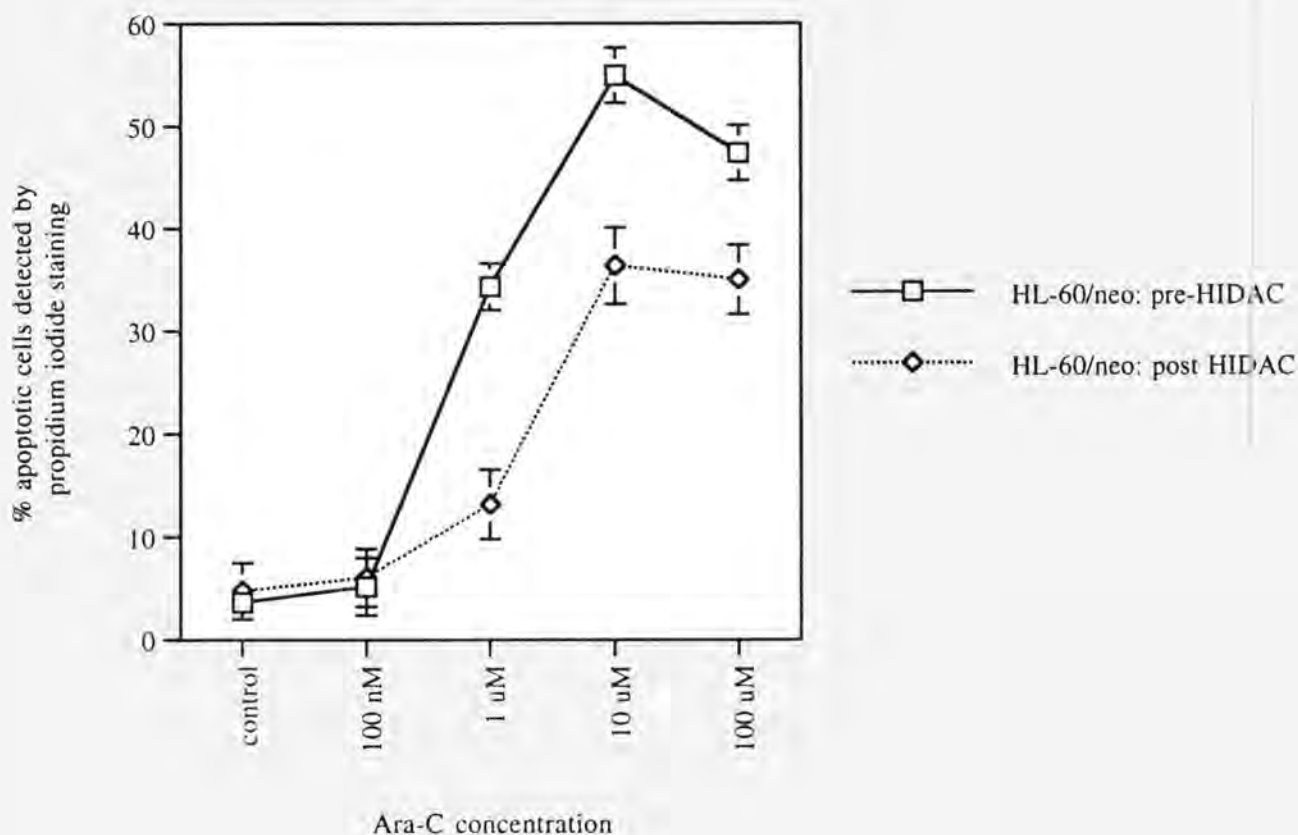
** HIDAC indicates treatment with 100μM Ara-C for 4 hours.

Figure 27a.

**ASSESSMENT OF CELL VIABILITY BY MTT ASSAY
IN HL-60/neo CELLS AFTER FIRST AND SECOND
TREATMENTS WITH ARA-C**



**FLOW CYTOMETRIC DETERMINATION OF APOPTOSIS
IN HL-60/neo CELLS AFTER FIRST AND SECOND
TREATMENTS WITH ARA-C**



CHAPTER V.

**Overexpression of p26Bcl-2 in acute myeloid leukemia HL-60 cells
blocks Ara-C-induced apoptosis, but does not increase repair of
Ara-C-induced DNA damage.**

CHAPTER V: OVEREXPRESSION OF p26Bcl-2 IN ACUTE MYELOID LEUKEMIA HL-60 CELLS BLOCKS ARA-C-INDUCED APOPTOSIS, BUT DOES NOT INCREASE REPAIR OF ARA-C-INDUCED DNA DAMAGE:

Abstract:

The effect of high intracellular levels of p26Bcl-2 on the repair of Ara-C-induced DNA damage was examined in AML HL-60 cells. For these studies, retrovirally-transfected HL-60/neo, and HL-60/Bcl-2 cells, which exhibited highest overexpression of p26Bcl-2, and by immunofluorescence measured 6.3 times higher Bcl-2 intensity than HL-60/neo cells, were utilized. As compared to untreated cells, treatment with high-dose Ara-C (100 μ M for 4 hours) markedly inhibited [³H]-thymidine incorporation in HL-60/neo as well as HL-60/Bcl-2 cells. This inhibition lasted up to 24 hours after Ara-C was removed from the culture condition. To determine whether the recovery of DNA synthesis occurs following its inhibition by Ara-C, the persistence of Ara-C-induced DNA lesions over time after Ara-C treatment was compared by two assays in HL-60/neo versus HL-60/Bcl-2 cells. By alkaline elution analysis, Ara-C-induced DNA strand breaks 4 and 24 hours following HIDAC treatment were demonstrated to be similar in amount between HL-60/neo and HL-60/Bcl-2 cells. Co-culture with aphidicolin, an inhibitor of repair synthesis of DNA, to the culture medium for 4 hours following HIDAC treatment resulted in similar increases in the elutable DNA fragments in both HL-60/neo and HL-60/Bcl-2. PCR of the genomic DNA, following HIDAC treatment of HL-60/neo and HL-60/Bcl-2 cells, demonstrated that the nonspecific damage to DNA templates caused a decrease in the ability of TaqDNA polymerase to amplify sequences from the *c-myc*, relative to *tPA* (amplified as a reference), gene. Regardless of the differences in numbers of apoptotic cells, the amplified *c-myc* gene products could be recovered at an equivalent rate in both HL-60/neo and HL-60/Bcl-2 cells following HIDAC treatment. Unscheduled DNA synthesis was also examined in the two cell lines. Flow cytometric determination of bromodeoxyuridine incorporation in S-phase versus non-S-phase cells after Ara-C treatment demonstrated that there was no significant difference in the unscheduled DNA synthesis in HL-60/neo, as compared to HL-60/Bcl-2 cells. Taken together, these data indicate that following HIDAC treatment, while overexpression of p26Bcl-2 blocks Ara-C-induced apoptosis and promotes greater cell viability, this is not due to an increase

in the repair of Ara-C-induced DNA damage as a result of p26Bcl-2 overexpression. These data show that the early events including DNA damage and its repair are not affected by overexpression of Bcl-2. Hence, they suggest distally operative protective role of p26Bcl-2 in preventing the conversion of Ara-C-induced potentially repairable DNA damage into lethal DNA fragmentation associated with apoptosis.

Introduction:

Damage to genomic DNA must be repaired in order for its efficient replication and for the survival of an organism. Lesions such as incorporated abnormal nucleotides and inter- or intra-strand cross-links must be removed from template DNA, excised as either a single base, as a nucleotide, or an oligonucleotide stretch. Repair of DNA damaged from chemicals has been best studied in *E. coli*, in which several DNA repair systems have been identified and well defined (reviewed in 367-370).

Nucleotide excision repair in eukaryotic cells is far more complex. The extensive proteins involved are more numerous, and are still under investigation. Human excinuclease itself requires the activity of at least 17 polypeptides (371, 372). The excision repair genes of *E. coli* (*uvrA*, *uvrB*, *uvrC*) show no homology to the known human excision repair genes (367). However, the excision repair genes of *S. cerevisiae* are highly homologous to some human excision repair genes, such as the *ercc* genes (367, 370). These genes were discovered by virtue of their ability to rescue excision repair-deficient mutant rodent cells when transfected, and were thus called excision repair cross complementing rodent repair deficiency (*ercc*) genes when cloned. The human *ercc-1* gene encodes a protein with various domains including a nuclear localization capability and a "helix-turn-helix" DNA-binding motif (370). The *ercc-2* and *ercc-3* genes encode DNA helicases responsible for unwinding DNA, and were cloned when discovered to correct incision defects and UV-sensitivity of rodent mutants (370, 373). Mismatch repair of DNA bases has been described as a specific type of nucleotide excision repair in eukaryotes. Most recently, mutations in DNA repair genes such as *Msh2* and *MLH1*, homologs of bacterial DNA mismatch repair genes *mutS* and *mutL*, have been associated with progression of hereditary nonpolyposis colorectal cancer (374, 375).

Repair of Ara-C DNA.

The majority of DNA damage caused by anticancer drugs can be eliminated from DNA by nucleotide excision repair (371). However, while several reports in the literature document the usage of Ara-C as an inhibitor of repair itself, and specifically, the inhibition of the gap-filling step during excision repair (376, 377), there are very few reports documenting the mechanism of repair of DNA with incorporated Ara-C residues. As previously described, 1- β -D-arabinofuranosylcytosine (Ara-C) differs from normal deoxycytidine by the presence of a β -OH group in the 2' position of the sugar (224, 225). When incorporated into DNA, this altered 3' terminal-OH group of Ara-C has less reactivity, and impedes efficient DNA chain elongation by DNA polymerase, not necessarily by inhibiting initiation, but by slowing extension of new DNA strands as illustrated by Ross (236, 237). Removal of the impaired base is required to restore normal DNA synthesis. It is predicted that the 3'-5' exonuclease activity associated with DNA polymerase itself could excise the arabinosyl residue (223). *In vitro* experiments in cell-free systems using purified mammalian DNA polymerase have demonstrated that excision of 1- β -D-arabinofuranosyladenosine (Ara-A) is necessary for further DNA synthesis. However, Tsang Lee *et al.* demonstrated that 6-mercaptapurine ribonucleotide 5'-monophosphate (6-MPR-P) increases incorporation of Ara-AMP into DNA by selectively inhibiting the 3'-5' exonuclease activity of DNA polymerase, and therefore preventing excision of incorporated Ara-AMP into DNA chains (378). In contrast, the exonuclease activity copurified and associated with herpes simplex virus type I DNA polymerase was also demonstrated to remove Ara-AMP residues in a GMP-dependent manner in an artificial system (379). DNA polymerase is then assumed to be able to proceed with repair synthesis.

Various studies have sought to define which DNA polymerase(s) are involved in mammalian repair synthesis. While DNA polymerase α is thought to be mainly responsible for DNA replication (380), both DNA polymerases α and β are involved in repair synthesis, and the extent to which each one is involved is dependent upon the type as well as concentration of the DNA damaging agent (380, 381). There are many conflicting reports in the literature concerning the roles of these two polymerase in DNA repair; however, Miller and Chinault have attempted to explain their involvement. Both can be inhibited by Ara-CTP to different extents (380, 382). However, DNA polymerase β may still be able to function, although not as efficiently, in replication and repair in the presence of Ara-C, and hence, Ara-CTP can be eventually

incorporated into internucleotide position through slow chain extension from the altered terminal Ara-C residue (223, 236). Subsequently, the removal of the impaired base may be difficult to detect (383).

Other DNA polymerases are extensively mentioned in the DNA repair literature. While DNA polymerase γ is thought not to be involved in mammalian repair synthesis (382), DNA polymerases δ and ϵ may be involved in DNA repair in conjunction with other accessory proteins such as proliferating cell nuclear antigen (PCNA), replication protein A (RPA), and RFC replication factor C (RPC) (367), as demonstrated in the repair of UV-induced DNA damage. Aroussekhra *et al.* report that complete repair of UV-induced DNA damage is achieved by the combined action of about 30 polypeptides including DNA polymerase ϵ , RFC, PCNA, and ligase I activities following incision activities achieved RPA, XPA, TFIIH, which contains XPB and XPD, XPC, UV-DDB, XPG, ERCC/XPF complex, and factor IF7 (384). Poly(ADP-ribose) polymerase (PARP) is also thought to be involved in the repair of different types of DNA damage in eukaryotes by virtue of its increased activity during the induction and repair of single-strand and double-strand DNA breaks (385-387). Also known as poly(ADP-ribose) transferase or poly(ADP-ribose) synthetase, PARP is an enzyme which converts NAD to nicotinamide and protein-linked ADP-ribose polymers (385, 388, 389), and is activated when it binds to damaged DNA. Activated PARP adds poly(ADP-ribose) chains to various nuclear polypeptides as well as itself, and this automodification facilitates its own release from damaged DNA to permit DNA repair enzymes to access DNA breaks (385, 390). PARP is also proposed to prevent DNA recombination processes and to facilitate DNA ligation (391). *In vitro* reconstitution studies have demonstrated, however, that several polymerases and even Klenow fragment of polymerase I are capable of performing repair synthesis, and illustrate that it is difficult to assign a specific polymerase to a specific repair situation (367, 384). However, while DNA polymerases δ and ϵ can also be inhibited by Ara-C (392), the roles of these polymerases, as well as the roles of the *ercc* gene product or the mismatch repair genes *msh2* and *mlh1*, have not yet been specifically implicated in repair of DNA with incorporated Ara-C residues, and are not specifically addressed in these studies.

Studies in this dissertation have demonstrated that Ara-C induces equivalent damage to genomic DNA in both HL-60/neo and HL-60 cells overexpressing Bcl-2 (HL-60/Bcl-2 cells)

(Chapter Three). However, lethal double-strand DNA breaks associated with Ara-C-induced apoptosis are prevented in Bcl-2-overexpressing cells (**Chapters Three and Four**). While these findings are consistent with previous reports which show no effect of Bcl-2 overexpression on early DNA damage (101-103), Bcl-2 may impede other genotoxic insults. Hashimoto *et al.* have recently demonstrated that although Bcl-2 overexpression in V79 Chinese hamster cells exhibited equivalent DNA strand breaks induced by the topoisomerase II inhibitor etoposide (VP-16) as compared to V79/neo cells, Bcl-2 overexpression blocked subsequent etoposide-induced DNA recombination by sister chromatid exchange and mutation frequency, leading to higher survival (393). Similarly, if Ara-C-induced DNA strand breaks still occur in HL-60/Bcl-2 cells, it is important to identify what Bcl-2 either promotes or inhibits such that progression to further DNA damage is impeded. Furthermore, **Chapter Four** of this thesis also shows that HL-60/neo or HL-60/Bcl-2 cells which sustain initial Ara-C-induced DNA damage, and yet survive over time, exhibit increased levels of Bcl-2. In order to explain the increased survival of HL-60/Bcl-2 cells after Ara-C treatment, the question was asked whether increased Bcl-2 levels promote more repair of Ara-C-induced DNA damage over time.

There are presently no instances documented in the literature where increased nucleotide excision repair contributes to drug resistance in cancers (371), save one report in which retroviral-mediated transfer of the O⁶-methylguanine DNA methyltransferase (*MGMT*) gene to bone marrow stem cells decreases the cytotoxicity of the chemotherapeutic alkylating agent 1,3-bis(2-chloroethyl)-1-nitrosourea (BCNU) by increasing the capacity for repair of DNA interstrand crosslinks in these target cells (394). By contrast, in the case of cisplatin-induced DNA damage, high mobility group (HMG)-domain proteins which bind to 1,2-intrastrand DNA cross-links caused by cisplatin inhibit their repair, and may affect response to chemotherapy (395-398). The studies in this chapter, examine whether AML cells which possess high levels of Bcl-2 and are resistant to the cytotoxic effects of Ara-C also possess increased repair capacity as assessed by incorporation of thymidine and thymidine analogs, and persistence of lesions in DNA templates.

Materials and Methods:

• **Drugs.** Ara-C and aphidicolin were both purchased from Sigma Chemical Co. (St. Louis, MO). Ara-C was prepared as described in **Chapter Two**. Aphidicolin was prepared as a 10 mM stock in dimethylsulfoxide (DMSO, Fisher Chemicals), and aliquots were stored at -20°C until just prior to use.

• **Transfection of HL-60 Cells.** HL-60/neo and HL-60/Bcl-2 cells were generated by retroviral-mediated transfection of HL-60 parental cells with the neomycin resistance gene alone or in combination with *bcl-2* cDNA as described in **Chapter Two**. Subcloning of HL-60/Bcl-2 cells by limiting dilution generated various clones with disparate levels of homogeneous overexpression of p26Bcl-2, as described in Chapter Four. Clonal population B, which exhibited p26Bcl-2 expression 6.3 times greater than HL-60/neo cells by immunofluorescence (described in **Chapters Two and Four**), was used for the studies presented in this chapter.

• **[³H] Thymidine [TdR] Incorporation:** The inhibitory effect of HIDAC on DNA synthesis, as reflected by inhibition of intracellular [³H]-TdR incorporation, was compared in HL-60/neo versus HL-60/Bcl-2 cells according to a previously described method (219, 399). Briefly, after incubation of HL-60/neo and HL-60/Bcl-2 cells with 100 μM Ara-C for 4 hours, the cells were washed and resuspended in fresh medium containing 0.5 μCi/ml [³H] thymidine (specific activity 65.6 Ci/mmol, Moravek Biochemicals, Brea, CA). The cells were then incubated at 37°C with 5% CO₂. 1 x 10⁶ cells were incubated for various time intervals, then centrifuged and the cell pellets resuspended in cold 10% trichloroacetic acid and stored overnight at 4°C. The cells were again centrifuged, resuspended in cold 10% TCA, and incubated for an additional hour on ice. After centrifugation, the cells were resuspended in 5% TCA, and incubated at 90°C for 30 minutes to extract DNA. The cells were again centrifuged, supernatants transferred into scintillation vials, and radioactive [³H] signal was counted in a Beckman scintillation counter (Columbia, MD). Amount of [³H] thymidine incorporated was expressed as cpm per million cells.

• **Alkaline Elution.** Alkaline elution was performed at different time points after Ara-C treatment exactly as described in **Chapter Three**.

• **Semi-Quantitative Polymerase Chain Reaction for Amplification of *c-myc* relative to *tPA* from HL-60/neo and HL-60/Bcl-2 Genomic DNA Templates after Ara-C Treatment:** HL-60/neo and HL-60/Bcl-2 cells were exposed to 100 μ M Ara-C for 4 hours, washed with warm sterile PBS, resuspended in fresh drug-free 1X RPMI media, and incubated for various intervals. Alternatively, as positive controls for DNA damage, HL-60/neo and HL-60/Bcl-2 cells in 6-well plates (Costar) were gently shaken on a rotating platform and irradiated with 20 J/m² (253.7nm) ultraviolet light for 10 minutes under a sterile culture hood using a germicidal lamp (Forma Scientific Biological Safety Cabinet, Lilburn, GA). This dosage of UV-irradiation induced internucleosomal DNA fragmentation and reduction of cell viability by trypan blue dye exclusion in HL-60/neo cells but not in HL-60/Bcl-2 cells, and was similar to dosages used by Martin *et al.* (400) and Islas and Hanawalt (401).

Genomic DNA was extracted from HL-60/neo and HL-60/Bcl-2 cells at various time points after Ara-C treatment or UV-irradiation as described previously in Chapter Three. 1 μ g genomic DNA from each condition was used for polymerase chain reaction with 150 μ M deoxynucleotide mix, 50 pmols of the appropriate primers, 1.5 mM MgCl₂, and 2.5 U AmpliTaq DNA polymerase (Perkin Elmer Cetus Corporation, Branchburg, NJ). For some experiments, 20 μ Ci/ml α ³²P-dCTP (specific activity 3000 Ci/mmol, ICN Biochemicals, Costa Mesa, CA), was included. For amplification of a 358-bp *c-myc* product from the sequence of exon III, the following PCR primers were used, as described by Harlow and Stewart (402):

5' (+, sense) primer: 5' -AAGGTCAGAGTCTGGATCAC - 3'

3' (-, antisense) primer: 5' -TAACTACCTTGGGGGCCTTT - 3'

For amplification of a 174-bp *tPA* product, the following PCR primers were used:

5' (+, sense) primer: 5' - GCCACCTGCGGCCTGAGACA - 3'

3' (+, antisense) primer: 5' - AGAGAGAATCCAGCAGGAGC - 3'

Reactions were overlaid with 50 μ l mineral oil prior to PCR. The following program was optimized for co-amplification of both products in a DNA Thermal Cycler (Model 480, Perkin Elmer, Branchburg, NJ): initial denaturation at 94°C for 3 minutes; denaturation at 94°C for 1 minute, annealing at 60°C for 1 minute, extension at 72°C for 2 minutes, for 26 cycles; final extension at 72°C for 5 minutes. Furthermore, the addition of the *tPA* primers was delayed until 3 cycles after the start of the PCR amplification with the *c-myc* primers, as used by Rinaudo *et al.* (403) and suggested by Kinoshita *et al.* (404). This was done in order to assure that the *tPA* and *c-myc* primers do not interfere with each other and allow greater *c-myc* amplification than could be obtained with simultaneous addition of both sets of primers. After PCR, mineral oil was removed by extraction with chloroform.

Radioactive PCR products were electrophoresed in standard 1.5-mm-thickness non-denaturing 8% polyacrylamide gels (Gel-Mix 8, GIBCO/BRL, Grand Island, NY). Dried gels were exposed overnight to Molecular Dynamics Phosphorimager cassette, and the bands quantitated using the ImageQuant program. Non-radioactive PCR products were electrophoresed in 3.0% agarose/1X TAE gels, stained with ethidium bromide, photographed utilizing UV transillumination, and the bands quantitated by horizontal scanning densitometry of the film negatives, by acquisition into Adobe Photoshop and utilizing NIH Image Version 1.57 programs (Macintosh). Ratios of *c-myc* amplification to *tPA* reference amplification were calculated and compared between samples.

Ara-C- and UV-induced lesion frequency in the *c-myc* gene in genomic DNA templates for each PCR product in each sample was calculated as described by Kalinowski *et al.* (405):

$$\text{lesion frequency (s)} = -\ln \frac{\text{intensity of amplification in drug-treated sample}}{\text{intensity of amplification in untreated control sample}}$$

•Enrichment of S Phase HL-60/neo and HL-60/Bcl-2 Cells by Centrifugal Elutriation: S phase HL-60/neo and HL-60/Bcl-2 cells were collected by centrifugal elutriation using a Beckman rotor and elutriation apparatus (Beckman Instruments, Columbia, MD). Based on the size of S phase cells, as compared to smaller G₁ phase cells and larger G₂ phase cells, S phase cells were obtained when PBS was washed over the cells at a previously optimized flow rate during centrifugation. This physical separation of cells is optimum for the purpose of this project in that synchronization of cells in S phase does not utilize thymidine or aphidicolin

treatments which may themselves cause DNA breaks and/or apoptosis in HL-60 cells. 500×10^6 of each of logarithmically growing HL-60/neo and HL-60/Bcl-2 cells were sequentially loaded into the rotor by pumping a cell suspension through attached tubing at an initial flow rate of 8 ml/min. The flow rate was then increased gradually by increments of 2 ml/min until S phase cells could be specifically collected when the flow rate reached 16 ml/min. The cell cycle status of this collected fraction was confirmed as S phase by propidium iodide staining and flow cytometric analysis for DNA content.

•Bromodeoxyuridine Incorporation and DNA Analysis by Flow Cytometry S phase HL-60/neo and HL-60/Bcl-2 cells collected by centrifugal centrifugation were exposed to 100 μM Ara-C for 4 hours, washed and resuspended in fresh medium containing 10 μM bromodeoxyuridine (BrdU, Sigma Chemical Co., St. Louis, MO). The Ara-C-treated cells were incubated at 37°C for several hours, and BrdU was allowed to incorporate into DNA. After various time intervals, 5×10^6 cells from each condition were fixed in 70% ethanol overnight at -20°C. Thermal denaturation of the DNA at low ionic strength to promote availability of the BrdU sites to the anti-BrdU antibody, as well as antibody staining, were performed by modifying previously described methods (406-409). After centrifugation the cells were washed in phosphate-buffered saline (PBS), recentrifuged, resuspended in 0.5 $\mu\text{g/ml}$ RNase A/PBS and incubated in a 37°C water bath for 30 minutes. The cells were then centrifuged, washed with PBS, resuspended in 0.1 M HCl/0.5% Triton X-100 in PBS, and incubated for 10 minutes on ice. After recentrifugation and washing in PBS, the cells were resuspended in distilled water and placed in a water bath at 95°C for 10 minutes. The cells were subsequently placed on ice for 10 minutes. After centrifugation and washing in PBS, the cell pellets were resuspended in 150 μl of mouse monoclonal anti-BrdU antibody (DAKO Corporation, Carpinteria, Calif.) (1:100 dilution in 0.5% Tween-20/5% FBS/PBS), and stained for 30 minutes at room temperature. The cells were then washed with 0.5% Tween-20/PBS, recentrifuged, and resuspended in 150 μl goat-anti-mouse fluorescein-isothiocyanate (FITC)-conjugated (Fab')₂ antibody fragment (DAKO Corporation, Carpinteria, Calif.) (1:30 dilution in 0.5% Tween-20/5% FBS/PBS). The cells were again washed with 0.5% Tween-20/PBS, recentrifuged, and subsequently resuspended in 10 $\mu\text{g/ml}$ propidium iodide solution in PBS. Flow cytometry was performed using a 488-nm excitation with 514-nm band-pass filter for fluorescein and a 600-nm long-pass filter for propidium iodide.

• **Statistical analysis.** Statistical analyses including unpaired t-test were performed as described in Chapters Three and Four.

Results:

• **[³H]-thymidine incorporation** into DNA was measured in control and Ara-C treated HL-60/neo and HL-60/Bcl-2 cells as a reflection of total DNA synthesis following treatment with 100 μM Ara-C treatment for 4 hours. **Figure 28** shows that equivalent and increasing amounts of [³H]-thymidine were incorporated into untreated HL-60/neo as well as HL-60/Bcl-2 cells over 24 hours. Treatment with 100 μM Ara-C inhibited [³H]-TdR incorporation in both HL-60/neo versus HL-60/Bcl-2 cells to an equivalent extent immediately following Ara-C treatment (**Figure 28**). In addition, **Figure 28** shows that although HIDAC treatment vastly inhibited [³H]-TdR incorporation in both cell lines, there was a significant difference in the recovery of [³H]-TdR incorporation at 24 hours following Ara-C treatment in HL-60/Bcl-2 as compared to HL-60/neo cells. Even when normalized for the percentage of cells remaining viable (using data presented for cell viability in **Chapter IV, Tables VIII and IX**), the amount of [³H]-thymidine by 24 hours after Ara-C treatment was significantly higher in HL-60/Bcl-2 cells than in HL-60/neo cells (data not shown). These results demonstrate initially, that HIDAC-induced inhibition of DNA synthesis is not affected by overexpression of Bcl-2 in AML cells. Therefore, by abrogating HIDAC-induced apoptotic cell death, high intracellular levels of Bcl-2 convert HIDAC from a cytotoxic to merely a cytostatic antileukemic drug (98). However, the higher amount of [³H]-TdR incorporation in HL-60/Bcl-2 cells at 24 hours after HIDAC treatment as compared to that of HL-60/neo cells (**Figure 29** and data in **Table XVII**) is a finding worthy of further explanation.

• **Alkaline Elution: Analysis of sustained damage over time.**

To determine the extent to which Ara-C-induced DNA strand breaks persisted in HL-60/neo versus HL-60/Bcl-2 clonal population B cells, over time, alkaline elution was performed immediately following, 4 and 24 hours after HL-60/neo and HL-60/Bcl-2 cells were exposed to

100 μ M Ara-C for 4 hours. The alkaline elution profiles were analyzed in order to test the hypothesis that after Ara-C treatment, if greater amounts or rates of repair take place in HL-60/Bcl-2 versus HL-60/neo cells, this would be evident by a reduction in the elution profile of DNA from HL-60/Bcl-2 cells at various time points after Ara-C treatment. **Figure 30** shows that as time progressed after HIDAC treatment, both HL-60/neo and HL-60/Bcl-2 cells sustained equivalent Ara-C-induced DNA strand damage, and increased amounts of Ara-C-induced DNA fragments were detected in both cell types immediately after, as well as 4 hours following Ara-C treatment. Ara-C-induced DNA strand breaks were not significantly different ($p > 0.05$) in HL-60/Bcl-2 cells as compared to HL-60/neo cells, by virtue of equivalent slopes of the DNA elution curves, and the total amounts of alkali elutable DNA collected from beginning to end of elution, from both HL-60/neo and HL-60/Bcl-2 cells immediately following and 4 hours after HIDAC treatment (see **Tables XVIII and XIX**). Furthermore, 100 μ M aphidicolin was added to the media in some conditions, and was used as an inhibitor of repair synthesis. The tetracyclid diterpinoid aphidicolin is also an inhibitor of DNA polymerase(s), but does not incorporate into the DNA strand as Ara-C does (243). It has been previously shown to increase alkaline elution profiles in Ara-C damaged HL-60 cells (243), and has been used as an inhibitor of repair synthesis in several instances in the literature (392, 410-413). When aphidicolin was added to the media as an inhibitor of DNA repair synthesis after removal of Ara-C, the rates of elution increased (as compared to that after Ara-C treatment alone) as previously noted (242), but were similar in both HL-60/neo and HL-60/Bcl-2 cells. Again, a comparison of the slopes of the elution curves, as well as the total amount of DNA eluted from the filters from HL-60/neo and HL-60/Bcl-2 cells showed that they were not dissimilar (see **Table XIX** for slopes). Although percentages of cells undergoing apoptosis were markedly different between the two cell lines (see **Table XX**), this data indicates that Ara-C-induced DNA strand breaks were not significantly different 4 hours following Ara-C treatment. They also suggest that the attempted repair of this damage may be occurring at similar rates in both cell lines.

Alkaline elution profiles of DNA from Ara-C-treated HL-60/neo and HL-60/Bcl-2 cells were again compared 24 hours following Ara-C treatment. Their slopes and the amount of total elutable DNA were not significantly different (data not shown). However, when the cells were co-cultured for 24 hours with aphidicolin after Ara-C treatment, it first appeared that more DNA was eluted overall from HL-60/Bcl-2 cells than from HL-60/neo cells when the percentage of DNA remaining at 18 hours of elution was subtracted from that remaining at 3 hours of elution

(Δ values). However, this result is deceptive since more apoptosis had occurred in HL-60/neo versus HL-60/Bcl-2 cells (see **Table XX**), yielding lower amounts of radioactively-labelled DNA from the remaining intact HL-60/neo cells that could be eluted from the filters. Apoptotic cells are essentially washed from the filters by the cell lysis technique used prior to elution (see **Table XX**). Loss of lower molecular weight apoptotic DNA fragments at alkaline pH 12.1 may be consistent with Ross' demonstration that shorter DNA fragments such as Okazaki fragments (described as 100-200-bp in length, ref. 233) are not elutable at pH 12.1 but at pH 11.0 (237) (please see description in **Introduction, Chapter One**). Thus, when using alkaline elution buffer at pH 12.1, in order to avoid discrepancies due to extensive apoptosis, comparison of elution curves at earlier time points following drug treatment are more useful in addressing the extent to which Ara-C-induced DNA damage persists.

• **Semi-quantitative PCR for *c-myc* and *tPA* products.**

An additional technique was implemented to detect differences in Ara-C induced DNA damage and repair in HL-60/neo versus HL-60/Bcl-2 cells by amplifying sequences of the transcriptionally active *c-myc* gene from genomic DNA of both cell types after Ara-C treatment by polymerase chain reaction (PCR). The principle for optimizing a quantitative PCR assay is based on the theory that any lesion in DNA will block amplification of the DNA template by Taq polymerase used in the PCR (405, 414) or other primer extension assays (415-417). Kalinowski *et al.* demonstrated in L1210 murine leukemia cells that DNA damage induced by UV irradiation or cisplatin correlated with inhibition of amplification of a segment of the transcriptionally active dihydrofolate reductase (DHFR) gene, and that repair of template DNA correlated with increased amplification and return or reappearance of the *DHFR* PCR product (405). *c-myc* is also a transcriptionally active gene (412). Since HL-60 cells possess high rates of transcription of and high levels of *c-myc*, the analysis of amplification of this proto-oncogene from genomic DNA was chosen for these thesis studies in the context of Ara-C-induced DNA damage between HL-60/neo and HL-60/Bcl-2 cells. The assay was made semi-quantitative by adding 1 μ g of genomic DNA to each PCR reaction and co-amplifying a sequence of the *tissue plasminogen activator (tPA)* gene, a reference gene which located on the same chromosome 8 as the *c-myc* gene (402).

Figure 31 is a DNA dose-response gel which demonstrates that using the conditions described in Materials and Methods, PCR amplification for both 358-bp *c-myc* and 174-bp *tPA* products were linear in both cell lines and increased predictably with increased amount of DNA added. **Figure 32** shows results of semi-quantitative PCR for *c-myc* and *tPA* co-amplification in Ara-C-treated (**Panel A**) and as positive controls for DNA damage, UV-irradiated (**Panel B**) HL-60/neo (lanes 1-5 for each) and HL-60/Bcl-2 (lanes 6-10 for each) cells at various time intervals after DNA damage. **Panel A** demonstrates that in both HL-60/neo and HL-60/Bcl-2 cells, as compared to amplification of 358-bp *c-myc* and 174-bp *tPA* products in untreated cells (lanes 1 and 6, respectively), that HIDAC treatment resulted in decreased intensity of PCR amplification of the *c-myc* product in genomic DNA relative to *tPA* immediately following Ara-C treatment (lanes 2 and 7). However, by this assay, the intensity of amplification of the PCR products was recovered and returned to at least that of control levels in both cell lines at 4 hours, and remained at 24 and 48 hours following Ara-C treatment (lanes 3, 4, 5 for HL-60/neo cells, and lanes 8, 9, 10 for HL-60/Bcl-2 cells, respectively). Similarly, to demonstrate the detection of DNA damage by this technique using another genotoxic source, genomic DNA from UV-irradiated HL-60/neo or HL-60/Bcl-2 cells as positive controls were subjected to the same PCR conditions. Diminished intensity of amplification of *c-myc* PCR products relative to *tPA* is also demonstrated in **Panel B** in both cell lines immediately following UV-irradiation (lanes 2 and 7 for HL-60/neo and HL-60/Bcl-2 cells, respectively). This disappearance of the *c-myc* product was prolonged 4 and 8 hours after UV-irradiation (lanes 3 and 8, 4 and 9), and recovered by 24 hours (lanes 5 and 10) in both cell lines. **Figure 30** also includes graphical representations of the numerical calculations presented in **Table XXI** for each set of PCR experiments in both HL-60/neo and HL-60/Bcl-2 cells. The graphs demonstrate the return of the lesion frequency value toward zero, suggesting that repair of the damage incurred to the genomic DNA templates used for PCR takes place. The graphs further suggest that repair and recovery occur to equivalent extents in both cell lines.

• **BrdU incorporation and flow cytometry**

In order to further examine the potential for increased repair in HL-60/Bcl-2 cells with increased survival capacity, a flow cytometric method was optimized to measure unscheduled DNA synthesis as a reflection of ongoing repair processes in HL-60/neo versus HL-60/Bcl-2 cells after Ara-C treatment. The technique of analyzing Bromodeoxyuridine (BrdU)

incorporation into cells in phases of the cell cycle other than S (the synthesis or scheduled replication phase) for the detection of DNA repair by flow cytometry was developed by Selden *et al.* as an improvement over existing techniques for measuring unscheduled DNA synthesis (417). In their study, human fibroblasts were originally irradiated with UV or incubated with various mutagens, and then pulsed with the thymidine analog 5-bromodeoxyuridine (BrdU). The cells were then labelled with both a fluorescein-isothiocyanate (FITC)-conjugated antibody to BrdU, as well as with propidium iodide for DNA content (418, 419). When the cells were subjected to flow cytometry and their cell cycle status determined, it was demonstrated that increases in BrdU intensity in cells outside of S phase were indicative of unscheduled DNA synthesis associated with repair synthesis. Additional studies with four direct-acting mutagens yielded consistent results to lend further credence to the use of this technique for the detection of UDS (418).

In **Chapters Three and Four**, it was demonstrated that high p26Bcl-2 levels confer upon HL-60 cells a greater survival advantage after Ara-C treatment. In order to provide an explanation for the increased survival of HL-60/Bcl-2 cells, this flow cytometric technique was optimized and applied to synchronized HL-60/neo and HL-60/Bcl-2 cells incorporation BrdU for various time intervals after Ara-C treatment. **Figure 33** shows that after centrifugal elutriation, the fourth fraction of either HL-60/neo or HL-60/Bcl-2 cells collected at 16 ml/min were indeed enriched for S-phase cells: up to 94.9% S-phase cells in the elutriated HL-60/Bcl-2 population, as compared to approximately 45.8% of cells in S-phase in the total HL-60/neo population or 48.2% cells in S-phase of the total HL-60/Bcl-2 population loaded onto the elutriator (average percentages are derived from Elite Multicycle Software analysis). These fractions collected were therefore utilized for further studies. This enrichment was performed in order to ensure that the majority of cells studied would indeed be affected by S-phase-specific Ara-C treatment, and their eventual progression into G₂ phase could be monitored flow cytometrically while comparing BrdU incorporation into cells in these phases.

Figure 34 shows histograms and graphs generated by flow cytometry software which illustrate the analysis of BrdU incorporation in various phases of the cell cycle. The left panels A and C of **Figure 34** illustrate “horseshoe” patterns of BrdU incorporation throughout the cell cycle in untreated elutriated HL-60/neo or HL-60/Bcl-2 cells pulsed with 10 μ M BrdU for 4 hours, with high levels of BrdU incorporation in S phase cells (“scheduled” or replicative

synthesis), and low levels in non-S-phase cells (“unscheduled” or repair synthesis). Each top histogram is followed underneath by a graphic representation illustrating that a large percentage of untreated cells exhibit high BrdU incorporation, and correspond to actively synthesizing S-phase cells. Much lower incorporation of BrdU occurs in untreated non-S-phase cells. Windows were drawn around particles corresponding to cells in each phase of the cell cycle, and the mean fluorescence intensity of BrdU incorporation for each window analyzed accordingly. The right panels B and D of **Figure 34** illustrate that when freshly elutriated HL-60/neo or HL-60/Bcl-2 S-phase cells are treated with 100 μ M Ara-C for 4 hours, then washed and pulsed with 10 μ M BrdU for 4 hours, the intensity of BrdU incorporation in S-phase cells is vastly decreased in both Ara-C-treated HL-60/neo and HL-60/Bcl-2 cells as compared with elutriated and untreated HL-60/neo and HL-60/Bcl-2 cells. The graphic representation underneath each histogram on the right-hand panel B and D of **Figure 34** further illustrate that in both elutriated HL-60/neo and HL-60/Bcl-2 cells treated with Ara-C, the majority of cells analyzed exhibit only a low intensity of BrdU fluorescence.

Table XXII shows quantitation of the mean fluorescence intensity for BrdU incorporation in the cell-cycle-phase windows drawn consistently for each sample analyzed by flow cytometry. This table also illustrates that the amount of BrdU incorporation in Ara-C-treated S-phase HL-60/neo or HL-60/Bcl-2 cells is significantly lower than that in untreated “control” S-phase HL-60/neo or HL-60/Bcl-2 cells. This table specifically illustrates that mean fluorescence intensity of BrdU incorporation is not significantly different ($p > 0.05$) in S-phase HL-60/neo or HL-60/Bcl-2 cells, or most importantly, in non-S-phase ($G_1 + G_2$) HL-60/neo or HL-60/Bcl-2 cells distinguished by flow cytometry. It was hypothesized that any increases in BrdU intensity detected in non-S-phase HL-60/Bcl-2 cells over HL-60/neo cells would indicate an increase in unscheduled DNA synthesis promoted by Bcl-2 overexpression. When HL-60/neo and HL-60/Bcl-2 cells continuously pulsed with BrdU for 12 and 24 hours after Ara-C treatment were also analyzed, it was consistently found that BrdU incorporation in non-S-phase cells was also not significantly different in HL-60/neo as compared to HL-60/Bcl-2 cells, reflecting no appreciable difference in unscheduled DNA synthesis (or repair synthesis) between the two cell lines.

Discussion:

The cytotoxic activity of HIDAC against AML cells is well documented to be responsible for its clinical efficacy in relapsed AML following treatment with conventional doses of Ara-C (335-339). Ara-C is also known to be a potent inhibitor of DNA synthesis (223). The results in this thesis demonstrate that although overexpression of Bcl-2 in HL-60/Bcl-2 cells abrogates the cytotoxic effects of HIDAC, as reflected by its inhibition of HIDAC-induced apoptosis, it does not significantly affect HIDAC-mediated DNA synthesis inhibition (**Figure 28**). Thus in the context of Bcl-2 overexpression in AML cells, these findings show that HIDAC may be acting only as a cytostatic anti-AML drug (98). **The eventual recovery of HIDAC-induced DNA synthesis inhibition in Bcl-2 overexpressing AML cells which escape apoptotic cell death may be a mechanism underlying clinical relapse in AML despite initial growth inhibitory effects of HIDAC.** The increased level of [³H]-TdR incorporation in HL-60/Bcl-2 cells 24 hours after Ara-C treatment as compared to that seen in HL-60/neo cells (see **Figure 29**) therefore prompted the subsequent studies presented in this chapter examining the potential for repair of Ara-C-induced DNA damage in HL-60/Bcl-2 cells as compared to HL-60/neo cells. As consistently demonstrated in this thesis, Ara-C induced much greater apoptosis and inhibition of viability in HL-60/neo cells than in HL-60/Bcl-2 cells. When the amounts of [³H]-TdR incorporation in both HL-60/neo and HL-60/Bcl-2 cells after Ara-C treatment are normalized for the percentage of viable non-apoptotic cells remaining after Ara-C treatment (not shown), based on data from flow cytometric analyses and MTT assays presented in **Chapters Three and Four**, the resultant [³H] TdR incorporation levels are still significantly higher in HL-60/ Bcl-2 cells as compared to HL-60/neo cells. These data are consistent with Miyashita and Reed's findings, where 697/Bcl-2 cells show slightly higher [³H]-TdR incorporation after drug treatment than 697/neo cells (98), but this difference was not further explained. These data indicate that Bcl-2 promotes greater cell viability, and possibly suggests higher capacity for recovery of DNA synthesis after Ara-C treatment. The contribution to the higher [³H] signal in TCA-extracted DNA from HL-60/Bcl-2 cells after HIDAC may be due to the incorporation activity in a higher number of surviving cells, however. Whether or not this increase in [³H]-TdR incorporation is due to increase in recovery of DNA synthesis by repair of Ara-C-induced DNA damage was then further assessed. Because of a paucity of techniques in the DNA repair literature for direct

evidence of repair of Ara-C-induced DNA damage, three indirect techniques for indications of repair were utilized.

Alkaline elution analysis for the persistence of Ara-C-induced DNA strand breaks over time, as well as for the potential effect of inhibition of repair synthesis by DNA polymerase-specific aphidicolin, also showed no conclusive evidence for difference in DNA profiles between Ara-C-treated HL-60/neo and HL-60/Bcl-2 cells up to 24 hours after Ara-C treatment. If it is hypothesized Bcl-2 overexpression that allows or causes increased repair of Ara-C-induced DNA strand breaks, it would be expected that the slopes of the elution curves from DNA from HL-60/Bcl-2 cells would be smaller in degree than those from DNA from HL-60/neo cells at several time points following Ara-C removal, indicating repair of the damage. In addition, it was hypothesized that if greater rates of repair synthesis occur in cells overexpressing Bcl-2, the presence of aphidicolin would cause less inhibition of active DNA polymerase activity, resulting in decreased elutable DNA from HL-60/Bcl-2 cells treated with HIDAC followed by aphidicolin, as compared with HL-60/neo cells. This also assumes that the process(es) of repair synthesis of Ara-C-induced DNA damage utilizes the DNA polymerase(s) affected by aphidicolin as its primary element(s). Since no differences were found in elution profiles of both cell lines after Ara-C treatment, and in the presence or absence of aphidicolin, these data offer no conclusive evidence that Bcl-2 overexpression confers upon HL-60 cells a greater potential for removal of Ara-C-induced DNA damage by the alkaline elution assay. Notably, the Ara-C-induced DNA damage, as detected by alkaline elution, persists up to 24 hours following Ara-C treatment in both HL-60/neo and HL-60/Bcl-2 cells, shown by greater percentage of elutable DNA fragments at 24 hours after Ara-C treatment as compared with previous time points (data not shown). The recovery of the integrity of damaged DNA from HL-60/neo or HL-60/Bcl-2 cells is thus not identified at these time points. It is further surmised that if the study was extended up to 48 hours after Ara-C treatment, the DNA profiles in both cell lines would demonstrate decreased slopes as more surviving cells recover from Ara-C-induced DNA damage. This has been demonstrated by Walton *et al.* (102) and Kamesaki *et al.* (103) that as nitrogen mustard- and etoposide-induced DNA damage, respectively, is repaired (to equivalent extents in cells which overexpress Bcl-2 as compared with parental cells), alkaline elution profiles over time are reduced, and less damaged DNA is eluted from the filters over time.

By a different assay, PCR-amplified *c-myc* relative to *tPA* products were shown to recover at equivalent rates over time after Ara-C-induced damage to genomic DNA templates in both HL-60/neo and HL-60/Bcl-2 cells. Repair of the actively transcribed *c-myc* gene in HL-60 cells is described as proficient (401), and this is potentially reflected in these data presented here in HL-60/neo and HL-60/Bcl-2 cells. It was noted, however, that the *c-myc* PCR products do not completely disappear initially in DNA of Ara-treated cells as do the DHFR products analyzed in UV-treated L1210 cells in Kalinowski's study, or even to the extent as the UV-irradiated HL-60/neo and HL-60/Bcl-2 cells used as positive controls in this Chapter. This is possibly due to the different types of DNA damage in each scenario. UV irradiation can produce single-strand breaks by virtue of forming UV photodimers, a structural lesion which severely impairs further extension from the altered DNA template (405). The potential impasse by the altered base Ara-C may not be as severe, since Ross and others have demonstrated that polymerization may still be able to occur, albeit much more slowly, from the Ara-C residue (236-237). In addition, the probability of detection of a DNA lesion into the genomic template is proportional to the size of the gene product amplified and analyzed by PCR. While smaller products are more efficiently amplified by Taq polymerase used in PCR than larger segments (420, 421), the smaller the product, the less damage may be detected in that region. While *c-myc* amplification intensity decreased after exposure to HIDAC in both HL-60/neo and HL-60/Bcl-2 cells, the 174-bp *tPA* product showed little change in amplification, most likely because of its size. Jennerwein and Eastman also examined the feasibility of detecting DNA damage in PCR products of various sizes. They found that bulky cisplatin-induced DNA adducts blocked amplification of various sequences of the hamster adenosine phosphoribosyltransferase gene in CHO cells to a significant extent in a 2-kbp fragment, to a moderate extent in a 750-bp fragment, and not at all in a 150-bp fragment (414). They concluded that smaller PCR fragments may be used in this context as references to normalize data for variations between samples (414). These examples may provide explanations as to why the *c-myc* and *tPA* products do not completely disappear when DNA from Ara-C- or UV-treated HL-60/neo and HL-60/Bcl-2 cells is amplified. It is notable, however, that the recovery of amplification of the *c-myc* product relative to the *tPA* product occurs in both cell lines, and shows an indication of equivalent rates of repair and/or recovery.

Furthermore, potential for repair synthesis was investigated by examining BrdU incorporation into HL-60/neo and HL-60/Bcl-2 cells elutriated to enrich for S-phase cells and

treated with Ara-C. Subsequent flow cytometry demonstrated that the amounts of BrdU incorporation after Ara-C treatment in non-S-phase cells were similar in both cell lines, regardless of the level of Bcl-2 expression. Therefore, despite Bcl-2-mediated blockade of apoptosis and Bcl-2-mediated enhancement of cell viability, rates of unscheduled DNA synthesis were not affected by the presence of higher intracellular levels of Bcl-2. In comparing the equivalent incorporation of BrdU in S- and non-S-phase cells as an indication of replicative and repair synthesis with the incorporation of [³H]-TdR in the total HL-60/neo and HL-60/Bcl-2 populations after Ara-C treatment, it is concluded that increased levels of [³H] thymidine incorporation may merely reflect contributions from a higher number of viable cells present in the population of HL-60 cells overexpressing Bcl-2.

If any indication of increased unscheduled DNA synthesis was observed in these experiments, increased repair of Ara-C-induced DNA damage in cells which overexpress p26Bcl-2 could be confirmed by assessment of sedimentation in isopyknic cesium chloride density gradients and measuring the buoyant density of BrdU-labelled DNA strands undergoing repair after HIDAC treatment and compared with BrdU-labelled DNA strands undergoing semiconservative synthesis (368, 401, 422). Furthermore, the effect of Bcl-2 on specific incision, polymerase, or ligation activities attributed to the removal and repair of Ara-C-induced DNA lesions would need to be investigated in order to be able to conclude whether increased repair is a direct result or a secondary effect of Bcl-2 overexpression. These latter assays have not been widely established in the literature. However, these data in this dissertation indicate no additional capacity for increased repair synthesis in cells which overexpress Bcl-2, and are consistent with previously published reports which found no effect of Bcl-2 overexpression on the rate of repair of etoposide- (VP-16-) induced single-strand breaks (103), or on nitrogen mustard- or camptothecin-induced DNA damage (101). While it is therefore assumed that cells with higher Bcl-2 levels are as capable of repairing Ara-C-induced DNA damage as cells with lower Bcl-2 levels, as evidenced by the PCR studies presented here, and by flow cytometric evidence of equivalent recovery of cell cycling through G₂/M-phase after Ara-C treatment (data not shown), it is concluded that cells which possess higher Bcl-2 levels have no greater repair capacity than cells with lower Bcl-2 levels. The data presented in this chapter suggest that regardless of the ability of HL-60 cells with disparate levels of p26Bcl-2 expression to repair DNA damage, this damage may nevertheless be a critical signal to activate a cellular pathway

leading to apoptosis. If the signalling pathway itself is blocked by Bcl-2, only apoptosis is inhibited or lessened. **It is therefore important to establish or identify how Bcl-2 inhibits the conversion of early DNA damage into lethal DNA damage in order to maintain cell viability without the contribution of increased DNA repair.** The proposed mechanism(s) of action of Bcl-2, including the antioxidant effect (120, 121), the interference with Ca^{2+} flux (10), and with nuclear protein trafficking associated with apoptosis (142, 144), have been discussed in **Chapters One and Three** of this dissertation. These potential mechanism(s) will be expanded upon in the next chapter, as they specifically apply to the inhibition of Ara-C-induced apoptosis.

FIGURE LEGENDS:

Figure 28: [³H]-thymidine incorporation in HL-60/neo and HL-60/Bcl-2 cells. HL-60/neo and HL-60/Bcl-2 cells were either untreated or exposed to 100 μM Ara-C (HIDAC) for 4 hours, then washed resuspended in drug-free media containing 0.5 μCi/ml [³H] thymidine. At various time points, 1 to 24 hours, 1 x 10⁶ cells were collected and DNA extracted with TCA, as described in the method in this chapter. [³H] thymidine incorporation was expressed as cpm per million cells, and bars in the figure (top and bottom panel) reflect the means ± S.E.M. for three experiments, tabulated in **Table XVII**.

Figure 29: [³H]-thymidine incorporation in HL-60/neo and HL-60/Bcl-2 cells after Ara-C treatment. Enlargement of bars in Figure 24 representing [³H] thymidine incorporation in HL-60/neo or HL-60/Bcl-2 cells at various time points after Ara-C treatment only, as described in the Figure 28 legend. Bars reflect means ± S.E.M. for three experiments, tabulated in **Table XVII**.

Figure 30: Alkaline Elution profiles for HL-60/neo (top) and HL-60/Bcl-2 (bottom) cells after Ara-C treatment are expressed as the percent DNA remaining on the polycarbonate filters, as described in Chapter Three methods. Data points on the curves represent the means of eluted DNA in three-hourly fractions collected over 18 hours (mean of three experiments, with standard error of mean [S.E.M.] tabulated in **Table XVII**). The results demonstrate that there is no significant difference in the amounts or the slope of the elution of DNA in Ara-C-treated HL-60/neo versus HL-60/Bcl-2 cells (please see data in **Table XIX**).

Figure 31: Dose-response curves for amplification of *c-myc/tPA* products by PCR. **Panel A** shows intensity of amplification of the 358-bp *c-myc* PCR product for given amounts of genomic DNA from HL-60/neo or HL-60/Bcl-2 cells added to the PCR reactions and amplified with the conditions listed in the text. The above graph is a representation of the intensity value assigned to radioactive *c-myc* bands in the dried polyacrylamide gel in **Panel B**, quantitated by a Phosphorimager. **Panel C** is a similar graphic representation of the intensity of amplification of the 174-bp *tPA* PCR product for given amounts of genomic DNA from HL-60/neo or HL-60/Bcl-2 cells, tabulated from the intensity value assigned to the radioactive *tPA* bands shown in Panel B. The intensity values demonstrate a predictable and linear increase in the amount of PCR products generated by the described cycle number, durations, and temperatures, as the amount of DNA added is also increased to 1000 ng (1 μg). Gel is representative of 2 experiments, each with similar results.

Figure 32: Determination of Ara-C- or UV-induced lesion frequency in the *c-myc* gene relative to *tPA*) by PCR of genomic DNA templates from HL-60/neo and HL-60/Bcl-2 cells. Genomic DNA was extracted from HL-60/neo or HL-60/Bcl-2 cells at various time points after Ara-C treatment or UV-irradiation (described in Materials and Methods), as described in Chapter Three. *c-myc* and *tPA* PCR products were co-amplified from 1 μg of each genomic DNA sample using the conditions and parameters listed Materials and Methods. 10 μl of each PCR reaction was then electrophoresed in 2.0% agarose/1X TAE gels, stained with ethidium bromide, and photographed utilizing UV transillumination.

Panel A represents PCR co-amplification of 358-bp *c-myc* and 174-bp *tPA* sequences in genomic DNA from HL-60/neo (lanes 1-5) and HL-60/Bcl-2 cells (lanes 6-10) immediately following HIDAC treatment (lanes 2,7) as well as 4, 24, and 48 hours after HIDAC treatment (lanes 3 and

8, 4 and 9, 5 and 10, respectively), as compared to untreated controls (lanes 1,6). M represents 123-bp ladder as the electrophoresis marker.

Genomic DNA from UV-irradiated cells was used as positive controls for DNA damage for this technique. **Panel B** represents the same technique performed on genomic DNA templates extracted from HL-60/neo (lanes 1-5) and HL-60/Bcl-2 (lanes 6-10) immediately following UV-irradiation (lanes 2,7) as well as 4, 8, and 24 hours following UV-irradiation (lanes 3 and 8, 4 and 9, 5 and 10, respectively), as compared with un-irradiated control cells (lanes 1,6).

Intensity of amplification of each band was quantitated by scanning densitometry of the film negative, and Ara-C-induced lesion frequency was calculated as described in the text. Graphical representations of the calculations for *c-myc* lesion frequency after each DNA damaging treatment tabulated in **Table XXI** are plotted beneath each PCR gel. Data represent mean \pm S.E.M. for n=4 experiments. Gels are also representative of four experiments, each with similar results.

Figure 33: Flow cytometric confirmation of enrichment of HL-60/neo and HL-60/Bcl-2 cells for S-phase cells by centrifugal elutriation. For each panel, 2×10^6 HL-60/neo or HL-60/Bcl-2 cells were fixed in ice-cold ethanol in -20°C for 1 hour, washed with PBS, and resuspended in $10 \mu\text{g/ml}$ propidium iodide containing $0.5 \mu\text{g/ml}$ RNase A before (**Panels A and C**) or after (**Panels B and D**) centrifugal elutriation and collection of cells eluted during flow of PBS through the elutriation chamber at 16 ml/min , as described in the text. Flow cytometry for DNA content was performed and percentage of cells in S-phase tabulated with Multicycle software. Panels B and D show that cells collected at flow rate 16 ml/min contained the greatest number of S-phase HL-60/neo or HL-60/Bcl-2 cells than other fractions collected by centrifugal elutriation, and were subsequently used for BrdU incorporation after Ara-C treatment.

Figure 34: Flow cytometric analysis of bromodeoxyuridine incorporation in elutriated HL-60/neo versus HL-60/Bcl-2 cells after Ara-C treatment. For each panel, elutriated S-phase HL-60/neo (**Panels A and B**) or HL-60/Bcl-2 (**Panels C and D**) cells were either left untreated (**Panels A and C**) or exposed to $100 \mu\text{M}$ Ara-C (**Panels B and D**). After 4 hours, cells were washed, resuspended in fresh drug-free media and pulsed with $10 \mu\text{M}$ BrdU for at least 4 hours. Cell samples fixed in ice-cold 70% ethanol were then processed and double-stained with anti-BrdU antibody and propidium iodide as described in the text. Flow cytometry was performed, and generated histogram representation of BrdU intensity in each phase of the cell cycle (top square of each panel, with **window B = apoptotic/sub- G_1 phase**; **window C = G_1 phase**; **window E = S phase**; **window D = G_2 phase**), as well as comparison of BrdU intensity per cell count (bottom square of each panel). Panels A and C show typical “horseshoe” pattern of high BrdU incorporation in S-phase and low BrdU incorporation in non-S-phase untreated HL-60/neo and HL-60/Bcl-2 cells. Panels B and D demonstrate the inhibition of BrdU incorporation in S phase in Ara-C-treated HL-60/neo as well as HL-60/Bcl-2 cells, with only the low incorporation of BrdU in the remaining non-S-phase cells.

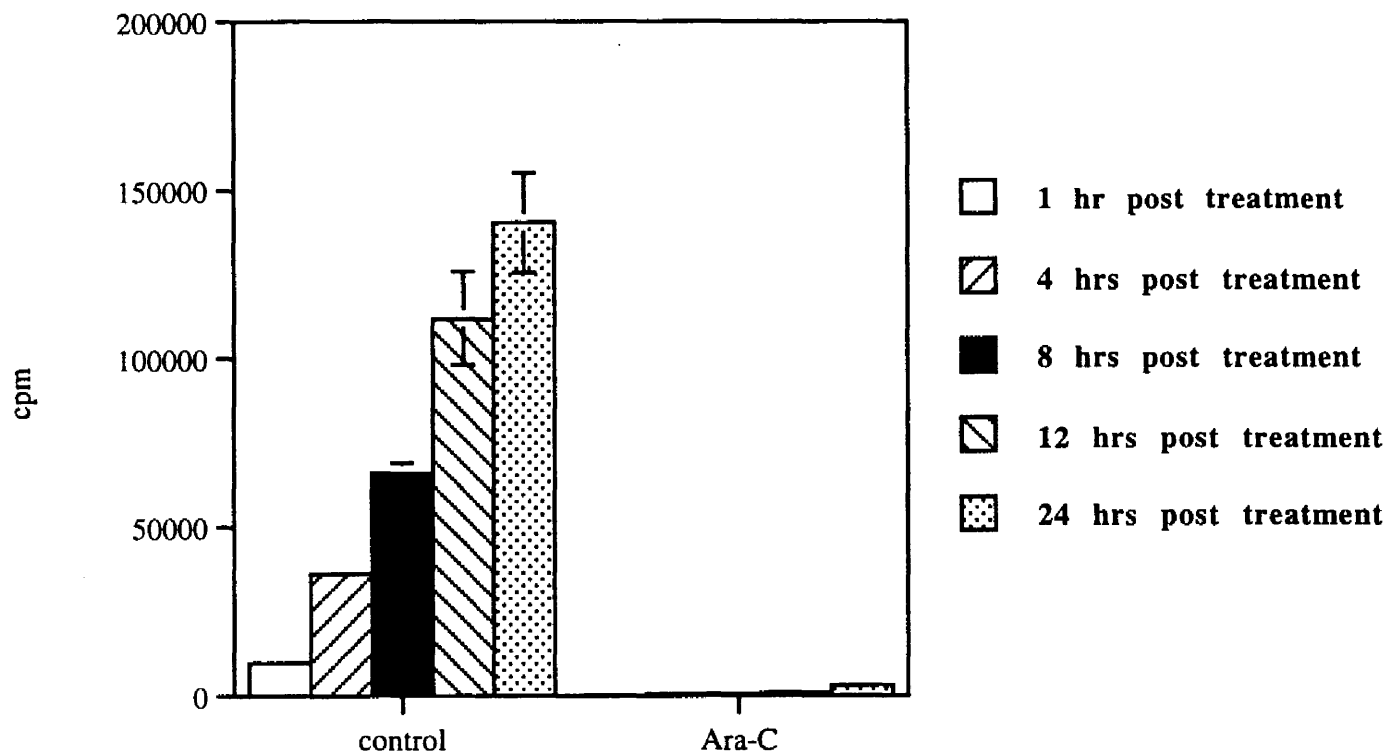
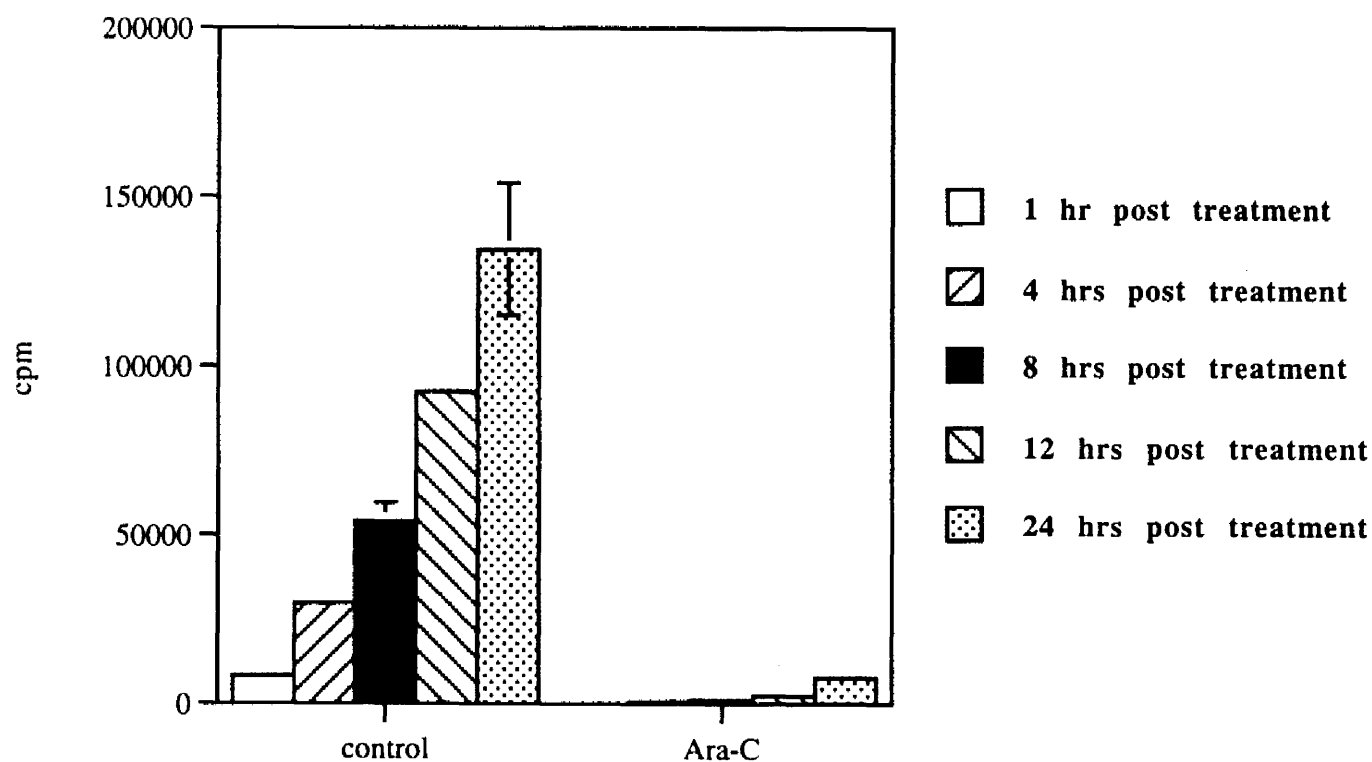
Figure 28.**[3-H] THYMIDINE INCORPORATION
IN HL-60/neo CELLS****[3-H] THYMIDINE INCORPORATION
IN HL-60/Bcl-2 CELLS**

Figure 29.

**[³H]-THYMIDINE INCORPORATION
IN HL-60/neo AND HL-60/Bcl-2 CELLS
AFTER ARA-C TREATMENT:**

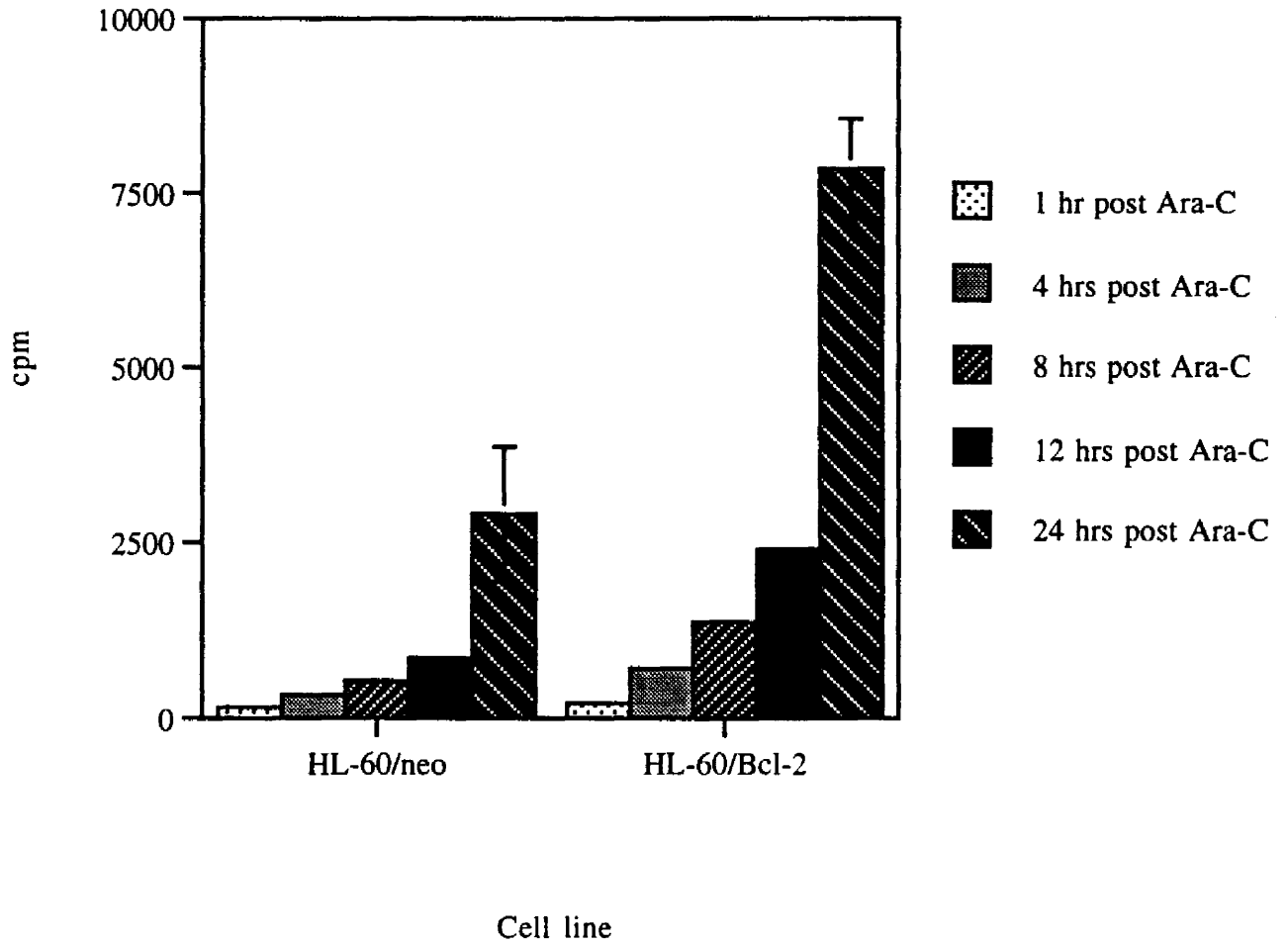


TABLE XVII.

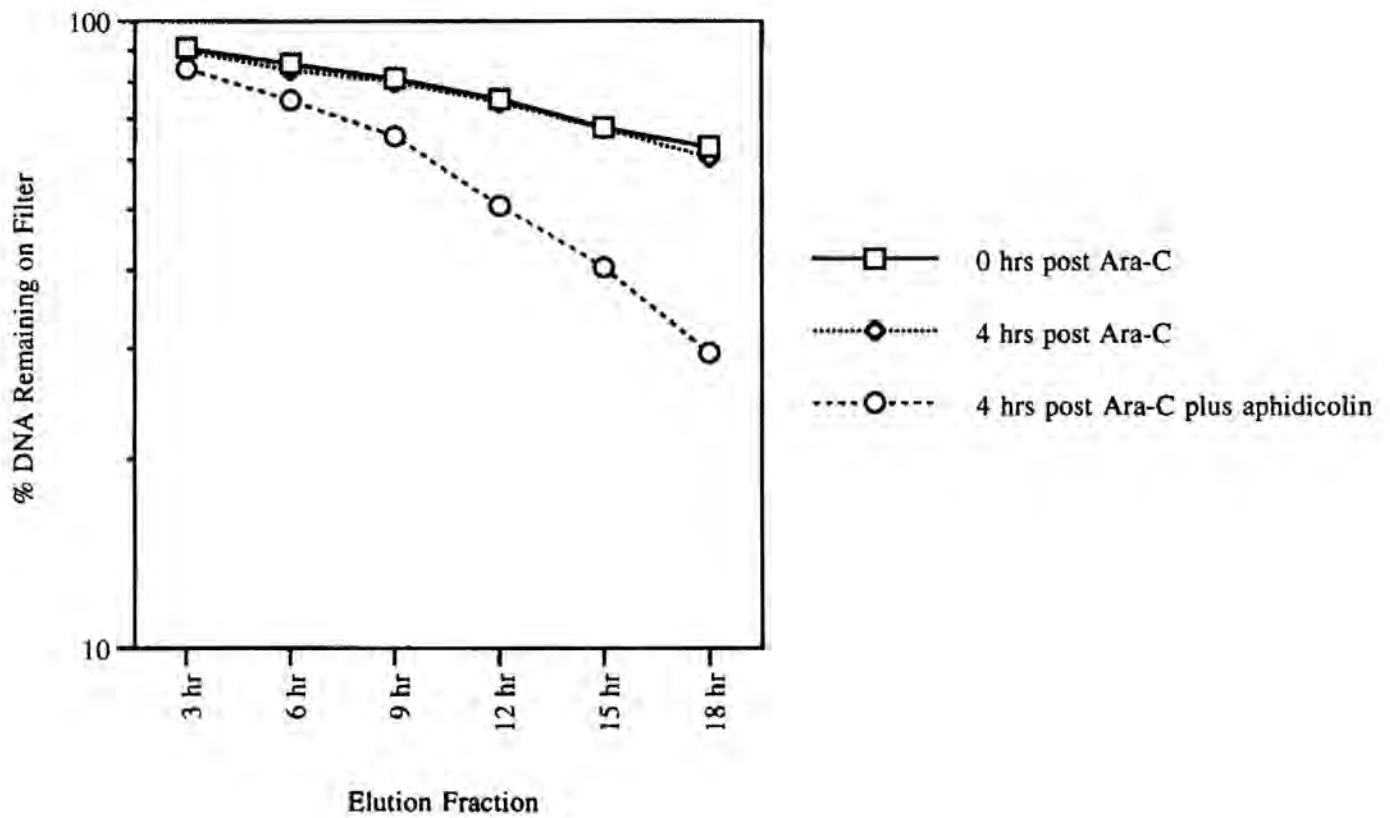
[³H]-THYMIDINE INCORPORATION
IN HL-60/neo VERSUS HL-60/Bcl-2 CELLS
AFTER ARA-C TREATMENT:*

<u>Condition:</u>	<u>[³H] counts of TCA extracts</u>	
	<u>HL-60/neo:</u>	<u>HL-60/Bcl-2:</u>
<u>Control:</u>		
1 hr	9652.5 ± 303.7	8183 ± 876.5
4 hrs	36031 ± 936.56	29845.7 ± 1437.5
8 hrs	65813 ± 3414.7	54116 ± 5450.3
12 hrs	111783.7 ± 13808.9	92410.7 ± 2164.9
24 hrs	140329.7 ± 14797.8	134608 ± 19530.2
<u>Post 100 μM Ara-C:</u>		
1 hr	149 ± 10.5	207.5 ± 22.6
4 hrs	334.3 ± 44.3	709.3 ± 100.1
8 hrs	540.3 ± 52.9	1363.7 ± 36.3
12 hrs	861.3 ± 81.9	2408.3 ± 139.1
24 hrs	2909 ± 964.4	7845 ± 718.9

* Values represent mean ± S.E.M. for n = 3 experiments. Values obtained in identically treated HL-60/neo versus HL-60/Bcl-2 cells are significantly different (p < 0.05) for post Ara-C samples.

Figure 30.

ALKALINE ELUTION IN HL-60/neo CELLS:



ALKALINE ELUTION IN HL-60/Bcl-2 CELLS:

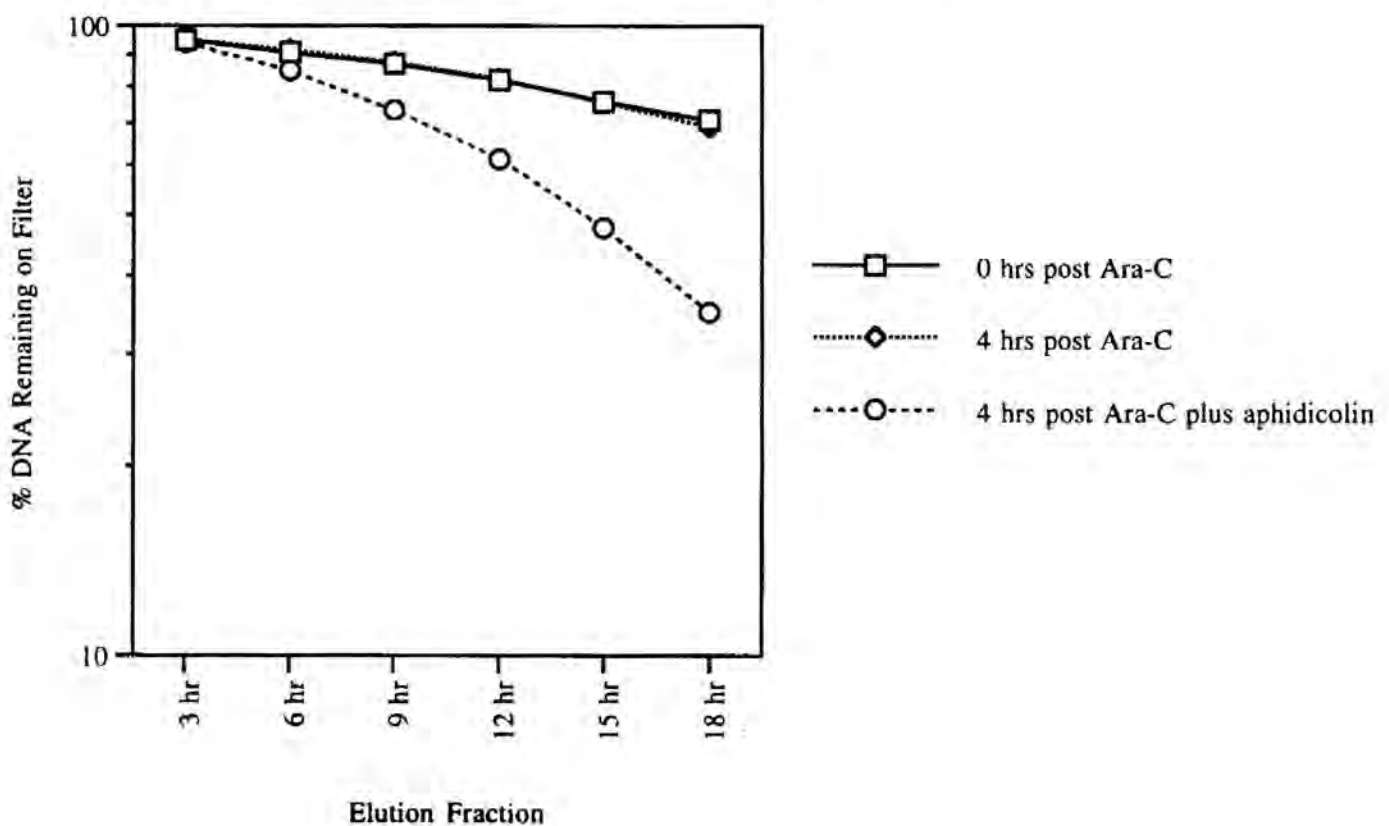


TABLE XVIII.**ALKALINE ELUTION IN HL-60/neo VERSUS HL-60/Bcl-2 CELLS:***

<u>Condition:</u>	<u>% DNA Remaining on Filter:</u>	
	<u>HL-60/neo:</u>	<u>HL-60/Bcl-2:</u>
<u>0 hrs post Ara-C:</u>		
3 hr fraction	92.11 ± 1.49	94.68 ± 0.38
6 hr fraction	86.28 ± 1.71	89.89 ± 0.61
9 hr fraction	81.57 ± 1.96	85.54 ± 1.13
12 hr fraction	76.20 ± 1.34	81.42 ± 0.80
15 hr fraction	69.58 ± 0.83	75.59 ± 0.66
18 hr fraction	60.98 ± 3.85	69.64 ± 0.26
<u>4 hrs post Ara-C:</u>		
3 hr fraction	89.46 ± 0.77	95.16 ± 1.34
6 hr fraction	83.56 ± 2.32	91.55 ± 1.82
9 hr fraction	79.89 ± 2.64	87.51 ± 2.55
12 hr fraction	74.17 ± 2.93	82.47 ± 3.19
15 hr fraction	67.33 ± 2.65	75.42 ± 3.87
18 hr fraction	60.63 ± 2.70	69.03 ± 4.68
<u>4 hrs post Ara-C, plus 100 μM aphidicolin:</u>		
3 hr fraction	84.04 ± 0.66	93.98 ± 1.45
6 hr fraction	74.77 ± 0.80	84.84 ± 2.87
9 hr fraction	65.50 ± 0.61	73.33 ± 5.23
12 hr fraction	50.68 ± 3.44	61.32 ± 6.08
15 hr fraction	40.35 ± 2.42	47.68 ± 6.06
18 hr fraction	29.52 ± 2.18	35.02 ± 4.04

* Values represent mean ± S.E.M. for n = 4 experiments.

TABLE XIX.

ALKALINE ELUTION IN HL-60/neo VERSUS HL-60/Bcl-2 CELLS
AFTER ARA-C TREATMENT:**

<u>Condition:</u>	<u>HL-60/neo:</u>		<u>HL-60/Bcl-2:</u>	
	<u>Δ:*</u>	<u>Slope of Elution Curve:</u>	<u>Δ:*</u>	<u>Slope of Elution Curve:</u>
0 hrs post Ara-C	31.13 ± 5.34	-2.06 ± 0.13	31.41 ± 6.39	-1.98 ± 0.18
4 hrs post Ara-C	32.49 ± 1.84	-2.41 ± 0.87	29.06 ± 5.17	-2.09 ± 0.58
4 hrs post Ara-C, plus 100 μM aphidicolin	54.52 ± 2.68	-3.61 ± 0.12	58.96 ± 2.89	-3.93 ± 0.36

* Δ (delta) represents the total percentage of DNA eluted from the filter under alkaline conditions between the earliest time point (3-hr fraction) and the latest time point (18-hr fraction), and represents the total amount of DNA eluted.

** Values represent mean ± S.E.M. for n = 4 experiments. Values obtained in identically HL-60/neo and HL-60/Bcl-2 cells are not significantly different (p > 0.05) for the above listed conditions.

TABLE XX.

**ALKALINE ELUTION IN HL-60/neo VERSUS HL-60/Bcl-2 CELLS
AFTER ARA-C TREATMENT;***

<u>Condition:</u>	<u>I. MORPHOLOGIC EVIDENCE OF APOPTOSIS IN CELLS USED FOR ALKALINE ELUTION ASSAY: _____</u>		<u>II. % DNA LYSED FROM FILTERS PRIOR TO ALKALINE ELUTION;*</u>	
	<u>HL-60/neo:</u>	<u>HL-60/Bcl-2:</u>	<u>HL-60/neo:</u>	<u>HL-60/Bcl-2:</u>
Control	2.41% ± 1.21	0.74% ± 0.47	4.56 ± 1.40	2.65 ± 0.90
4 hrs post Ara-C	40.51% ± 5.37	3.60% ± 1.83	26.83 ± 3.27	4.43 ± 1.86
4 hrs post Ara-C, plus aphidicolin	43.04% ± 10.37	11.62% ± 3.07	18.56 ± 4.84	5.40 ± 2.53
24 hrs post Ara-C	46.56% ± 1.36	5.08% ± 1.03	24.18 ± 5.95	9.59 ± 3.89
24 hrs post Ara-C	82.93% ± 10.30	18.90% ± 2.22	59.21 ± 10.99	12.02 ± 2.16

* Values represent mean ± S.E.M. for n = 4 experiments, and demonstrate that apoptotic cells are lysed from filters and may not be included in DNA eluted from filters under alkaline conditions.

** % DNA lysed from filters =
$$\frac{\text{Raw lysis counts}}{\text{Total counts} = \text{lysis} + \text{fraction accumulation} + \text{NaOH wash} + \text{DNA counts on filter}}$$

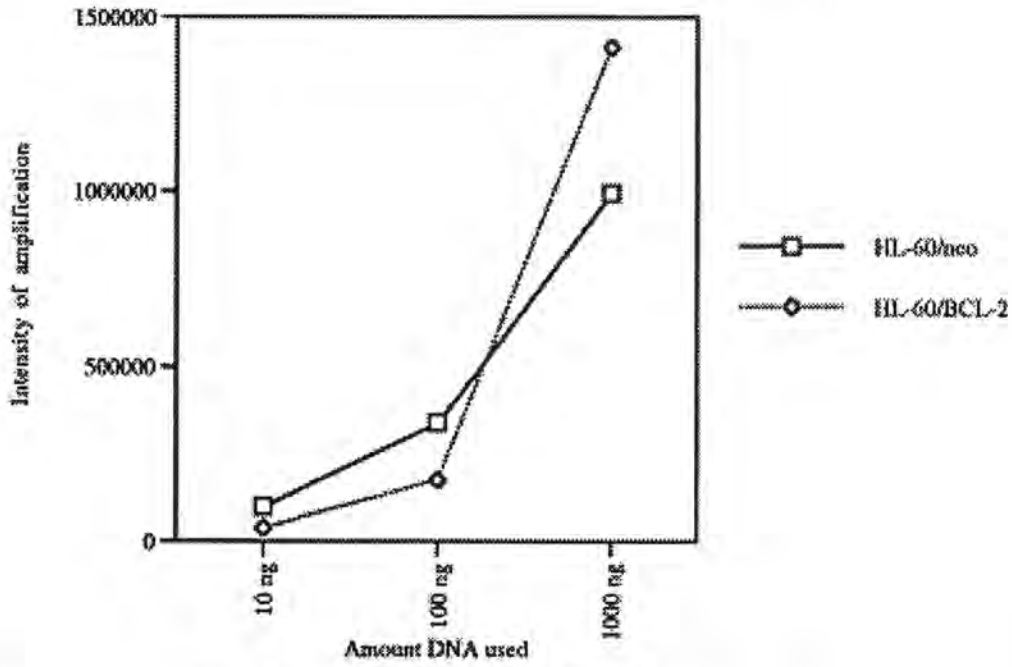
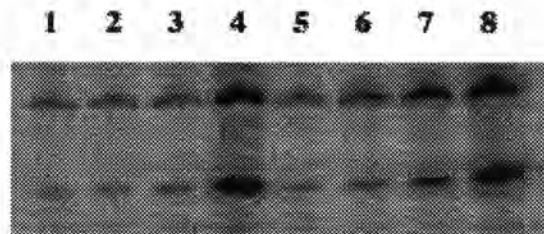
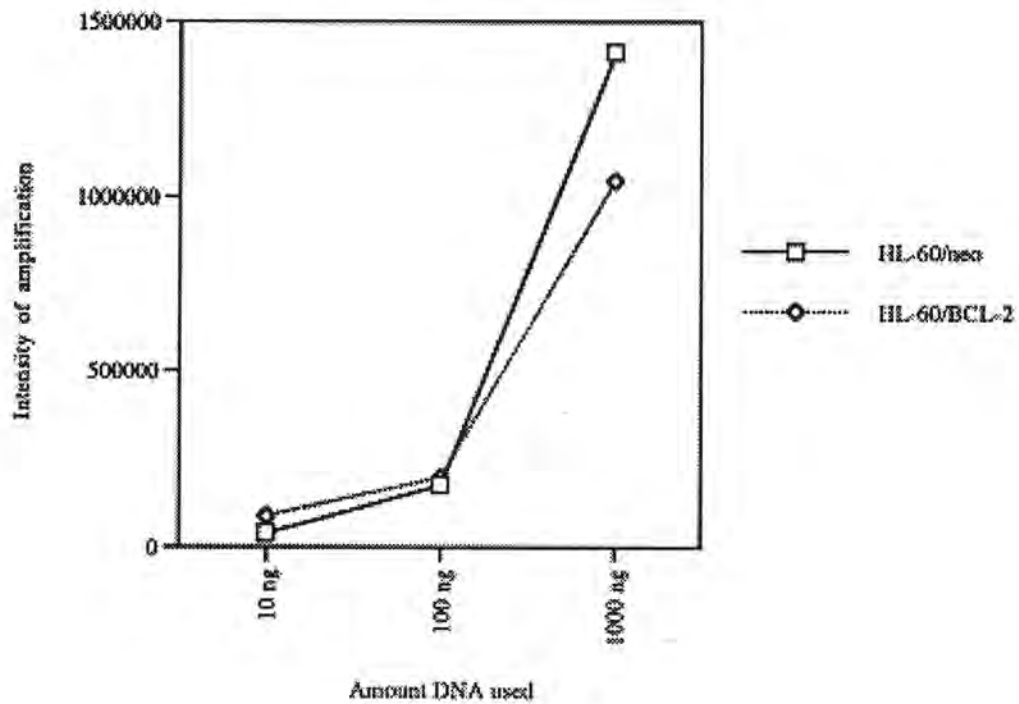
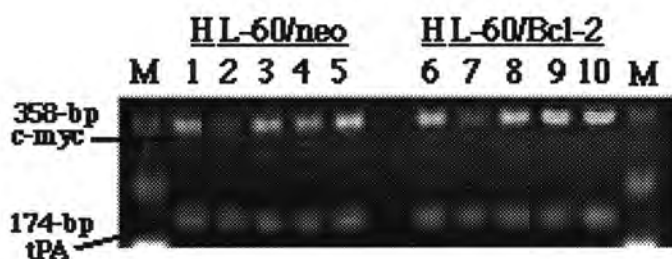
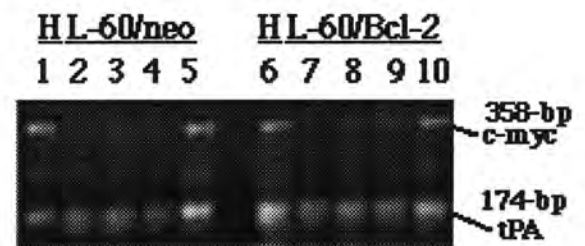
Figure 31.**A. e-myc PCR PRODUCT DOSE-RESPONSE CURVE****B.****C. IPA PCR PRODUCT DOSE RESPONSE CURVE**

Figure 32

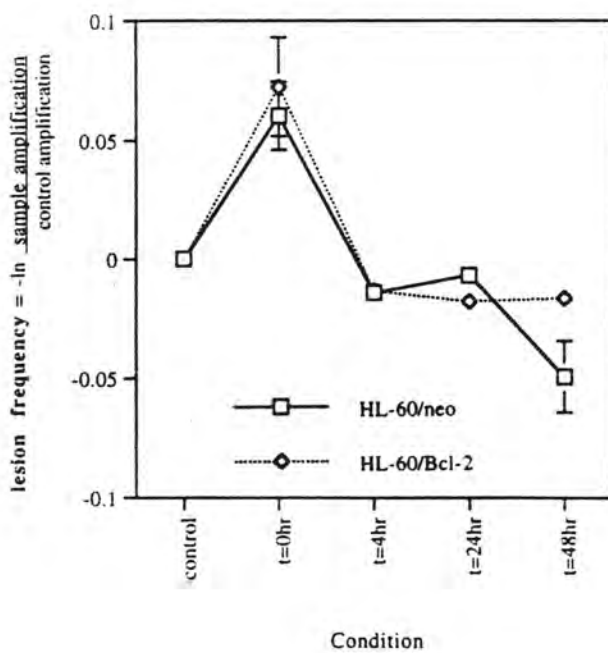
A. Ara-C



B. U.V.



c-myc LESION FREQUENCY
IN GENOMIC DNA TEMPLATES
AFTER ARA-C TREATMENT:



c-myc LESION FREQUENCY
IN GENOMIC DNA TEMPLATES
AFTER UV-IRRADIATION:

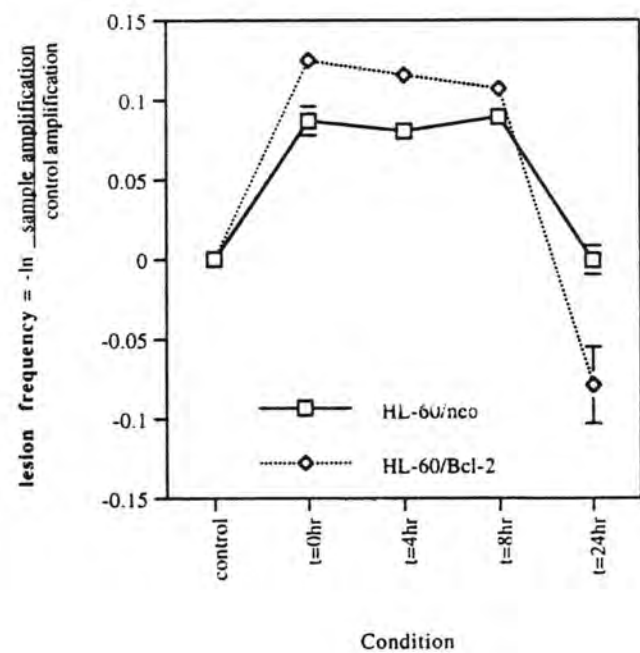


TABLE XXI.

**DETERMINATION OF *c-myc* LESION FREQUENCY BY PCR
IN HL-60/neo AND HL-60/Bcl-2 GENOMIC DNA TEMPLATES
AFTER ARA-C TREATMENT (OR UV-IRRADIATION)***

$$\text{lesion frequency} = -\ln \frac{\text{c-myc amplification for treated sample}}{\text{c-myc amplification for untreated sample}}$$

<u>Condition:</u>	<u>HL-60/neo:</u>	<u>HL-60/Bcl-2:</u>
<u>I. post Ara-C treatment:</u>		
0 hrs	0.0604 ± 0.0248	0.0724 ± 0.0206
4 hrs	-0.0141 ± 0.0104	-0.0134 ± 0.0087
24 hrs	-0.0068 ± 0.0036	-0.0178 ± 0.0101
48 hrs	-0.0494 ± 0.0259	-0.0165 ± 0.0091
<u>II. post UV-irradiation:</u>		
0 hrs	0.0871 ± 0.0288	0.0983 ± 0.0423
4 hrs	0.0804 ± 0.0267	0.0906 ± 0.0398
8 hrs	0.0895 ± 0.0295	0.0829 ± 0.0375
24 hrs	-0.0009 ± 0.0290	-0.0590 ± 0.0441

* Values represent mean ± S.E.M. for n = 4 experiments.

Values obtained for HL-60/Bcl-2 cells are not significantly different (p < 0.05) as compared with identically treated HL-60/neo cells (with exception of HL-60/Bcl-2 cells 24 hours post UV-irradiation).

Figure 33.

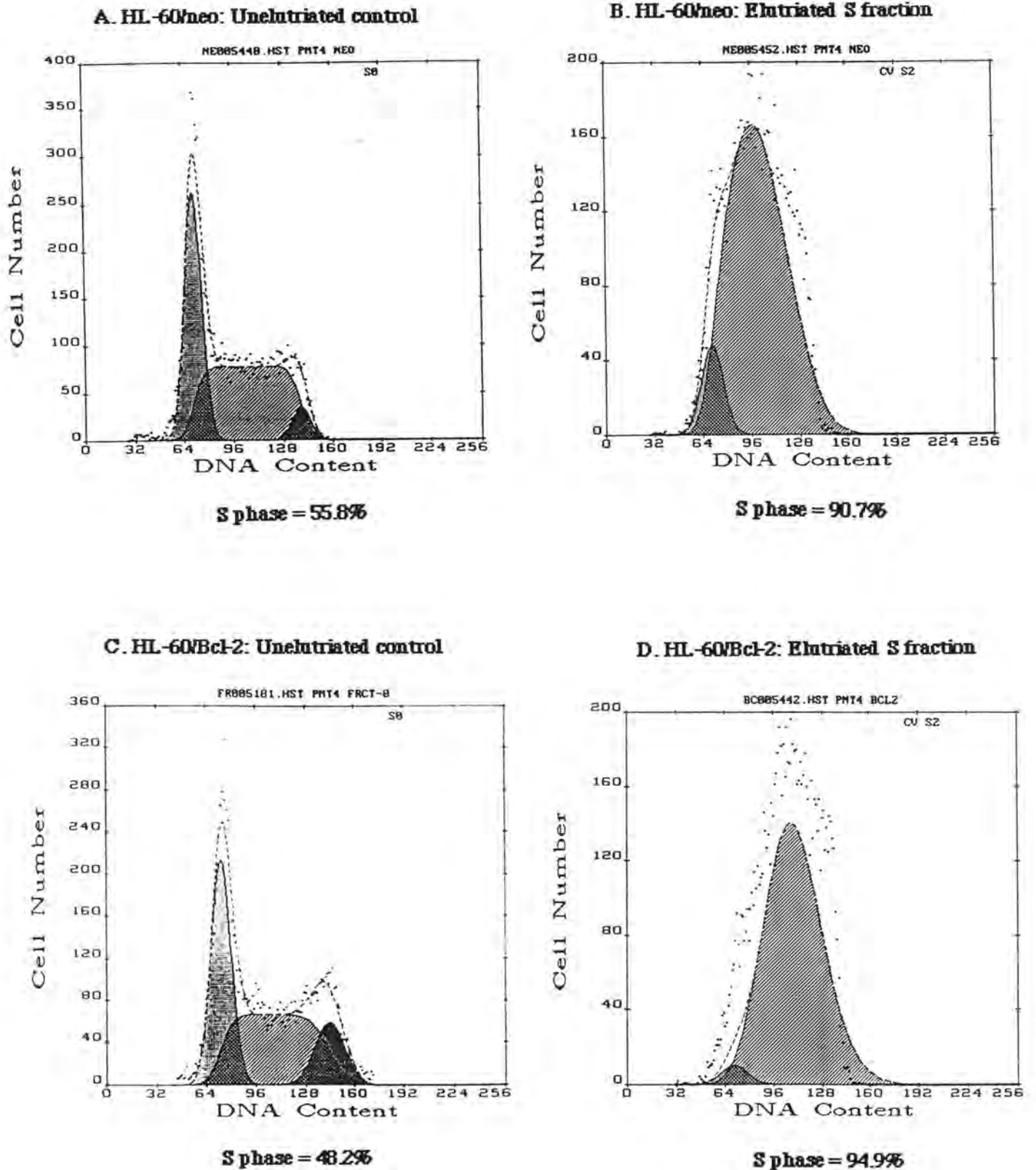
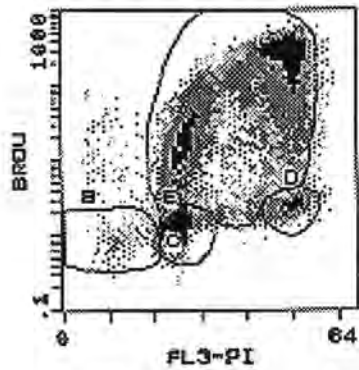
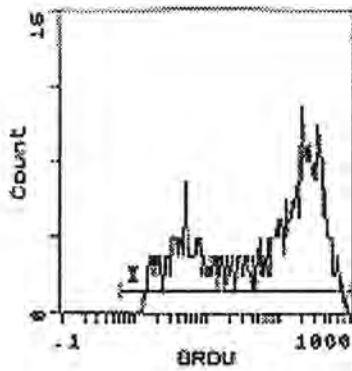


Figure 34.

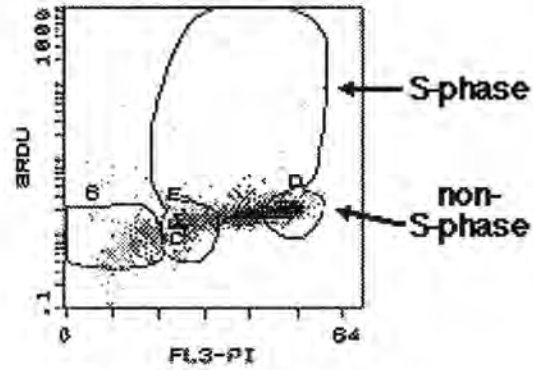
**A. HL-60/neo: Control
+ 10 μ M BrdU, 4 hrs**



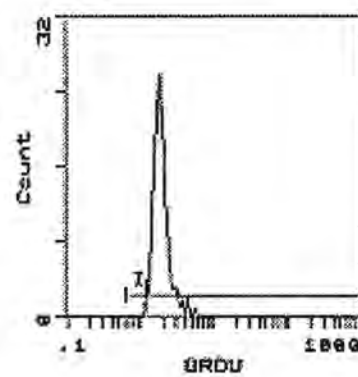
G: E



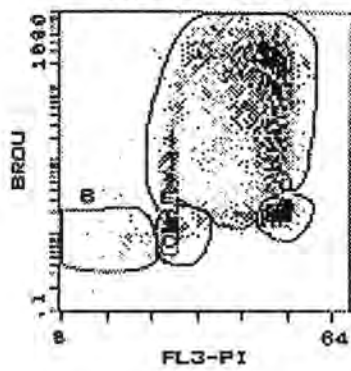
**B. HL-60/neo: 4 hrs post Ara-C
+ 10 μ M BrdU, 4 hrs**



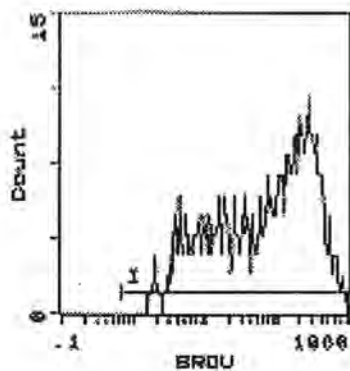
G: E



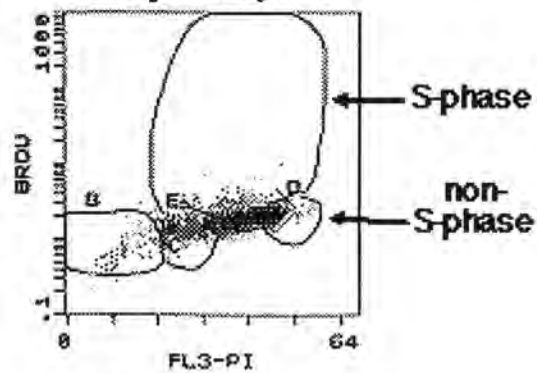
**C. HL-60/Bcl-2: Control
+ 10 μ M BrdU, 4 hrs**



G: E



**D. HL-60/Bcl-2: 4 hrs post Ara-C
+ 10 μ M BrdU, 4 hrs**



G: E

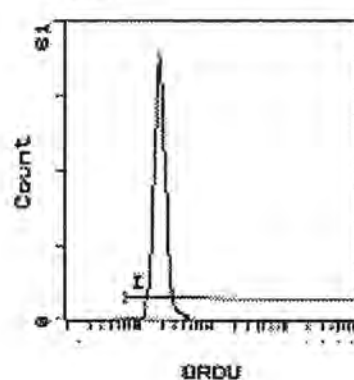


TABLE XXII.

**FLOW CYTOMETRIC ANALYSIS OF BROMODEOXYURIDINE INCORPORATION
IN ELUTRIATED HL-60/neo VERSUS HL-60/Bcl-2 CELLS
AFTER ARA-C TREATMENT:***

I. HL-60/neo CELLS:

<u>Condition:</u>	<u>S-phase cells:</u> <u>mean FITC-BrdU:</u>	<u>non-S-phase cells:</u> <u>(G1 + G2)</u> <u>mean FITC-BrdU:</u>	<u>RATIO:</u> <u>S-BrdU: non-S-BrdU:</u>
control 4 hrs	202.81 ± 24.14	16.50 ± 5.27	14.88 ± 1.23
4 hrs post Ara-C	5.38 ± 2.57	9.15 ± 4.51	0.60 ± 0.01
12 hrs post Ara-C	8.69 ± 2.41	12.37 ± 8.32	1.04 ± 0.51
24 hrs post Ara-C	33.75 ± 15.02	23.46 ± 6.58	1.73 ± 0.35

II. HL-60/Bcl-2 CELLS:

<u>Condition:</u>	<u>S-phase cells:</u> <u>mean FITC-BrdU:</u>	<u>non-S-phase cells:</u> <u>(G1 + G2)</u> <u>mean FITC-BrdU:</u>	<u>RATIO:</u> <u>S-BrdU: non-S-BrdU:</u>
control 4 hrs	213.57 ± 53.46	12.64 ± 1.62	14.72 ± 2.77
4 hrs post Ara-C	5.56 ± 2.86	9.69 ± 4.70	0.57 ± 0.02
12 hrs post Ara-C	6.22 ± 3.02	11.10 ± 7.36	0.68 ± 0.18
24 hrs post Ara-C	28.58 ± 23.96	21.22 ± 5.31	1.29 ± 0.68

* Values represent mean ± S.E.M. for n = 4 experiments.

Values obtained for identically treated HL-60/neo versus HL-60/Bcl-2 cells are not significantly different (p > 0.05).

CHAPTER VI.

Mechanism(s) of action of Bcl-2:

General Discussion and

Future Studies.

CHAPTER VI: MECHANISM(S) OF ACTION OF Bcl-2: GENERAL DISCUSSION AND FUTURE STUDIES

A. Introduction:

In **Chapter Three** of this dissertation, it was demonstrated that overexpression of Bcl-2 inhibited Ara-C-induced apoptosis and the concomitant loss of cell viability without affecting the early steps of Ara-C metabolism, Ara-C DNA incorporation, and Ara-C-induced DNA strand breaks. Studies in **Chapter Four** showed that the survival advantage and the degree of inhibition of apoptosis correlated with the degree of Bcl-2 overexpression. **Chapter Four** also demonstrated that cells which survived Ara-C treatment exhibited a transcriptional up-regulation of *bcl-2* mRNA, as well as increase in p26Bcl-2 levels, regardless of their original endogenous level of Bcl-2 expression. Furthermore, these increases in Bcl-2 levels were shown to be biologically relevant since surviving HL-60 cells were more resistant to a second exposure of Ara-C. In **Chapter Five**, it was investigated whether the overexpression of Bcl-2 conferred survival advantage following Ara-C treatment by virtue of improving the repair of Ara-C-induced early DNA damage. As noted previously, both the Ara-C-mediated DNA synthesis inhibition as well as Ara-C-induced early DNA damage was similar in HL-60/neo and HL-60/Bcl-2 cells. The repair of this DNA damage was compared by several assays, and was found to be similar in rate in HL-60/neo versus HL-60/Bcl-2 cells. These assays included analysis of DNA strand breaks by alkaline elution, assessment of lesion frequency in DNA by PCR-based DNA amplification, and flow cytometric determination of unscheduled DNA synthesis by virtue of incorporation of Bromodeoxyuridine (BrdU) into non-S-phase cells. The data presented in Chapters Three through Five define Ara-C-induced intracellular events into proximal, which lead to more distal and lethal events, those that are proximal involving the metabolism of Ara-C and its incorporation into and damage of DNA, from those that are distal and related to biochemical and morphologic features of apoptotic cell death. The anti-apoptotic effect of Bcl-2 overexpression results from inhibition of these distal events, and therefore inhibition of a critical “switchpoint” in intracellular signalling which converts DNA damage into a signal by which the progression to apoptosis commences (see **Figure 35** for illustration). Exactly what this signal includes remains to be elucidated. This chapter will explore several possibilities for Bcl-2

mechanism of action, and includes discussion of various gene expressions and potential molecular transducers affected by Ara-C or affected in apoptosis in general.

Figure 36 highlights several other intracellular effects of Ara-C. Some have been associated with apoptosis, while the role of other events mediating or regulating Ara-C-induced apoptosis have not been defined. These events have been categorized into two groups in this figure: in the first group are early response genes and signal transduction proteins which have been described to be induced by Ara-C exposure, and include transcription factor *NFκB*, *H1 histone*, *c-jun*, *c-abl*, SAP kinase, p34^{cdc2} kinase (254-259, 265, 268); the second listed group refers to alternate targets affected by Ara-CDP choline, and include DAG formation, PKC signalling, and ceramide formation, as previously described in Chapter One of this thesis. Whether Bcl-2-mediated inhibition of Ara-C-induced apoptosis involves interaction with or modification of these alternate targets has not been previously addressed. In addition, whether Bcl-2 overexpression affects the trafficking or activation of other proteins currently associated with the induction of apoptosis in other systems described in the literature, also represents a unique set of questions which have not been previously addressed.

B. Disparate levels of gene expressions induced in HIDAC-treated HL-60/Bcl-2 cells as compared with HIDAC-treated HL-60/neo cells.

In addition to the expressions of *bcl-2*-related genes and gene products presented here in this thesis, various other gene expressions have also been studied in HL-60/Bcl-2 cells as compared with HL-60/neo cells in the context of Ara-C-induced apoptosis. Analyses of these gene expressions were undertaken in order to address separate questions which might explain Bcl-2 function in Bcl-2-mediated blockade of Ara-C-induced apoptosis.

1. *c-jun* mRNA hyperinduction in HIDAC-treated HL-60/Bcl-2 cells as compared with HIDAC-treated HL-60/neo cells:

c-jun is a member of a family of early response genes which encode for sequence-specific bZIP DNA-binding proteins (423). *c-Jun* can either homodimerize, or heterodimerize with *c-Fos* protein to form the AP-1 (activator protein-1) transcription factor involved in the transcriptional regulation of genes responsive to phorbol esters or growth factors (424). Therefore, AP-1 can

modulate the transcription of a variety of genes which may affect cell proliferation and differentiation (425). Recent reports have implicated protein kinase C (PKC) activation as a step leading to the induction of *c-jun* in the molecular cascade leading to apoptosis by antileukemic drugs which include Ara-C (261, 426). However, it has been recently demonstrated that its role in apoptosis may probably be indirect (262). *c-jun* may play a more critical role in Ara-C-induced maturation than apoptosis, since U937 cells expressing a mutant c-Jun protein exhibit Ara-C-induced apoptosis to an equivalent extent as in parental U937 cells, but are more resistant to Ara-C-induced features of maturation (263).

Figure 35, Panel A, shows hyperinduction (approximately 5-fold) of *c-jun* mRNA in HIDAC-treated HL-60/Bcl-2 cells as compared to *c-jun* mRNA induction in identically treated HL-60/neo cells. This effect was also previously demonstrated by Bullock *et al.* in pre-B leukemia 697/Bcl-2 cells treated with HIDAC, as well as mitoxantrone, as compared to levels of *c-jun* mRNA induction in identically-treated 697-neo cells (262).

If Bcl-2 overexpression increases *c-jun* induction, it may be worthwhile to explore the mechanism by which this hyperinduction occurs, as well as what genes are responsive downstream of AP-1 as either direct or indirect targets of Bcl-2-mediated protection against Ara-C-induced apoptosis. c-Jun, as well as c-Fos, are reported to induce the expression of metallothionein genes involved in the detoxification of heavy metals, whose promoters contain AP-1 sites (427). In addition, c-jun/AP-1 activity may either reflect or play a role in the oxidative state of a cell. For example, the transcriptional activity of DNA binding of AP-1 has been reported to be affected by the regulation of reduction-oxidation status of a conserved cysteine residue in the DNA-binding domains of both Fos and Jun proteins (428, 429). Meyer *et al.* describe AP-1 itself as an antioxidant-responsive factor since DNA binding and transactivation by AP-1 were induced in HeLa cells following treatment with antioxidants such as *N*-acetyl-L-cysteine, and was suppressed by H₂O₂ treatment (430). Similarly, intracellular glutathione (GSH) levels are also known to regulate Fos/Jun induction (431). In addition, a downstream target for this AP-1-mediated activity is the glutathione-*S*-transferase gene (GST), which functions to detoxify mammalian cells and remove toxic compounds such as mutagens and carcinogens. Furthermore, as mentioned in the introduction to this thesis, computer analysis of the *bcl-2* cDNA sequence indicates that several AP-1 sites exist downstream of the *bcl-2* open reading frame, and may reflect sites for the potential posttranscriptional regulation of *bcl-2* itself if the AP-1 protein is also increased and is biologically significant in Bcl-2-overexpressing cells.

Because of the regulation of c-jun/AP-1 by redox and GSH levels, the antioxidant theory of Bcl-2 mechanism of action seemed an attractive hypothesis which might fit this situation presented in this chapter, since Bcl-2 was shown to suppress oxidant-induced apoptosis, scavenge free radicals (120), and increase GSH levels (121) in neural cells and in lymphoma cells (122). However, **Ara-C itself is not known to induce the generation of reactive oxygen species (ROS)** such as H₂O₂, superoxide (O₂⁻) or hydroxyl radicals (OH[•]), as does γ -irradiation, UV light, or low concentrations of H₂O₂ (432). It also remains unclear whether ROS play a universal role in the induction of apoptosis. In addition, Ara-C is not among the compounds known to be conjugated to thiols and subsequently removed from cells by GSTs (433). It remains yet to be confirmed whether Bcl-2 functions in an antioxidant role, either in the context of Ara-C-induced apoptosis or universally. As concluded in the Introduction to this dissertation, the increased antioxidant properties of cells which overexpress Bcl-2 may only be a secondary effect of Bcl-2-mediated inhibition of apoptosis and cytotoxicity.

2. Increased *c-myc* mRNA expression in HL-60/Bcl-2 cells:

As mentioned previously in the introduction of this thesis, *c-myc* and *bcl-2* oncogenes have been demonstrated to cooperate in the progression of tumorigenesis and the acquisition of drug resistance (89, 108). Bcl-2 overexpression has been demonstrated to block *c-myc* apoptotic function but not its proliferative function (107). **Figure 37, Panel B**, shows approximately 5-fold increase in the endogenous level of *c-myc* in untreated HL-60/Bcl-2 cells (lane 3) as compared to the endogenous level in untreated HL-60/neo cells (lane 1). In addition, *c-myc* expression decreases in HL-60/neo cells treated with HIDAC for 4 hours (lane 2), consistent with studies in the literature (262). This decrease in *c-myc* expression as a result of HIDAC treatment for 4 hours is not as pronounced in HL-60/Bcl-2 cells (lane 4), as a result of higher endogenous levels. These data represent a new scenario in which delivery of *bcl-2* cDNA to and overexpression of p26Bcl-2 in HL-60 cells by retroviral-mediated transfection increases, either directly or indirectly, *c-myc* levels, and may affect cell survival and proliferative capacity. Baer *et al.* have demonstrated dysregulation in *c-myc* mRNA in patient-derived AML cells, suggesting a possible contribution to the genesis of AML (352). However, whether increase in *c-myc* levels or in *c-jun* induction is due to Bcl-2 overexpression or due to retroviral-mediated transfection of these cells needs to be clarified, since the corroborating experiment recently reported by Bullock

et al. utilized 697/neo and 697/Bcl-2 cells also transfected with the same retroviral constructs (262).

High levels of *c-jun* mRNA have been shown to be expressed in proliferating cells, for example, and has also been associated with inhibition of differentiation (425, 434). *c-myc* mRNA levels are also high in proliferating cells (44, 45). These findings suggest that increased *c-jun* and *c-myc* levels in HIDAC-treated cells overexpressing Bcl-2 may indicate an increase in their proliferative ability as compared to that in HL-60/neo cells. However, this has not necessarily been observed in culture of the HL-60/Bcl-2 cells used in these studies presented in this thesis.

C. Proposal for Bcl-2-mediated blockade of p34^{cdc2} kinase nuclear trafficking or and/or premature activation; and review of other documented mechanisms:

Recently, Bcl-2 overexpression was demonstrated to block cytoplasmic to nuclear trafficking of p53 (144) as well as cell cycle-dependent kinases *cdc2* and *cdk2* (142). Cyclin-dependent p34^{cdc2} kinase is a highly regulated serine threonine kinase related to mitosis. It forms an active complex with regulatory subunit cyclin B, and its dephosphorylation controls entry of cells into mitosis (142, 435-437). The resultant breakdown of the cell membrane and chromatin condensation are features of mitosis which are also characteristic of apoptosis (438). As mentioned in the introduction of this thesis, recent studies have shown that premature activation of p34^{cdc2} kinase precedes the onset of granzyme B- or taxol-induced apoptosis (143, 269), as well as etoposide- or nitrogen mustard-induced apoptosis in HL-60 cells (439). The only study which links Ara-C to an effect on p34^{cdc2} kinase is the recent report that 15 minutes' exposure of HL-60 cells to HIDAC causes phosphorylation of p34^{cdc2} kinase, which reduces its activity (268). **Whether subsequent dephosphorylation and activation of p34^{cdc2} kinase occurs after a longer exposure to HIDAC, i.e., 4 hours' exposure, concomitant with the induction of apoptosis, has not been additionally examined.** A further important question to address would be whether Bcl-2 has the ability to block nuclear trafficking of p34^{cdc2} kinase or its premature activation in the context of Ara-C-induced apoptosis. In regards to p53 trafficking, however,

HL-60 cells do not possess p53 expression due to deletions in the *p53* gene (286), and therefore this examination would be in the context of **p53-independent** Ara-C-induced apoptosis.

For completeness, it is also essential to mention two other proposed mechanisms of action for Bcl-2 which appear in the literature. These include **association with R-ras and Raf-1 kinase signal transduction proteins** (134, 138), and the demonstrated **inhibition by Bcl-2 of Ca²⁺ repartitioning from the endoplasmic reticulum to the mitochondria associated with the onset of apoptosis** in growth factor-deprived cells (10) or in thapsigargin-treated cells (127). Whether these actions are among the mechanism for Bcl-2-mediated blockade of Ara-C-induced apoptosis remains to be addressed, given that **there is no documentation that Ara-C itself causes changes in intracellular calcium levels in mediating its cytotoxicity**. Ras is also not mentioned in the current literature as a specific target or effect of Ara-C treatment, as it is associated with taxol treatment, for example (139). While Ara-C can also stimulate MAP kinase, its connection to a Ras-related pathway in the context of apoptosis remains to be elucidated, especially since Ras may also be involved in similar PKC-dependent and PKC-independent pathways (88). Furthermore, it would also be of interest to study whether Bcl-2 interaction with mutated Ras is of functional significance for the signalling of apoptosis in HL-60 cells, for example, which harbor *N-ras* mutations, as described in **Chapter Two** of this dissertation. The interaction of Ras with Bcl-2 may also be dependent on the type of stimulus inducing the signal transduction leading to apoptosis. Because Bcl-2 inhibits a final common pathway of apoptosis (70, 89-111), its interaction with Ras (and vice versa) may not necessarily be a universal characteristic of Bcl-2-mediated inhibition of apoptosis.

D. Proposal for Bcl-2-mediated blockade of protease cascade(s) preceding the onset of apoptosis:

Historically, the biochemical hallmark and endpoint of most forms of apoptosis has been universally described in the literature as double-stranded DNA fragmentation. The events leading up to and specifically causing this DNA fragmentation remain to be clarified. This thesis illustrates that early DNA strand damage induced by Ara-C progresses to double-strand DNA fragmentation associated with apoptosis in HL-60/neo cells, but the pathway by which this early

(potentially reparable) damage is converted to irreversible lethal double-strand DNA damage is not known. New insights into the molecular events of apoptosis, however, have come from the identification of a new category of components associated with the onset of apoptosis. These are **cysteine protease cascades**, which include the interleukin-1 β (IL-1 β) converting enzyme (ICE) family previously mentioned in the introduction of this thesis, and now its related proteins most recently described (440).

Protease cascades and their inhibitors is a relatively new concept in the study of apoptosis but is not novel to human physiology. Coagulation is a complex and tightly regulated system in which the interaction of various proteolytic pathways culminate in a final common pathway resulting in the formation of a functional insoluble fibrin clot. Circulating plasma proteins first become activated upon contact with damaged vascular tissue, and their active forms in turn stimulate through **enzymatic cleavage**, the subsequent **activation** of several clotting factors from their inactive forms in an orderly manner (441). Antagonists of this dynamic system exist in order to maintain balance between blood flow and coagulation. Synthetic calcium chelators, which compete with the clotting factors which require Ca²⁺ for their activation, are used *ex vivo*. Protein C and Protein S are vitamin-K-dependent polypeptides which neutralize factors V and VIII in their activated states, and may also activate fibrinolysis in an interrelated pathway (441). The most important specific anticoagulant, however, is antithrombin III, a **serine protease inhibitor** which preferentially binds to and neutralizes thrombin and other serine proteases in the coagulation cascade (441).

Apoptosis is also described as being tightly regulated, and its orderly execution is now linked to protease cascade(s). As mentioned previously, cytotoxic T-lymphocytes and natural killer cells induce apoptosis in target cells by virtue of pore-forming proteins and serine proteases stored in their cytoplasmic granules. These proteases include granzyme B (or fragmentin-2), which can cleave proteins at aspartate (Asp) residues (34), and by itself, granzyme B is sufficient to induce apoptosis in target cells. The *C. elegans* cell death gene *ced-3* was recently found to have significant homology to the mammalian *Ice* gene (27), which converts its substrate, inactive pro-IL-1 β , to its active form by cleavage of pro-IL-1 β , also at Asp residues. Overexpression of *Ice* in Rat-1 fibroblasts was also demonstrated to cause apoptosis (30), further suggesting that proteolytic gene products can execute apoptosis. In addition,

cisplatin-induced apoptosis also induces expression of ICE in murine and human malignant glioma cells, and can be inhibited by the tetrapeptide ICE inhibitor Ac-YVAD-cmk (442). However, ICE itself may not be responsible for the universal mediation of apoptosis, as demonstrated by the study by Kuido *et al.*, in which lymphoid cells of ICE (-/-) deficient mice were still found to be sensitive to dexamethasone- or radiation-induced apoptosis (33). Other recently discovered proteases and ICE/ced-3 homologs, however, may be involved in other pathways which lead to a final common induction of apoptosis: these include Nedd-2/Ich-1, CPP32 β /Yama, Tx/Ich-2, and Mch-2, each of which, like ICE, contain a conserved pentameric peptide QACRG, which includes an active cysteine site for its own cleavage and activation (reviewed in 34, 342). Each of these ICE family members have been shown to induce apoptosis in various cell types when individually overexpressed (reviewed in 34, 342). In neutrophils, granzyme B can also directly activate the ICE-like cysteine protease and zymogen pro-CPP32 β /Yama (443). Even in *Drosophila*, an ICE-like protease may be involved in apoptosis induced by the death effector REAPER (RPR), since ICE-like protease inhibitor Z-VAD-fmk abrogates its death activity (444).

The ICE-like proteases, when activated, target specific downstream substrates, including poly(ADP-ribose) polymerase (PARP), U1 small nuclear ribonucleoprotein, Lamin B1, α -fodrin, topoisomerase I, lamins, and, most recently, β -actin and retinoblastoma protein (34, 445). Each of these have been demonstrated to undergo degradation due to activation of cysteine proteases when apoptosis is induced in various cells systems (reviewed in 26, 34, 446). For example, PARP is cleaved at DEVD 216 - G 217, and the site which surrounds this area is similar to that site cleaved in pro-IL-1 β by ICE (FEAD 27- G 28) (446, 447). This cleavage site may be similar in other substrates. Mashima *et al.* have subsequently demonstrated that the small peptide Z-Asp-CH2-DBB, a selective inhibitor of the activity of ICE-family proteases, prevents apoptosis in U937 cells induced by Ara-C, VP-16, camptothecin, and adriamycin, by competing with the cleavage site in proteolysable substrates (448). In addition, Emoto *et al.* have found that the ICE family inhibitor YVAD blocks proteolytic activation of another substrate, protein kinase C δ , as well as subsequent internucleosomal DNA fragmentation induced by ionizing radiation in U937 cells (449). Furthermore, **Bcl-2 overexpression in these cells also blocks these events** (449), consistent with studies by Kondo *et al* (442).

Cleavage of poly (ADP-ribose) polymerase (PARP) is an important specific event accomplished by an ICE-like protease at the onset of apoptosis (446). In HL-60 cells, Kaufmann *et al.* have demonstrated that incubation with a variety of chemotherapeutic agents including Ara-C, induces internucleosomal DNA fragmentation, and is consistently accompanied by cleavage of 116-kD native PARP polypeptide to a 85-kD fragment as seen by Western blot (384), as well as 25-29-kD fragment(s) also demonstrated by Soldatenkov *et al.* (450). Kaufmann *et al.* describe PARP as being involved in the repair of different types of DNA damage by virtue of its increased activity during the induction of single-strand and double-strand DNA breaks, as previously mentioned in **Chapter Five**. Its cleavage to an inactive form may contribute to the demise of HL-60 cells exposed to chemotherapeutic agents, γ -irradiation, and protein synthesis inhibitors (384). Interestingly, Kaufmann *et al.* also showed that while 116-kD PARP is cleaved to a smaller 85-kD fragment after exposure of HL-60 cells to Ara-C, PARP is maintained as a 116-kD polypeptide in identically treated K562 cells, which are resistant to apoptosis (385).

Recently, the ICE-like protease CPP32 β /Yama, also known as **apopain**, was specifically demonstrated to **catalyze the cleavage of PARP** (reviewed in 447, 451, 452), and represents a step proximal to this molecular event recently described as a marker for the onset of apoptosis (385, 450). ProCPP32 β /Yama is comprised of two subunits of mass 17 kD and 12 kD which are released when the proenzyme is activated by cleavage (447). CPP32 β /Yama-induced cleavage of PARP has been shown to be specifically prevented by CrmA, an inhibitor of ICE encoded by the cowpox virus, and a member of the serpin family of protease inhibitors (453), which on its own can protect serum-deprived Rat1 fibroblasts from apoptosis due to serum withdrawal when overexpressed (34). In addition, PARP can also be cleaved by a newly identified CPP32 homologs. CPP32/Mch2, or CMH1, is another cysteine protease whose overexpression in COS cells induces apoptosis but is not associated with cleavage of the interleukin-1 β precursor itself (454). Mch3 has also been recently isolated and has the highest homology to CPP32 β /Yama. It has been shown that upon cleavage, the 17 kDa subunit of CPP32 can form a heteromer with the 12 kDa subunit of proMch3 α , which, in turn, can also activate the degradation of PARP during apoptosis (455). The involvement of the CPP32 family of ICE-like proteases in drug-induced apoptosis is in to process of further clarification.

As an addendum to this dissertation, the question was asked, based on newly generated hypotheses, whether Bcl-2 has the ability to specifically block CPP32 β /Yama activation and PARP degradation associated with Ara-C-induced apoptosis in HL-60 cells. To this end, **Figure 38** illustrates preliminary evidence for Bcl-2-mediated interference in proteolytic cascade(s) possibly engaged during Ara-C-induced apoptosis. The top Western blot in **Panel A** shows that when HL-60/neo cells are exposed to HIDAC (lane 2), a 32-kD band corresponding to intact full-length pro-CPP32 β /Yama, decreases in intensity. Smaller species ranging from 20 to 11kD, as demonstrated by Tewari in BJAB cells undergoing anti-Fas-induced apoptosis (411), or detected by Nicholson *et al.* (456), were not detected in this instance using the extraction and centrifugation technique listed in the legend. As documented in the literature, this active form of CPP32 β /Yama most recently associated with the induction of apoptosis is now capable of degrading its downstream target PARP prior to the irreversible onset of DNA fragmentation and apoptosis. The Western blot presented in **Figure 38, Panel B**, demonstrates that HL-60/neo cells, which into subsequently undergo Ara-C-induced apoptosis, also show evidence for disappearance or degradation of 116-kD intact PARP into 85-kD smaller fragments in lane 2 as compared to control HL-60/neo (lane 1), similar to Kaufmann's findings (385). Identically treated HL-60/Bcl-2 cells, however, do not show decrease of pro-Yama levels (**Panel A**, lane 4) or degradation of PARP into smaller fragments (**Panel B**, lane 4), as compared to that seen in HL-60/neo cells. Parenthetically, the effect of HIDAC-induced Yama activation and its blockade by Bcl-2 overexpression was also studied at the RNA level. This places, for the first time, **Bcl-2-mediated blockade of Ara-C-induced apoptosis** distal to Ara-C-induced DNA damage but proximal to Yama activation, protease cascade induction and subsequent PARP degradation just prior to endonucleolytic DNA fragmentation associated with apoptosis. This concept is confirmed in the March 1, 1996 publication by Chinnaiyan *et al.*, in which Jurkat cells overexpressing either Bcl-2 (or Bcl-x_L) inhibited staurosporine-induced Yama and ICE-like ICE-LAP3 activation and subsequent PARP degradation (457). Furthermore, Boulakia *et al.* have presently demonstrated that Bcl-2 mediated suppression of adenovirus E1A-induced apoptosis occurs in conjunction with prevention of E1A-induced processing of pro-CPP32/Yama and subsequent cleavage of PARP as well (458). Whether PARP degradation in the scenario presented in this thesis is also due to the activity of CPP32 homolog Mch3 or Mch3/Yama heterodimers (455) was not further addressed.

Given that CPP32 β /Yama is activated during chemotherapeutic drug-induced apoptosis, a further intriguing question still remains as to how nuclear DNA damage can trigger a cytoplasmic cascade of protease activation, whose amplification results in endonucleolytic DNA fragmentation. In the context of drug-induced apoptosis, the signal(s) which directly catalyze the induction of these protease cascades have yet to be identified. Conversely, an important question to address is how proteolytic cleavage of the components of these cytoplasmic cascades can ultimately result in the double-strand DNA fragmentation characteristic of apoptosis, consistent with inferences from the demonstration by Lazebnik *et al.* that cytoplasmic extracts of mitotically arrested cells can induce events of apoptosis in isolated nuclei (459). As described in the introduction to **Chapter Five**, PARP has been associated with DNA repair. Therefore its degradation by the cytoplasmic proteases may inhibit its repair activity. However, as is also mentioned in Chapter Five, PARP in its active form catalyzes the poly(ADP-ribosyl)ation of various nuclear polypeptides by conversion of NAD to nicotinamide and protein-linked ADP-ribose polymers (385). How these additional poly(ADP-ribosyl) groups affect the targeted nuclear proteins may be variable. However, one important target for poly(ADP-ribosyl)ation is a Ca²⁺/Mg²⁺-dependent endonuclease. As early as 1975, it was described that poly(ADP-ribosyl)ation of a purified Ca²⁺/Mg²⁺-dependent endonuclease occurs readily, and inhibits its activity (460, 461). In addition, Nelipovich *et al.* reported that preincubation of thymocyte nuclei with NAD (the substrate for PARP) prevented Ca²⁺/Mg²⁺-induced DNA degradation, and decreased endonuclease activity (462). Furthermore, this effect was reversed by increased concentrations of nicotinamide, which inhibits poly(ADP-ribose) polymerase (463). Schwartzman and Cidlowski suggest that the inhibition of PARP during the induction of apoptosis may be responsible for the activation of the Ca²⁺/Mg²⁺-dependent endonuclease described here, and that in the absence of an apoptotic signal the endonuclease is kept in a repressed state due to the addition of poly (ADP-ribose) polymers to the enzyme by PARP (2). In addition, PARP has also been found to poly(ADP-ribosyl)ate histone H1 in the early induction of apoptosis in UV-irradiated HL-60 cells (464), and may facilitate internucleosomal DNA fragmentation by making nuclear chromatin more susceptible to cleavage by the putative endonuclease at its targets between the histone octamers. While the Ca²⁺/Mg²⁺-dependent endonuclease or other endonuclease(s) responsible for the fragmentation of DNA associated with apoptosis have not yet been unequivocally identified, this proposal still remains a valid possibility to explain the onset of the final events of apoptosis.

Figure 39, therefore, illustrates a model for the proposed role of Bcl-2 in a protease cascade associated with apoptosis. **Because Bcl-2 inhibits the progression of early DNA damage**, in the case of Ara-C-induced apoptosis, for example, **to double-strand DNA fragmentation**, it is possible that it may function to keep the responsible endonuclease inactive by inhibiting the degradation of PARP. Inhibition of PARP degradation by Bcl-2 may be the result of Bcl-2-mediated inhibition of the conversion of a protease(s) such as CPP32 β /Yama to its active form, and thus may ultimately keep the putative endonuclease in a repressed state.

If PARP is not degraded in Bcl-2-overexpressing cells, it might be hypothesized that these cells have greater capacity for DNA repair. However, although intact PARP is suggested to allow DNA repair enzymes to access DNA breaks (385, 390), Bcl-2-overexpressing cells, which show blockade of PARP degradation, were shown in **Chapter Five** to have no absolute increased capacity for repair of Ara-C-induced DNA damage, even though PARP itself has not been specifically implicated in repair of Ara-C-induced DNA damage. This further indicates that regardless of a cell's capacity for DNA repair, a critical irreversible switchpoint for apoptosis may exist separate from repair events. This irreversible pathway may lie in the induction of the protease cascade described above. This cascade may ultimately channel the final events of apoptosis, dependent upon inhibition of PARP-associated endonuclease derepression, rather than on inhibition of PARP-associated DNA repair.

Because the exact signal(s) which catalyze(s) the initial induction of the protease cascade is not known. The induction of the protease cascade may also be the result of an alternate signal not directly related to Ara-C DNA damage. Therefore, it also remains a possibility, that the progression of Ara-C-induced DNA damage to the final induction of apoptosis is not as direct, as depicted in such models as **Figures 7, 36, and 39**. The signal(s) leading to protease activation could possibly be due to Ara-C effects on ceramide generation, transcription factor activation, and/or protein kinase activation, as mentioned in **Chapter One**. These events may be due to Ara-C interaction with these alternate targets or due to cellular response to Ara-C-induced DNA damage, and represent points for further study and clarification.

E. Further speculations.

The mechanism by which Bcl-2 mediates the inhibition of the protease cascade still needs to be addressed. Taking the above various proposed mechanisms into account, and given the subcellular residence of Bcl-2, which includes the nuclear membrane, the endoplasmic reticulum, and the outer mitochondrial membrane, a further model is given in **Figure 40** which attempts to illustrate possible Bcl-2 function in the inhibition of apoptosis. Since studies have not been done which examine the location of Bcl-2 during exposure of leukemia cells to apoptotic stimuli, it is assumed that Bcl-2 remains anchored in the described membranes of its residence. If Bcl-2 overexpression leads to an inhibition of the proteolytic cleavage of degradative CPP32 β /Yama in a cytoplasmic cascade, it is hypothesized that **Bcl-2 may function universally in blocking the trafficking of a signal from damaged DNA from the nucleus to the cytoplasm.** If so, this signal(s) which may be responsible for the induction of the protease cascade may not then be able to reach the zymogen pro-CPP32 β /Yama, and thus PARP will not be degraded. Ultimately, the Ca²⁺/Mg²⁺-dependent endonuclease will remain repressed. Bcl-2 may therefore exist in a conformational state which may physically inhibit trafficking of ultimate apoptotic signals toward death effectors. This is partially supported by studies showing that Bcl-2 overexpression prohibits translocation of cdk's (142) or p53 (144) to the nucleus, conversely, and thus can build up in the cytoplasm during inhibition of apoptosis by Bcl-2. Phosphorylation of Bcl-2 may change its conformation and not allow Bcl-2 to perform its protective function. However, phosphorylation of Bcl-2 may occur only in certain cases, and may not be a universal effect of drug treatment, since Ara-C treatment has not been shown in this thesis or other studies to cause phosphorylation of Bcl-2.

This model in **Figure 40** is specific in that it includes the aspects of Ara-C-induced apoptosis studied in HL-60 cells. This model may be relevant for other drugs as well, since Bcl-2 can block apoptosis induced by a wide variety of stimuli. The final death effectors involved in these processes may include different ICE family members in different cell lines, and different Bcl-2 family members may be utilized as well to block apoptosis in other systems, representing tissue-specific expressions of universal processes. If the apoptotic signal comes from alternate targets of Ara-C action, however, the protective role of Bcl-2, given its residence in the previously described membranes, is not as obvious, especially since these alternate targets in the context of apoptosis after several hours' exposure to Ara-C has not been proven. Whether

nuclear envelope or the nuclear lamina disassembly concomitant with the onset of apoptosis (465) interferes with Bcl-2 function is also a consideration for the universality of this model. However, Bcl-2 has been shown to possess at least partial anti-apoptotic activity even if not anchored to intracellular membranes (77, 164), and may still be functional in the cytoplasm to impede access of apoptotic signals to the protease cascade(s).

As stated previously, **the ultimate goal of studies such as these presented in this dissertation is to target specific sites or events in Bcl-2-mediated inhibition of Ara-C-induced apoptosis, in order to improve the antileukemic efficacy of Ara-C.** The data and speculations presented in this dissertation hopefully provide further directions toward the ultimate elucidation of the mechanism of action of Bcl-2 at a **distal** event in the induction of apoptosis. This achievement will then provide opportunities to target the action of Bcl-2, and thus improve present chemotherapy treatments in leukemias and other cancers, by decreasing drug resistance due to Bcl-2 and other members of this new class of oncogenes which inhibit apoptosis. While the mechanism of action of Bcl-2 is still unknown, it is speculated at present that perhaps gene therapy, targeted to the functional domains for heterodimerization and proper action of Bcl-2 or its homologs, may be beneficial, by disrupting the proper formation of those dimers which may inhibit the apoptotic process in leukemia cells whose eradication is desired. This may then be useful in regaining the maintenance of cell numbers in the bone marrow environment, which, as described by Reed, is normally regulated physiologically in achieving a balance between cell proliferation and cell death (70).

FIGURE LEGENDS:

Figure 35: Preliminary illustration of Bcl-2-mediated blockade of the progression of apoptosis induced by DNA damage.

Figure 36: Preliminary illustration of possibilities for Bcl-2-mediated interference with known signalling events induced by Ara-C.

Figure 37. Hyperinduction of for *c-jun* mRNA expressions by Northern blots in HIDAC-treated HL-60/Bcl-2 cells as compared with HIDAC-treated HL-60/neo cells; and increased *c-myc* mRNA expression in HL-60/Bcl-2 cells. Total RNA was extracted from HL-60/neo or HL-60/Bcl-2 clonal population B cells either untreated (lanes 1,3) or immediately following treatment with HIDAC for 4 hours (lanes 2,4) by the guanidinium thiocyanate-phenol-chloroform method by Chomczynski *et al.* (466, 467), and 10 µg per condition electrophoresed in 1.8% agarose/MOPS/formaldehyde gel as described in Chapter Three. Northern blots were hybridized with the following 32-P-labelled cDNA probes utilizing a previously described method (468):

For **Panel A**, human *c-jun* was a 1.8-kb *BamHI/EcoRV* fragment purified from pBluescript SK(+), and was the kind gift of Dr. Donald Kufe, Dana Farber Cancer Center, Boston, MA);.

For **Panel B**, human *c-myc* was a 1.3-kb *EcoRI/ClaI* fragment purifies from pMC445, and was the kind gift of Dr. R. Dalla Favera, Columbia University, NY;

For **Panel C**, human *b-actin* was a 600-bp *EcoRI/BamHI* fragment purifies from pBluescript KSII(+), and was the kind gift of Dr. James S. Norris, Medical University of South Carolina, Charleston, SC).

The blots are representative of experiments performed three times, each with similar results.

Figure 38: Western blot analysis for Bcl-2-mediated inhibition of cleavage of pro-CPP32β/Yama and degradation of its target PARP. Total protein was extracted from untreated (lanes 1,3) or HIDAC (lanes 2,4) treated HL-60/neo (lanes 1,2) and HL-60/Bcl-2 clonal population B cells (lanes 3,4) utilizing an extraction buffer enriched with protease inhibitors (142.5 mM KCl, 5 mM MgCl₂, 10 mM HEPES, pH 7.2, 1 mM EGTA, 0.02% NP-40, 0.2 mM PMSF [Sigma], 0.2 TIU/ml aprotinin, 0.7 mg/ml pepstatin, 1 mg/ml leupeptin [all from Sigma]). For **Panel A**, 20 µg total protein from each condition was electrophoresed in 12.5% SDS-polyacrylamide gel and hybridized as described in the Western blotting method in Chapter Two with a mouse monoclonal anti-CPP32β/pro-Yama antibody (#C31720, Transduction Laboratories, Lexington, Kentucky, 1:2000 dilution). For analysis of Ara-C-induced PARP degradation in **Panel B**, 50 µg total protein from each condition was electrophoresed in 7.5% SDS-polyacrylamide gel and hybridized with rabbit polyclonal antiserum to PARP (the kind gift of Dr. Ernest Kun, San Francisco State University, Tiburon, CA, Octamer, Inc., Mill Valley, CA; 1:2000 dilution). A resultant nonspecific 55 kD band after polyclonal anti-PARP antiserum is also displayed in Panel C to demonstrate equal loading of protein samples.

The results are representative of three experiments, each with similar results.

Figure 39: Proposed model for Bcl-2-mediated blockade of protease cascade(s) preceding the onset of apoptosis.

Figure 40: Proposed model for Bcl-2 function in blocking Ara-C-induced apoptosis in HL-60 cells. While Bcl-2 is known to reside in the nuclear envelope, the endoplasmic reticulum (ER), and the outer mitochondrial membrane, it is proposed that the more significant location for Bcl-2 in interfering with Ara-C-induced apoptosis is that of the nuclear envelope near nuclear pore complexes (NPC's), since Ca^{2+} fluxes observed at the ER and mitochondria are not known to be involved in Ara-C-induced apoptosis. Bcl-2 may function in impeding the trafficking of either: (a) an apoptotic signal resulting from nuclear DNA damage to its effectors in the cytoplasm which activate the protease cascade; or (b) activated Yama from the cytoplasm as it targets its nuclear substrate poly(ADP-ribose) polymerase (PARP). Hypothesis (a) may be more likely since the cleavage of Yama to its smaller active form is also blocked by Bcl-2, indicating the Bcl-2-mediated blockade occurs proximal to the activation of the protease cascade. Simultaneously, Bcl-2 may be promoting cell survival by sequestering Bax through heterodimerization.

Figure 35.

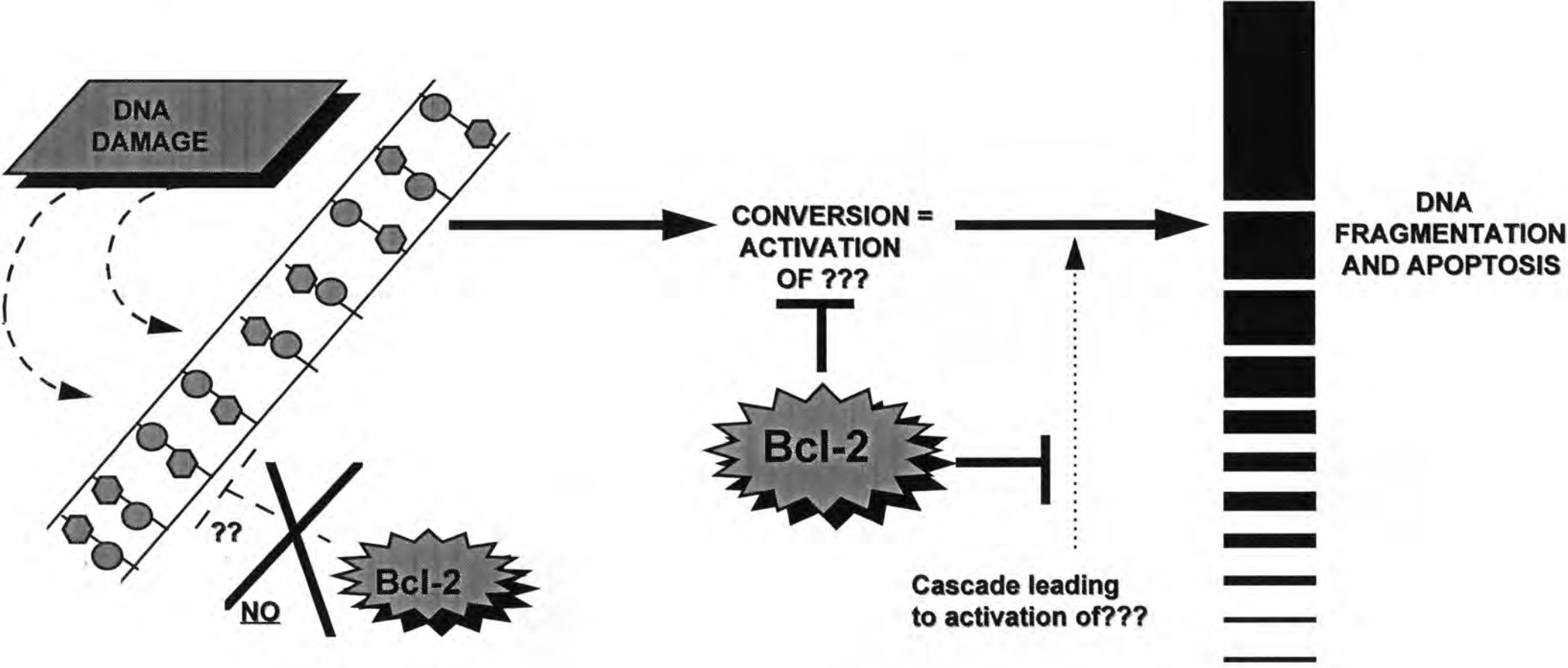


Figure 36.

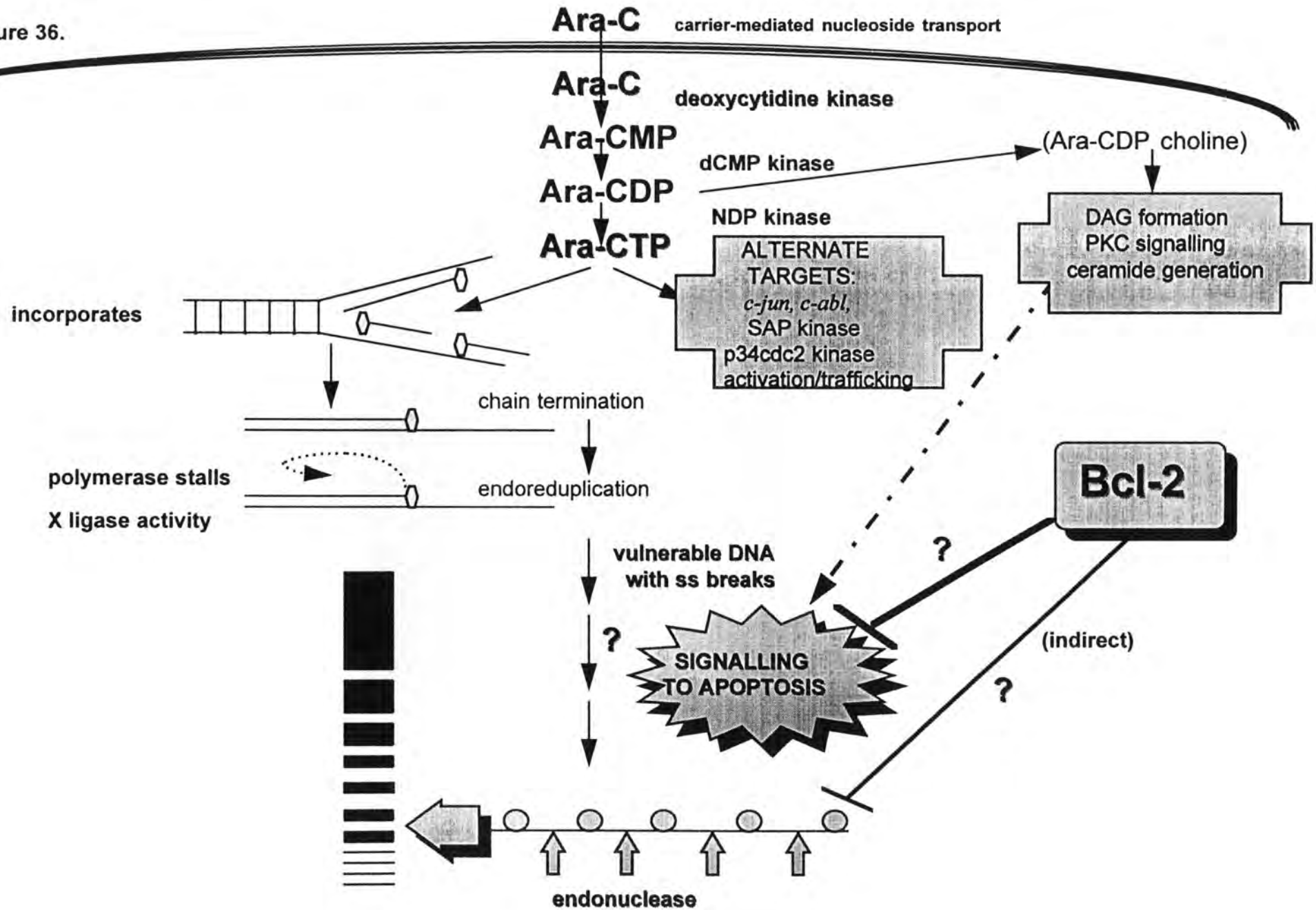


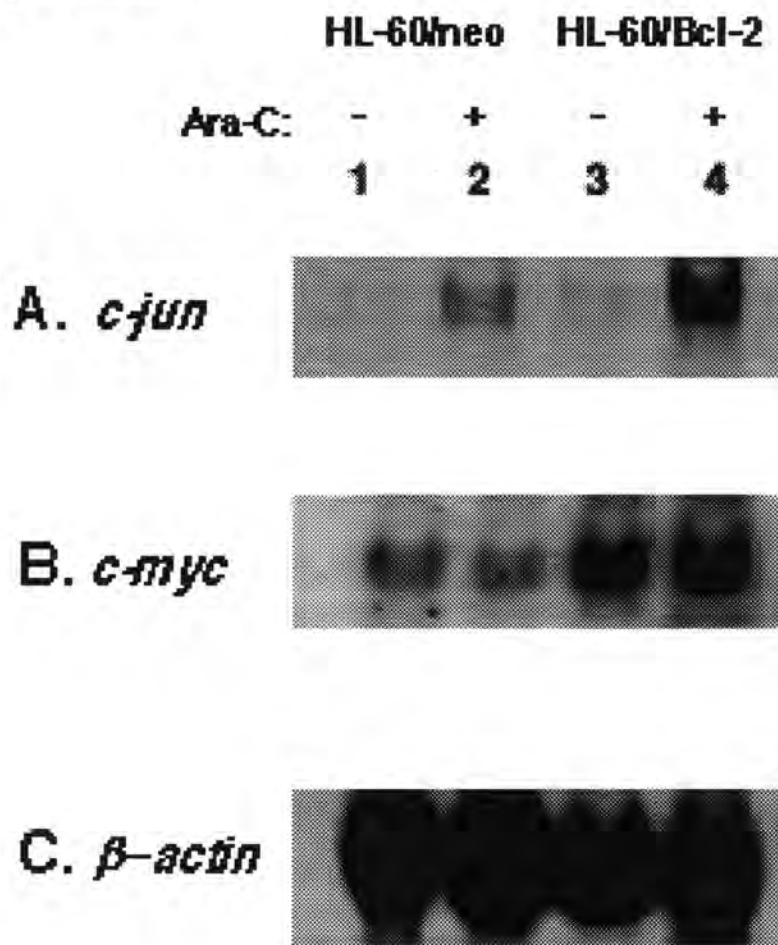
Figure 37.

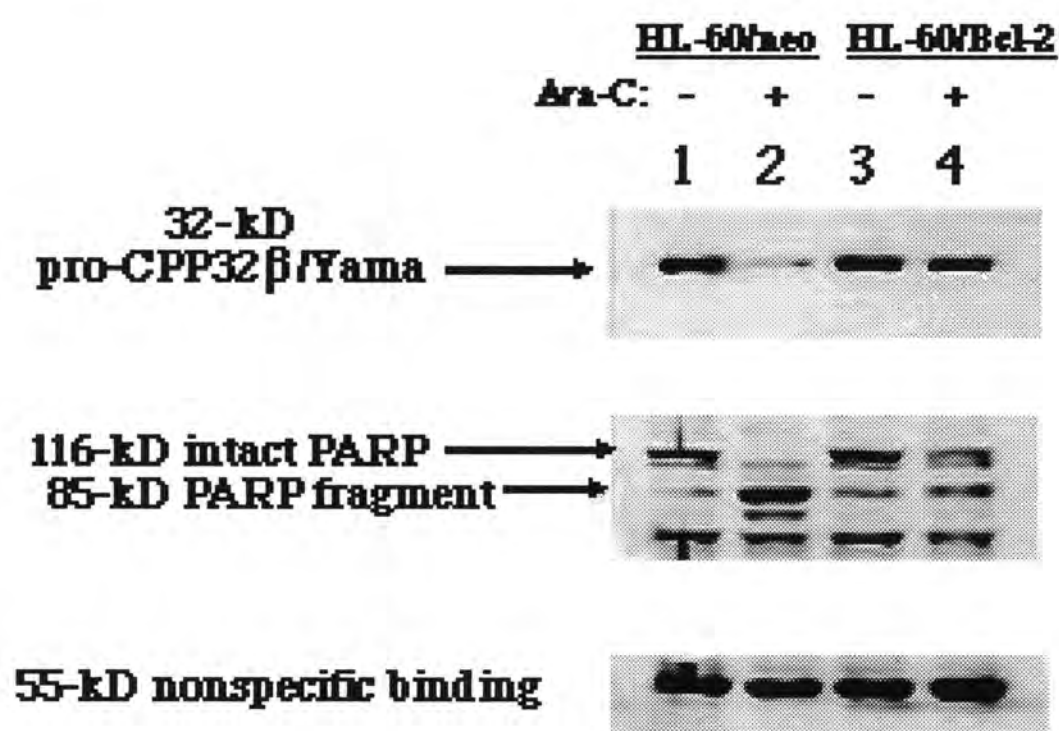
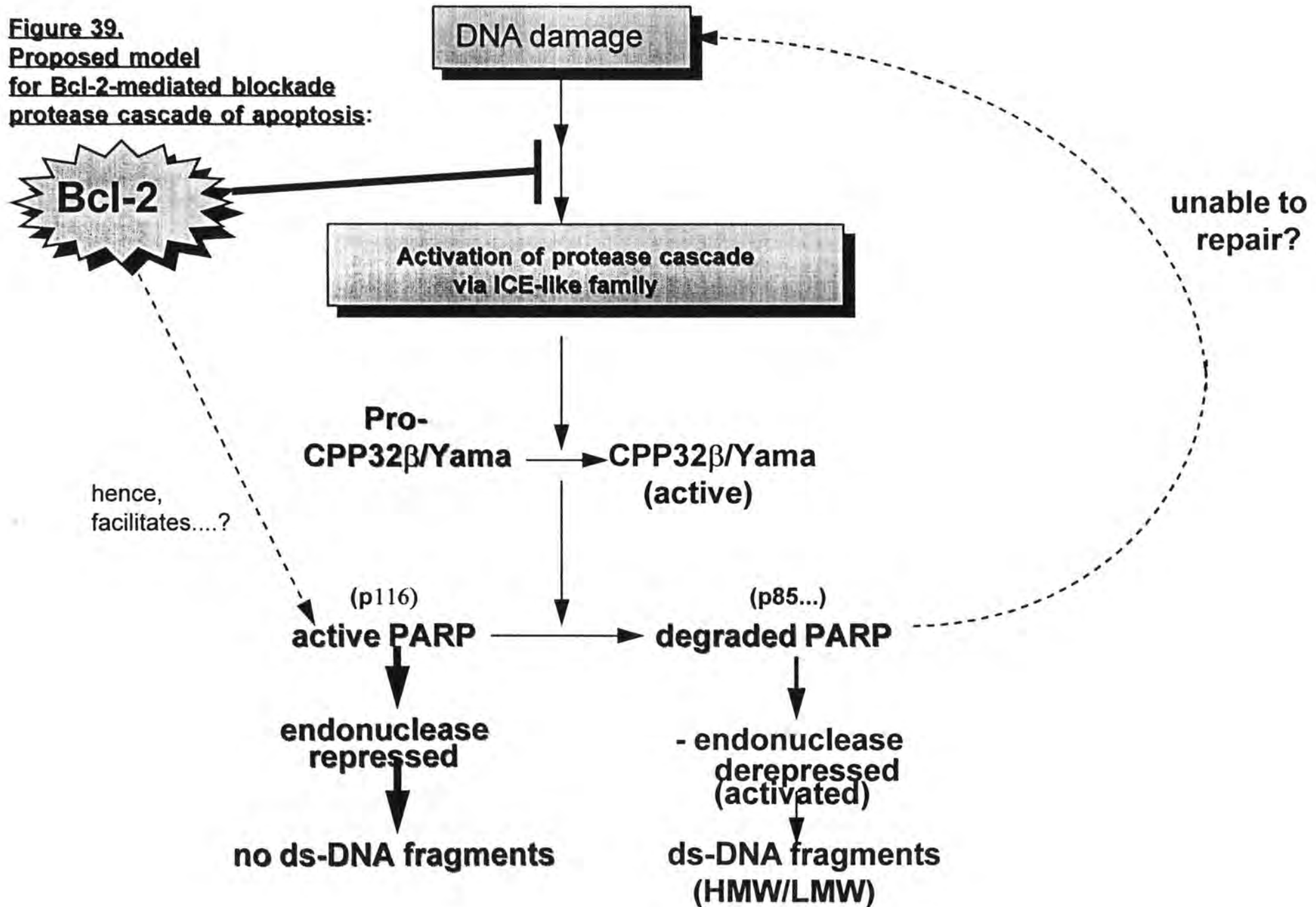
Figure 38.

Figure 39.
Proposed model
for Bcl-2-mediated blockade
protease cascade of apoptosis:



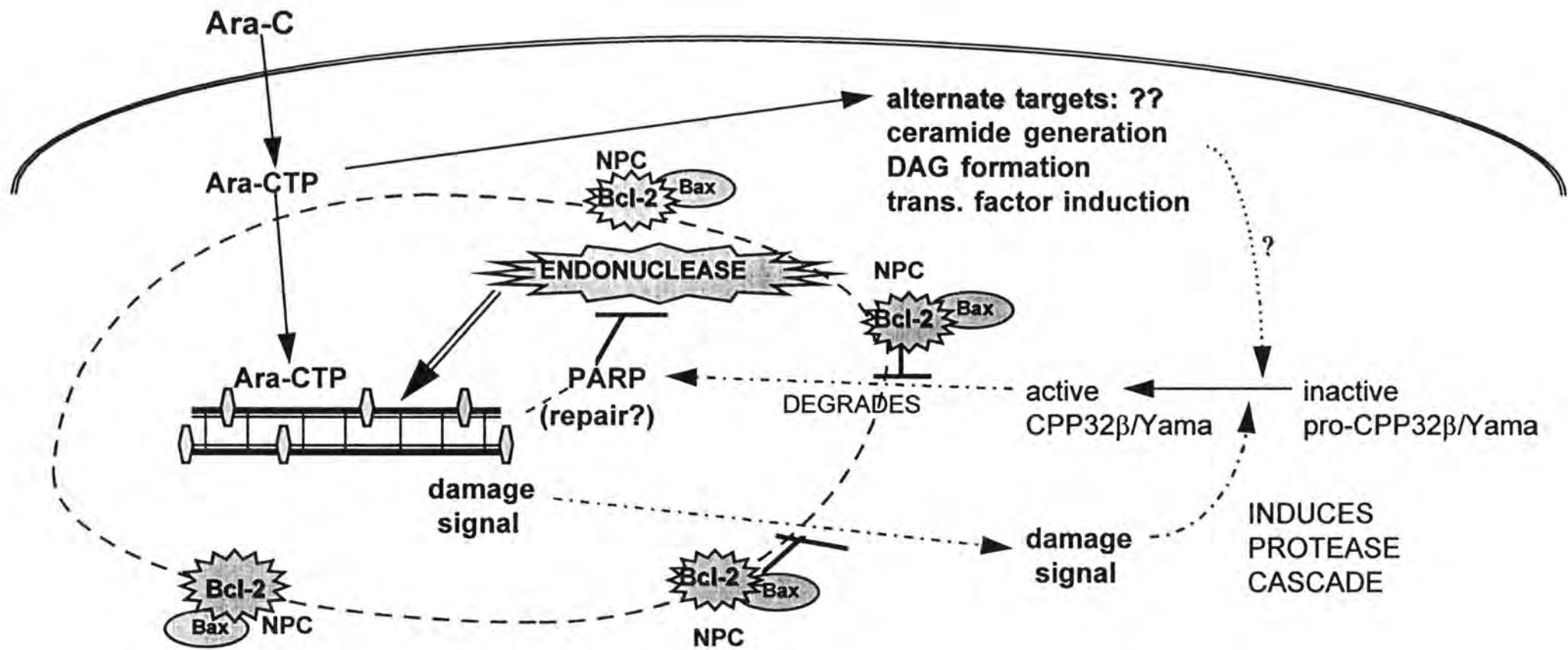


Figure 40.
Proposed model for Bcl-2 function:
Potential role as an inhibitor of the trafficking of apoptotic signals or effectors to their targets.

LIST OF REFERENCES:

1. Majno G, I Joris. Review: Apoptosis, oncosis, and necrosis: An overview of cell death. American Journal of Pathology 146 (1): 3-15, 1995.
2. Schwartzman RA, JA Cidlowski. Apoptosis: The biochemistry and molecular biology of programmed cell death. Endocrine Reviews 14 (2): 133-151, 1993.
3. Wyllie AH, JFR Kerr, AR Currie. Cell death: The significance of apoptosis. International Review of Cytology 68: 251-305, 1980.
4. Trump BF, JK Berezsky, RA Cowley. The cellular and subcellular characteristics of acute and chronic injury with emphasis on the role of calcium. In: Pathophysiology of shock, anoxia, and ischemia, RA Cowley, BF Trump, eds. Baltimore: Williams and Williams, 1982. pp. 6-46.
5. Chien KR, J Abrams, A , JT Martin, JL Farber. Accelerated phospholipid degradation and associated membrane dysfunction in irreversible, ischemic liver cell injury. The Journal of Biological Chemistry 253: 4809-4817, 1978.
6. Afanas'ev VN, BA Korol', YA Mantsygin, PA Nelipovich, VA Pechatnikov, SR Umansky. Flow cytometry and biochemical analysis of DNA degradation characteristic of two types of cell death. Federation of European Biochemical Societies Letters 194 (2): 347-350, 1986.
7. Lockshin RA, Z Zakeri. Programmed cell death and apoptosis. In: Apoptosis: The molecular basis of cell death, LD Tomei, FO Cope, eds. Current Communications in Cell and Molecular Biology, Volume 3. New York: Cold Spring Harbor Laboratory Press, 1991. pp. 47-60.
8. Gerchenson LE, RJ Rotello. Apoptosis: A different type of cell death. FASEB Journal 6: 2450-2455, 1992.
9. McConkey DJ, P Nicotera, P Hartzell, G Bellomo, AH Wyllie, S Orrenius. Glucocorticoids activate a suicide process in thymocytes through an elevation of cytosolic Ca²⁺ concentration. Archives of Biochemistry and Biophysics 269: 365-370, 1989.
10. Baffy G, T Miyashita, JR Williamson, JC Reed. Apoptosis induced by withdrawal of Interleukin-3 [IL-3] from an IL-3-dependent hematopoietic cell line is associated with repartitioning of intracellular calcium and is blocked by enforced Bcl-2 oncoprotein production. The Journal of Biological Chemistry 268: 6511-6519, 1993.
11. Li J, A Eastman. Apoptosis in an interleukin-2-dependent cytotoxic T-lymphocyte cell line is associated with intracellular acidification: Role of the Na⁺/H⁺ antiport. The Journal of Biological Chemistry 270 (7): 3203-3211, 1995.
12. Savill J, I Dransfield, N Hogg, C Haslett. Vitronectin receptor-mediated phagocytosis of cells undergoing apoptosis. Nature 343: 170-173, 1990.

13. Wyllie AH. Glucocorticoid-induced thymocyte apoptosis is associated with endogenous endonuclease activation. Nature 284: 555-556, 1980.
14. Peitsch MC, B Polzar, H Stephan, T Crompton, HR MacDonald, HG Mannherz, J Tschopp. Characterization of the endogenous deoxyribonuclease involved in nuclear DNA degradation during apoptosis (programmed cell death). The EMBO Journal 12 (1): 371-377, 1993.
15. Brown DG, X-M Sun, GM Cohen. Dexamethasone-induced apoptosis involves cleavage of DNA to large fragments prior to internucleosomal DNA fragmentation. The Journal of Biological Chemistry 268 (5): 3037-3039, 1993.
16. Cohn GM, X-M Xun, H Fearnhead, M MacFarlane, DG Brown, RT Snowden, D Dinsdale. Formation of large molecular weight fragments of DNA is a key committed step of apoptosis in thymocytes. Journal of Immunology 153: 507-516, 1994.
17. Hockenbery D. Review: Defining apoptosis. American Journal of Pathology 146 (1): 16-19, 1995.
18. Ellis RE, J Yuan, RH Horvitz. Annual Review of Cellular Biology 7: 663-698, 1991.
19. Bellamy COC, RDG Malcolmson, DJ Harrison, AH Wyllie. Cell death in health and disease: The biology and regulation of apoptosis. Seminars in Cancer Biology 6: 3-16, 1995.
20. Thompson CB. Apoptosis in the pathogenesis and treatment of disease. Science 267: 1456-1462, 1995.
21. Dive C, CA Evans, AD Whetton. Induction of apoptosis: New targets for cancer chemotherapy. Seminars in Cancer Biology 3: 417-427, 1992.
22. Gunji H, S Kharbanda, D Kufe. Induction of internucleosomal DNA fragmentation in human myeloid leukemia cells by 1- β -D-arabinofuranosylcytosine. Cancer Research 51: 741-743, 1991.
23. Ray S, V Ponnathpur, Y Huang, C Tang, ME Mahoney, AM Ibrado, G Bullock, K Bhalla. 1- β -D-arabinofuranosylcytosine-, mitoxantrone-, and paclitaxel-induced apoptosis in HL-60 cells: Improved method for detection of internucleosomal DNA fragmentation. Cancer Chemotherapy and Pharmacology 34: 365-371, 1994.
24. Bhalla K, AM Ibrado, E Tourkina, CQ Tang, ME Mahoney, Y Huang. Taxol induces internucleosomal DNA fragmentation associated with programmed cell death in human myeloid leukemia cells. Leukemia 7 (4): 563-568, 1993.
25. Bhalla K, AM Ibrado, E Tourkina, C Tang, S Grant, G Bullock, Y Huang, V Ponnathpur, ME Mahoney. High-dose mitoxantrone induced programmed cell death or apoptosis in human myeloid leukemia cells. Blood 82 (10): 3133-3140, 1993.
26. Hermann S. Apoptosis: Mechanisms and genes of cellular suicide. Science 267: 1445-1449, 1995.

27. Yuan J, S Shaham, S Ledoux, HM Ellis, HR Horvitz. The *C. elegans* cell death gene *ced-3* encodes a protein similar to mammalian Interleukin-1 β -converting enzyme. Cell 75: 641-652, 1993.
28. Derretti DP, CJ Kozolosky, B Mosley, N Nelson, K VanNess, TA Greenstreet, CJ March, SR Kronheim, T Druck, LA Cannizzaro, K Huebner, RA Black. Molecular cloning of the Interleukin-1 β -converting enzyme. Science 256: 97-100, 1992.
29. Kumar S, Y Tomoka, M Noda. Identification of a set of genes with developmentally down-regulated expression in the mouse brain. Biochemical and Biophysical Research Communications 185: 1155-1161, 1992.
30. Miura M, H Zhu, R Rotello, EA Hartweig, J Yuan. Induction of apoptosis in fibroblasts by IL-1 β converting enzyme, a mammalian homolog of the *C. elegans* cell death gene *ced-3*. Cell 75: 653-660, 1993.
31. Wang L, M Miura, L Bergeron, H Zhu, J Yuan. *Ich-1*, an *Ice/ced-3*-related gene encodes both positive and negative regulators of programmed cell death. Cell 78: 739-750, 1994.
32. Shi L, C-M Kam, JC Powers, R Aebersold, AH Greenberg. Purification of three cytotoxic lymphocyte granule serine proteases that induce apoptosis through distinct substrate and target cell interactions. Journal of Experimental Medicine 176: 152-1529, 1992.
33. Kuida K, JA Lippke, G Ku, MW Harding, DJ Livingston, MS-S Su, RA Flavell. Altered cytokine export and apoptosis in mice deficient in interleukin-1 β -converting enzyme. Science 267: 2000-2003, 1995.
34. Martin SJ, DR Green. Protease activation during apoptosis: Death by a thousand cuts? Cell 82: 349-352, 1995.
35. Nagata S, P Goldstein. The Fas death factor. Science 267: 1449-1456, 1995.
36. Itoh N, S Nagata. A novel protein domain required for apoptosis: Mutational analysis of Fas antigen. The Journal of Biological Chemistry 268 (15): 10932-10937, 1993.
37. Yonhara S, A Ishii, M Yonehara. A cell-killing monoclonal antibody (anti-Fas) to a cell surface antigen co-downregulated with the receptor of tumor necrosis factor. Journal of Experimental Medicine 169: 1747-1756, 1989.
38. Rouvier E, M-F Luciani, P Goldstein. Fas involvement in Ca²⁺-independent T-cell-mediated cytotoxicity. Journal of Experimental Medicine 177: 195-200, 1993.
39. Hsu H, J Xiong, DV Goeddel. The TNF Receptor-1-associated protein TRADD signals cell death and NF κ B activation. Cell 81: 495-504, 1995.
40. Chinnaiyan AM, K O'Rourke, M Tewari, VM Dixit. FADD, a novel death domain-containing protein, interacts with the death domain of Fas and initiates apoptosis. Cell 81: 505-512, 1995.

41. Stanger BZ, P Leder, T-H Lee, E Kim, B Seed. RIP: A novel protein containing a death domain that interacts with Fas/APO-1 (CD 95) in yeast and causes cell death. Cell 81: 513-524, 1995.
42. Cleveland JL, JN Ihle. Contenders in FasL/TNF death signalling. Cell 81: 479-482, 1995.
43. Evan GI, AH Wyllie, CS Gilbert, TD Littlewood, H Land, M Brooks, CM Waters, LZ Penn, DC Hancock. Induction of apoptosis in fibroblasts by c-myc protein. Cell 69: 119-128, 1992.
44. Westin E, F Wong-Staal, E Gelmann, R Dalla-Favera, T Papas, J Lautenberger, E Alessandra, E Reddy, S Tronick, S Aaronson, R Gallo. Expression of cellular homologues of retroviral oncogenes in human hematopoietic cells. Proceedings of the National Academy of Sciences, USA 79: 2490-2494, 1982.
45. Reitsma P, P Rothberg, S Astrin, J Trial, Z Bar-shavit, S Hall, S Teitelbaum, A Kahn. Regulation of *myc* gene expression in HL-60 leukemia cell by a vitamin D metabolite. Nature 306: 492-494, 1983.
46. Asken DS, RA Ashmun, BD Simmons, JL Cleveland. Constitutive *c-myc* expression in an Il-3-dependent myeloid cell line suppresses cell cycle arrest and accelerates apoptosis. Oncogene 6: 1915-1922, 1991.
47. Shi Y, JM Glynn, LJ Guilbert, TG Cotter, RP Bissonnette, DR Green. Role for *c-myc* in activation-induced apoptotic cell death in T cell hybridomas. Science 257: 212-214, 1993.
48. Canman CE, MB Kastan. Induction of apoptosis by tumor suppressor genes and oncogenes. Seminars in Cancer Biology 6: 17-25, 1995.
49. Baker SJ, S Markowitz, ER Fearon, JKV Wilson, B Vogelstein. Suppression of human colorectal carcinoma cell growth by wild-type p53. Science 249: 912-915, 1990.
50. Papathanasiou MA, NC Kerr, JH Robbins, OW McBride, I Alamo Jr, SF Barrett, ID Hickson, AJ Fornace Jr. Induction by ionizing radiation of the gadd 45 gene in cultured human cells: Lack of mediation by protein kinase C. Molecular and Cellular Biology 11: 1006-1016, 1991.
51. El-Deiry WS, JW Harper, PM O'Connor, VE Velculescu, CE Canman, J Jackman, JA Pietenpol, M Burrell, DE Hill, Y Wang, KG Wiman, WE Mercer, MB Kastan, KW Kohn, SJ Elledge, KW Kinzler, B Vogelstein. WAF1/CIP1 is induced in p53-mediated G₁ arrest and apoptosis. Cancer Research 54: 1169-1174, 1994.
52. Kastan MB, O Onyekwere, D Sidransky, B Vogelstein, RW Craig. Participation of p53 protein in the cellular response to DNA damage. Cancer Research 51: 6304-6311, 1991.
53. Chen C-Y, JD Oliner, Q Zahn, AJ Fornace Jr, B Vogelstein, MB Kastan. Interactions between p53 and MDM2 in a mammalian cell cycle checkpoint pathway. Proceedings of the National Academy of the Sciences, USA 91: 2684-2688, 1994.
54. Wyllie FS, MF Haughton, JA Bond, JM Rowson, CJ Jones, D Wynford-Thomas. S-phase cell-cycle arrest following DNA damage is independent of the p53/p21^{WAF1} signalling pathway. Oncogene 12: 1077-1082, 1996.

55. Kastan MB, O Onyekwere, D Sidransky, B Vogelstein, RW Craig. Participation of p53 protein in the cellular response to DNA damage. Cancer Research 51: 6304-6311, 1991.
56. Levine AJ, J Momand, CA Finlay. The p53 tumor suppressor gene. Nature 351: 453-455, 1991.
57. Lotem J, L Sachs. A mutant p53 antagonizes the deregulated c-myc-mediated enhancement of apoptosis and decreases in leukemogenicity. Proceedings of the National Academy of the Sciences, USA 92: 9672-9676, 1995.
58. Yonisch-Rouach E, D Resnitzky, J Lotem, L Sachs, A Kimchi, M Oren. Wild-type p53 induces apoptosis of myeloid leukemia cells that is inhibited by interleukin-6. Nature 352: 345-347, 1991.
59. Yonisch-Rouach E, D Grunwald, S Wilder, A Kimchi, E May, J Lawrence, P May, M Oren. p53-mediated cell death: Relationship to cell cycle control. Molecular and Cellular Biology 13: 1415-1523, 1993.
60. Lowe SW, HE Ruley, T Jacks, DE Housman. p53-dependent apoptosis modulates the cytotoxicity of anticancer agents. Cell 74: 957-967, 1993.
61. Fisher DE, S Bodis, S Lowe, C Takemoto, D Housman, T Jacks. Restoration of apoptosis in p53 deficient tumor cells [abstract]. Blood 84 (10): 430, 1994.
62. Miyashita T, S Krajewski, M Krajewska, H-G Wang, HK Lin, DA Liebermann, B Hoffman, JC Reed. Tumor suppressor p53 is a regulator of *bcl-2* and *bax* gene expression *in vitro* and *in vivo*. Oncogene 9: 1799-1805, 1994.
63. Selvkumaran M, H-K Lin, T Miyashita, H-G Wang, S Krajewski, JC Reed, B Hoffman, D Liebermann. Immediate early up-regulation of *bax* expression by p53 but not TGF β 1: A paradigm for distinct apoptotic pathways. Oncogene 9: 1791-1798, 1994.
64. Miyashita T, JC Reed. Tumor suppressor p53 is a direct transcriptional activator of the human *bax* gene. Cell 80: 293-299, 1995.
65. Ben-Neriah Y. GQ Daley, A-M Mes-Masson, ON Witte, D Baltimore. The chronic myelogenous leukemia-specific p210 product is the product of the *bcr/abl* hybrid gene. Science 233: 212-214, 1986.
66. GQ Daley, RA Van Etten, D Baltimore. Induction of chronic myelogenous leukemia in mice by the p210 *bcr/abl* gene of the Philadelphia chromosome. Science 247: 824-830, 1990.
67. Evans CA, PJ Owen-Lynch, AD Whetton, C Dive. Activation of the Abelson tyrosine kinase activity is associated with suppression of apoptosis in hemopoietic cells. Cancer Research 53: 1735-1738, 1993.
68. Bedi A, BA Zehnbaauer, JP Barber, SJ Sharkis, RJ Jones. Inhibition of apoptosis by bcr-abl in chronic myelogenous leukemia. Blood 83: 2038-2044, 1994.

69. McGahon A, R Bissonnette, M Schmitt, KM Cotter, DR Green, TG Cotter. *bcr-abl* maintains resistance of chronic myelogenous leukemia cells to apoptotic cell death. Blood 83: 1179-1187, 1994.
70. Reed JC. Bcl-2 and the regulation of programmed cell death. Mini-review: Cellular Mechanisms of disease series. The Journal of Cell Biology 124 (1-2): 1-6, 1994.
71. Tsujimoto Y, J Coosman, E Jaffe, C Croce. Involvement of the *bcl-2* gene in human follicular lymphoma. Science (Wash, D.C.) 228: 1440-1443, 1985.
72. Krajewski SS, S Tanaka, S Takayama, MJ Schibler, W Fenton, JC Reed. Investigations of the subcellular distribution of the Bcl-2 oncoprotein: Residence in the nuclear envelope, endoplasmic reticulum, and outer mitochondrial membranes. Cancer Research 53: 4701-4714, 1993.
73. Tsujimoto Y, CM Croce. Analysis of the structure, transcripts, and protein products of *bcl-2*, the gene involved in human follicular lymphoma. Proceedings of the National Academy of Sciences, USA 83: 5214-5218, 1986.
74. Seto M, U Jaeger, RD Hockett, W Graninger, S Bennett, P Goldman, SJ Korsmeyer. Alternative promoters and exons, somatic mutation and deregulation of the *Bcl-2-Ig* fusion gene in lymphoma. EMBO Journal 7 (1): 123-131, 1988.
75. Wilson BE, E Mochon, LM Boxer. Induction of *bcl-2* expression by phosphorylated CREB proteins during B-cell activation [abstract]. Blood 86 (10): 327a, 1995.
76. DiCroce PA, TG Krontiris. The *bcl-2* major breakpoint region is a sequence- and cell-cycle specific binding site of the Ku antigen. Proceedings of the National Academy of the Sciences, USA 92: 10137-10141, 1995.
77. Tanaka S, K Saito, JC Reed. Structure-function analysis of the Bcl-2 oncoprotein. Addition of a heterologous transmembrane domain to portions of the Bcl-2 β protein restores function as a regulator of cell survival. The Journal of Biological Chemistry 268 (15): 10920-10926, 1993.
78. Lewin B. Genes IV. Oxford: Oxford University Press, 1994.
79. Young RL, SJ Korsmeyer. A negative regulatory element in the *bcl-2* 5'-untranslated region inhibits expression from an upstream promoter. Molecular and Cellular Biology 13 (6): 3686-3697, 1993.
80. Miyashita T, M Harigai, M Hanada, JC Reed. Identification of a p53-dependent negative response element in the *bcl-2* gene. Cancer Research 54: 3131-3135, 1994.
81. Hewitt SM, S Hamada, TJ McDonnell, FJ Rauscher III, GF Saunders. Regulation of the proto-oncogenes *bcl-2* and *c-myc* by the Wilms' tumor suppressor gene *WT1*. Cancer Research 55: 5386-5389, 1995.
82. Harigai M, T Miyashita, M Hanada, JC Reed. A *cis*-acting element in the *bcl-2* gene controls expression through translational mechanisms. Oncogene 12: 1369-1374, 1996.

83. May WS, Tyler PG, DK Armstrong, NE Davidson. Role for serine phosphorylation of Bcl-2 in an antiapoptotic signalling pathway triggered by IL-3, EPO, and bryostatin [abstract]. Blood 82 (10): 1738, 1993.
84. May WS, PG Tyler, T Ito, DK Armstrong, KA Qatsha, NE Davidson. Interleukin-3 and bryostatin-1 mediated hyperphosphorylation of Bcl-2 α in association with suppression of apoptosis. The Journal of Biological Chemistry 269 (43): 26865-26870, 1994.
85. Haldar S, N Jena, CM Croce. Inactivation of Bcl-2 by phosphorylation. Proceedings of the National Academy of Sciences, USA 92: 4507-4511, 1995.
86. Haldar S, J Chintapalli, CM Croce. Taxol induces Bcl-2 phosphorylation and death of prostate cancer cells. Cancer Research 56: 1253-1255, 1996.
87. Chen CY, DV Faller. Direction of p21^{ras}-generated signal towards cell growth or apoptosis is determined by protein kinase C and Bcl-2. Oncogene 11: 1487-1498, 1995.
88. Chen CY, DV Faller. Phosphorylation of Bcl-2 protein and association with p21^{Ras} in Ras-induced apoptosis. The Journal of Biological Chemistry 271 (5): 2376-2379, 1996.
89. Vaux D, S Cory, J Adams. *Bcl-2* gene promotes hemopoietic cell survival and cooperates with *c-myc* to immortalize pre-B cells. Nature 335: 440-442, 1988.
90. Borzillo GV, K Endo, Y Tsujimoto. Bcl-2 confers growth and survival advantage to Interleukin-7-dependent early pre-B-cells which become factor independent by a multistep process in culture. Oncogene 7 (5): 869-876, 1992.
91. Nunez G, L London, D Hockenbery, M Alexander, JP McKearn, SJ Korsmeyer. Deregulated *Bcl-2* gene expression selectively prolongs survival of growth-factor-deprived hemopoietic cell lines. Journal of Immunology 144 (9): 3602-3610, 1990.
92. Allsopp TE, S Wyatt, HF Peterson, AM Davies. The proto-oncogene *bcl-2* can selectively rescue neurotrophic factor-dependent neurons from apoptosis. Cell 73: 295-307, 1993.
93. Fairbairn LJ, GJ Cowling, BM Reipert, TM Dexter. Suppression of apoptosis allow differentiation and development of a multipotent hemopoietic cell line in the absence of added growth factors. Cell 74: 823-832, 1993.
94. Naumovski L, ML Cleary. Bcl-2 inhibits apoptosis associated with terminal differentiation of HL-60 myeloid leukemia cells. Blood 83 (8): 2261-2267, 1994.
95. Hanada M, S Krajewski, S Tanaka, D Cazals-Hatem, BA Spengler, RA Ross, JL Biedler, JC Reed. Regulation of Bcl-2 oncoprotein levels with differentiation of human neuroblastoma cells. Cancer Research 53: 4978-4986, 1993.
96. Alnemri ES, TF Fernandes, S Haldar, CM Croce, G Litwack. Involvement of Bcl-2 in glucocorticoid-induced apoptosis of human pre-B leukemias. Cancer Research 52: 491-495, 1992.

97. Miyashita T, JC Reed. *bcl-2* gene transfer increases relative resistance of S49.1 and WEHI7.2 lymphoid cells to cell death and DNA fragmentation induced by glucocorticoids and multiple chemotherapeutic drugs. Cancer Research 52: 5407-5411, 1992.
98. Miyashita T, JC Reed. Bcl-2 oncoprotein blocks chemotherapy-induced apoptosis in a human leukemia cell line. Blood 81 (1): 151-157, 1992.
99. Kondo S, D Yin, T Morimura, Y Oda, H Kikuchi, J Taneuchi. Transfection with a *bcl-2* expression vector protects transplanted bone marrow from chemotherapy-induced myelosuppression. Cancer Research 54: 2928-2933, 1994.
100. Dole M, G Nunez, AK Merchant, J Maybaum, CK Rode, CA Bloch, VP Castle. Bcl-2 inhibits chemotherapy-induced apoptosis in neuroblastoma. Cancer Research 54: 3253-3259, 1994.
101. Walton MI, D Whyson, PM O'Connor, D Hockenbery, SJ Korsmeyer, KW Kohn. Constitutive expression of human *bcl-2* modulates nitrogen mustard and camptothecin-induced apoptosis. Cancer Research 53: 1853-1861, 1993.
102. Fisher TC, AE Milner, CD Gregory, AL Jackman, G Wynne Aherne, JA Hartley, C Dive, JA Hickman. Bcl-2 modulation of apoptosis induced by anti-cancer drugs: Resistance to thymidylate stress is independent of classical resistance pathways. Cancer Research 53: 3321-3326, 1993.
103. Kamesaki S, H Kamesaki, TJ Jorgensen, A Tanizawa, Y Pommier, J Cossman. Bcl-2 inhibits etoposide-induced apoptosis through its effect on events subsequent to topoisomerase II-induced DNA strand breaks and their repair. Cancer Research 53: 4251-4256, 1993.
104. Tang C, MC Willingham, JC Reed, T Miyashita, S Ray, V Ponnathpur, Y Huang, ME Mahoney, G Bullock, K Bhalla. High levels of p26Bcl-2 oncoprotein retard taxol-induced apoptosis in human pre-B leukemia cells. Leukemia 8 (11): 1960-1969, 1994.
105. Wang Y, L Szekely, I Okan, G Klein, Kg Wiman. Wild-type p53-triggered apoptosis is inhibited by *bcl-2* in a *v-myc*-induced T-cell lymphoma line. Oncogene 8: 3426-3431, 1993.
106. Chiou S-K, L Rao, E White. Bcl-2 blocks p53-dependent apoptosis. Molecular and Cellular Biology 14 (4): 2556-2563, 1994.
107. Bissonnette RP, F Echeverri, A Mahboubi, DR Green. Apoptotic cell death induced by *c-myc* is inhibited by *bcl-2*. Nature 359: 552-554, 1992.
108. Fanidi A, EA Harrington, GI Evan. Cooperative interaction between *c-myc* and *bcl-2* proto-oncogenes. Nature 359: 554-556, 1992.
109. Sanchez-Garcia I, G Grutz. Tumorigenic activity of the *bcr-abl* oncogenes is mediated by *bcl-2*. Proceedings of the National Academy of the Sciences, USA 92: 5287-5291, 1995.
110. Strasser A, RL Anderson. Bcl-2 and thermotolerance cooperate in cell survival. Cell Growth and Differentiation 6: 799-805, 1995.

111. Cleary ML, SD Smith, J Sklar. Cloning and structural analysis of cDNAs for *bcl-2* and a hybrid *bcl-2*/immunoglobulin transcript resulting from the t(14;18) translocation. Cell 47:19-28, 1986.
112. Henderson S, D Huen, M Rowe, C Dawson, G Johnson, A Rickinson. Epstein-Barr virus-coded BHRF1 protein, a viral homologue of Bcl-2, protects human B-cells from programmed cell death. Proceedings of the National Academy of the Sciences, USA 90: 8479-8483, 1993.
113. Takayama S, DL Cazals-Hatem, S Kitada, S Tanaka, T Miyashita, LR Hovey, D Huen, A Rickinson, P Veerapndian, S Krajewski, K Saito, JC Reed. Evolutionary conservation of function among mammalian, avian, and viral homologs of the Bcl-2 oncoprotein: structure-function implications. DNA and Cell Biology 12 (9) : 679-692, 1993.
114. Henderson S, M Rowe, C Gregory, D Croom-Carter, F Wang, R Longnecker, E Kieff, A Rickinson. Induction of *bcl-2* expression by Epstein-Barr virus latent membrane protein 1 protects infected B cells from programmed cell death. Cell 65: 1107-1116, 1991.
115. Finke J, R Fritzen, P Ternes, P Trivedi, KJ Bross, W Lange, R Mertelsmann, G Dolken. Expression of *bcl-2* in Burkitt's lymphoma cell lines: Induction by latent Epstein-Barr virus genes. Blood 80: 459-469, 1992.
116. Neilan J, Z Lu, C Afonso, G Kutish, M Sussman, DL Rock. An African Swine Fever virus gene with similarity to the *bcl-2* proto-oncogene and the Epstein-Barr virus gene BHRF-1. Journal of Virology 67: 4341-4394, 1993.
117. Hockenbery D, G Nunez, C Milliman, RD Schreiber, SJ Korsmeyer. Bcl-2 is an inner mitochondrial membrane protein that blocks programmed cell death. Nature 348: 334-336, 1990.
118. Mah SP, LT Zhong, Y Liu, A Roghani, RH Edwards, DE Bredesen. The proto-oncogene *bcl-2* inhibits apoptosis in PC12 cells. Journal of Neurochemistry 60: 1183-1186, 1993.
119. Zhong L-T, T Sarafian, DJ Kane, AC Charles, SP Mah, RH Edwards, DE Bredesen. *bcl-2* inhibits death of central neural cells induced by multiple agents. Proceedings of the National Academy of Sciences, USA 90: 4533-4537, 1993.
120. Hockenbery DM, ZN Oltvai, X-M Yin, CL Milliman, SJ Korsmeyer. Bcl-2 functions in an antioxidant pathway to prevent apoptosis. Cell 75: 241-251, 1993.
121. Kane DJ, TA Sarafian, R Anton, H Hahn, E Butler Gralla, J Selverstone Valentine, T Ord, DE Bredesen. Bcl-2 inhibition of neural death: Decreased generation of reactive oxygen species. Science 262: 1274-1277, 1993.
122. Meyn RE, N Mirkovic, DW Voehringer, MD Story. Bcl-2 inhibits radiation-induced apoptosis by upregulating the antioxidant properties of the cell [abstract]. Proceedings of the American Association for Cancer Research 37: 159, 1996.
123. Shimizu S, Y Eguchi, W Kamiike, Y Itoh, J Hasegawa, K Yamabe, Y Otsuki, H Matsuda, Y Tsujimoto. Induction of apoptosis as well as necrosis by hypoxia and predominant prevention of apoptosis by Bcl-2 and Bcl-x_L. Cancer Research 56: 2161-2166, 1996.

124. Shimizu S, Y Eguchi, H Kosaka, W Kamiike, H Matsuda, Y Tsujimoto. Prevention of hypoxia-induced cell death by Bcl-2 and Bcl-x_L. Nature 374: 811-813, 1995.
125. Jacobson MD, MC Raff. Programmed cell death and Bcl-2 protection in very low oxygen. Nature 374: 814-816, 1995.
126. Steinman HM. The Bcl-2 oncoprotein functions as a pro-oxidant. The Journal of Biological Chemistry 270 (8): 3487-3490, 1995.
127. Lam M, G Dubyak, L Chen, G Nunez, RL Miesfeld, CW Distelhorst. Evidence that Bcl-2 represses apoptosis by regulating endoplasmic reticulum-associated Ca²⁺ fluxes. Proceedings of the National Academy of the Sciences, USA 91: 6569-6573, 1994.
128. Distelhorst C, T McCormick. Bcl-2 acts downstream from Ca²⁺ fluxes to inhibit apoptosis in thapsigargin- and glucocorticoid-treated mouse lymphoma cells [abstract]. Proceedings of the American Association for Cancer Research 37: 163, 1996.
129. Distelhorst C, M Lam, T McCormick. Bcl-2 inhibits oxygen radical mediated depletion of the endoplasmic reticulum calcium pool [abstract]. Proceedings of the American Association for Cancer Research 37: 164, 1996.
130. McCormick T, K McColl, C Distelhorst. Bcl-2 overexpression enables WEHI7.2 cells to upregulate GRP78 in response to thapsigargin [abstract]. Proceedings of the American Association for Cancer Research 37: 165, 1996.
131. Jacobson MD, JF Burne, MP King, T Miyashita, JC Reed, MC Raff. Bcl-2 blocks apoptosis in cell lacking mitochondrial DNA. Nature 361:365-369, 1993.
132. Marchetti P, SA Susin, D Decaudin, S Gamen, M Castedo, T Hirsch, N Zamzami, J Naval, A Senik, G Kroemer. Apoptosis-associated derangement of mitochondrial function in cells lacking mitochondrial DNA. Cancer Research 56: 2033-2038, 1996.
133. Smets LA, J Van den Berg, D Acton, B Top, H Van Rooij, M Verwijs-Janssen. *Bcl-2* expression and mitochondrial activity in leukemia cells with different sensitivity to glucocorticoid-induced apoptosis. Blood 84 (5): 1613-1619, 1994.
134. Fernandez-Sarabia MJ, JR Bischoff. Bcl-2 associates with the *ras*-related protein R-*ras* p23. Nature 366: 274-275, 1993.
135. Haldar S, C Beatty, Y Tsujimoto, CM Croce. *Bcl-2a* encodes a novel small molecular weight GTP binding protein. Nature : 195-198, 1989.
136. Monica K, Z Chen-Levy, ML Cleary. Small G proteins are expressed ubiquitously in lymphoid cells and do not correspond to Bcl-2. Nature 346: 189-191, 1990.
137. Kinoshita T, T Yokota, K Arai, A Miyajima. Regulation of Bcl-2 expression by oncogenic Ras protein in hematopoietic cells. Oncogene 10: 2207-2212, 1995.

138. Wang H-G, T Miyashita, S Takayama, T Sato, T Torigoe, S Krajewski, S Tanaka, L Hovey III, J Troppmair, UR Rapp, JC Reed. Apoptosis regulation by interaction of Bcl-2 protein and raf-1-kinase. Oncogene 9:2751-2756, 1994.
139. H-G Wang, UR Rapp, JC Reed. Investigations of Raf-1 kinase interactions with Bcl-2 family proteins [abstract]. Blood 86 (1): 588a, 1995.
140. Blagoskonny M, T Schulte, P Nguyen, J Trepel, L Neckers. Raf-1-dependent Bcl-2 phosphorylation by taxol: A novel apoptotic signal transduction pathway [abstract]. Proceedings of the American Association for Cancer Research 37: 88, 1996.
141. Blagoskonny MV, T Schulte, P Nguyen, J Trepel, LM Neckers. Taxol-induced apoptosis and phosphorylation of Bcl-2 protein involves c-Raf-1 and represents a novel c-Raf-1 signal transduction pathway. Cancer Research 56: 1851-1854, 1996.
142. Meikrantz W, S Gisselbrecht, SW Tam, R Schlegel. Activation of cyclin A-dependent protein kinases during apoptosis. Proceedings of the National Academy of the Sciences, USA 91: 3754-3758, 1994.
143. Shi L, WK Nishioka, J Th'ng, EM Bradbury, DW Litchfield, AH Greenberg. Premature p34^{cdc2} activation required for apoptosis. Science 263: 1143-1145, 1994.
144. Ryan JL, E Prochownik, CA Gottlieb, IJ Apel, R Merino, G Nunez, MF Clarke. *c-myc* and *bcl-2* modulate p53 function by altering p53 subcellular trafficking during the cell cycle. Proceedings of the National Academy of the Sciences, USA 91: 5878-5882, 1994.
145. Jacobson MD, JF Burne, MC Raff. Programmed cell death and Bcl-2 protection in the absence of a nucleus. EMBO Journal 13 (8):1899-1910, 1994.
146. Willingham MC, K Bhalla. Transient mitotic phase localization of Bcl-2 oncoprotein in human carcinoma cells and its possible role in prevention of apoptosis. The Journal of Histochemistry and Cytochemistry 42 (4): 441-450, 1994.
147. Boise LH, M Gonzalez-Garcia, CE Postema, L Ding, T Lindsten, LA Turka, X Mao, G Nunez, CB Thompson. *Bcl-x*, a *bcl-2*-related gene that functions as a dominant regulator of apoptotic cell death. Cell 74: 597-608, 1993.
148. Datta R, Y Manome, N Taneja, LH Boise, R Weichselbaum, CB Thompson, CA Slapak, D Kufe. Overexpression of *bcl-x_L* by cytotoxic drug exposure confers resistance to ionizing radiation-induced internucleosomal DNA fragmentation. Cell Growth and Differentiation 6: 363-370, 1995.
149. Dole MG, R Jasty, MJ Cooper, CB Thompson, G Nunez, VP Castle. *Bcl-x_L* is expressed in neuroblastoma cells and modulates chemotherapy-induced apoptosis. Cancer Research 55: 2576-2582, 1995.
150. Gauthier ER, L Piche, G Lemieux, R Lemieux. Role of *bcl-x_L* in the control of apoptosis in murine myeloma cells. Cancer Research 56: 1451-1456, 1996.

151. Fang W, JJ Rivard, JA Ganser, TW LeBien, KA Nath, DL Mueller, TW Behrens. Bcl-x_L rescues WEHI231 B lymphocytes from oxidant-mediated death following diverse apoptotic stimuli. Journal of Immunology 155: 66-75, 1995.
152. Krajewski S, M Krajewska, A Shabaik, H-G Wang, S Irie, L Fong, JC Reed. Immunohistochemical analysis of *in vivo* patterns of *bcl-x* expression. Cancer Research 54: 5501-5507, 1994.
153. Sumantran VN, MW Ealovega, G Nunez, MR Clarke, MS Wicha. Overexpression of Bcl-x_S sensitizes MCF-7 cells to chemotherapy-induced apoptosis. Cancer Research 55: 2507-2510, 1995.
154. Ealovega MW, PK McGinnis, VN Sumantran, MF Clarke, MS Wicha. *bcl-x_S* gene therapy induces apoptosis of human mammary tumors in nude mice. Cancer Research 56: 1965-1969, 1996.
155. Clark MF, IJ Apel, MA Benedict, PG Eipers, V Sumantran, M Gonzalez-Garcia, M Doedens, N Fukunaga, B Davidson, JE Dick, AJ Minn, LH Boise, CB Thompson, M Wicha, G Nunez. A recombinant *bcl-x_S* adenovirus selectively induces apoptosis in cancer cells but not in normal bone marrow cells. Proceedings of the National Academy of Sciences, USA 92: 11024-11028, 1995.
156. Minn AJ, LH Boise, CB Thompson. Bcl-x_S antagonizes the protective effects of Bcl-x_L. The Journal of Biological Chemistry 271 (11): 6306-6312, 1996.
157. Gonzalez-Garcia M, I Garcia, L Ding, S O'Shea, LH Boise, CB Thompson, G Nunez. *Bcl-x* is expressed in embryonic and postnatal neural tissues and functions to prevent neural cell death. Proceedings of the National Academy of Sciences, USA 92: 4304-4308, 1995.
158. Park JR, ID Bernstein, DM Hockenbery. Primitive human hematopoietic precursors express *bcl-x* but not Bcl-2. Blood 86 (3): 868-876, 1995.
159. Motoyama N, F Wang, KA Roth, H Sawa, K Nakayama, K Nakayama, I Negishi, S Senju, Q Zhang, S Fujii, DY Loh. Massive cell death of immature hematopoietic cells and neurons in *bcl-x*-deficient mice. Science 267: 1506-1510, 1995.
160. Veis DJ, CM Sorenson, JR Shutter, SJ Korsmeyer. *Bcl-2*-deficient mice demonstrate fulminant lymphoid apoptosis, polycystic kidneys, and hypopigmented hair. Cell 75: 229-250, 1993.
161. Oltvai ZN, CL Milliman, SJ Korsmeyer. Bcl-2 heterodimerizes *in vivo* with a conserved homolog, bax, that accelerates programmed cell death. Cell 74: 609-619, 1993.
162. Yin X-M, ZA Oltvai, SJ Korsmeyer. BH1 and BH2 domains of Bcl-2 are required for inhibition of apoptosis and heterodimerization with Bax. Nature 369: 321-323, 1994.
163. Hanada M, C Aime'-Sempe', T Sato, JC Reed. Structure-function analysis of Bcl-2 protein. Identification of conserved domains important for homodimerization with Bcl-2 and heterodimerization with Bax. The Journal of Biological Chemistry 270 (20): 11962-11969, 1995.

164. Borner C, I Martinou, C Mattmann, M Irmeler, E Schaerer, J-C Martinou, J Tschopp. The protein Bcl-2 α does not require membrane attachment but two conserved domains to suppress apoptosis. The Journal of Cell Biology 126: 1059-1068, 1994.
165. Cheng E H-Y, B Levine, LH Boise, CB Thompson, JM Hardwick. Bax-independent inhibition of apoptosis by Bcl-x_L. Nature 379: 554-556, 1996.
166. Oltvai ZN, SJ Korsmeyer. Checkpoints of dueling dimers foil death wishes. Cell 79: 189-192, 1994.
167. Krajewski S, M Krajewska, A Shabaik, T Miyashita, H-G Wang, JC Reed. Immunohistochemical determination of in vivo distribution of Bax, a dominant inhibitor of Bcl-2. American Journal of Pathology 145 (6): 1323-1336, 1994.
168. Kozpas KM, T Yang, HL Buchan, P Zhou, RW Craig. *Mcl1*, a gene expressed in programmed myeloid cell differentiation, has sequence similarity to *bcl-2*. Proceedings of the National Academy of Sciences, USA 90: 3516-3520, 1993.
169. Krajewski S, S Bodrug, R Gascoyne, K Berean, M Krajewska, JC Reed. Immunohistochemical analysis of mcl-1 and Bcl-2 proteins in normal and neoplastic lymph nodes. American Journal of Pathology 145 (3): 515-525, 1994.
170. Reynolds JE, T Yang, L Qian, JD Jenkinson, P Zhou, A Eastman, RW Craig. Mcl-1, a member of the *bcl-2* family, delays apoptosis induced by c-Myc overexpression in Chinese hamster ovary cells. Cancer Research 54: 6348-6352, 1994.
171. Lomo J, EB Smeland, S Krajewski, JC Reed, HK Blomhoff. Expression of Bcl-2 homologue Mcl-1 correlates with survival of peripheral blood B-lymphocytes. Cancer Research 56 (1): 40-43, 1995.
172. Lin EY, A Orloffsky, M Bergar, MB Prystowsky,. Characterization of *A1*, a novel hemopoietic-specific early-response gene with sequence similarity to *bcl-2*. Journal of Immunology 151: 1979-1988, 1993.
173. Nunez G, MF Clarke. The Bcl-2 family of proteins: Regulators of cell death and survival. Trends in Cell Biology 4: 399-403, 1994.
174. Lin EY, A Orloffsky, H-G Wang, JC Reed, MB Prystowsky. A1, a Bcl-2 family member, prolongs cell survival and permits myeloid differentiation. Blood 87 (3): 983-992, 1996.
175. Yang E, J Zha, J Jockel, LH Boise, CB Thompson, SJ Korsmeyer. Bad, a heterodimeric partner for Bcl-x_L and Bcl-2, displaces Bax and promotes cell death. Cell 80: 285-291, 1995.
176. Takayama S, T Sato, S Krajewski, K Kochel, S Irie, JA Millan, JC Reed. Cloning and functional analysis of Bag-1: A novel Bcl-2-binding protein with anti-cell death activity. Cell 80: 279-284, 1995.

177. Farrow SN, JHM White, I Martinou, T Raven, K-T Pun, CJ Grinham, J-C Martinou, R Brown. Cloning of a *bcl-2* homologue by interaction with adenovirus E1B 19K. Nature 374: 731-733, 1995.
178. Keifer MC, MJ Brauer, VC Powers, JJ Wu, SR Umansky, LD Tomei, PJ Barr. Modulation of apoptosis by the widely distributed Bcl-2 homologue Bak. Nature 374: 736-739, 1995.
179. Chittenden T, EA Harrington, R O'Connor, C Flemington, RJ Lutz, GI Evan, BC Guild. Induction of apoptosis by the Bcl-2 homologue Bak. Nature 374: 733-736, 1995.
180. Choi SS, I-C Park, JW Yon, YC Sung, S-I Hong, H-S Shin. A novel Bcl-2 related gene, Bfl-1, is overexpressed in stomach cancer and preferentially expressed in bone marrow. Oncogene 11: 1693-1698, 1995.
181. Gillet G, M Guerin, A Trembleau, G Brun. A *bcl-2*-related gene is activated in avian cells transformed by the Rous sarcoma virus. EMBO Journal 14 (7): 1372-1381, 1995.
182. Hengartner MO and RH Horvitz. *C.elegans* cell survival gene *ced-9* encodes a functional homolog of the mammalian proto-oncogene *bcl-2*. Cell 76:665-676, 1994.
183. Hengartner MO, HR Horvitz. Activation of *C. elegans* cell death protein *ced-9* by an amino acid substitution in a domain conserved in Bcl-2. Nature 369: 318-320, 1994.
184. Das R, EP Reddy, D Chatterjee, DW Andrews. Identification of a novel Bcl-2 related gene, BRAG-1, in human glioma. Oncogene 12: 947-951, 1996.
185. Boyd JM, GJ Gallo, B Elanovan, AB Houghton, S Malstrom, BJ Avery, RG Ebb, T Subramanian, T Chittenden, RJ Lutz, G Chinnadurai. Bik, a novel death-inducing protein shares a distinct sequence motif with Bcl-2 family proteins and interacts with viral and cellular survival-promoting proteins. Oncogene 11: 1921-1928, 1995.
186. Chittenden T, C Flemington, AB Houghton, RG Ebb, GJ Gallo, B Elanovan, G Chinnadurai, RJ Lutz. A conserved domain in Bak, distinct from BH1 and BH2, mediates cell death and protein binding functions. The EMBO Journal 14 (22): 5589-5596, 1995.
187. Zha H, C Aime-Sempe, T Sato, JC Reed. Pro-apoptotic protein Bax heterodimerizes with Bcl-2 and homodimerizes with Bax via a novel domain (BH3) distinct from BH1 and BH2 [abstract]. Proceedings of the American Association for Cancer Research 37: 221, 1996.
188. Zha H, C Aime-Sempe, T Sato, JC Reed. Pro-apoptotic protein Bax heterodimerizes with Bcl-2 and homodimerizes with Bax via a novel domain (BH3) distinct from BH1 and BH2. The Journal of Biological Chemistry 271 (13): 7440-7444, 1996.
189. Hunter JJ, TG Parslow. A peptide sequence from Bax that converts Bcl-2 into an activator of apoptosis. The Journal of Biological Chemistry 271 (5): 8521-8524, 1996.
190. Wang H-G, S Takayama, C Aime-Sempe, UR Rapp. Bcl-2 interacting protein, BAG-1, binds to and activates the kinase Raf-1 [abstract]. Proceedings of the American Association for Cancer Research 37: 173, 1996.

191. Craig RW. The *bcl-2* gene family. Seminars in Cancer Biology 6: 35-43, 1995.
192. Sato T, M Hanada, S Bodrug, S Irie, N Iwama, LH Boise, CB Thompson, E Golemis, L Fong, H-G Wang, JC Reed. Interactions among members of the Bcl-2 protein family analyzed with a yeast two-hybrid system. Proceedings of the National Academy of Sciences, USA 91: 9238-9242, 1994.
193. McDonnell TJ, P Troncoso, SM Brisbay, C Logothetis, LWK Chung, J-T Hsieh, S-M Tu, ML Campbell. Expression of the proto-oncogene *bcl-2* in the prostate and its association with emergence of androgen-independent prostate cancer. Cancer Research 52: 6940-6944, 1992.
194. Mariano, MT, L Moretti, A Donelli, M Grantini, G Montagnani, AU DiPrisco, G Torelli, U Torelli, F Narni. *Bcl-2* gene expression in hematopoietic cell differentiation. Blood 80 (3): 768-775, 1992.
195. Jiwa NM, P Kanavaros, P van der Valk, JMM Walboomers, A Horstman, W Vos, H Mullnik, CJLM Meijer. Expression of *c-myc* and *bcl-2* oncogene products in reed-Sternberg cells independent of presence of Epstein-Barr virus. Journal of Clinical Pathology 46: 211-217, 1993.
196. Tanaka S, D Louie, J Kant, JC Reed. Application of a PCR-mismatch technique to the *bcl-2* gene: Detection of point mutations in *bcl-2* genes of malignancies with a t(14;18). Leukemia 6 (suppl. 3): 15S-19S, 1992.
197. Gribben JG, AS Freedman, SD Woo, K Blake, RS Shu, G Freeman, JA Longtine, GS Pinkus, LM Nadler. All advanced stage non-Hodgkin's lymphomas with a PCR-amplifiable breakpoint of *bcl-2* have residual cells contenting *bcl-2* rearrangements at evaluation and after treatment. Blood 78 (12): 3275-3280, 1991.
198. Kodo E, S Nakamura, H Onoue, Y Matsuo, T Yoshino, H Aoki, K Hayashi, K Takahashi, J Minowada, S Nomura, T Akagi. Detection of Bcl-2 protein and *bcl-2* mRNA in normal and neoplastic lymphoid tissues by immunohistochemistry and in situ hybridization. Blood 80 (8): 2044-2051, 1992.
199. Pettersson M, H Jernberg-Wiklund, L-G Larsson, C Sundstrom, I Givol, Y Tsujimoto, K Nilsson. Expression of the *bcl-2* gene in human multiple myeloma cell lines and normal plasma cells. Blood 79 (2): 495-502, 1992.
200. Delia D, A Aiella, D Soligo, E Fontanella, C Melani, F Pezzella, MA Pierotti, G DellaPorta. *Bcl-2* proto-oncogene expression in normal and neoplastic human myeloid cells. Blood 79 (5): 1291-1298, 1992.
201. Bullock G, A Nawabi, S Ray, Y Huang, K Bhalla. Mechanisms and partial reversal of resistance to antileukemic drug-induced apoptosis in CML blast crisis K562 cells [abstract]. Blood 84 (10): 610, 1994.
202. Ray S, G Bullock, G Nunez, JC Reed, S Krajewski, C Tang, AM Ibrado, Y Huang, K Bhalla. Enforced expression of Bcl-x_S induces differentiation and sensitizes CML-blast crisis K562 cells to Ara-C-mediated differentiation and apoptosis. Manuscript submitted.

203. Benito A, D Grillot, G Nunez, JL Ferna'ndez-Luna. Regulation and function of Bcl-2 during differentiation-induced cell death in HL-60 promyelocytic cells. American Journal of Pathology 146 (2): 481-490, 1995.
204. Campos L, J-P Rouault, O Sabido, P Oriol, N Roubi, C Vasselon, E Archimbaud, J-P Magnud, D Guyotat. High expression of Bcl-2 protein in AML cells is associated with poor response to chemotherapy. Blood 81 (11): 3091-3096, 1993.
205. Campos L, O Sabido, JP Rouault, D Guyotat. Effects of *bcl-2* antisense oligodeoxynucleotides on in vitro proliferation and survival of normal marrow progenitors and leukemic cells. Blood 84: 595-600, 1994.
206. Keith FJ, DA Bradbury, Y-M Zhu, NH Russell. Inhibition of *bcl-2* with antisense oligonucleotides induces apoptosis and increases the sensitivity of AML blasts to Ara-C. Leukemia 9: 131-138, 1995.
207. Lichtman MA. Acute myelogenous leukemia. In: Williams' Hematology, Fifth Edition, E Beutler, MA Lichtman, BS Coller, TJ Kipps, eds. New York: McGraw-Hill, Inc., 1995. pp. 272-298.
208. Friedreich N. Ein neuer Fall von Leukamie. Archives of Pathologic Anatomy 12: 37, 1857.
209. Ebstein W. Ueber die acute Leukamie und Pseudoleukamie. Deutsch Archives of Klinical Medicine 44: 343, 1889.
210. Fraenkal A. Ueber acute Leukamie. Deutsch Medikal Wochenschr. 21: 639, 1895.
211. Sacher RA, RA McPherson, eds. Widmann's Clinical Interpretation of Laboratory Tests, Tenth Edition. Philadelphia: FA Davis Company, 1991. pp. 139.
212. Cormack DH, ed. Hematopoietic differentiation. Ham's Histology. Philadelphia: J.B. Lippincott Co., 1987. pp.219-230.
213. Adams JM, S Cory. Oncogene cooperation in leukemogenesis. Cancer Survival 15: 119, 1992.
214. Larson RA, DP Sandler, MM LeBeau. Acute leukemia: Biology and treatment. In: Hematology 1994: Education Program of the American Society of Hematology. The American Society of Hematology, 1994. pp. 34-42.
215. Wiernik PH, PLC Banks, DC Case Jr, et al. Cytarabine plus idarubicin or daunorubicin as induction and consolidation therapy for previously untreated adult patients with acute myeloid leukemia. Blood 79 (2): 313-319, 1992.
216. Berman E, G Heller, J Santors. Results of a randomized trial comparing idarubicin and cytosine arabinoside with daunorubicin and cytosine arabinoside in adult patients in the newly diagnosed acute myelogenous leukemia. Blood 77 (8): 1666-1674, 1991.

217. Phillips GL, DE Reece, JD Shepard *et al.* High-dose cytarabine and daunorubicin induction and postremission chemotherapy for the treatment of acute myelogenous leukemia in adults. Blood 77 (7): 1429-1435, 1991.
218. Appelbaum FR, J Downing, C Willman. The biology and therapy of acute myelogenous leukemia. In: Hematology 1995: Education Program of the American Society of Hematology. The American Society of Hematology, 1995. pp. 23-35.
219. Bhalla K, R Nayak, S Grant. Isolation and characterization of a deoxycytidine kinase-deficient human promyelocytic leukemic cell line highly resistant to 1- β -D-arabinofuranosylcytosine. Cancer Research 44: 5029-5037, 1984.
220. Baer MR, CD Bloomfield. Multidrug resistance in acute myeloid leukemia. Journal of the National Cancer Institute 83 (10): 663-665, 1991.
221. Porwit-MacDonald A, K Ivory, S Wilkinson, K Wheatley, L Wong, G Janossy. Bcl-2 protein expression in normal human bone marrow precursors and in acute myelogenous leukemia. Leukemia 9: 1191-1198, 1995.
222. Deng G, C Lane, S Kornblau, A Goodacre, V Snell, M Andreef, AB Deisseroth. Bcl-2 and Bcl-xL are expressed at higher levels in poor prognosis (monosomy 5 and monosomy 7) acute myeloid leukemia (AML) cells than in good prognosis [inversion 16 and t(8;21)] AML cells [abstract]. Proceedings of the American Association for Cancer Research 37: 157, 1996.
223. Kufe DW, DR Spriggs. Biochemical and cellular pharmacology of cytosine arabinoside. Seminars in Oncology 12 (2), suppl.5: 34-48, 1985.
224. Chabner BA. Cytidine analogues. In: Cancer Chemotherapy: Principles and Practice, BA Chabner and JM Collins, eds. New York: JB Lippincott, Co., 1990. pp.154-179.
225. Chabner BA. Cytidine analogues. In: Cancer Chemotherapy and Biotherapy: Principles and Practice, second edition, BA Chabner and DL Longo, eds. Philadelphia: Lippincott-Raven Publishers, 1996. pp.213-233.
226. Plagemann PGW, R Marz, RM Wohlheter. Transport and metabolism of deoxycytidine and 1- β -D-arabinofuranosylcytosine into cultured Novikoff rat hepatoma cells, relationship to phosphorylation, and regulation of triphosphate synthesis. Cancer Research 38: 978-989, 1978.
227. Wiley JS, SP Jones, WH Swayer, ARP Paterson. Cytosine arabinoside influx and nucleoside transport sites in acute leukemia. Journal of Clinical Investigation 69: 479-489, 1982.
228. Raza A, K Ucar, HD Preisler, G Mayers. *In vitro* and *in vivo* assessment of sensitivity to Ara-C in myeloid leukemia. Seminars in Oncology 12 (2): 9-19, 1985.
229. Kawasaki H, H Kuwabara, H Hori, M Higashigawa, T Ohkuba, M Sakurai. Intracellular dCTP/Ara-CTP ratio and the cytotoxic effect of Ara-C. Cancer Investigation 9(4): 409-413, 1991.
230. Kufe DW, PP Major, EM Egan, GP Beardsley. Correlation of cytotoxicity with incorporation of Ara-C into DNA. The Journal of Biological Chemistry 255 (19): 8997-9000, 1980.

231. Major PP, EM Egan, GP Beardsley, MD Minden, DW Kufe. Lethality of human myeloblasts correlates with the incorporation of arabinofuranosylcytosine into DNA. Proceedings of the National Academy of Sciences, USA 78 (5): 3235-3239, 1981.
232. Woodcock DM, RM Fox, IA Cooper. Evidence for a new mechanism of cytotoxicity of 1- β -D-arabinofuranosylcytosine. Cancer Research 39: 1418-1424, 1979.
233. Fernandes DJ, CV Catapano. Nuclear matrix targets for anticancer agents. Cancer Cells 3 (4): 134-140, 1991.
234. Woodcock DM, IA Cooper. Evidence for double replication of chromosomal DNA segments as a general consequence of DNA replication inhibition. Cancer Research 41: 2483-2490, 1981.
235. Perrino FW, HL Mekosh. Incorporation of cytosine arabinoside monophosphate into DNA at internucleotide linkages by human DNA polymerase α . The Journal of Biological Chemistry 267 (32): 23043-23051, 1992.
236. Ross DD, DP Cuddy, N Cohen, DR Hensley. Mechanistic implications of alterations in HL-60 nascent DNA after exposure to 1- β -D-arabinofuranosylcytosine. Cancer Chemotherapy and Pharmacology 31: 61-70, 1992.
237. Ross DD, S-RS Chen, DP Cuddy. Effects of 1- β -D-arabinofuranosylcytosine on DNA replication intermediates monitored by pH-step alkaline elution. Cancer Research 50: 2658-2666, 1990.
238. Mikita T, Beardsley GP. Functional consequences of the arabinofuranosylcytosine structural lesion in DNA. Biochemistry 27: 4698-4705, 1988.
239. Downes CS, ARS Collins. Effects of DNA replication inhibitors on UV excision repair in synchronized human cells. Nucleic Acids Research 10 (17): 5357-5368, 1982.
240. Frankfurt OS. Inhibition of DNA repair and enhancement of cytotoxicity of alkylating agents. International Journal of Cancer 48: 916-923, 1991.
241. Holmberg M, E Gumauska. Chromosome-type exchange aberrations are induced by inhibiting repair of UVC-induced DNA lesions in quiescent human lymphocytes. Mutation Research 232: 261-266, 1991.
242. Dunn WC, JD Regan. Inhibition of DNA excision repair in human cells by arabinofuranosyl cytosine: Effect on normal and xeroderma pigmentosum cells. Molecular Pharmacology 15: 367-374, 1979.
243. Fram RJ, DW Kufe. DNA strand breaks caused by inhibitors of DNA synthesis: 1- β -D-arabinofuranosylcytosine and aphidicolin. Cancer Research 42: 4056-4053, 1982.
244. Zittoun J, J Marquet, JC David, D Maniey, R Zittoun. A study of the mechanisms of cytotoxicity of Ara-C in three human leukemic cell lines. Cancer Chemotherapy and Pharmacology 24: 251-255, 1989.

245. Zittoun J, J Marquet, JC David. Mechanism of inhibition of DNA ligase activity in Ara-C-treated cells. Leukemia Research 15 (2/3): 157-164, 1991.
246. Grem JL, F Geoffroy, PM Politi, DP Cuddy, DD Ross, D Nguyen, SM Steinberg, CJ Allegra. Determinants of sensitivity to 1- β -D-arabinofuranosylcytosine in HCT 116 and NCI-H630 human colon carcinoma cells. Molecular Pharmacology 48: 305-315, 1995.
247. Lauzon GJ, ARP Paterson, AW Belch. Formation of 1- β -D-arabinofuranosylcytosine diphosphate choline in neoplastic and normal cells. Cancer Research 38: 1730-1733, 1978.
248. Hawtrey AO, T Scott-Burden, G Robertson. Inhibition of glycoprotein and glycolipid synthesis in hamster embryo cells by cytosine arabinoside and hydroxyurea. Nature 252: 58-60, 1974.
249. Kucera GL, RL Capizzi. 1- β -D-arabinofuranosylcytosine-diphosphate choline is formed by the reversal of cholinephosphotransferase and not via cytidyltransferase. Cancer Research 52: 3886-3891, 1992.
250. Strum JC, GW Small, SB Pauig, LW Daniel. 1- β -D-arabinofuranosylcytosine stimulates ceramide and diglyceride formation in HL-60 cells. The Journal of Biological Chemistry 269 (22): 15493-15497, 1994.
251. Obeid LM, CM Linardic, LA Karolak, YA Hannun. Programmed cell death induced by ceramide. Science 259: 1769-1771, 1993.
252. Chen M, J Quintans, Z Fuks, C Thompson, DW Kufe, RR Weichselbaum. Suppression of bcl-2 messenger RNA production may mediate apoptosis after ionizing radiation, tumor necrosis factor α , and ceramide. Cancer Research 55: 991-994, 1995.
253. Jarvis WD, S Grant, RN Kolesnick. Ceramide and the induction of apoptosis. Clinical Cancer Research 2: 1-6, 1996.
254. Brach MA, SM Kharbanda, F Herrmann, DW Kufe. Activation of the transcription factor κ B in human KG-1 myeloid leukemia cells treated with 1- β -D-arabinofuranosylcytosine. Molecular Pharmacology 41: 60-63, 1991.
255. Datta R, S Kharbanda, DW Kufe. Transcriptional and posttranscriptional regulation of H1 histone gene expression by 1- β -D-arabinofuranosylcytosine. Molecular Pharmacology 41: 64-68, 1991.
256. Kharbanda S, ML Sherman, D Kufe. Transcriptional and posttranscriptional regulation of *c-jun* gene expression by arabinofuranosylcytosine in human myeloid leukemia cells. Journal of Clinical Investigation 86: 1517-1523, 1990.
257. Datta R, Kharbanda S, D Kufe. Regulation of *jun-B* gene expression by 1- β -D-arabinofuranosylcytosine in human myeloid leukemia cells. Molecular Pharmacology 38: 435-439, 1990.

258. Kharbanda S, E Huberman, D Kufe. Activation of the *jun-D* gene during treatment of human myeloid leukemia cells with 1- β -*D*-arabinofuranosylcytosine. Biochemical Pharmacology 45: 2055-2061, 1993.
259. Kharbanda S, A Saleem, E Rubin, V Sukhutme, J Blenis, D Kufe. Activation of the early growth response 1 gene and nuclear pp90^{rsk} in human myeloid leukemia cells by 1- β -*D*-arabinofuranosylcytosine. Biochemistry 32: 9137-9142, 1993.
260. Brach MA, F Herrmann, DW Kufe. Activation of the AP-1 transcription factor by arabinofuranosylcytosine in myeloid leukemia cells. Blood 79 (3): 728-734, 1992.
261. Kharbanda S, R Datta, D Kufe. Regulation of *c-jun* gene expression in HL-60 leukemia cells by 1- β -*D*-arabinofuranosylcytosine. Potential involvement of a protein kinase C dependent mechanism. Biochemistry 30: 7947-7952, 1991.
262. Bullock G, S Ray, J Reed, T Miyashita, AM Ibrado, Y Huang, K Bhalla. Evidence against a direct role for the induction of *c-jun* expression in the mediation of drug-induced apoptosis in human acute leukemia cells. Clinical Cancer Research 1 (5): 559-564, 1995.
263. Grant S, AJ Freemerman, MJ Birrer, J Chelliah, WD Jarvis. Differential role of c-jun in 1- β -*D*-arabinofuranosylcytosine-induced differentiation versus apoptosis in U937 human myeloid leukemia cells [abstract]. Blood 86 (10): 1299, 1995.
264. Kharbanda S, Y Emoto, H Kasaki, A Saleem, D Kufe. 1- β -*D*-arabinofuranosylcytosine activates serine/threonine protein kinases and c-jun gene expression in phorbol ester-resistant myeloid leukemia cells. Molecular Pharmacology 46: 67-72, 1994.
265. Saleem A, R Datta, Z-M Yuan, S Kharbanda, D Kufe. Involvement of stress-activated protein kinase in the cellular response to 1- β -*D*-arabinofuranosylcytosine and other DNA damaging agents. Cell Growth and Differentiation 6: 1651-1658, 1995.
266. Verheij M, R Bose, XH Lin, B Yao, WD Jarvis, S Grant, MJ Birrer, E Szabo, LI Zon, JM Kyriakis, A Haimovitz-Friedman, Z Fuks, RN Kolesnick. Requirement for ceramide-initiated SAPK/JNK signalling in stress-induced apoptosis. Nature 380: 75-79, 1996.
267. Kharbanda S, P Pandey, R Ren, B Mayer, L Zon, D Kufe. c-Abl activation regulates induction of the SEK1/stress-activated protein kinase pathway in the cellular response to 1- β -*D*-arabinofuranosylcytosine. The Journal of Biological Chemistry 270 (51): 307278-30281, 1995.
268. Yuan Z-M, S Kharbanda, D Kufe. 1- β -*D*-arabinofuranosylcytosine activates tyrosine phosphorylation of p34^{cdc2} and its association with the src-like p56/p53^{lyn} kinase in human myeloid leukemia cells. Biochemistry 34: 1058-1063, 1995.
269. Donaldson KL, GL Goolsby, PA Kiener, AF Wahl. Activation of p34^{cdc2} coincident with taxol-induced apoptosis. Cell Growth and Differentiation 5: 1041-1050, 1994.
270. Benito A, M Silva, D Grillot, G Nunez, JL Fernandez-Luna. Apoptosis induced by erythroid differentiation of human leukemia cell lines is inhibited by Bcl-x_L. Blood 87 (9): 3837-3843, 1996.

271. Collins SJ. The HL-60 promyelocytic leukemia cell line: Proliferation, differentiation, and cellular oncogene expression. Blood 70 (5): 1233-1244, 1987.
272. Bi S, T Hughes, J Bungey, A Chase, P de Fabitiis, JM Goldman. p53 in chronic myeloid leukemic cell lines. Leukemia 6 (8): 839-842, 1992.
273. Collins S, R Gallo, R Gallagher. Continuous growth and differentiation of human myeloid leukemic cells in suspension culture. Nature 270: 347-349, 1977.
274. Gallagher R, S Collins, J Trujillo, M McCredie, M Ahearn, S Tsai, R Metzgar, G Aulakh, R Ting, F Ruscetti, R Gallo. Characterization of the continuous, differentiating myeloid cell line (HL-60) from a patient with acute promyelocytic leukemia. Blood 54: 713-733, 1979.
275. Lapidot T, C Sirard, J Vormoor, B Murdoch, T Hoang, J Caceres-Cortes, M Minden, B Paterson, MA Caligiuri, JE Dick. A cell initiating human acute myeloid leukemia after transplantation into SCID mice. Nature 367: 645-648, 1994.
276. Collins S, Ruscetti F, R Gallagher, R Gallo. Terminal differentiation of human promyelocytic leukemia cells induced by dimethyl-sulfoxide and other polar compounds. Proceedings of the National Academy of Sciences, USA: 75 (4): 2458-2462, 1978.
277. Breitman T, S Selonick, S Collins. Induction of differentiation of the human promyelocytic leukemia cell line (HL-60) by retinoic acid. Proceedings of the National Academy of Sciences, USA 77 (5): 2936-2941, 1980.
278. McCarthy D, J SanMiguel, H Freake, P Green, H Zola, D Catovsky, J Goldmann. 1,25 dihydroxyvitamin D₃ inhibits proliferation of human promyelocytic leukemia (HL-60) cells and induces monocyte-macrophage differentiation in HL-60 and normal human bone marrow cells. Leukemia Research 7: 51-57, 1983.
279. Tanaka H, E Abe, C Miyaura, Y Shiina, T Suda. 1-alpha-dihydroxy-vitamin D₃ induces differentiation of human promyelocytic leukemia cells (HL-60) into monocyte-macrophages but not into granulocytes. Biochemical and Biophysical Research Communications 117 (1): 86-92, 1983.
280. Rovera G, D Santoli, C Damsky. Human promyelocytic leukemia cells in culture differentiate into macrophage-like cells when treated with phorbol ester. Proceedings of the National Academy of Sciences, USA 76 (6): 2779-2783, 1979.
281. Rovera G, T O'Brien, L Diamond. Induction of differentiation in human promyelocytic leukemia cells by tumor promoters. Science 204: 868-870, 1979.
282. Collins S, M Groudine. Amplification of endogenous *myc*-related DNA sequences in a human myeloid leukemia cell line. Nature 298: 679-681, 1982.
283. Dalla Favera R, F Wong-Staal, R Gallo. Oncogene amplification in promyelocytic cell line HL-60 and primary leukemia cells of the same patient. Nature 299: 61-63, 1982.

284. Bos J, M Verlaan-de Vries, A Jansen, G Veeneman, J van Boom, A vander Eb. Three different mutations in codon 61 of the human *N-ras* gene detected by synthetic oligonucleotide hybridization. Nucleic Acids Research 12 (23): 9155-9163, 1984.
285. Murray M, J Cunningham, L Parada, F Dautry, P Lebowitz, R Weinberg. The HL-60 transforming sequence: A *ras* oncogene coexisting with alter *myc* genes in hematopoietic tumors. Cell 33: 749-757, 1983.
286. Wolf D, V Rotter. Major deletions in the gene encoding the p53 tumor antigen cause lack of p53 expression in HL-60 cells. Proceedings of the National Academy of Sciences, USA 82 (13): 790-794, 1985.
287. Imamura J, I Miyoshi, HP Koeffler. p53 in hematologic malignancies. Blood 84 (8): 2412-2421, 1994.
288. Grignani F, M Fagioli, M Alcaly, L Longo, PP Pandolfi, E Donti, A Biondi, F LoCoco, F Grignani, PG Pelicci. Acute promyelocytic leukemia: From genetics to treatment. Blood 83 (1): 10-25, 1994.
289. Grignani F, PF Ferrucci, U Testa, G Talamo, M Fagioli, M Alcaly, A Mencarelli, F Grignani, C Peschii, I Nicoletti, PG Pelicci. The acute promyelocytic leukemia-specific PML-RAR α fusion protein inhibits differentiation and promotes survival of myeloid precursor cells. Cell 74: 423-431, 1993.
290. Chen Z, F Guidez, P Rousselot, A Agadir, S-J Chen, Z-Y Wang, L Degos, A Zelent, S Waxman, C Chomienne. PLZF-RAR α fusion proteins generated from the variant t(11;17)(q23;q21) translocation in acute promyelocytic leukemia inhibit ligand-dependent transactivation of wild-type retinoic acid receptors. Proceedings of the National Academy of Sciences, USA 91: 1178-1182, 1994.
291. Rousselot J, B Hardas, A Patel, F Guidez, J Gaken, S Castagne, A Dejean, H de The', L Degos, F Farzaneh, C Chomienne. The *PML-RAR α* gene product of the t(15;17) translocation inhibits retinoic acid-induced granulocytic differentiation and mediated transactivation in human myeloid cells. Oncogene 9 (2): 545-551, 1994.
292. Mu Z-M, K-V Chin, J-H Liu, G Lozano, K-S Chang. *PML*, a growth suppressor disrupted in acute promyelocytic leukemia. Molecular and Cellular Biology 14 (10): 6858-6867, 1994.
293. Cano RJ, JS Colome'. Microbiology. St. Paul: West Publishing Company, 1986.
294. Sambrook J, EF Fritsch, T Maniatis. Subcloning. In: Molecular Cloning: A Laboratory Manual, Second Edition. Cold Spring Harbor, NY: Cold Spring Harbor Press, 1989. Appendix F.
295. Sambrook J, EF Fritsch, T Maniatis. In situ hybridization of bacterial colonies. Transferring small numbers of colonies to nitrocellulose filters. In: Molecular Cloning: A Laboratory Manual, Second Edition. Cold Spring Harbor, NY: Cold Spring Harbor Press, 1989. pp. 1.98-1.99.

296. Sambrook J, EF Fritsch, T Maniatis. Collection of superhelical plasmid DNA from cesium chloride gradients containing ethidium bromide. In: Molecular Cloning: A Laboratory Manual, second edition. Cold Spring Harbor Press, 1989, pp. 1.45.
297. Sambrook J, EF Fritsch, T Maniatis. Detection and analysis of proteins expressed from cloned genes. In: Molecular Cloning: A Laboratory Manual, Second Edition. Cold Spring Harbor, NY: Cold Spring Harbor Press, 1989. pp. 18.69-18.71.
298. Lin F-T, MD Lane. CCAAT/enhancer binding protein α is sufficient to initiate the 3T3-L1 adipocyte differentiation program. Proceedings of the National Academy of Sciences, USA 91: 8757-8761, 1994.
299. Cepko C, B Roberts, R Mulligan. Construction and applications of a highly transmissible murine retrovirus shuttle vector. Cell 37: 1053, 1984.
300. Alnemri ES, NM Robertson, TF Fernandes, CN Croce, G Litwack. Overexpressed full-length human Bcl-2 extends the survival of baculovirus-infected Sf9 insect cells. Proceedings of the National Academy of Sciences, USA 89: 7295-7299, 1992.
301. Aubin R, M Weinfeld, MC Paterson. Polybrene/DMSO-assisted gene transfer. In: Gene Transfer and Expression Protocols, EJ Murray, ed. Methods in Molecular Biology, Vol.7. Clifton, NJ: The Humana Press, Inc., 1991, p. 35.
302. Monaghan P, D Robertson, TAS Amos, MJS Dyer, DY Mason, MF Greaves. Ultrastructural localization of Bcl-2 protein. Journal Histochemistry and Cytochemistry 40 (12): 1819-1825, 1992.
303. Pezzella F, AGD Tse, JL Cordell, KAF Pulford, KC Gatter, DY Mason. Expression of the *bcl-2* oncogene protein is not specific for the 14;18 chromosomal translocation. American Journal of Pathology 137 (2): 225-232, 1990.
304. Willingham MC, MM Cornwell, CO Cardarelli, MM Gottesman, I Pastan. Single cell analysis of daunomycin uptake and efflux in multidrug-resistant and -sensitive KB cells: Effects of verapamil and other drugs. Cancer Research 46: 5941-5946, 1986.
305. Gilboa E. Retroviral gene transfer: Application to human therapy. In: Retroviruses and disease, H Hanafusa, A Pinter, ME Pullman, eds. San Diego: Academic Press, Inc., 1992. pp. 95-112.
306. Ray J, FH Gaye. Gene transfer into established and primary fibroblast cell lines: Comparison of transfection methods and promoters. Biotechniques 13 (4): 598-603, 1992.
307. Coffin JM. Retroviridae and their replication. Virology, 2nd edition, BN Fields, DM Knipsey, *et al.*, eds. New York: Raven Press, Ltd., 1990. pp. 1437-1489.
308. Temin HM. Retrovirus vectors for gene transfer: Efficient integration into and expression of exogenous DNA in vertebrates cell genomes. In: Gene Transfer, R Kucherlapati, ed. New York: Plenum Press, 1990.
309. Goff SP. Genetics of retroviral integration. Annual Review of Genetics 26: 527-544, 1992.

310. Collins SJ, KA Robertson, LM Mueller. Retinoic acid-induced granulocytic differentiation of HL-60 myeloid leukemia cells is mediated directly through the retinoic acid receptor (RAR- α). Molecular and Cellular Biology 10 (5): 2154-2163, 1990.
311. Hock RA, AD Miller, WRA Osborne. Expression of human adenosine deaminase from various strong promoters after gene transfer into human hematopoietic cell lines. Blood 74 (2): 876-881, 1989.
312. Kaleko M, JV Garcia, WRA Osborne, AD Miller. Expression of human adenosine deaminase in mice after transplantation of genetically-modified bone marrow. Blood 75 (8): 1733-1741, 1990.
313. Palmer TD, AR Thompson, AD Miller. Production of human factor IX in animals by genetically modified skin fibroblasts: Potential therapy for hemophilia B. Blood 73 (2): 438-445, 1989.
314. Mavilio F, G Ferrari, S Rossini, N Nobili, C Bonini, G Casorati, C Traversari, C Bordignon. Peripheral blood lymphocytes as target cells of retroviral vector-mediated gene transfer. Blood 83 (7): 1988-1997, 1994.
315. Sorrentino BP, SJ Brandt, D Bodine, M Gottesman, I Pastan, A Cline, AW Nienhuis. Selection of drug-resistant bone marrow cells in vivo after retroviral transfer of human *mdr1*. Science 257: 99-103, 1992.
316. DelaFlor-Weiss E, C Richardson, M Ward, A Himelstein, L Smith, S Podda, M Gottesman, I Pastan, A Bank. Transfer and expression of the human multidrug resistance gene in mouse erythroleukemia cells. Blood 80 (12): 3106-3111, 1992.
317. Korsmeyer SJ. Bcl-2 initiates a new category of oncogenes: Regulators of cell death. Blood 4: 879-886, 1992.
318. Major PP, EM Egan, DJ Herrick, DW Kufe. Effect of Ara-C incorporation on deoxyribonucleic acid synthesis in cells. Biochemical Pharmacology 31 (18): 2937-2940, 1982.
319. Huang P, W Plunkett. Fludarabine- and gemcitabine-induced apoptosis: Incorporation of analogs into DNA is a critical event. Cancer Chemotherapy and Pharmacology 36: 181-188, 1995.
320. Oberhammer F, JW Wilson, D Dive, ID Morris, JA Hickman, AE Wakeling, PR Walker, M Sikorska. Apoptotic death in epithelial cells: Cleavage of DNA to 200 and/or 50 kb fragments prior to or in the absence of internucleosomal fragmentation. EMBO Journal, 12: 36789-36984, 1993.
321. Sambrook J, EF Fritsch, T Maniatis. Preparation of DNA-agarose plugs for pulsed-field gel electrophoresis. In: Molecular Cloning: A Laboratory Manual, Second Edition. Cold Spring Harbor, NY: Cold Spring Harbor Press, 1989. pp. 6.54.
322. Darzynkiewicz Z, S Bruno, G DelBino, W Gorczyca, MA Hotz, P Lassotta, F Traganos. Features of apoptotic cells measured by flow cytometry. Cytometry 13: 795-808, 1992.

323. Aiello A, D Delia, MG Bornello, D Biassoni, R Giardini, E Fontanella, F Pezzella, K Pulford, M Pierotti, G Della Poarta. Flow cytometric detection of the mitochondrial Bcl-2 protein in normal and neoplastic human lymphoid cells. Cytometry 13: 502-509, 1992.
324. Gong J, F Traganos, Z Darzynkiewicz. A selective procedure for DNA extraction from apoptotic cells applicable for gel electrophoresis and flow cytometry. Analytical Biochemistry 218: 314-319, 1994.
325. Sladowski D, SJ Steer, RH Clothier, M Balls. An improved MTT assay. Journal of Immunological Methods 157: 203-207, 1993.
326. te Boekhorst PAW, B Lowenberg, P Sonneveld. Enhanced chemosensitivity in acute myeloid leukemia by hematopoietic growth factors: A comparison of the MTT assay with clonogenic assay. Leukemia 7 (10): 1637-1644, 1993.
327. Garrett C, DV Santi. A rapid and sensitive high pressure liquid chromatographic assay for deoxyribonucleoside triphosphate in cell extracts. Analytical Biochemistry 99: 268-273, 1979.
328. Heinemann V, W Plunkett. Modulation of deoxynucleotide metabolism by the deoxycytidylate deaminase inhibitor 3,4,5,6-tetrahydrodeoxyuridine. Biochemical Pharmacology 38 (22): 4115-4121, 1989.
329. Bhalla K, C Holladay, Z Arlin, S Grant, AM Ibrado, M Jasiok. Treatment with IL-2 plus GM-CSF improves the selectivity of Ara-C in vitro against AML blasts. Blood 78: 2674-2679, 1991.
330. Kohn KW, E Ewig, AG Regina, LC Erickson, LA Zwelling. Measurement of strand breaks and cross-links by alkaline elution. In: DNA repair: A laboratory manual of research procedures, Vol. 1: Part B, EC Friedberg, PC Hanawalt, eds. New York: Marcel Dekker, Inc., 1981.
331. Catapano CV, M Broggin, E Erba, M Ponti, L Mariani, L Citti, M D'Incalci. In vitro and in vivo methazolastone-induced DNA damage and repair in L-1210 leukemia cells sensitive and resistant to chloroethylnitrosourea. Cancer Research 47: 4884-4889, 1987.
332. Kohn KW. Principles and practice of DNA filter elution. Pharmacology and Therapeutics 49: 55-77, 1991.
333. Kirkwood BR. Essentials of medical statistics. Oxford: Blackwell Scientific Publications, 1988.
334. Milton JS. Statistical methods in the biological and health sciences, second edition. New York: McGraw-Hill, Inc., 1992.
335. Heinemann V, U Jehn. Rationales for a pharmacologically optimized treatment of acute nonlymphocytic leukemia with cytosine arabinoside. Leukemia 4: 790-796, 1990.
336. Bolwell BJ, PA Cassileth, RP Gale. High dose cytarabine: A review. Leukemia 2: 253-260, 1995.

337. Herzig RH, SN Wolff, HM Lazarus, GL Phillips, C Karanes, GP Herzig. High-dose cytosine arabinoside therapy for refractory leukemia. Blood 62: 361-369, 1983.
338. Damon LE, W Plunkett, CA Linker. Plasma and cerebrospinal fluid pharmacokinetics of 1- β -*D*-arabinofuranosylcytosine and 1- β -*D*-arabinofuranosyluracil following repeated intravenous administration of intermediate-dose 1- β -*D*-arabinofuranosylcytosine. Cancer Research 51: 4141-4145, 1991.
339. Rustum YM, RAP Raymakers. 1- β -*D*-arabinofuranosylcytosine in therapy of leukemia: Preclinical and clinical overview. Pharmacology and Therapeutics 56: 307-321, 1992.
340. Riva CM, YM Rustum, HD Preisler. Pharmacokinetics and cellular determinants of response to 1- β -*D*-arabinofuranosylcytosine (Ara-C). Seminars in Oncology XII (2), Suppl. 3: 1-8, 1985.
341. Afanas'ev VN, BA Korol', YA Mantsygin, PA Nelipovich, VA Pechatnikov, SR Umansky. Flow cytometric and biochemical analysis of DNA degradation characteristic of two types of cell death. FEBS Letters 194 (2): 347-350, 1986.
342. Vaux DL, A Strasser. The molecular biology of apoptosis. Proceedings of the National Academy of the Sciences, USA 93: 2239-2244, 1996.
343. Bullock G, S Ray, G Nunez, Y Huang, AM Ibrado, K Bhalla. High levels of Bcl-x_L or Bcl-2 inhibits Ara-C-induced apoptosis but not Ara-C DNA incorporation or colony growth of human AML HL-60 cells. Manuscript submitted.
344. Huang P, LE Robertson, S Wright, W Plunkett. High molecular weight DNA fragmentation: A critical event in nucleoside analogue-induced apoptosis in leukemia cells. Clinical Cancer Research 1: 1005-1013, 1995.
345. Hu XF, A Slater, DM Wall, P Kantharidis, JD Parkin, A Cowman, JR Zalcberg. Rapid up-regulation of *mdr-1* expression by anthracyclines in a classical multidrug-resistant cell line. British Journal of Cancer 71: 931-936, 1995.
346. Noonan KE, C Beck, TA Holzmayer, JE Chin, JS Wunder, IL Andrulis, AF Gazdar, CL Willman, B Griffith, DD Von Hoff, IB Roninson. Quantitative analysis of *mdr-1* (multidrug resistance) gene expression in human tumors by polymerase chain reaction. Proceedings of the National Academy of Sciences, USA 87: 7160-7164, 1990.
347. Kartner N, V Ling. Multidrug resistance in cancer. Scientific American 260 (3): 44-51, 1989.
348. Jonsson K, N Dahlberg, U Tiddefelf, C Paul, G Andersson. Characterization of an anthracycline-resistant human promyelocyte leukemia (HL-60) cell line with an elevated *mdr-1* gene expression. Biochemical Pharmacology 49(6): 755-762, 1995.
349. Chaudhary PM, IB Roninson. Induction of multidrug resistance in human cells by transient exposure to different chemotherapeutic drugs. Journal of the National Cancer Institute 85: 632-639, 1993.

350. Zhao J-Y, M Ikeguchi, T Eckersberg, MT Kuo. Modulation of multidrug resistance gene expression by dexamethasone in cultured hepatoma cells. Endocrinology 133 (2): 521-528, 1993.
351. Gorczyca W, J Gong, Z Darzynkiewicz. Detection of DNA strand breaks in individual apoptotic cells by the *in situ* terminal deoxynucleotidyl transferase. Cancer Research 53: 1945-1951, 1993.
352. Baer MR, P Augustinos, AJ Kinniburgh. Defective *c-myc* and *c-myb* RNA turnover in acute myeloid leukemia cells. Blood 79 (5): 1319-1326, 1992.
353. Manome Y, RR Weichselbaum, DW Kufe, HA Fine. Effect of Bcl-2 on ionizing radiation and 1- β -D-arabinofuranosylcytosine-induced internucleosomal DNA fragmentation and cell survival in human myeloid leukemia cells. Oncology Research 5(3): 139-144, 1993.
354. Yin DX, RT Schimke. Bcl-2 expression delays drug-induced apoptosis but does not increase clonogenic survival after drug treatment in HeLa cells. Cancer Research 55: 4922-4928, 1995
355. Cuende E, JE Ales'-Martinez, L Ding, M Gonzalez-Garcia, C Martinez-A, G Nunez. Programmed cell death by *bcl-2*-dependent and independent mechanisms in B lymphoma cells. EMBO Journal 42: 1555-1560, 1993.
356. Tang C, Y Huang, VS Ponnathpur, S Ray, ME Mahoney, G Bullock, AM Ibrado, K Bhalla. Combined antileukemic activity of pIXY321 and Ara-C against human acute myeloid leukemia cells. Leukemia and Lymphoma 15: 445-451, 1994.
357. Andreeff M, S Jiang, U Consoli, J Brandes, G Sanchez-Williams, A Deisseroth, E Estey. In vivo regulation of Bcl-2 expression in AML progenitors by granulocyte-colony stimulating factor (G-CSF) and direct evidence for selection of Bcl-2⁺⁺ cells by induction chemotherapy of AML [abstract]. Blood 86 (10): 511, 1995.
358. Chresta CM, JRW Masters, JA Hickman. Hypersensitivity of human testicular tumors to etoposide-induced apoptosis is associated with functional p53 and a high Bax:Bcl-2 ratio. Cancer Research 56: 1834-1841, 1996.
359. Thomas A, S El-Rouby, JC Reed, S Krajewski, R Silber, M Potmesil, EW Newcomb. Drug-induced apoptosis in B-cell chronic lymphocytic leukemia: Relationship between p53 gene mutation and *bcl-2*/*bax* ratios in drug resistance. Oncogene 12: 1055-1062, 1996
360. Bhalla K, C Tang, AM Ibrado, S Grant, E Tourkina, C Holladay, M Hughes, ME Mahoney, Y Huang. Granulocyte-macrophage colony-stimulating factor/Interleukin-3 fusion protein (pIXY321) enhances high-dose Ara-C-induced programmed cell death or apoptosis in huma myeloid leukemia cells. Blood 80 (11): 2883-2890, 1993.
361. Perreault J, R Lemieux. Rapid apoptotic cell death of B-cell hybridomas in absence of gene expression. Journal of Cellular Physiology 156: 286-293, 1993.
362. Schwarze MMK, RG Hawley. Prevention of myeloma cell apoptosis by ectopic *bcl-2* expression of interleukin 6-mediated up-regulation of *bcl-x_L*. Cancer Research 55: 2262-2265, 1995.

363. Han Z, D Chatterjee, J Early, P Pantazis, EA Hendrickson, JH Wyche. Isolation and characterization of an apoptosis-resistant variant of human leukemia HL-60 cells that has switched expression from *bcl-2* to *bcl-x_L*. Cancer Research 56: 1621-1628, 1996.
364. Lee K, C Dive, JA Hickman. Induction of *bcl-x_L* following treatment of the murine B-leukemia cell line L1210 with the topoisomerase II inhibitor etoposide [abstract]. Proceedings of the American Association for Cancer Research 37: 2820, 1996.
365. Yin DX, RT Schimke. Manuscript in preparation. In: Bcl-2 expression delays drug-induced apoptosis but does not increase clonogenic survival after drug treatment in HeLa cells. Cancer Research 55: 4922-4928, 1995.
366. Liliemark JO, W Plunkett. Regulation of 1- β -D-arabinofuranosylcytosine 5'-triphosphate accumulation in human myeloid cells by deoxycytidine 5'-triphosphate. Cancer Research 46: 1079-1083, 1986.
367. Sancar A. Excision repair in mammalian cells. The Journal of Biological Chemistry 270 (27): 15915-15918, 1995.
368. Friedberg EC. DNA Repair. New York: WH Freeman and Company, 1985.
369. Friedberg EC. The molecular biology of nucleotide excision repair of DNA: Recent progress. Journal of Cell Science, suppl.6: 1-23, 1987.
370. Hoeijmakers JHJ, D Bootsma. Molecular genetics of eukaryotic DNA excision repair. Cancer Cells 2 (10): 311-320, 1990.
371. Sancar A. Mechanisms of DNA excision repair. Science 266: 1954-1956, 1994.
372. Mu D, DS Hsu, A Sancar. reaction mechanism of human DNA repair excision nuclease. The Journal of Biological Chemistry 271 (14): 8285-8294, 1996.
373. Gozukara EM, CN Parris, CA Weber, EP Salazar, MM Seidman, JF Watkins, L Prakash, KH Kraemer. The human DNA repair gene, *ERCC2 (XPD)*, corrects ultraviolet hypersensitivity and ultraviolet hypermutability of a shuttle vector replicated in xeroderma pigmentosum group D cells. Cancer Research 54: 3837-3844, 1994.
374. Leach FS, K Polyak, M Burrell, KA Johnson, D Hill, MG Dunlop, AH Wyllie, P Peltomaki, A de la Chapelle, SR Hamilton, KW Kinzler, B Vogelstein. Expression of the human mismatch repair gene *hMSH2* in normal and neoplastic tissues. Cancer Research 56: 235-240, 1996.
375. Palombo F, M Hughes, O Truong, J Hsuan, J Jiricny. Mismatch repair and cancer. Nature 367: 417, 1994.
376. Fenech M, J Rinaldi, J Surrales. The origin of micronuclei induced by cytosine arabinoside and its synergistic interaction with hydroxyurea in human lymphocytes. Mutagenesis 9 (3): 273-277, 1994.

377. Antoccia A, F Palitti, T Raggi, C Catena, C Tanzarella. Lack of effect of inhibitors of DNA synthesis/repair on the ionizing radiation-induced chromosomal damage in G₂ stage of ataxia-telangiectasia cells. International Journal of Radiation Biology 66 (3): 309-317, 1994.
378. Tsang Lee MYW, JJ Byrnes, KM Downey, AG Soo. Mechanism of inhibition of deoxyribonucleic acid synthesis by 1- β -D-arabinofuranosyl adenosine triphosphate and its potentiation by 6-mercaptopurine ribonucleoside 5'-monophosphate. Biochemistry 19: 215-219, 1980.
379. Derse D, Y-C Cheng. Herpes simplex virus type I polymerase. Kinetic properties of the associated 3'-5' exonuclease activity and its role in araCMP incorporation. The Journal of Biological Chemistry 256 (16): 8525-8530, 1981.
380. Miller MR, DN Chinault. Evidence that DNA polymerases α and β participate differentially in DNA repair synthesis induced by different agents. The Journal of Biological Chemistry 257 (10): 46-49, 1982.
381. Sobol RW, JK Horton, R Kuhn, H Gu, RK Singhal, R Prasad, K Rajewsky, SH Wilson. Requirement of mammalian DNA polymerase- β in base-excision repair. Nature 379:183-186, 1996.
382. Miller MR, DN Chinault. The roles of DNA polymerases α , β , and γ in DNA repair synthesis induced in hamster and human cells by different DNA damaging agents. The Journal of Biological Chemistry 257 (17): 10204-10209, 1982.
383. Bublely GJ, CS Crumpacker, LE Schnipper. Repair of DNA following incorporation of 1- β -D-arabinofuranosylcytosine into herpes simplex virus type I. Cancer Research 44: 1813-1818, 1984.
384. Aboussekhra A, M Biggerstaff, MKK Shivji, JA Vilpo, V Moncollin, VN Podust, M Protic, U Hubscher, J-M Egly, RD Wood. Mammalian DNA nucleotide excision repair reconstituted with purified protein components. Cell 80: 859-868, 1995.
385. Kaufmann SH, S Desnoyers, Y Ottaviano, NE Davidson, GG Poirier. Specific proteolytic cleavage of poly(ADP-ribose) polymerase: An early marker of chemotherapy-induced apoptosis. Cancer Research 53: 3976-3985, 1993.
386. Stierum RH, MH van Herwijnen, GJ Hageman, JC Kleinjans. Increased poly(ADP-ribose) polymerase activity during repair of (+/-)-anti-benzo[a]pyrene diolepoxide-induced DNA damage in human peripheral blood lymphocytes in vitro. Carcinogenesis 15 (4): 745-751, 1994.
387. Malanga M, FR Althaus. Poly(ADP-ribose) molecules formed during DNA repair in vivo. The Journal of Biological Chemistry 269 (26): 17691-17696, 1994.
388. Althaus FR, C Richer. ADP-ribosylation of proteins. Enzymology and biological significance. Molecular and Biological Biochemistry and Biophysics 37: 1-126, 1987.
389. DeMurcia G, A Huletsky, GG Poirier. Review: modulation of chromatin structure by poly(ADP-ribosyl)ation. Biochemistry and Cellular Biology 66: 626-635, 1988.

390. Satoh MS, T Lindahl. Role of poly(ADP-ribose) formation in DNA repair. Nature 356: 356-358, 1992.
391. Chatterjee S, NA Berger. Growth-phase-dependent response to DNA damage in poly(ADP-ribose) polymerase deficient cell lines: Basis for a new hypothesis describing the role of poly(ADP-ribose) polymerase in DNA replication and repair. Molecular and Cellular Biochemistry 138: 61-69, 1994.
392. Mirzayans R, B Andrais, MC Paterson. Synergistic effect of aphidicolin and 1-beta-D-arabinofuranosylcytosine on the repair of the gamma-ray-induced DNA damage in normal human fibroblasts. International Journal of Radiation Biology 62 (4): 417-425, 1992.
393. Hashimoto H, S Chatterjee, NA Berger. Inhibition of etoposide (VP-16)-induced DNA recombination and mutant-frequency by Bcl-2 protein overexpression. Cancer Research 55: 4029-4035, 1995.
394. Maze R, JP Carney, MR Kelley, BJ Glassner, DA Williams, L Samson. Increasing DNA repair methyltransferase levels via bone marrow stem cell transduction rescues mice from the toxic effects of 1,3-bis(2-chloroethyl)-1-nitrosourea, a chemotherapeutic alkylating agent. Proceedings of the National Academy of the Sciences, USA 93: 206-210, 1996.
395. Pil PM, SJ Lippard. Specific binding of chromosomal protein HMG1 to DNA damaged by the anticancer drug cisplatin. Science 256: 234-237, 1994.
396. Hughes EN, BN Engelsberg, PC Billings. Purification of nuclear proteins that bind to cisplatin-damaged DNA: Identity with high mobility group proteins 1 and 2. The Journal of Biological Chemistry 267: 13520-13527, 1992.
397. Treiber DK, X Zhai, HM Jantzen, JM Essigmann. Cisplatin-DNA adducts are molecular decoys for the ribosomal RNA transcription factor hUBF (human upstream binding factor). Proceedings of the National Academy of Sciences, USA 91: 5672-5676, 1994.
398. Huang JC, DB Zambli, JT Reardon, SJ Lippard, A Sancar. HMG-domain proteins specifically inhibit the repair of the major DNA adduct of the anticancer drug cisplatin by human excision nuclease. Proceedings of the National Academy of Sciences, USA 91: 10394-10398, 1994.
399. Freshney RI. Rates of DNA synthesis. In: Culture of animal cells: A manual of basic technique, Third Edition. New York: Wiley-Liss, Inc., 1994. pp. 227-228.
400. Martin SJ, AJ McGahon, WK Nishioka, D LaFace, X Guo, J Th'ng, EM Bradbury, DR green. p34^{cdc2} and apoptosis. Science 269: 106-107, 1995.
401. Islas AL, PC Hanawalt. DNA repair in the *MYC* and *FMS* proto-oncogenes in ultraviolet light-irradiated human HL-60 promyelocytic cells during differentiation. Cancer Research 55: 336-341, 1995.
402. Harlow SP, CC Stewart. Quantitation of *c-myc* gene amplification by a competitive PCR assay system. PCR Methods and Application 3: 163-168, 1993.

403. Rinaudo MS, K Su, LA Falk, S Haldar, RA Mufson. Human interleukin-3 receptor modulates *bcl-2* mRNA and protein levels through protein kinase C in TF-1 cells. Blood 86 (1): 80-88, 1995.
404. Kinoshita T, J Inamura, N Hirokazu, K Shimotohno. Quantification of gene expression over a wide range by the polymerase chain reaction. Analytical Biochemistry 206: 231-235, 1992.
405. Kalinowski DP, S Illenye, B VanHouten. Analysis of DNA damage and repair in murine leukemia L1210 cells using a quantitative PCR assay. Nucleic Acids Research 20 (13): 3485-3494, 1992.
406. Dolbeare F. BrdUrd-DNA analysis by flow cytometry. In: Flow Cytometry, Z Darzynkiewicz, ed. Cold Spring Harbor, NY: Cold Spring Harbor Press, 1993.
407. Dolbeare F, W Beisker, MG Pallavicini, M Vanderlaan, JW Gray. Cytochemistry for bromodeoxyuridine/DNA analysis: Stoichiometry and sensitivity. Cytometry 6: 521-530, 1985.
408. Hoy CA, LC Seamer, RT Schimke. Thermal denaturation of DNA for immunochemical staining of incorporated bromodeoxyuridine (BrdUrd): Critical factors that affect the amount of fluorescence and the shape of BrdUrd/DNA histogram. Cytometry 10: 718-725, 1989.
409. Dolbeare F, JR Selden. Immunochemical quantitation of bromodeoxyuridine: Application to cell-cycle kinetics. In: Methods in Cell Biology, Flow Cytometry, Second Edition, Vol.41, Part A, Z Darzynkiewicz, JP Robinson, HA Crissman, eds. San Diego: Academic Press, 1994. pp. 297-316.
410. Frankfurt OS, D Seckinger, EV Sugarbaker. Inhibition of DNA repair in cells treated with a combination of alkylating agents. Anticancer Research 13 (4): 947-952, 1993.
411. Niggli HJ. Aphidicolin inhibits excision repair of UV-induced pyrimidine photodimers in low serum cultures of mitotic and mitomycin-C-induced postmitotic human skin fibroblasts. Mutation Research 295 (3): 125-13, 1993.
412. Mirzayans R, K Dietrich, MC Paterson. Aphidicolin and 1-beta-D-arabinofuranosylcytosine strongly inhibit transcriptionally active DNA repair in normal human fibroblasts. Carcinogenesis 14 (2): 2621-2626, 1993.
413. Gera JF, C Fady, A Gardner, FJ Jacoby, KB Briskin, A Lichtenstein. Inhibition of DNA repair with aphidicolin enhances sensitivity of targets to tumor necrosis factor. Journal of Immunology 151 (7): 3746-3757, 1993.
414. Jennerwein MM, A Eastman. A polymerase chain reaction-based method to detect cisplatin adducts in specific genes. Nucleic Acids Research 19 (22): 6209-6214, 1991.
415. Axelrod JD, J Majors. An improved method for footprinting yeast genes in vivo using Taq polymerase. Nucleic Acids Research 17 (1): 171-183, 1989.
416. Ponti M, SM Forrow, RL Souhami, M D'Incalci, JA Hartley. Measurement of the sequence specificity of covalent DNA modification by antineoplastic agents using Taq DNA polymerase. Nucleic Acids Research 19 (11): 2929-2932, 1991.

417. Denissenko MF, S Venkatachalam, EY Yamaski, AA Wani. Assessment of DNA damage and repair in specific genomic regions by quantitative immuno-coupled PCR. Nucleic Acids Research 22 (12): 2351-2359, 1994.
418. Selden JR, F Dolbeare, JH Clair, WW Nichols, JE Miller, KN Kleemeyer, RJ Hyland, JG DeLuca. Statistical confirmation that immunofluorescent detection of DNA repair in human fibroblasts by measurement of bromodeoxyuridine incorporation is stoichiometric and sensitive. Cytometry 14: 154-167, 1993.
419. Selden JR, F Dolbeare. A flow cytometric technique for detection of DNA repair in mammalian cells. In: Methods in Cell Biology: Flow Cytometry, Second Edition, Vol.42, Part B, Z Darzynkiewicz, JP Robinson, HA Crissman, eds. San Diego: Academic Press, 1994.
420. Erlich HA. PCR Technology: Principles and applications for DNA amplification. New York: Stockton Press, 1989. pp. 1-16.
421. McPherson MJ, P Quirke, GR Taylor. PCR: A Practical Approach. Oxford: IRL Press, 1991. pp. 1-14.
422. Cleaver JE. Repair replication of mammalian cell DNA: Effects of compounds that inhibit DNA synthesis or dark repair. Radiation Research 37: 334-348, 1969.
423. Angel P, EA Allegeretto, ST Okino, K Hattori, WJ Boylwo, T Hunter, M Karin. Oncogene *jun* encodes a sequence-specific trans-activator similar to AP-1. Nature 332: 166-171, 1988.
424. Chiu R, WJ Boyle, J Meek, T Smeal, T Hunter, M Karin. The c-fos protein interacts with c-jun/AP-1 to stimulate transcription of AP-1 responsive genes. Cell 54: 541-552, 1988.
425. Angel P, M Karin. The role of *jun*, *fos*, and the AP-1 complex in cell proliferation and transformation. Biochimica Biophysica Acta 1072: 129-157, 1991.
426. Jarvis WD, LF Povirk, AJ Turner, RS Traylor, DA Gewirtz, GR Pettit, S Grant. Effects of Bryostatin 1 and other pharmacological activators of protein kinase C on 1- β -D-arabinofuranosylcytosine-induced apoptosis in HL-60 human promyelocytic leukemia cells. Biochemical Pharmacology 47: 839-852, 1994.
427. Grunicke HH, F Uberall. Protein kinase C modulation. Seminars in Cancer Biology 3: 351-360, 1992.
428. Abate C, L Patel, FJ Rauscher III, T Curran. Redox regulation of Fos and Jun DNA-binding activity in vitro. Science 249: 1157-1161, 1990.
429. Ng L, D Forrest, T Curran. Differential roles for Fos and Jun in DNA-binding: redox-dependent and independent functions. Nucleic Acids Research 21(5): 5831-5837, 1993.
430. Meyer M, R Scheck, PA Baeurle. H₂O₂ and antioxidants have opposite effects on activation of NF κ B and AP-1 in intact cell: AP-1 as secondary antioxidant-responsive factor. The EMBO Journal 12(5): 2005-2015, 1993.

431. Bergelson S, R Pinkus, V Daniel. Intracellular glutathione levels regulate Fos/Jun induction and activation of glutathione *S*-transferase gene expression. Cancer Research 54: 36-40, 1994.
432. Schreck R, K Albermann, PA Baeuerle. Free Radical Research Communications 17: 221-237, 1992.
433. Pinkus R, S Bergelson, V Daniel. Phenobarbital induction of AP-1 binding activity mediates activation of glutathione *S*-transferase and quinone reductase gene expression. Biochemistry Journal 290: 637-640, 1993.
434. Procownik EV, MJ Smith, K Snyder, D Emeagwali. Amplified expression of transfected jun family members inhibits erythroleukemia differentiation. Blood 76: 1830-1837, 1990.
435. Morgan DO. Principles of CDK regulation. Nature 374: 131-134, 1995.
436. Gazitt Y, GW Eros. Fluctuations and ultrastructural localization of oncoproteins and cell cycle regulatory proteins during growth and apoptosis of synchronized AGF cells. Cancer Research 54: 950-956, 1994.
437. King RW, PK Jackson, MW Kirschner. Mitosis in transition. Cell 79: 563-571, 1994.
438. Nurse P. Universal control mechanism regulating onset of M-phase. Nature 344: 503-508, 1990.
439. Shimizu T, PM O'Connor, KW Kohn, Y Pommier. Unscheduled activation of cyclin B1/cdc2 kinase in human promyelocytic cell line HL-60 cells undergoing apoptosis induced by DNA damage. Cancer Research 55: 228-231, 1995.
440. Schwartz SM, MR Bennett. Commentary: Death by any other name. American Journal of Pathology 147(2): 229-234, 1995.
441. Sacher RA and RA McPherson. Coagulation cascade. Widmann's Clinical Interpretation of Laboratory Tests, Tenth Edition. Philadelphia: FA Davis Company, 1991. pp.190-195.
442. Kondo S, BP Barna, T Morimura, J Takeuchi, J Yuan, A Akbask, GH Barnett. Interleukin-1 β -converting enzyme mediates cisplatin-induced apoptosis in malignant glioma cells. Cancer Research 55: 6166-6171, 1995.
443. Darmon AJ, DW Nicholson, RC Bleakley. Activation of the apoptotic protease CPP32 by cytotoxic T-cell-derived granzyme B. Nature 377: 446-448, 1995.
444. Pronk GJ, K Ramer, P Amri, LT Williams. Requirement of an ICE-like protease for induction of apoptosis and ceramide generation by REAPER. Science 271: 808-810, 1996.
445. An B, QP Dou. Cleavage of retinoblastoma protein during apoptosis: An interleukin-1 β -converting enzyme-like protease as candidate. Cancer Research 56: 438-442, 1996.
446. Lazebnik YA, SH Kaufmann, S Desnoyers, GG Poirier, WC Earnshaw. Cleavage of poly (ADP-ribose) polymerase by a proteinase with properties like ICE. Nature 37: 346-347, 1994.

447. Nicholson DW, A Ali, NA Thornberry, JP Vaillancourt, CK Ding, M Gallant, Y Gareau, PR Griffin, M Labelle, YA Lazebnik, NA Munday, SM Raju, ME Smulson, TT Yamin, VL Yu, DK Miller. Identification and inhibition of the ICE/Ced-3 protease necessary for mammalian apoptosis. Nature 376: 37-43, 1995.
448. Mashima T, M Naito, N Fujita, K Noguchi, T Tsuruo. Identification of actin as a substrate of ICE and an ICE-like protease and involvement of an ICE-like protease but not ICE in VP-16-induced U937 apoptosis. Biochemical and Biophysical Research Communications 217 (3): 1185-1192, 1995.
449. Emoto Y, Y Manome, G Meinhardt, H Kisaki, S Kharbanda, M Robertson, T Ghayur, WW Wong, R Kamen, R Weichselbaum, D Kufe. Proteolytic activation of protein kinase C δ by an ICE-like protease in apoptotic cells. The EMBO Journal 14 (24): 6148-6156, 1995.
450. Soldatenkov VA, S Prasad, V Notario, A Dritschilo. Radiation-induced apoptosis of Ewing's sarcoma cells: DNA fragmentation and proteolysis of poly(ADP-ribose) polymerase. Cancer Research 55: 4240-4242, 1995.
451. Tewari M, LT Quan, K O'Rourke, S Desnoyers, Z Zheng, DH Beidler, GG Poirier, GS Salvesen, VM Dixit. Yama/ CPP32 β , a mammalian homolog of ced-3, is a CrmA-inhibitable protease that cleaves the death substrate poly(ADP-ribose) polymerase. Cell 81: 801-809, 1995.
452. Fernandes-Alnemri T, G Litwack, ES Alnemri. CPP32, a novel human apoptotic protein with homology to *Caenorhabditis elegans* cell death protein ced-3 and mammalian interleukin-1 β -converting enzyme. The Journal of Biological Chemistry 269: 30761-30764, 1994.
453. Tewari M, WG Telford, RA Miller, VM Dixit. CrmA, a poxvirus-encoded serpin, inhibits cytotoxic T-lymphocyte-mediated apoptosis. The Journal of Biological Chemistry 270 (39): 22705-22708, 1995.
454. Lippke JA, Y Gu, C Sarnecki, PR Caron, M S-S Su. Identification and characterization of CPP32/Mch2 homolog 1, a novel cysteine protease similar to CPP32. The Journal of Biological Chemistry 271 (4): 1825-1828, 1996.
455. Fernandes-Alnemri T, A Takahari, R Armstrong, J Krels, L Fritz, KJ Tomaselli, L Wang, Z Yu, CM Croce, G Salvesen, WC Earnshaw, G Litwack, ES Alnemri. Mch3, a novel human apoptotic cysteine protease highly related to CPP32. Cancer Research 55: 6045-6052, 1995.
456. Tewari M, VM Dixit. Fas- and tumor necrosis factor-induced apoptosis is inhibited by the poxvirus crmA gene product. The Journal of Biological Chemistry 270 (7): 3255-3260, 1995.
457. Chinnaiyan AM, K Orth, K O'Rourke, H Duan, GG Poirier, VM Dixit. Molecular ordering of the cell death pathway: Bcl-2 and Bcl-xL function upstream of the ced-3-like apoptotic proteases. The Journal of Biological Chemistry 271 (9): 4573-4576, 1996.
458. Boulakia CA, G Chen, FWH Ng, JG Teodoro, PE Branton, DW Nicholson, GG Poirier, GC Shore. Bcl-2 and adenovirus E1B 19 kDa protein prevent E1A-induced processing of CPP32 and cleavage of poly(ADP-ribose) polymerase. Oncogene 12: 529-535, 1996.

459. Lazebnik YA, S Cole, CA Cooke, WG Nelson, WC Earnshaw. Nuclear events of apoptosis *in vitro* in cell-free mitotic extracts: A model system for analysis of the active phase of apoptosis. Journal of Cell Biology 123 (1): 7-22, 1993.
460. Yoshihara K, Y Tanigawa, L Burzio, SS Koide. Evidence for adenosine diphosphate ribosylation of Ca^{2+} - Mg^{2+} -dependent endonuclease. Proceedings of the National Academy of the Sciences, USA 72 (1): 289-293, 1975.
461. Tanaka Y, K Yoshihara, A Itaya, T Kamiya, SS Koide. Mechanism of the inhibition of the Ca^{2+} - Mg^{2+} -dependent endonuclease of bull seminal plasma induced by ADP-ribosylation. The Journal of Biological Chemistry 259: 6579-6585, 1984.
462. Nelipovich PA, LV Nikonova, SR Umansky. Inhibition of poly(ADP-ribose) polymerase as a possible reason for activation of Ca^{2+} - Mg^{2+} -dependent endonuclease in thymocytes of irradiated rats. International Journal Radiation Biology 53: 749-765, 1988.
463. Marks DI, RM Fox. DNA damage, poly (ADP-ribosyl)ation and apoptotic cell death as a potential common pathway of cytotoxic drug action. Biochemical Pharmacology 42 (10): 1859-1867, 1991.
464. Yoon YS, KW Wang, YS Kim, KH Choi, CO Joe. Poly(ADP-ribosyl)ation of histone H1 correlates with internucleosomal DNA fragmentation during apoptosis. The Journal of Biological Chemistry 271 (15): 9129-9134, 1996.
465. Bellamy COC, RDG Malcolmson, DJ Harrison, AH Wyllie. Cell death in health and disease: the biology and regulation of apoptosis. Seminars in Cancer Biology 6: 3-16, 1995.
466. Chirgwin J, H Przybyla, R McDonald, W Rutter. Isolation of biologically active ribonucleic acid from sources enriched in ribonuclease. Biochemistry 18: 5294-5299, 1979.
467. Chomczynski P, N Sacchi. Single-step method of RNA isolation by acid guanidinium thiocyanate-phenol-chloroform extraction. Analytical Biochemistry 162: 156-159, 1987.
468. Thomas PS. Hybridization of denatured RNA and small DNA fragments transferred to nitrocellulose. Proceedings of the National Academy of Sciences, USA 77: 5201-5205, 1980.

Biographical Sketch

GLORIA JOAN BULLOCK

DATE OF BIRTH:

12/13/68

EDUCATION:

1990 B.S. Biology, LeMoyne College, Syracuse, N.Y.

RESEARCH EXPERIENCE:

1989 Student of Summer Undergraduate Research Program,
Roswell Park Cancer Institute, Buffalo, N.Y.

PUBLICATIONS:

1. ARTICLES FROM THIS DISSERTATION:

- Chapter III has been submitted for publication:

Gloria Bullock, Swapan Ray, John C. Reed, Stanislaw Krajewski, Ana Maria Ibrado, Yue Huang, Amir Nawabi, and Kapil Bhalla. Intracellular metabolism of high dose Ara-C and resulting DNA fragmentation and apoptosis of human AML cells possessing disparate levels of p26Bcl-2 protein. Submitted to Leukemia.

Gloria Bullock, Swapan Ray, Gabriel Nunez, Yue Huang, Amir Nawabi, Kapil Bhalla. High levels of Bcl-x_L or Bcl-2 inhibit Ara-C-induced apoptosis but not Ara-C DNA incorporation and resulting inhibition of DNA synthesis or colony growth of human AML HL-60 cells. Submitted to Blood.

- Chapter III has been presented:

Gloria Bullock, Swapan Ray, John C. Reed, Stanislaw Krajewski, Ana Maria Ibrado, Yue Huang, and Kapil Bhalla. Intracellular metabolism of high dose Ara-C and resulting DNA fragmentation and apoptosis of human AML cells possessing disparate levels of p26Bcl-2 and p29Bcl-x_L [abstract]. Blood 86 (10): 515, 1995.

Gloria Bullock, Amir Nawabi, Swapan Ray, Ana Maria Ibrado, Caroline Tang, Yue Huang, and Kapil Bhalla. High Intracellular p26Bcl-2 levels block high-dose Ara-C-induced DNA fragmentation and apoptosis of human myeloid leukemia cells [abstract]. Proceedings of the American Association for Cancer Research 36: 415, 1995.

- Chapter IV will be submitted for presentation:

Gloria Bullock, John C. Reed, Toshiyuki Miyashita, Kapil Bhalla. Intracellular levels of overexpression of p26Bcl-2 determine the response to Ara-C-induced apoptosis over time in human myeloid leukemia HL-60 cells. Abstract in preparation for the American Society of Hematology.

- Chapter IV will be submitted for publication:

Gloria Bullock, GuoFu Fang, Shuli Li, Gian G. Re, Mark C. Willingham, John C. Reed, Toshiyuki Miyashita, Kapil Bhalla. *bcl-2* expression is induced in AML cells which survive treatment with HIDAC. Manuscript in preparation.

- Chapter V will be submitted for publication:

Gloria Bullock, Swapan Ray, Carlo V. Catapano, John C. Reed, Toshiyuki Miyashita, Kapil Bhalla. High intracellular levels of p26Bcl-2 blocks Ara-C-induced apoptosis but does not increase repair of Ara-C-induced DNA damage in acute myeloid leukemia HL-60 cells. Manuscript in preparation.

- A summary of this dissertation will be submitted for publication:

Gloria Bullock and Kapil Bhalla. Evolving concepts of Ara-C-induced AML cell death: A review. Manuscript in preparation.

2. ARTICLES RELATED TO THIS DISSERTATION:

- Part of Chapter II has been submitted for publication:

Swapan Ray, **Gloria Bullock**, Gabriel Nunez, John C. Reed, Stanislaw Krajewski, Caroline Tang, Ana Maria Ibrado, Yue Huang, Kapil Bhalla. Enforced expression of Bcl-x_s induces differentiation and sensitizes CML-blast crisis K562 cells to Ara-C-mediated differentiation and apoptosis. Manuscript submitted to Cell Growth and Differentiation.

- Part of chapter VI of this dissertation has been published:

Gloria Bullock, Swapan Ray, John C. Reed, Toshiyuki Miyashita, Ana Maria Ibrado, Yue Huang, Kapil Bhalla. Evidence against a direct role for the induction of *c-jun* expression in the mediation of drug-induced apoptosis in human acute leukemia cells. Clinical Cancer Research 1(5): 559-564, 1995.

3. OTHER PUBLICATIONS:

Gloria Bullock, Caroline Tang, Elena Tourkina, Ana Maria Ibrado, Jose Lutsky, Yue Huang, Mary Ella Mahoney, Kapil Bhalla. Effect of combined treatment with IL-3 and IL-6 on 4-Hydroperoxycyclophosphamide-induced programmed cell death or apoptosis in human myeloid leukemia cells. Experimental Hematology 21: 1640-1647, 1993.

Kapil Bhalla, **Gloria Bullock**, Jose Lutsky, Charles Holladay, Ana Maria Ibrado, Michelle Jasiok, Shivandra Singh. Effect of combined treatment with IL-3 and IL-6 on 4-Hydroperoxycyclophosphamide-mediated reduction of glutathione levels and cytotoxicity in normal and leukemic bone marrow progenitor cells. Leukemia 6 (8): 814-819, 1992.